

Electronic Supplementary Information for

Syntheses and structural aspects of six-membered palladacyclic complexes derived from *N,N',N''*-triarylguanidines with N- or S-thiocyanate ligand

Priya Saxena,^a Jisha Mary Thomas,^b Chinnappan Sivasankar^b and Natesan Thirupathi,*^a

^a*Department of Chemistry, University of Delhi, Delhi 110 007, India. Email:*
tmat@chemistry.du.ac.in, thirupathi_n@yahoo.com

^b*Department of Chemistry, School of Physical, Chemical and Applied Sciences,*
Pondicherry University, Puducherry 605014, India

Materials and methods

Cyclopalladated *N,N',N''*-triarylguanidines, **I–V**^{1–3} and 1,3,5-triaza-7-phosphaadamantane (PTA)⁴ were prepared following the literature procedures. KSCN, 3,5-Me₂C₅H₃N, 4-MeC₅H₄N, P(OCH₂)₃CEt, PMe₃ and P(NMe₂)₃ were procured from commercial vendors and used as received. Solvents were distilled following the standard procedures and stored at ambient condition prior to use. Elemental analyses were performed on an Elementar Analysensysteme GmbH VarioEL V3.00. The IR spectral data were obtained on a Shimadzu IR435 spectrometer using KBr pellet and CHCl₃ solution of the analyte in the frequency range 400–4000 cm^{−1}. ¹H NMR and ¹³C{¹H} NMR spectra were recorded on a Jeol ECX 400 MHz spectrometer operating at field strengths of 400 and 100.5 MHz,

respectively. $^{13}\text{C}\{\text{H}\}$ NMR spectra were recorded for the saturated CDCl_3 solution of the analyte with at least 5000 scans in each case. Fewer number of carbon signals than anticipated were observed in the ^{13}C NMR spectra of **4**, **11**, **13**, **14**, **16** and **17**, presumably due to overlapping peaks as well as low intensity of some of the peaks of the minor isomers of **4** and **16**. $^{31}\text{P}\{\text{H}\}$ NMR spectra were recorded on a Jeol ECX 400 NMR spectrometer operating at 161.8 MHz with 85% H_3PO_4 as the external standard. The electrospray ionization mass spectra (ESI-MS) were recorded on Waters Q-TOF Premier Micromass, Bruker Micro TOF-Q II and MicroMass Quattro II instruments. MALDI-TOF mass spectra were recorded on Applied Biosystems 4700 Proteomics Analyser 34800031 using α -cyano-4-hydroxycinnamic acid (CHCA) as matrix with MeOH or MeCN as carrier solvent. Melting points were measured on a Perkin Elmer DSC instrument (Model: Pyrex 6).

X-ray crystallography

Intensity data of suitably sized crystals of **2**, **4**, **5**· CH_2Cl_2 , **6**·PhMe, **9**·MeOH, **10**·PhMe, **11**·1/3 CH_2Cl_2 ·1/3 H_2O , **13**·PhMe, **15**·2PhMe, **16**· CHCl_3 , **17** and **18**·PhMe were collected on an Oxford Xcalibur S diffractometer (4-circle κ goniometer, Sapphire-3 CCD detector, ω scans, graphite monochromator, and a single wavelength enhanced X-ray source with MoK α radiation).⁵ Pre-experiment, data collection, data reduction, and absorption corrections were performed with the CrysAlisPro software suite.⁶ Intensity data of suitably sized crystals of **8**·2/3PhMe was collected on a Bruker AXS SMART-APEX diffractometer with a CCD area detector, graphite monochromator. The frames were collected by ω , ϕ , and 2 θ rotation at 10 s per frame with SMART.⁷ The measured intensities were reduced to F^2 and corrected for absorption with SADABS.⁸ The structures of complexes were solved

by direct methods using SIR 92,⁹ which revealed the atomic positions, and refined using the SHELX-97 program package¹⁰ and SHELXL97 (within the WinGX program package¹¹). Non-hydrogen atoms were refined anisotropically. C–H/N–H hydrogen atoms were placed in geometrically calculated positions by using a riding model. The molecular structures were created with the Olex2 program.¹² Images of Hydrogen-bond interactions in the crystal lattice of **8**·MeOH was created with the Diamond program.¹³

Computational details

The geometries of the monomeric and dimeric NCS and SCN linkage isomers were optimized using the density functional theory (B3LYP).^{14–16} N, P, O, S, C and H atoms were described using the 6-31G* basis set¹⁷ and the metal atom Pd was described using the LANL2DZ basis set.^{18–21} The solvent correction (for methanol) was carried out using the polarized continuum mode.^{22–24} The computational analysis was done using the Gaussian 09 software.²⁵

References

- 1 K. Gopi, N. Thirupathi, M. Nethaji, *Organometallics*, 2011, **30**, 572–583.
- 2 K. Gopi, P. Saxena, N. Thirupathi, M. Nethaji, *Polyhedron*, 2013, **52**, 1041–1052.
- 3 P. Elumalai, N. Thirupathi, M. Nethaji, *J. Organomet. Chem.*, 2013, **741–742**, 141–147.
- 4 D. J. Daigle, T. J. Decuir, J. B. Robertson, D. J. Daresbourg, *Inorg. Synth.*, 1998, **32**, 40–43.

- 5 ENHANCE, Oxford Xcalibur Single Crystal Diffractometer, version 1.171.34.40; Oxford Diffraction Ltd: Oxford, U.K., 2006.
- 6 CrysAlisPro, version 1.171.34.40; Oxford Diffraction Ltd: Oxford, U.K., 2006.
- 7 SMART, Bruker Molecular Analysis Research Tool, version 5.0; Bruker Analytical X-ray Systems: Madison, WI, 2000.
- 8 SAINT-NT, version 6.04; Bruker Analytical X-ray Systems: Madison, WI, 2001.
- 9 A. Altomare, G. Cascarano, C. Giacovazzo, A. Guagliardi, M. C. Burla, G. Polidori, M. Camalli, *J. Appl. Crystallogr.*, 1994, **27**, 435–436.
- 10 Sheldrick, G. M. SHELXL-97, Program for crystal structure refinement; University of Gottingen: Gottingen, Germany, 1997.
- 11 L. J. Farrugia, *J. Appl. Crystallogr.*, 1999, **32**, 837–838.
- 12 O. V. Dolomanov, L. J. Bourhis, R. J. Gildea, J. A. K. Howard, H. Puschmann, *J. Appl. Cryst.*, 2009, **42**, 339–341.
- 13 Klaus, B. DIAMOND, version 3.0 c; University of Bonn: Bonn, Germany, 2004.
- 14 A.D. Becke, *Phys. Rev. A.*, 1988, **38**, 3098–3100.
- 15 A.D. Becke, *J. Chem. Phys.*, 1993, **98**, 1372–1377.
- 16 A.D. Becke, *J. Chem. Phys.*, 1993, **98**, 5648–5652.
- 17 R. Krishnan, J. S. Binkley, R. Seeger, J. A. Pople, *J. Chem. Phys.*, 1980, **72**, 650–654.
- 18 T. H. Dunning Jr., P. J. Hay, in: H.F. Schaefer III. (Ed.), *Modern Theoretical Chemistry*, Plenum, New York, 1976.
- 19 P. J. Hay, W. R. Wadt, *J. Chem. Phys.*, 1985, **82**, 270–283.
- 20 W. R. Wadt, P. J. Hay, *J. Chem. Phys.*, 1985, **82**, 284–298.

- 21 P. J. Hay, W. R. Wadt, *J. Chem. Phys.*, 1985, **82**, 299–310.
- 22 M. T. Cancès, B. Mennucci, J. Tomasi, *J. Chem. Phys.*, 1997, **107**, 3032–3041.
- 23 M. Cossi, V. Barone, B. Mennucci, J. Tomasi, *Chem. Phys. Lett.*, 1998, **286**, 253–260.
- 24 B. Mennucci, J. Tomasi, *J. Chem. Phys.*, 1997, **106**, 5151–5158.
- 25 M. J. Frisch, G. W. Trucks, H. B. Schlegel, G. E. Scuseria, M. A. Robb, J. R. Cheeseman, J. A. Montgomery Jr., T. Vreven, K. N. Kudin, J. C. Burant, J. M. Millam, S. S. Iyengar, J. Tomasi, V. Barone, B. Mennucci, M. Cossi, G. Scalmani, N. Rega, G. A. Petersson, H. Nakatsuji, M. Hada, M. Ehara, K. Toyota, R. Fukuda, J. Hasegawa, M. Ishida, T. Nakajima, Y. Honda, O. Kitao, H. Nakai, M. Klene, X. Li, J. E. Knox, H. P. Hratchian, J. B. Cross, C. Adamo, J. Jaramillo, R. Gomperts, R. E. Stratmann, O. Yazyev, A. J. Austin, R. Cammi, C. Pomelli, J. W. Ochterski, P. Y. Ayala, K. Morokuma, G. A. Voth, P. Salvador, J. J. Dannenberg, V. G. Zakrzewski, S. Dapprich, A. D. Daniels, M. C. Strain, O. Farkas, D. K. Malick, A. D. Rabuck, K. Raghavachari, J. B. Foresman, J. V. Ortiz, Q. Cui, A. G. Baboul, S. Clifford, J. Cioslowski, B. B. Stefanov, G. Liu, A. Liashenko, P. Piskorz, I. Komaromi, R. L. Martin, D. J. Fox, T. Keith, M. A. Al- Laham, C. Y. Peng, A. Nanayakkara, M. Challacombe, P. M. W. Gill, B. Johnson, W. Chen, M. W. Wong, C. Gonzalez, J. A. Pople, Gaussian09, rev. A.02, Gaussian, Inc., Wallingford CT, 2009.

Table S1 Crystallographic data for **2**, **4**, **5·CH₂Cl₂**, **6·PhMe** and **8·2/3PhMe**

	2	4	5·CH₂Cl₂	6·PhMe	8·2/3PhMe
Formula	C ₄₆ H ₄₄ N ₈ S ₂ Pd ₂	C ₅₂ H ₅₆ N ₈ S ₂ Pd ₂	C ₃₁ H ₃₃ Cl ₂ N ₅ O ₃ SPd	C ₃₇ H ₃₉ N ₅ SPd	C _{33.67} H _{39.33} N ₇ O ₃ SPPd
Fw	985.81	1069.97	732.98	692.19	759.48
Temperature (K)	298(2)	298(2)	298(2)	298(2)	298(2)
Wavelength (λ)	0.71073	0.71073	0.71073	0.71073	0.71073
Crystal system	Orthorhombic	Monoclinic	Monoclinic	Triclinic	Triclinic
Space group	<i>Pbca</i>	<i>P2₁/c</i>	<i>P2₁/n</i>	<i>P</i> $\bar{1}$	<i>P</i> $\bar{1}$
<i>a</i> (Å)	14.0567(6)	11.6247(5)	14.0233(5)	10.1830(7)	13.502(5)
<i>b</i> (Å)	16.0971(7)	14.8522(5)	13.5565(5)	11.6661(5)	14.691(5)
<i>c</i> (Å)	18.918(1)	14.4971(6)	16.9737(8)	14.8821(5)	29.759(5)
α (deg)	90	90	90	69.549(3)	97.088(5)
β (deg)	90	91.424(4)	89.870(4)	78.925(4)	92.815(5)
γ (deg)	90	90	90	74.569(5)	112.468(5)
Volume (Å ³)	4280.6(3)	2502.2(2)	3226.8(2)	1587.1(1)	5383(3)
<i>Z</i>	4	2	4	2	6
ρ_{calcd} (g cm ⁻³)	1.530	1.420	1.509	1.448	1.406
<i>F</i> (000)	2000	1096	1496	716	2348
$\mu(\text{Mo K}\alpha)$ (mm ⁻¹)	0.981	0.845	0.845	0.685	0.663
θ range (deg)	2.90–26.37	3.08–26.37	2.91–26.37	2.94–26.37	1.39–26.37
No. of reflns collected	19693	19401	14116	12051	78394
No. of reflns used	4371	5119	6421	6488	21700
Parameters	265	291	393	353	1261
R ₁ [$I > 2\sigma(I)$] ^a	0.0438	0.0603	0.0430	0.0483	0.0578
wR ₂ (all reflns) ^b	0.1214	0.1497	0.1249	0.1335	0.2205
GooF on F^2 ^c	1.184	1.212	0.986	1.036	1.065
Largest diff peak/hole (e·Å ⁻³)	0.590/-0.445	1.058/-0.345	1.366/-1.264	1.045/-0.599	1.666/-1.098

^aR₁ = $\sum |F_o| - |F_c| / \sum |F_o|$; ^bwR₂ = { $\sum [w(F_o^2 - F_c^2)^2] / \sum [w(F_o^2)^2]$ }^{1/2}; ^cS = { $\sum [w(F_o^2 - F_c^2)^2] / (n-p)$ }^{1/2}

Table S2 Crystallographic data for **9**·MeOH, **10**·PhMe, **11**·1/3CH₂Cl₂·1/3H₂O and **13**·PhMe

	9 ·MeOH	10 ·PhMe	11 ·1/3CH ₂ Cl ₂ ·1/3H ₂ O	13 ·PhMe
Formula	C ₃₀ H ₃₈ N ₇ O ₄ SP Pd	C ₃₆ H ₄₂ N ₇ SPPd	C _{29.33} H _{28.33} N ₄ O _{6.33} SPCl _{0.67} Pd	C ₃₃ H ₃₉ N ₄ O ₃ PSPd
Fw	730.10	742.20	731.29	709.11
Temperature (K)	298(2)	298(2)	298(2)	298(2)
Wavelength (λ)	0.71073	0.71073	0.71073	0.71073
Crystal system	Monoclinic	Triclinic	Triclinic	Triclinic
Space group	C2/c	P $\bar{1}$	P $\bar{1}$	P $\bar{1}$
<i>a</i> (Å)	28.988(2)	10.9066(5)	10.7843(4)	9.2297(3)
<i>b</i> (Å)	11.4580(7)	12.8213(6)	19.7675(6)	11.1576(4)
<i>c</i> (Å)	20.238(2)	12.8595(6)	23.7030(7)	16.1202(5)
α (deg)	90	72.737(4)	101.376(3)	72.627(3)
β (deg)	104.786(8)	73.456(4)	99.035(2)	76.087(3)
γ (deg)	90	69.959(4)	95.764(3)	85.936(2)
Volume (Å ³)	6499.1(8)	1579.3(1)	4847.0(3)	1537.87(9)
Z	8	2	2	2
ρ_{calcd} (g cm ⁻³)	1.492	1.561	1.503	1.531
<i>F</i> (000)	3008	768	2228	732
μ (Mo K α) (mm ⁻¹)	0.731	0.745	0.791	0.765
θ range (deg)	2.83–26.37	3.27–26.37	3.03–26.37	2.97–26.37
No. of reflns collected	26060	22288	74879	22504
No. of reflns used	6638	6435	19822	6282
Parameters	401	372	1172	344
R ₁ [$I > 2\sigma(I)$] ^a	0.0258	0.0537	0.0577	0.0337
wR ₂ (all reflns) ^b	0.0632	0.1434	0.1544	0.0977
GooF on F^2 ^c	1.071	1.104	1.062	1.078
Largest diff peak/hole (e·Å ⁻³)	0.579/-0.401	1.130/-1.484	1.510/-1.222	0.746/-0.716

^aR₁ = $\sum |F_o| - |F_c| / \sum |F_o|$; ^bwR₂ = $\{\sum [w(F_o^2 - F_c^2)^2] / \sum [w(F_o^2)^2]\}^{1/2}$; ^cS = $\{\sum [w(F_o^2 - F_c^2)^2] / (n-p)\}^{1/2}$

Table S3 Crystallographic data for **15**·2PhMe, **16**·CHCl₃, **17** and **18**·PhMe

	15 ·2PhMe	16 ·CHCl ₃	17	18 ·PhMe
Formula	C ₄₃ H ₅₆ N ₇ O ₃ PSPd	C ₃₀ H ₄₁ N ₇ PSCl ₃ Pd	C ₂₉ H ₄₀ N ₄ O ₃ P ₂ SPd	C ₃₆ H ₄₈ N ₄ P ₂ SPd
Fw	888.38	775.48	693.05	737.18
Temperature (K)	298(2)	298(2)	298(2)	298(2)
Wavelength (λ)	0.71073	0.71073	0.71073	0.71073
Crystal system	Triclinic	Triclinic	Orthorhombic	Monoclinic
Space group	<i>P</i> ī	<i>P</i> ī	<i>Pbca</i>	<i>Cc</i>
<i>a</i> (Å)	10.9588(5)	11.6013(5)	11.3614(3)	28.592(2)
<i>b</i> (Å)	13.9322(8)	12.8550(6)	13.7572(3)	9.0068(2)
<i>c</i> (Å)	15.0765(6)	13.2434(7)	41.720(1)	19.446(1)
α (deg)	112.290(4)	110.543(4)	90	90
β (deg)	97.668(4)	98.363(4)	90	129.889(10)
γ (deg)	108.324(5)	96.758(3)	90	90
Volume (Å ³)	1936.4(2)	1799.2(2)	6520.8(3)	3842.4(4)
<i>Z</i>	2	2	8	4
ρ_{calcd} (g cm ⁻³)	1.524	1.431	1.412	1.274
<i>F</i> (000)	928	796	2864	1536
μ (Mo Kα) (mm ⁻¹)	0.627	0.872	0.766	0.649
θ range (deg)	2.88–26.37	3.22–26.37	2.93–26.37	3.08–26.37
No. of reflns collected	24363	26544	92009	25542
No. of reflns used	7924	7346	6661	7854
Parameters	419	396	361	407
R ₁ [$I > 2\sigma(I)$] ^a	0.0476	0.0473	0.0490	0.0250
wR ₂ (all reflns) ^b	0.1394	0.1348	0.1048	0.0654
GooF on F^2 ^c	1.077	1.034	1.225	1.083
Largest diff peak/hole (e·Å ⁻³)	1.050/-0.664	0.800/-0.685	0.743/-1.631	0.401/-0.514

^aR₁ = $\sum |F_o| - |F_c| / \sum |F_o|$; ^bwR₂ = $\{\sum [w(F_o^2 - F_c^2)^2] / \sum [w(F_o^2)^2]\}^{1/2}$; ^cS = $\{\sum [w(F_o^2 - F_c^2)^2] / (n-p)\}^{1/2}$

Table S4 Selected bond distances (\AA) and angles (deg) for **2** and **4**

	2	4
N(4)–Pd(1)	2.112(4)	2.105(4)
N(1)–Pd(1)	2.055(3)	2.052(4)
C(17)–Pd(1)/C(19)–Pd(1)	1.989(4)	1.999(5)
Pd(1)–S(1)	2.324(1)	2.336(1)
C(23)–S(1)/C(26)–S(1)	1.660(4)	1.655(5)
C(23)–N(4)/C(26)–N(4)	1.138(5)	1.149(6)
N(1)–C(1)	1.287(5)	1.315(6)
N(2)–C(1)	1.360(5)	1.350(7)
N(3)–C(1)	1.360(5)	1.345(7)
N(4)–Pd(1)–S(1)	91.79(9)	91.2(1)
C(17)–Pd(1)–S(1)/C(19)–Pd(1)–S(1)	87.5(1)	88.0(1)
C(17)–Pd(1)–N(1)	87.2(1)	88.8(2)
N(1)–Pd(1)–N(4)	93.5(1)	92.3(2)
N(1)–Pd(1)–S(1)	174.44(9)	173.7(1)
C(17)–Pd(1)–N(4)/C(19)–Pd(1)–N(4)	179.2(2)	176.8(2)
N(4)–C(23)–S(1)/N(4)–C(26)–S(1)	179.2(4)	178.2(5)

Table S5 Selected bond distances (\AA) and angles (deg) for **5**·CH₂Cl₂ and **6**·PhMe

	5 ·CH ₂ Cl ₂	6 ·PhMe
Pd(1)–C(17)	1.986(3)	1.995(4)
Pd(1)–N(1)	2.024(3)	2.014(3)
Pd(1)–N(5)	2.159(3)	2.154(3)
Pd(1)–N(4)	2.018(3)	2.007(4)
N(4)–C(23)	1.117(5)	1.152(6)
S(1)–C(23)	1.621(5)	1.617(5)
N(1)–C(1)	1.308(4)	1.306(5)
N(2)–C(1)	1.351(4)	1.354(5)
N(3)–C(1)	1.344(4)	1.358(4)
C(17)–Pd(1)–N(1)	88.7(1)	88.6(1)
N(1)–Pd(1)–N(5)	91.1(1)	92.8(1)
N(5)–Pd(1)–N(4)	88.7(1)	86.0(1)
N(4)–Pd(1)–C(17)	91.5(1)	92.7(2)
C(17)–Pd(1)–N(5)	177.1(1)	178.3(1)
N(1)–Pd(1)–N(4)	178.7(1)	178.0(1)
C(23)–N(4)–Pd(1)	162.8(4)	173.9(4)

Table S6 Selected bond distances (\AA) and angles (deg) for **8**·2/3PhMe, **9**·MeOH and **10**·PhMe

	8 ·2/3PhMe	9 ·MeOH	10 ·PhMe
Pd(1)–C(17)	1.990(6)	2.004(2)	1.987(4)
Pd(1)–N(1)	2.082(5)	2.099(2)	2.095(3)
Pd(1)–S(1)/Pd(1)–N(7)	2.083(6)	2.4330(6)	2.096(4)
Pd(1)–P(1)	2.237(2)	2.2387(5)	2.2481(9)
N(7)–C(29)	1.119(8)	1.146(4)	1.154(6)
S(1)–C(29)	1.657(8)	1.636(3)	1.625(4)
N(1)–C(1)	1.300(8)	1.314(2)	1.311(5)
N(2)–C(1)	1.360(8)	1.370(2)	1.363(5)
N(3)–C(1)	1.353(8)	1.343(2)	1.365(5)
C(17)–Pd(1)–N(1)	87.3(2)	85.73(7)	85.9(1)
N(1)–Pd(1)–S(1)/N(1)–Pd(1)–N(7)	93.3(2)	88.39(5)	94.3(1)
S(1)–Pd(1)–P(1)/N(7)–Pd(1)–P(1)	87.5(8)	94.93(2)	86.08(9)
C(17)–Pd(1)–P(1)	92.4(2)	91.20(5)	93.5(1)
C(17)–Pd(1)–S(1)/C(17)–Pd(1)–N(7)	175.9(3)	173.71(5)	179.1(1)
N(1)–Pd(1)–P(1)	173.0(2)	171.35(5)	179.2(2)
C(29)–S(1)–Pd(1)/C(29)–N(7)–Pd(1)	160.5(6)	108.10(9)	163.3(3)

Table S7 Selected bond distances (\AA) and angles (deg) for **11**·1/3CH₂Cl₂·1/3H₂O, **13**·PhMe, **15**·2PhMe and **16**·CHCl₃

	11 ·1/3CH ₂ Cl ₂ ·1/3H ₂ O	13 ·PhMe	15 ·2PhMe	16 ·CHCl ₃
Pd(1)–C(17)	2.011(5)	1.991(3)	2.009(4)	2.014(3)
Pd(1)–N(1)	2.077(4)	2.086(2)	2.113(2)	2.101(3)
Pd(1)–N(4)/Pd(1)–N(7)	2.077(4)	2.093(3)	2.076(4)	2.087(3)
Pd(1)–P(1)	2.208(1)	2.2501(7)	2.2597(8)	2.2601(9)
N(4)–C(29)/N(4)–C(26)/N(7)–C(29)	1.144(6)	1.156(4)	1.146(5)	1.146(5)
S(1)–C(29)/S(1)–C(26)	1.633(5)	1.623(3)	1.636(4)	1.636(4)
N(1)–C(1)	1.310(6)	1.300(3)	1.299(4)	1.297(4)
N(2)–C(1)	1.356(7)	1.365(3)	1.365(4)	1.357(4)
N(3)–C(1)	1.347(6)	1.357(3)	1.360(5)	1.357(4)
C(17)–Pd(1)–N(1)	88.0(2)	86.3(1)	86.5(1)	87.2(1)
N(1)–Pd(1)–N(4)/ N(1)–Pd(1)–N(7)	89.3(2)	92.25(9)	89.6(1)	89.6(1)
N(4)–Pd(1)–P(1)/ N(7)–Pd(1)–P(1)	90.6(1)	87.19(8)	90.66(8)	90.52(9)
C(17)–Pd(1)–P(1)	92.0(1)	95.09(8)	93.37(9)	92.8(1)
C(17)–Pd(1)–N(4)/ C(17)–Pd(1)–N(7)	176.4(2)	172.8(1)	176.0(1)	174.5(1)
N(1)–Pd(1)–P(1)	179.9(1)	172.96(7)	175.44(7)	176.95(8)
C(29)–N(4)–Pd(1)/C(26)–N(4)–Pd(1)/ C(29)–N(7)–Pd(1)	172.4(4)	158.6(3)	176.6(3)	170.2(4)

Table S8 Selected bond distances (\AA) and angles (deg) for **17** and **18·PhMe**

	17	18·PhMe
Pd(1)–P(1)	2.327(1)	2.3163(7)
Pd(1)–P(2)	2.308(1)	2.3260(7)
Pd(1)–C(3)	2.014(3)	2.028(2)
Pd(1)–N(4)	2.080(4)	2.085(3)
N(4)–C(26)	1.149(5)	1.153(4)
S(1)–C(26)	1.634(4)	1.629(3)
N(1)–C(1)	1.390(4)	1.380(3)
N(2)–C(1)	1.278(4)	1.286(3)
N(3)–C(1)	1.373(4)	1.388(3)
P(1)–Pd(1)–C(3)	88.2(1)	89.35(7)
C(3)–Pd(1)–P(2)	88.2(1)	87.54(8)
P(2)–Pd(1)–N(4)	93.2(1)	93.87(8)
N(4)–Pd(1)–P(1)	90.3(1)	89.23(8)
P(1)–Pd(1)–P(2)	175.51(4)	176.33(3)
C(3)–Pd(1)–N(4)	177.7(1)	178.5(1)
C(26)–N(4)–Pd(1)	168.4(3)	177.1(3)

Table S9 Selected bond distances (\AA) and angles (deg) of optimized NCS coordinated complex **8**

Pd1-P1	2.3134	P1-Pd1-C1	97.03204
Pd1-C1	2.01547	C1-Pd1-N1	86.65862
Pd1-N1	2.12233	N1-Pd1-N2	92.80097
Pd1-N2	2.12492	N2-Pd1-P1	83.29273
N2-C2	1.18391	Pd1-N2-C2	164.09074
C2-S1	1.63508	N2-C2-S1	179.62968

Table S10 Selected bond distances (\AA) and angles (deg) of optimized SCN coordinated complex **9**

Pd1-P1	2.31475	P1-Pd1-C1	92.30552
Pd1-C1	2.03535	C1-Pd1-N1	85.1815
Pd1-N1	2.14768	N1-Pd1-S1	90.22251
Pd1-S1	2.51584	S1-Pd1-P1	92.28301
N2-C2	1.17458	Pd1-S1-C2	103.7699
C2-S1	1.68358	S1-C2-N2	177.7553

Table S11 Selected bond distances (\AA) and angles (deg) of optimized NCS coordinated complex **8'**

Pd1-P1	2.321	P1-Pd1-C1	95.71
Pd1-C1	2.030	C1-Pd1-N1	88.95
Pd1-N1	2.030	N1-Pd1-N2	86.29
Pd1-N2	2.149	N2-Pd1-P1	89.19
N2-C2	1.183	Pd1-N2-C2	144.82
C2-S1	1.642	N2-C2-S1	178.99

Table S12 Selected bond distances (\AA) and angles (deg) of optimized SCN coordinated complex **9'**

Pd1-P1	2.309	P1-Pd1-C1	97.02
Pd1-C1	2.043	C1-Pd1-N1	88.71
Pd1-N1	2.045	N1-Pd1-S1	89.12
Pd1-S1	2.540	S1-Pd1-P1	85.44
N2-C2	1.172	Pd1-S1-C2	99.47
C2-S1	1.682	S1-C2-N2	179.02

Table S13 Selected bond lengths (\AA) and bond angles (deg) of the methanol mediated NCS bound modified Pd dimeric complex **8''**

Pd1-P1	2.321	P1-Pd1-C1	95.71
Pd1-C1	2.030	C1-Pd1-N1	88.95
Pd1-N1	2.030	N1-Pd1-N2	86.29
Pd1-N2	2.149	N2-Pd1-P1	89.19
N2-C2	1.183	N2-C2-S1	178.99
C2-S1	1.642	Pd1-N2-C2	144.82
S1-H2'	2.403	P1'-Pd1'-C1'	95.32
O1'-H1'	2.603	C1'-Pd1'-N1'	88.94
Pd1'-P1'	2.326	N1'-Pd1'-N2'	88.10
Pd1'-C1'	2.030	N2'-Pd1'-P1'	87.79
Pd1'-N1'	2.050	N2'-C2'-S1'	179.08
Pd1'-N2'	2.118	Pd1'-N2'-C2'	163.32
N2'-C2'	1.183		
C2'-S1'	1.637		
S1'-H2	2.392		
O1-H1	2.485		

Table S14 Selected bond lengths (\AA) and bond angles (deg) of the methanol mediated SCN bound modified Pd dimeric complex **9''**

Pd1-P1	2.296	P1-Pd1-C1	94.40
Pd1-C1	2.037	C1-Pd1-N1	85.98
Pd1-N1	2.076	N1-Pd1-S1	88.79
Pd1-S1	2.557	S1-Pd1-P1	89.97
S1-C2	1.681	N2-C2-S1	178.00
C2-N2	1.174	Pd1-S1-C2	92.81
N2-H2'	1.871	P1'-Pd1'-C1'	97.02
O1'-H1'	2.482	C1'-Pd1'-N1'	88.71
Pd1'-P1'	2.309	N1'-Pd1'-S1'	89.12
Pd1'-C1'	2.043	S1'-Pd1'-P1'	85.44
Pd1'-N1'	2.045	N2'-C2'-S1'	179.02
Pd1'-S1'	2.540	Pd1'-S1'-C2'	99.47
S1'-C2'	1.682		
C2'-N2'	1.172		
N2'-H2	1.914		
O1-H1	2.693		

Cartesian coordinates of the optimized NCS coordinated complex **8**

Pd	1.00294100	0.07230800	0.56489500
P	3.17079300	0.47178800	-0.13700000
O	-1.75858000	-2.76419200	-0.38929100
O	-4.72215800	-1.53545900	-1.84498700
O	-2.43807100	4.01779000	-0.10461900
N	-1.03544800	-0.41047600	0.90571200
N	-3.17387300	-0.34311600	-0.07267300
H	-3.10182700	-1.32324900	-0.33988800
N	-1.73453100	1.50447800	-0.20456800
H	-2.48161400	1.93841600	-0.73018100
N	5.40575300	1.96994800	-0.84729500
N	4.89403700	0.02150900	-2.27631300
N	5.83346600	-0.31821100	-0.01650500
N	1.53883800	-1.95903400	0.24592600

S	2.34450900	-4.40316000	-0.90460900
C	-1.96016800	0.23348600	0.23482100
C	-1.29371000	-1.61737100	1.61600600
C	-1.13413000	-1.61522300	3.00460600
H	-0.88616300	-0.67403300	3.48647800
C	-1.27036900	-2.78666100	3.74938700
H	-1.14401700	-2.76168400	4.82774100
C	-1.55238600	-3.98569100	3.09711100
H	-1.64688400	-4.90939100	3.66120800
C	-1.71133100	-4.01288500	1.71030700
H	-1.92080100	-4.95209300	1.21145000
C	-1.58641700	-2.83552300	0.96845000
C	-1.71963500	-3.97215100	-1.14756000
H	-1.75672900	-3.66244800	-2.19321500
H	-2.58449100	-4.61146000	-0.92665800
H	-0.78698400	-4.51493500	-0.96157400
C	-4.37087300	0.30423900	-0.43210600
C	-4.80312100	1.50568300	0.13752400
H	-4.18495900	1.99544600	0.88169100
C	-6.02307100	2.07462300	-0.24015200
H	-6.33771000	3.01038700	0.21232300
C	-6.83580700	1.43161500	-1.16830300
H	-7.78896000	1.86294300	-1.45973100
C	-6.43321900	0.21319300	-1.72726200
H	-7.07440700	-0.28645000	-2.44439400
C	-5.20955300	-0.34985000	-1.36778600
C	-5.52737300	-2.28560600	-2.74148600
H	-4.95791400	-3.18733700	-2.97213300
H	-5.71821100	-1.72980300	-3.66846400
H	-6.48419700	-2.56475100	-2.28186200

C	-0.79137300	2.40295500	0.35288300
C	0.46684800	1.99852400	0.81867700
C	1.26390700	2.97096800	1.45079500
H	2.21814100	2.68512600	1.88065000
C	0.86057300	4.30141500	1.53956600
H	1.50406400	5.03486700	2.01904000
C	-0.36385500	4.71138400	1.00318800
H	-0.66548300	5.75074500	1.06216700
C	-1.19521000	3.75667300	0.42349400
C	-2.88957500	5.36244700	-0.13455000
H	-3.87087300	5.33816100	-0.61206000
H	-2.21345800	5.99862800	-0.72003500
H	-2.98687600	5.77496100	0.87799000
C	4.06571500	2.12664700	-0.26239500
H	3.47180700	2.81685700	-0.87190800
H	4.16053900	2.57585800	0.73177100
C	3.48099700	-0.10443900	-1.90118000
H	3.16345400	-1.14840500	-1.98361500
H	2.86283700	0.48747900	-2.58618700
C	4.55793900	-0.49610200	0.68833600
H	4.66264100	-0.16703600	1.72884700
H	4.27707300	-1.55337700	0.70095500
C	5.34801400	1.41760200	-2.21089400
H	4.68650500	2.04089600	-2.82245500
H	6.35731500	1.46682800	-2.63506400
C	5.75652000	-0.79878300	-1.40772700
H	6.76934000	-0.78270300	-1.82568600
H	5.39295200	-1.83076900	-1.41271800
C	6.25649700	1.08886600	-0.02805300
H	7.27328700	1.13444400	-0.43421100

H	6.27916200	1.46701000	0.99995200
C	1.87365300	-2.98542300	-0.23993700

Cartesian coordinates of the optimized SCN coordinated complex 9

Pd	-1.00519900	-0.34179700	0.33645300
P	-3.15531100	0.15521600	-0.36217800
S	-1.22625200	-2.74827400	-0.36316800
O	2.20803200	-2.78477400	-0.64773800
O	4.90267000	-0.95460000	-2.06048300
O	2.00011500	4.00351500	0.37528400
N	1.08712800	-0.63695900	0.72061700
N	3.21163700	-0.18361500	-0.18212100
H	3.27650900	-1.13863500	-0.52834800
N	1.54601700	1.46944400	-0.14911300
H	2.23568500	2.04913600	-0.60879600
N	-5.00884400	1.99532900	-1.33701000
N	-5.87983800	0.23709400	0.16861600
N	-5.23393800	-0.32258200	-2.14841100
N	-3.84840200	-3.46938300	0.51454000
C	1.93013700	0.19441800	0.15248200
C	1.52496600	-1.81636600	1.38922900
C	1.34267800	-1.90001700	2.77257000
H	0.91895900	-1.03973000	3.28192800
C	1.67628700	-3.05661900	3.47722400

H	1.52618400	-3.09837300	4.55193200
C	2.18847300	-4.15631600	2.79138200
H	2.44368600	-5.06753400	3.32506200
C	2.37298700	-4.09893700	1.40844900
H	2.76504600	-4.96214600	0.88244500
C	2.04240100	-2.93654600	0.70822600
C	2.42840300	-3.94633700	-1.43877800
H	3.40583000	-4.39930200	-1.22737400
H	2.40256400	-3.60765800	-2.47581300
H	1.63354500	-4.68168600	-1.27344400
C	4.32191600	0.64297900	-0.44143700
C	4.59976800	1.80967900	0.27668800
H	3.92311100	2.12441100	1.06309000
C	5.73912600	2.56723400	-0.00962000
H	5.93452300	3.47242000	0.55762500
C	6.62672700	2.14724200	-0.99526000
H	7.51908200	2.72534500	-1.21661500
C	6.38072900	0.96569800	-1.70367100
H	7.08116600	0.64142100	-2.46485500
C	5.23623900	0.21576500	-1.43493000
C	5.78954000	-1.47004900	-3.04156000
H	5.89935100	-0.77628900	-3.88478800
H	5.33841500	-2.39868900	-3.39500300
H	6.77840800	-1.68332500	-2.61564500

C	0.53071900	2.17492800	0.54865900
C	-0.67022100	1.57319200	0.93914900
C	-1.54255800	2.32703400	1.74528600
H	-2.45858900	1.87664600	2.11717900
C	-1.26630600	3.65348300	2.07235900
H	-1.96366500	4.22071100	2.68393400
C	-0.10228500	4.27384600	1.60762300
H	0.09783500	5.31067400	1.85184800
C	0.80343100	3.52748600	0.85720700
C	2.31236900	5.37271700	0.57969600
H	1.56063900	6.02719200	0.12026300
H	3.27873800	5.53456500	0.09852700
H	2.39296700	5.61028800	1.64827500
C	-3.60058600	1.89754100	-0.92929000
H	-3.39719300	2.60987300	-0.12483400
H	-2.95595900	2.17017700	-1.77336500
C	-4.60583700	-0.11447700	0.80897000
H	-4.61442600	-1.16801000	1.10438100
H	-4.46696100	0.49500900	1.70968800
C	-3.85965900	-0.74970400	-1.86123100
H	-3.21839000	-0.54941400	-2.72688100
H	-3.84062000	-1.82359600	-1.66826700
C	-5.92055700	1.64987400	-0.23206200
H	-5.68651200	2.27716900	0.63527700

H	-6.94154000	1.88052800	-0.55736900
C	-6.13486400	-0.60243600	-1.01576100
H	-7.16236200	-0.41497200	-1.34796900
H	-6.04013400	-1.65477900	-0.73366500
C	-5.30706300	1.10669800	-2.47218000
H	-6.32514500	1.32737000	-2.81337800
H	-4.61381900	1.32699900	-3.29163700
C	-2.76045100	-3.18324400	0.17671200

Cartesian coordinates of the optimized NCS coordinated modified complex 8'

Pd	0.90840000	-0.63599700	0.00792500
P	1.26148000	-2.88129700	0.47711200
O	-4.02763000	1.42066700	0.21637000
N	0.75113700	1.37590400	-0.21449900
N	-0.07610800	3.50980200	0.25933600
H	0.89407000	3.80209300	0.39030500
N	-1.48051700	1.66238900	0.36465100
H	-2.23264200	2.33826100	0.42354000
N	3.03483200	-0.32544500	0.04337500
S	5.08487000	1.58087300	-0.33576500
C	-0.23501600	2.15444100	0.13915100
C	-1.93489700	0.35434100	0.08330600
C	-1.11420900	-0.76936200	-0.10779700
C	-1.75798400	-1.97830000	-0.44193300

H	-1.17193300	-2.86650300	-0.65779600
C	-3.14234300	-2.08236700	-0.53124500
H	-3.60022100	-3.03590500	-0.78087600
C	-3.95238200	-0.96847400	-0.29747200
H	-5.03130900	-1.05006600	-0.35432000
C	-3.34820500	0.24732600	-0.00101800
C	-5.42875000	1.46246900	-0.07080100
H	-5.71666600	2.50924900	0.02770400
H	-5.99533600	0.86549100	0.65089300
H	-5.62211000	1.11622800	-1.09302200
C	3.89971200	0.46512800	-0.12212900
H	1.64673300	1.84950000	-0.26651700
H	-0.74030000	4.00272300	0.84527600
H	1.27099100	-3.83756200	-0.56479000
H	2.51280500	-3.17620100	1.05374400
H	0.41947700	-3.57105500	1.37551700

Cartesian coordinates of the optimized SCN coordinated modified complex 9'

Pd	1.07459500	-0.22249400	-0.31505600
P	1.99315400	-2.24290600	0.32142800
O	-4.11337400	0.74689700	0.51869200
N	0.44786800	1.68505500	-0.70443700
N	-0.86512600	3.61270800	-0.38318900
H	-0.04285100	4.19984900	-0.34507300

N	-1.69448300	1.53393900	0.18281300
H	-2.54493500	2.04633100	0.38588600
C	-0.65391000	2.25791000	-0.30419700
C	-1.89276500	0.14181600	0.04440600
C	-0.88364200	-0.79617700	-0.21553100
C	-1.28615100	-2.12979100	-0.42647200
H	-0.55246900	-2.88595200	-0.68577000
C	-2.61696500	-2.52235200	-0.32504200
H	-2.89110100	-3.56048700	-0.49321700
C	-3.60764100	-1.59352900	0.00678900
H	-4.64132900	-1.90443800	0.10169300
C	-3.24438400	-0.26535100	0.19303500
C	-5.48803200	0.43522900	0.72264500
H	-5.94916400	1.35718900	1.07836100
H	-5.60367600	-0.34564300	1.48460400
H	-5.95907400	0.10237000	-0.21090300
C	3.88164700	0.78231100	1.02534400
H	1.17059600	2.31286500	-1.03941000
H	-1.67055600	3.97541500	0.12249000
H	2.98999100	-2.14836800	1.31261900
H	2.70457500	-2.98808600	-0.64331500
H	1.21388600	-3.28415400	0.87367200
N	4.17799800	0.92929900	2.14937900
S	3.47760600	0.55242900	-0.59111300

Cartesian coordinates of the optimized methanol mediated NCS coordinated modified dimeric complex 8"

Pd	4.07910500	-1.52388700	-0.16920100
P	5.43470000	-3.21021800	0.67033800
O	-1.14897500	-2.38588100	-0.91876800
N	2.96017500	0.08274100	-0.70649900
N	1.08523700	1.47754000	-0.66750200
H	1.72380800	2.24625100	-0.45503200
N	0.83360600	-0.82373500	-0.47461000
H	-0.15363400	-0.64676300	-0.61604000
N	5.69537000	-0.13275800	0.09887000
S	6.50985800	2.54468300	-0.28631700
C	1.66834800	0.23948700	-0.60500800
C	1.17550400	-2.18745800	-0.61592700
C	2.47442200	-2.71466200	-0.52860700
C	2.61692600	-4.09784200	-0.76126400
H	3.60343400	-4.55144000	-0.76400000
C	1.52707400	-4.92425800	-1.01526600
H	1.67864000	-5.98800600	-1.17857700
C	0.23399900	-4.39727700	-1.05790700
H	-0.61757200	-5.04104100	-1.24329000
C	0.06195500	-3.03141600	-0.86840600
C	-2.28994700	-3.10903500	-1.39055500
H	-3.08548500	-2.37003200	-1.48721000

H	-2.59628300	-3.87310200	-0.66902600
H	-2.08078800	-3.56288500	-2.36650500
C	6.04704000	0.98492500	-0.06704600
Pd	-3.45386600	0.88627400	0.28864300
P	-2.83636200	-0.68148700	1.89165100
O	-0.31009900	5.12125900	-0.57435300
N	-3.99492500	2.10859200	-1.26623600
N	-3.52482500	3.45107100	-3.15183600
H	-4.41849700	3.17994100	-3.53906500
N	-2.10798100	3.44796000	-1.32693900
H	-1.53544200	4.07945300	-1.87194300
N	-4.91116600	-0.49588000	-0.38331500
S	-6.52169100	-2.79133000	-0.68137200
C	-3.25072700	2.98013900	-1.88205900
C	-1.68570700	3.30349700	0.01319500
C	-2.13886800	2.30786400	0.89919000
C	-1.65357400	2.37629800	2.22300900
H	-2.01063800	1.67328400	2.96804000
C	-0.72674500	3.33210400	2.62687700
H	-0.37628300	3.34728000	3.65532900
C	-0.22934900	4.26869200	1.71607200
H	0.50963600	4.99811800	2.02516200
C	-0.71144100	4.25705000	0.41230600
C	0.87482000	5.89056000	-0.35635600

H	1.06481300	6.41159200	-1.29629000
H	1.72372800	5.24100100	-0.11240900
H	0.72311800	6.63031600	0.43902800
C	-5.59449600	-1.45432100	-0.50179600
H	-4.83716600	1.81287300	-1.74693900
H	3.47822000	0.95492700	-0.71009600
H	-3.28304800	4.41497000	-3.34524800
H	0.16524300	1.57637800	-0.25363000
C	-4.54893900	-4.81261300	2.33898600
H	-4.90437700	-5.76852500	1.92807700
H	-3.70484200	-5.01826300	3.00393300
H	-5.36050800	-4.36712700	2.93270600
C	3.38495300	2.92058000	1.69769800
H	2.36238900	2.85134400	2.07697700
H	3.91121300	3.72126200	2.23303400
H	3.90246200	1.97218800	1.88378100
O	-4.08138900	-3.93819100	1.32246500
H	-4.83453000	-3.73097700	0.72934700
O	3.29177300	3.20397700	0.29875500
H	4.21211300	3.20747000	-0.04971700
H	-3.26573000	-2.01243700	1.68369300
H	-3.30863800	-0.45994100	3.20497900
H	-1.46840000	-0.86125000	2.18000700
H	6.12970800	-4.07399300	-0.20770000

H	6.52470000	-2.76405800	1.44372600
H	4.91149900	-4.18858200	1.54265200

Cartesian coordinates of the optimized methanol mediated SCN coordinated modified dimeric complex 9"

Pd	-4.80751800	0.69491200	-0.48818200
P	-6.32916300	1.85069600	0.78414500
O	0.18523000	1.15590400	1.10940300
N	-3.40732100	-0.49197100	-1.45826700
N	-1.77485200	-2.17576800	-1.00866400
H	-2.34194800	-2.74130800	-1.63662800
N	-1.81210600	-0.18807500	0.19319400
H	-0.90814200	-0.49551200	0.53377400
C	-2.39141400	-0.93985100	-0.77012700
C	-2.02815900	1.20821600	0.35553000
C	-3.22913700	1.86072100	0.05823700
C	-3.25729600	3.26075300	0.14251500
H	-4.15895800	3.80686100	-0.11767200
C	-2.13189200	3.97460400	0.55658500
H	-2.17561200	5.05902900	0.61865700
C	-0.94761300	3.32215900	0.91112700
H	-0.07942400	3.89223900	1.23166100
C	-0.90074400	1.93229100	0.81234500
C	1.40451600	1.80053400	1.48826000
H	2.10266000	0.99185600	1.71004200

H	1.26487700	2.43503200	2.36884800
H	1.79589900	2.40776400	0.66772000
C	-5.65292000	-2.31405400	-0.35472100
Pd	4.44429200	-0.09391100	-0.68438800
P	6.09115900	0.52117800	0.81241500
O	1.05116300	-4.03813400	0.53202100
N	2.89398200	-0.37338100	-1.98883500
N	0.69382700	-0.93981600	-2.60646800
H	0.58340000	-0.07193100	-3.11332600
N	1.65866500	-1.89337600	-0.73850600
H	0.80014200	-2.43053200	-0.70036400
C	1.78660400	-1.03076800	-1.77948800
C	2.70477200	-2.44405300	0.03537600
C	3.98535000	-1.89023300	0.17369500
C	4.93210600	-2.63706500	0.90234400
H	5.95325500	-2.28174100	0.99346800
C	4.60629100	-3.84385100	1.51305800
H	5.36220200	-4.39273800	2.06846700
C	3.30676800	-4.35259800	1.43133200
H	3.05066800	-5.28435100	1.92167000
C	2.35878600	-3.65192500	0.69574700
C	0.59581000	-5.22038700	1.18267500
H	-0.47947500	-5.25841100	1.00518500
H	0.78367600	-5.17025700	2.26244800

H	1.08749200	-6.11080600	0.77086100
C	4.26108400	3.16369100	-0.88516900
H	2.88551200	0.25569700	-2.78437100
H	-3.82038000	-1.17614800	-2.08366200
H	-0.17348800	-1.34108700	-2.25613800
H	-1.69326500	-2.72157700	-0.13079700
C	2.04318800	6.38840700	1.92950200
H	1.32521000	6.71969400	2.68715700
H	3.04906200	6.69437600	2.25832500
H	1.81700300	6.91836200	0.99039300
C	-2.52272500	-3.29940400	2.56234900
H	-1.49968800	-3.28207600	2.94889600
H	-3.12670400	-3.95476300	3.20435900
H	-2.93382300	-2.28195500	2.61246600
O	1.91927100	4.98580400	1.80770100
H	2.56153200	4.68507300	1.13110900
O	-2.46701400	-3.78770400	1.22583300
H	-3.38392800	-3.75642300	0.86019700
H	5.98350600	1.84079000	1.29420100
H	7.42777600	0.55469400	0.36022700
H	6.28915600	-0.15772400	2.03565600
H	-6.10231900	3.18243600	1.19454900
H	-7.64812600	1.97943700	0.29865800
H	-6.61966100	1.28047400	2.04101400

N	-4.97583600	-3.17401200	0.06889100
N	3.74581500	3.94159900	-0.17647900
S	-6.58240900	-1.07290000	-1.00296800
S	5.02589000	2.06008200	-1.89815700

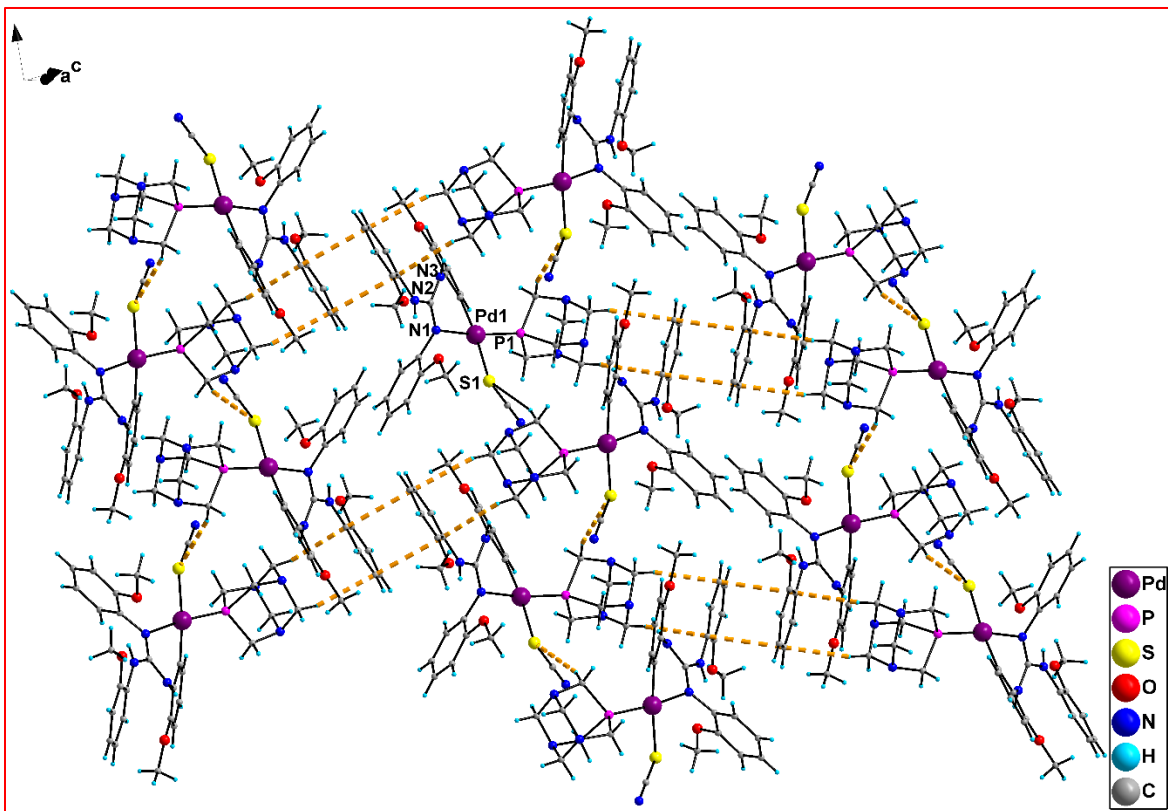


Fig. S1 C–H \cdots π , $\pi\cdots\pi$ and C–H \cdots S interactions present in the crystal lattice of **9**·MeOH. The sulfur atom of thiocyanate is involved in intermolecular C–H \cdots S hydrogen bond with PTA in the neighboring molecule related by 2-fold screw axis. The 2-anisyl ring of the N(H)Ar unit of the reference molecule forms a π -stacking interaction ($\pi\cdots\pi = 3.587 \text{ \AA}$) with the 2-anisyl ring of the N(H)Ar unit of the inversion related adjacent molecule. Further, the same 2-anisyl ring of the reference molecule also forms C–H \cdots π interactions with the C-H protons of PTA from a two-fold screw axis related adjacent molecule.

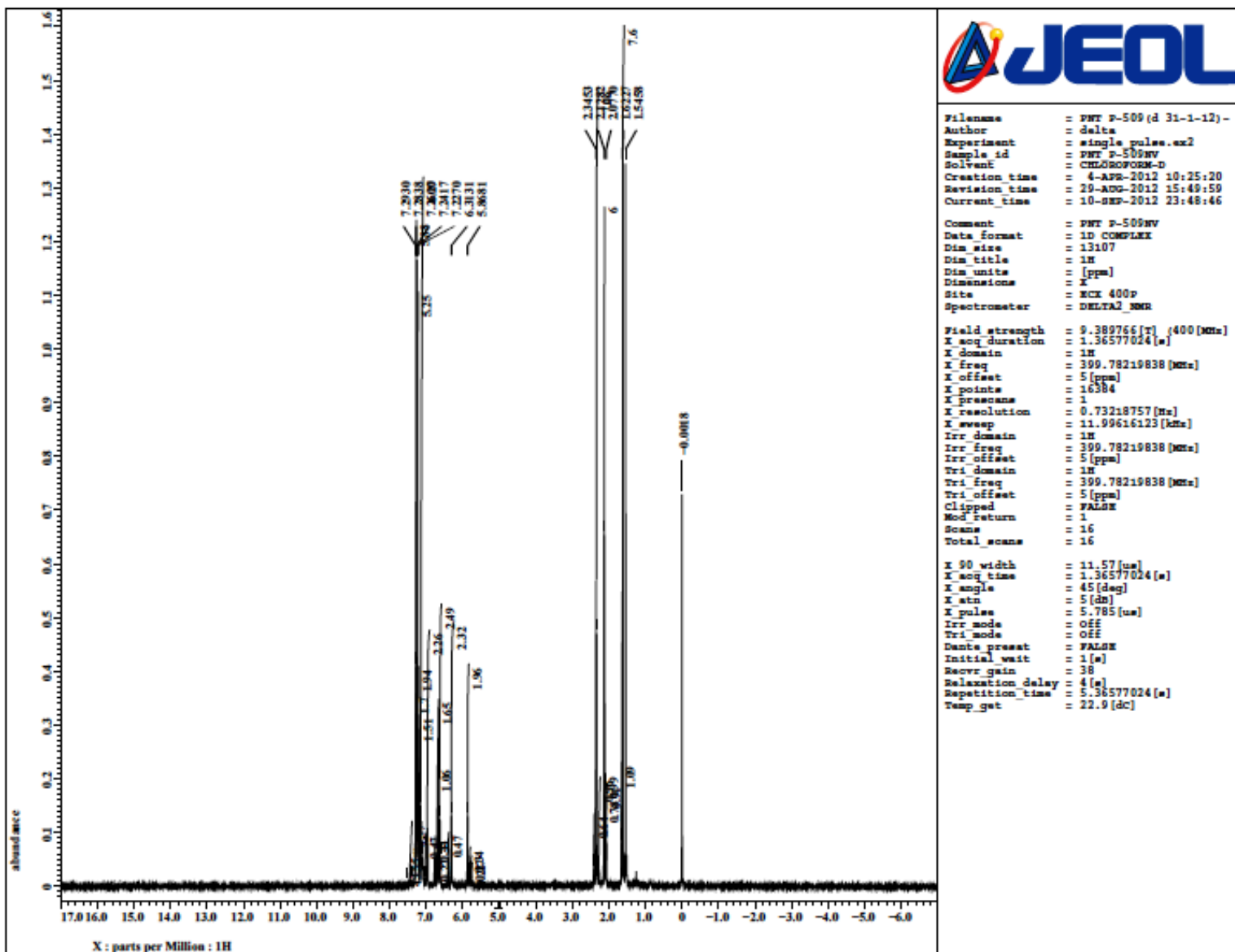


Fig. S2 ^1H NMR spectrum of **2** (CDCl_3 , 400.0 MHz).

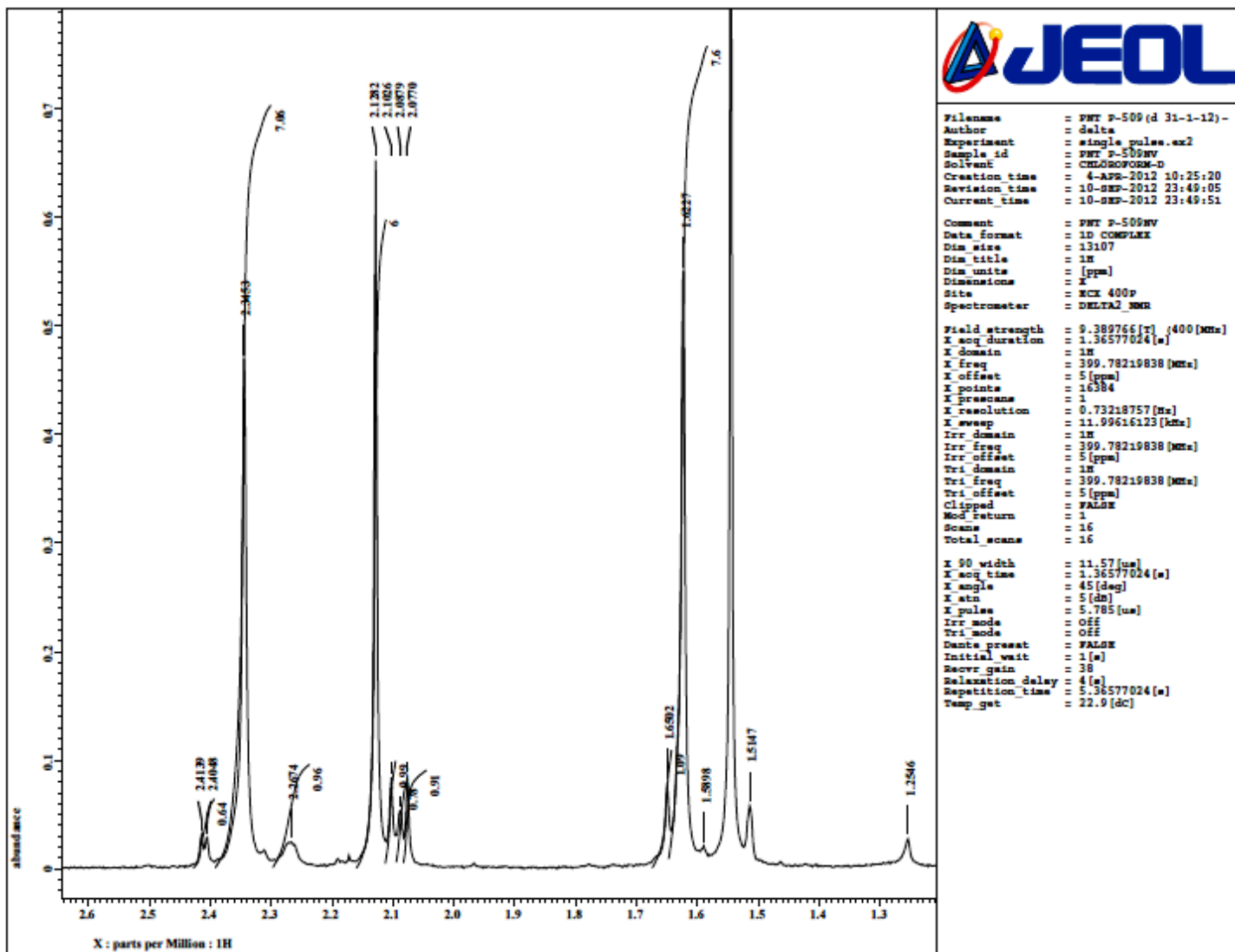


Fig. S3 Expansion of ^1H NMR spectrum of **2** (CDCl_3 , 400.0 MHz).

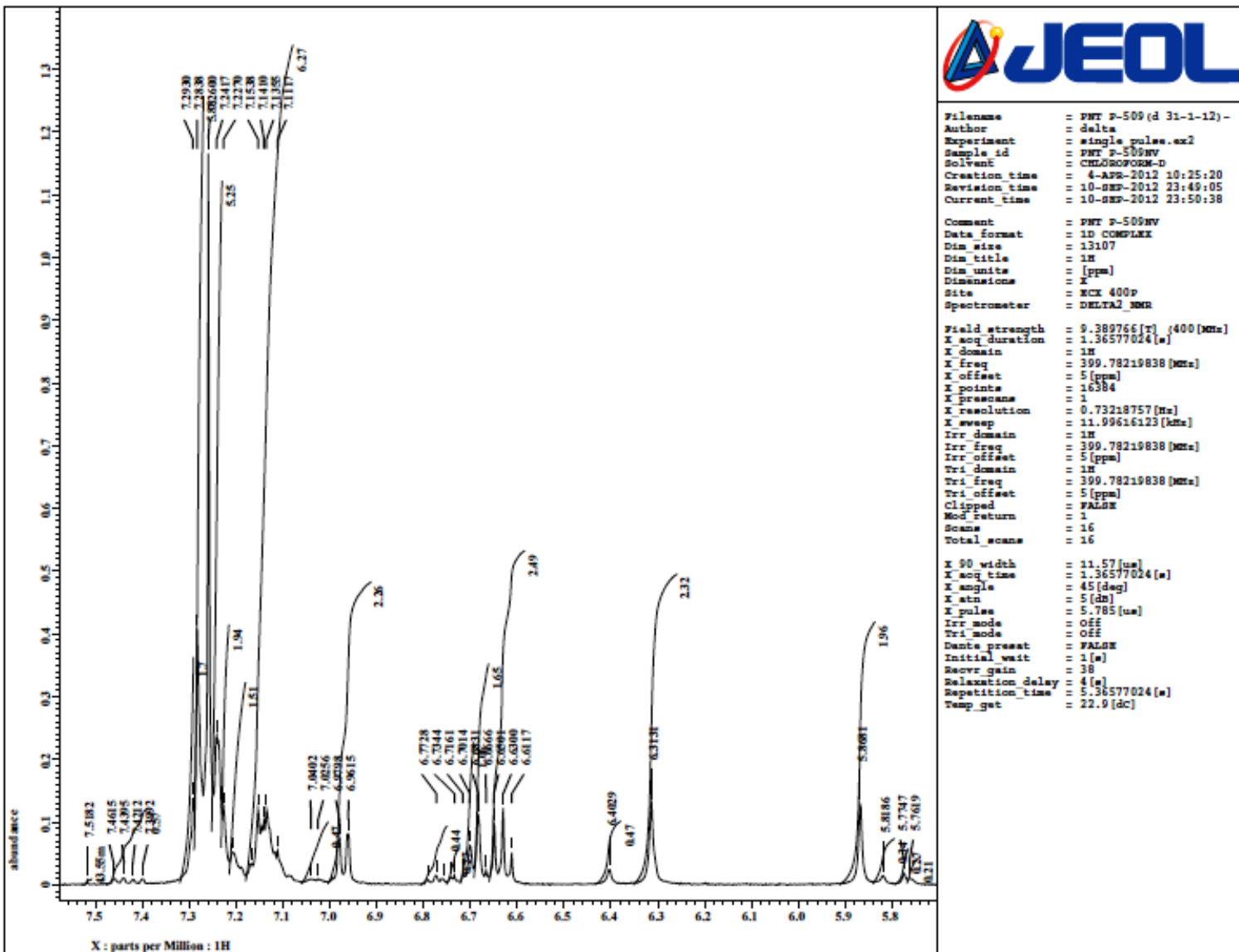


Fig. S4 Expansion of ¹H NMR spectrum of **2** (CDCl₃, 400.0 MHz).

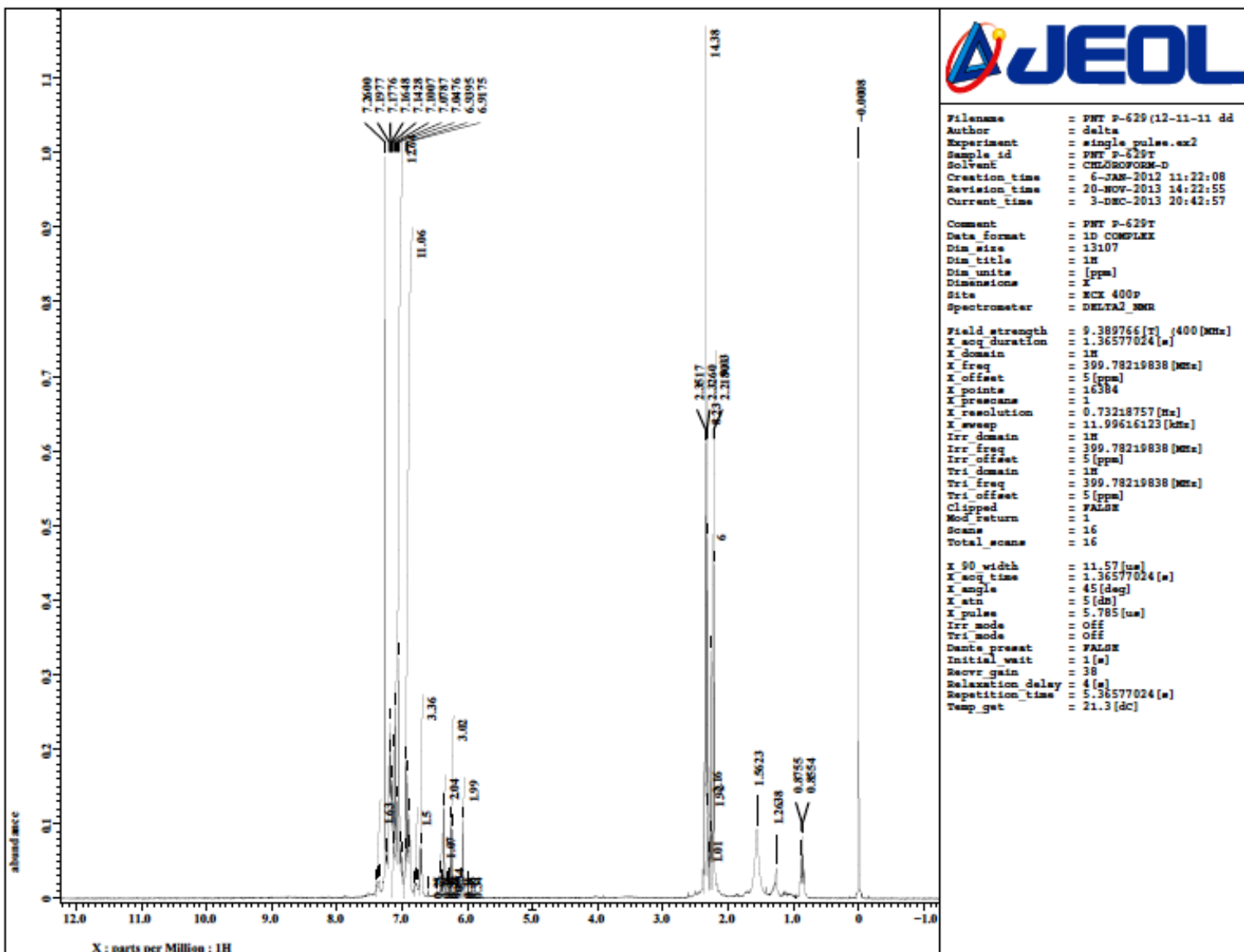


Fig. S5 ^1H NMR spectrum of **3** (CDCl_3 , 400.0 MHz).

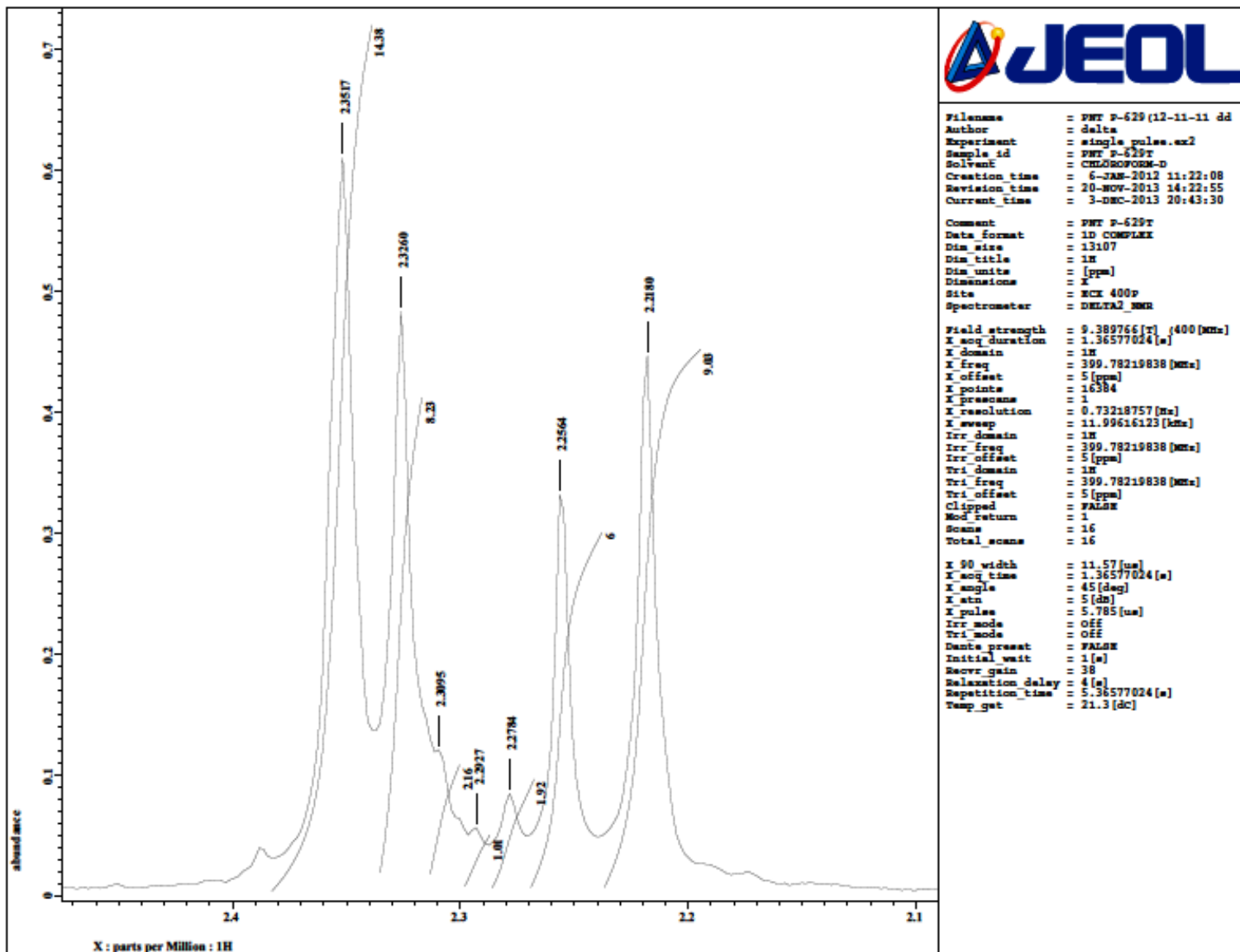


Fig. S6 Expansion of ¹H NMR spectrum of **3** (CDCl₃, 400.0 MHz).

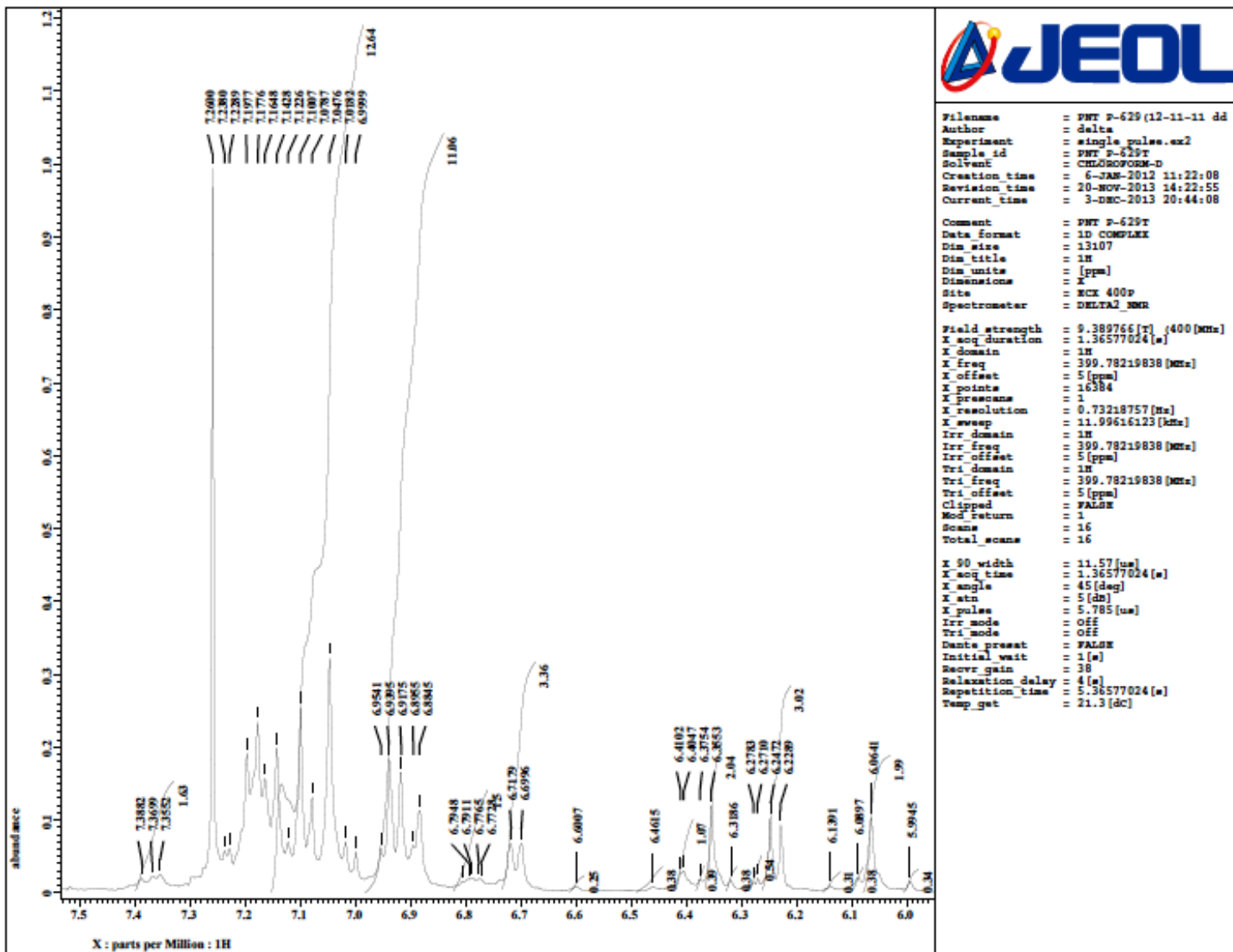


Fig. S7 Expansion of ^1H NMR spectrum of **3** (CDCl_3 , 400.0 MHz).

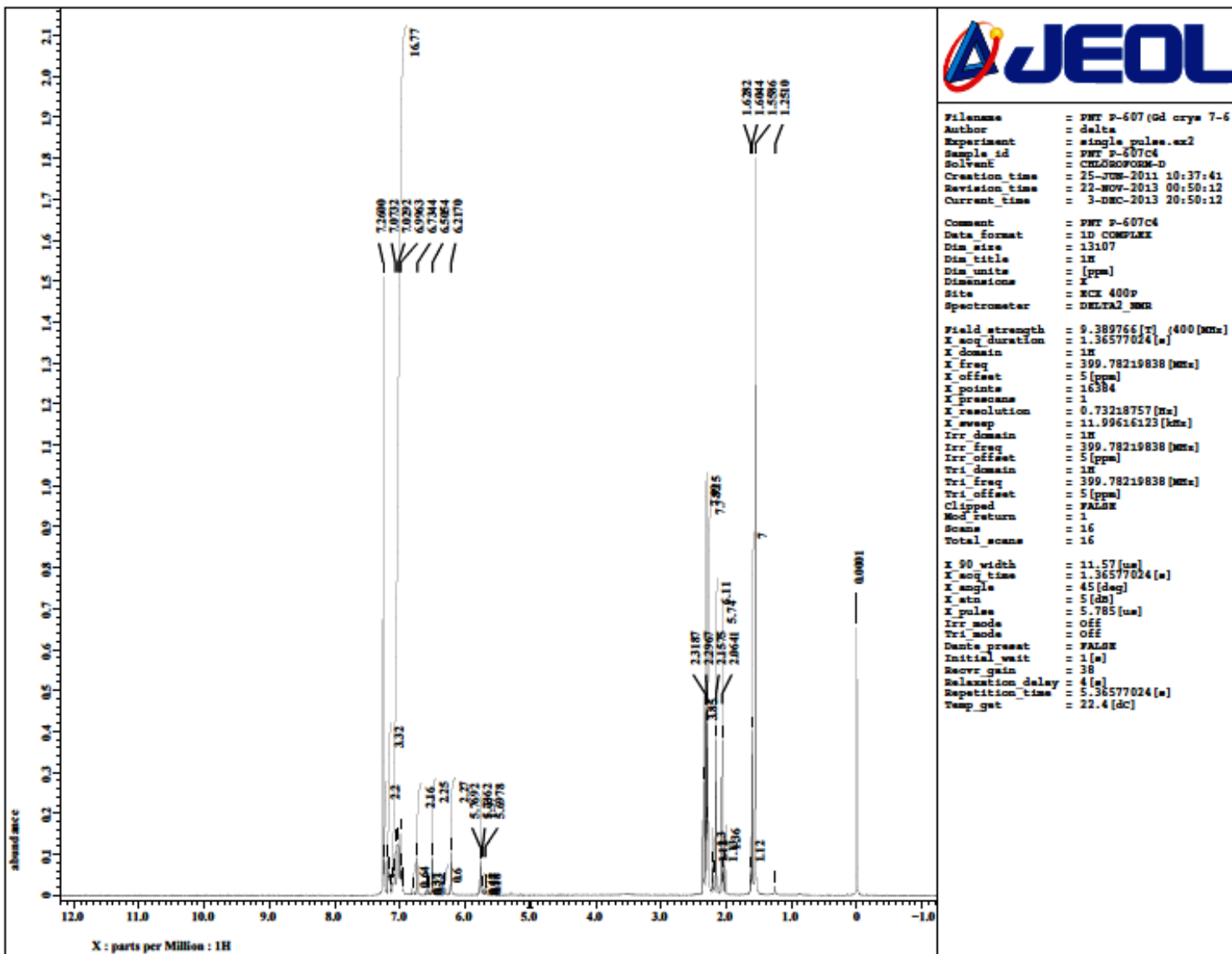


Fig. S8 ^1H NMR spectrum of **4** (CDCl_3 , 400.0 MHz).

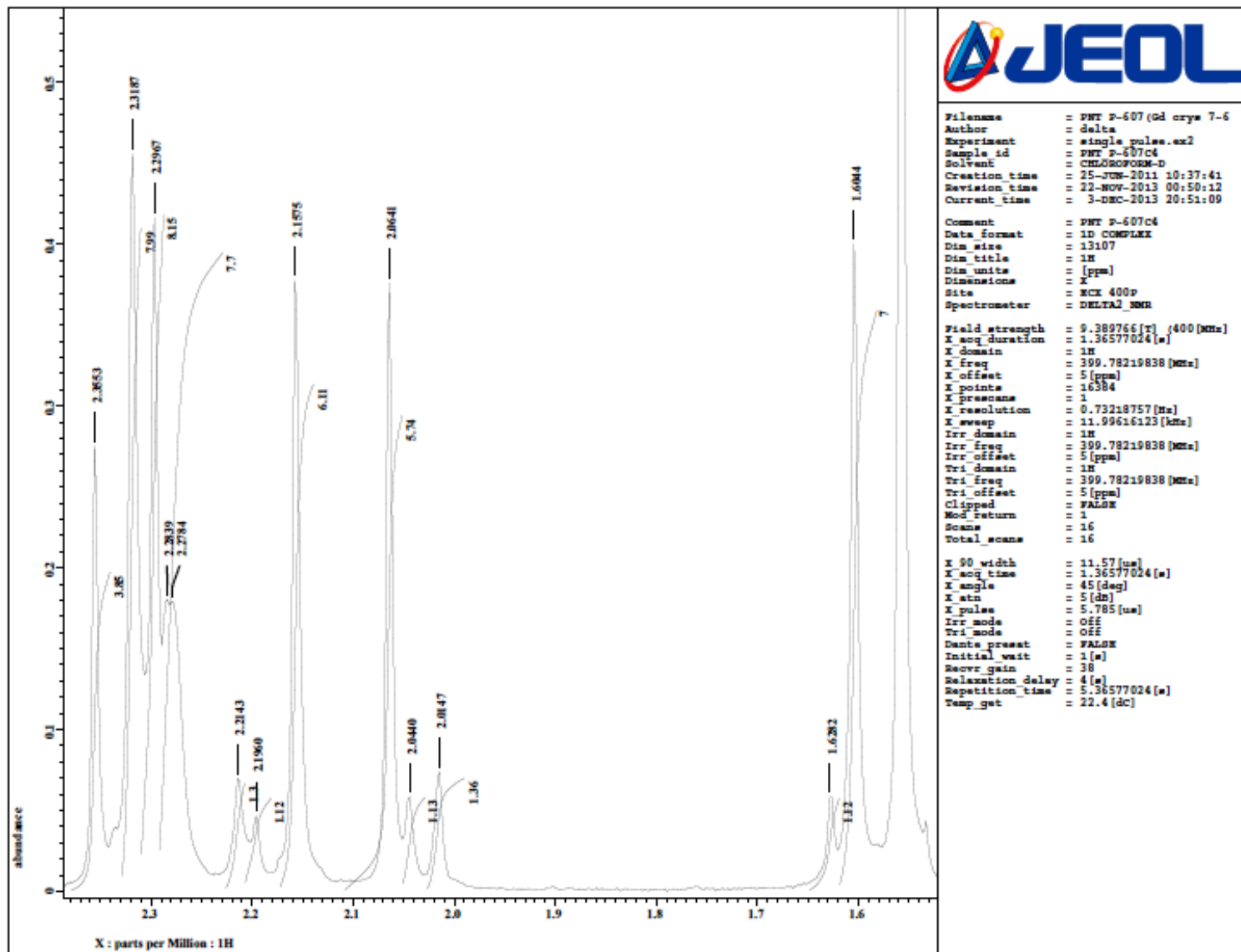


Fig. S9 Expansion of ^1H NMR spectrum of **4** (CDCl_3 , 400.0 MHz).

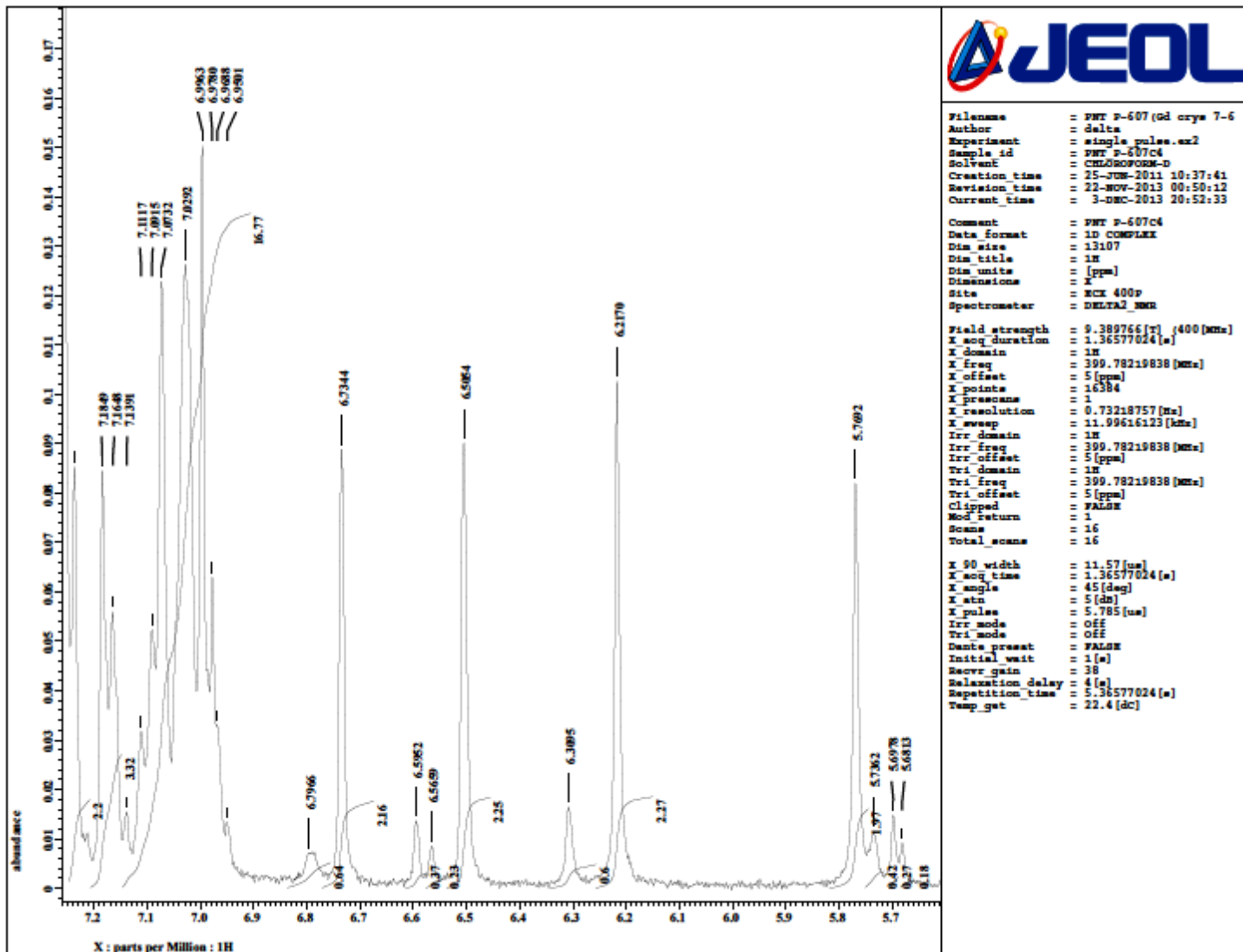


Fig. S10 Expansion of ^1H NMR spectrum of **4** (CDCl_3 , 400.0 MHz).

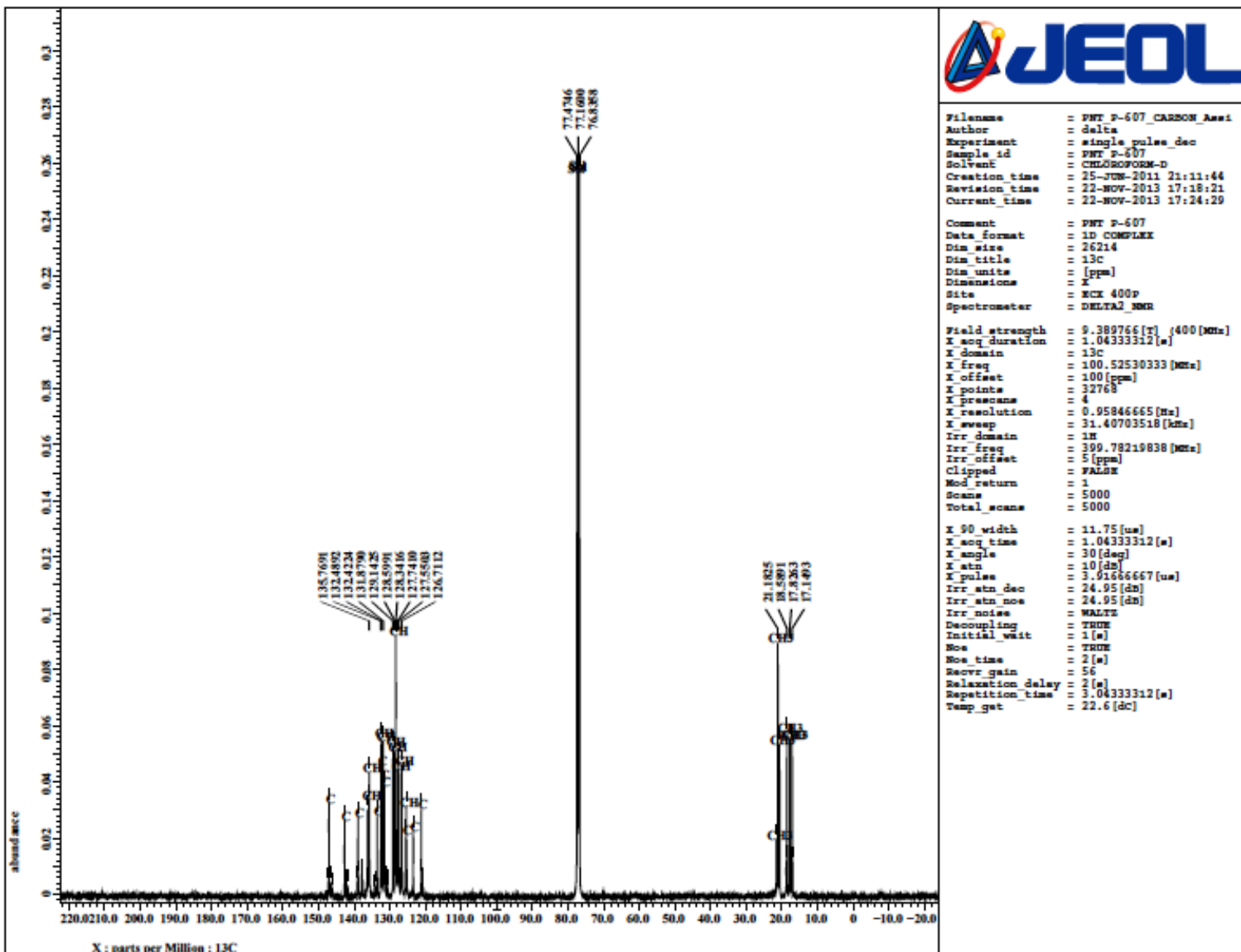


Fig. S11 ^{13}C NMR spectrum of **4** (CDCl_3 , 100.5 MHz).

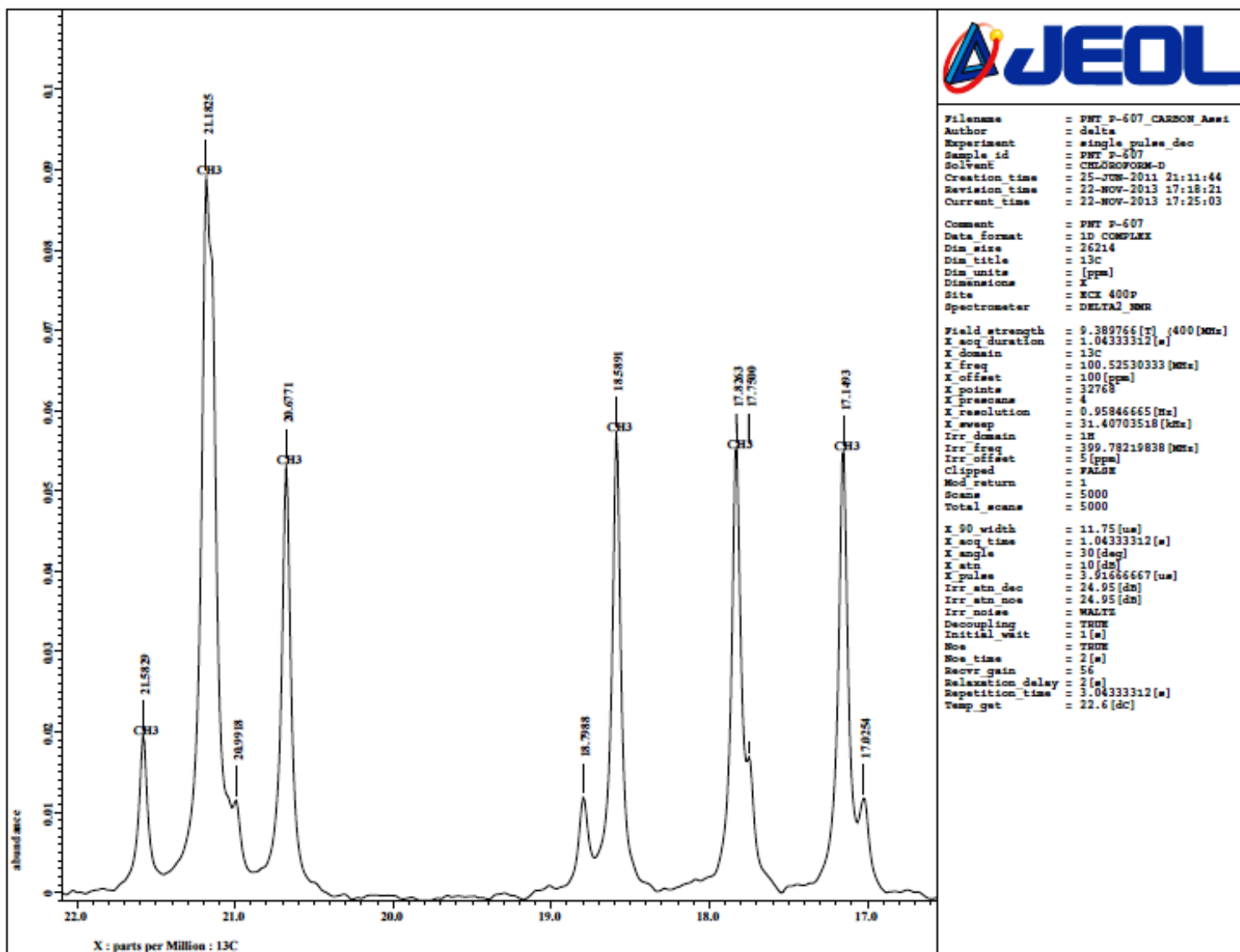


Fig. S12 Expansion of ^{13}C NMR spectrum of **4** (CDCl_3 , 100.5 MHz).

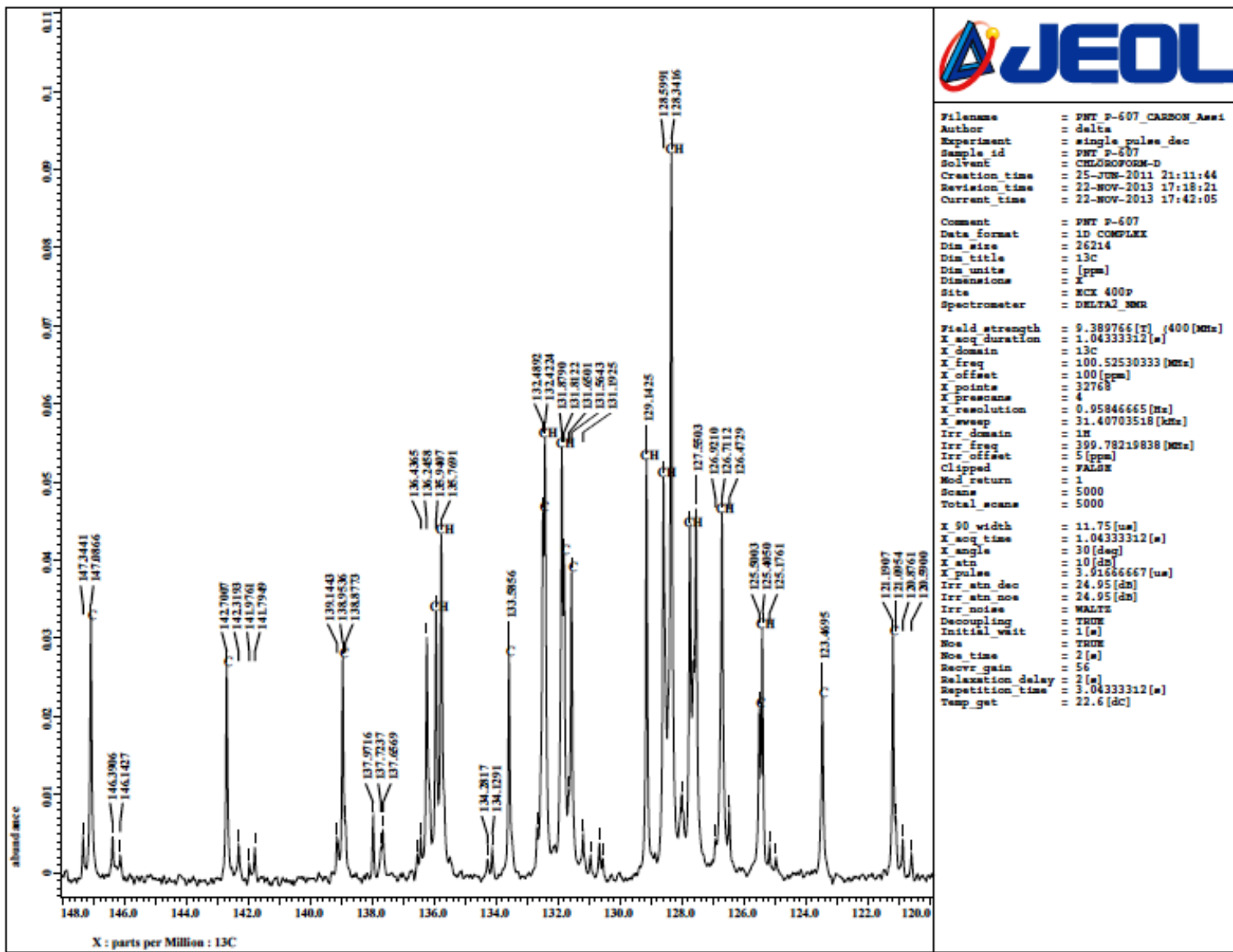


Fig. S13 Expansion of ^{13}C NMR spectrum of **4** (CDCl_3 , 100.5 MHz).

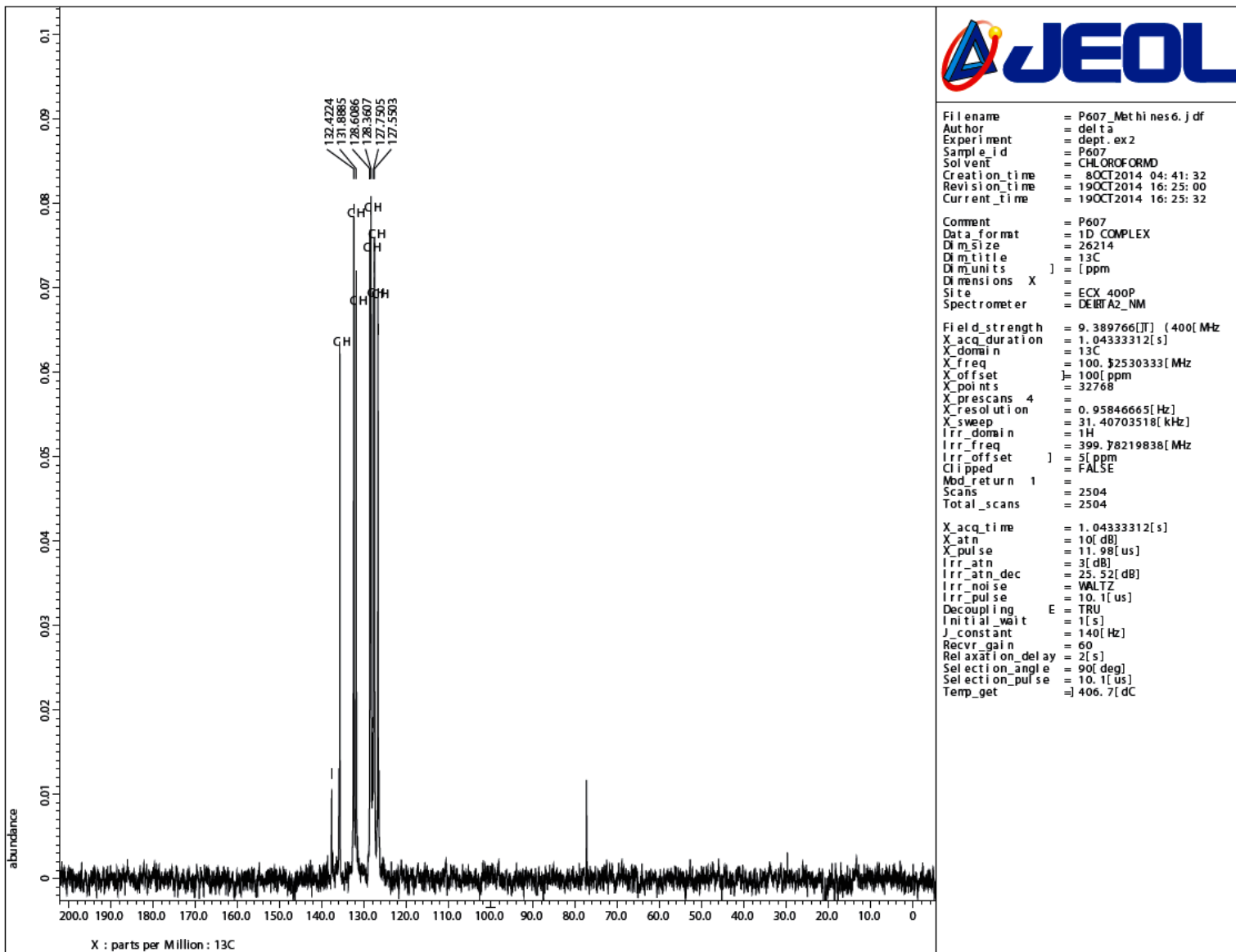


Fig. S14 DEPT 90 NMR spectrum of **4** (CDCl_3 , 100.5 MHz).

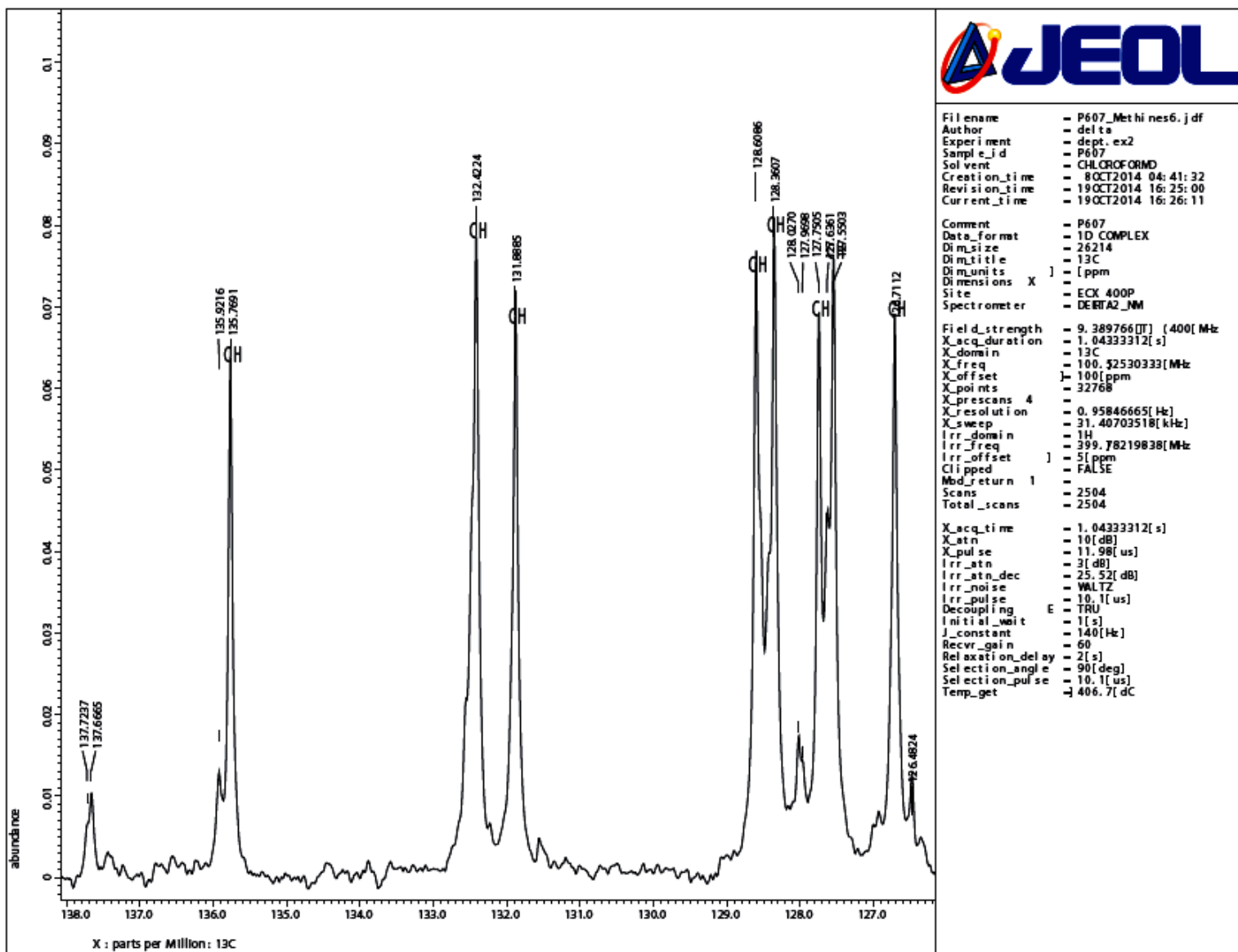


Fig. S15 Expansion of DEPT 90 NMR spectrum of 4.

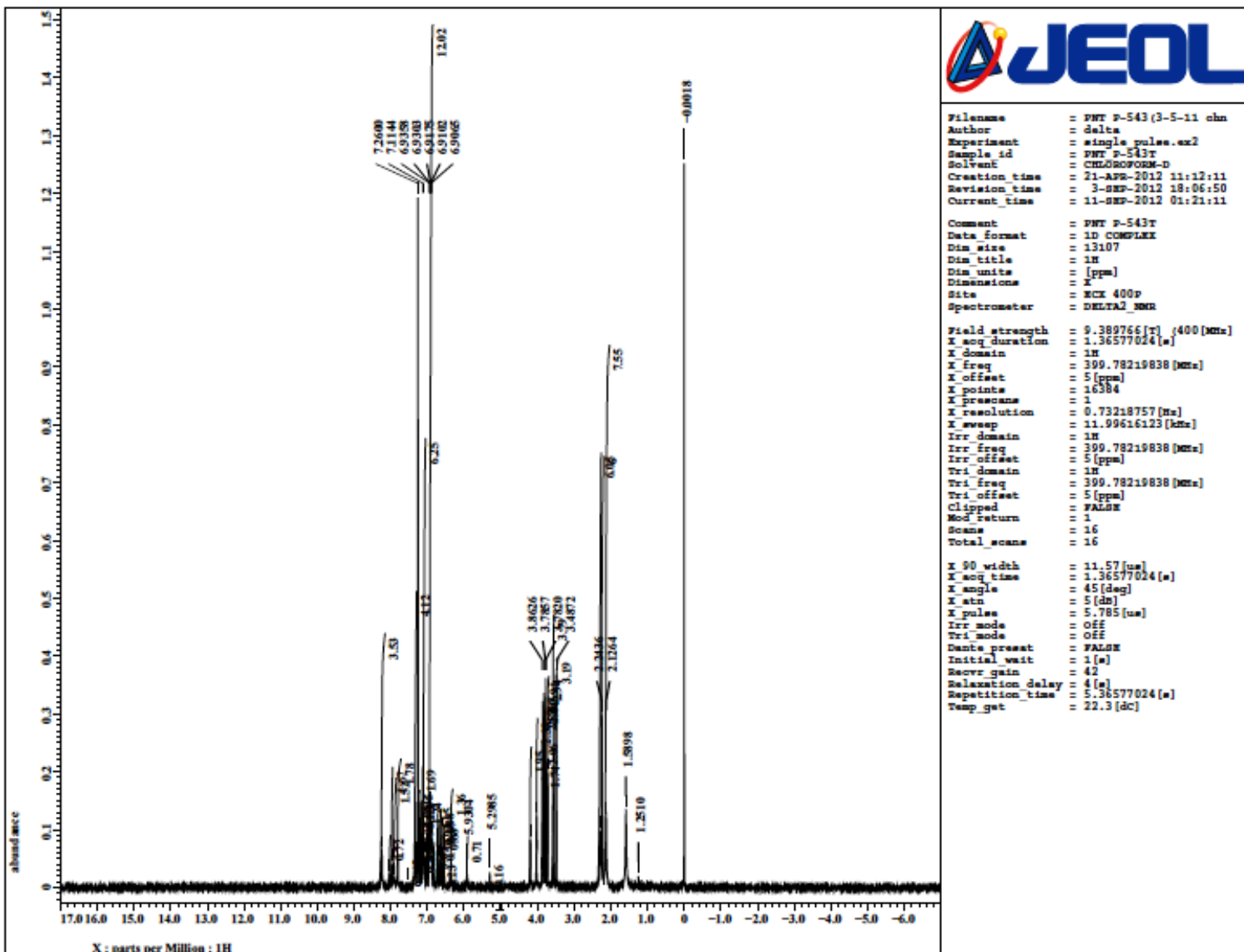


Fig. S16 ^1H NMR spectrum of **5** (CDCl_3 , 400.0 MHz).

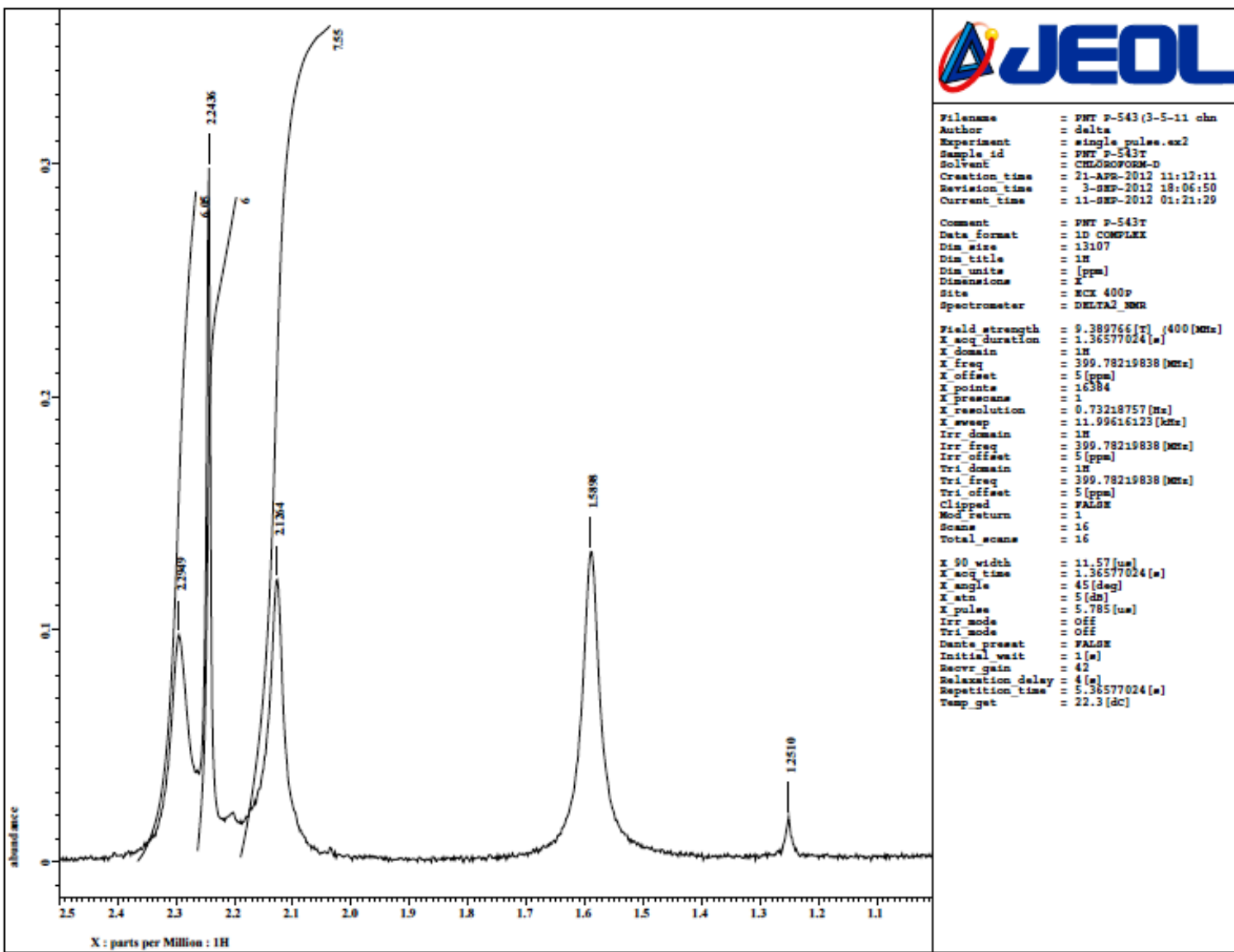


Fig. S17 Expansion of ^1H NMR spectrum of **5** (CDCl_3 , 400.0 MHz).

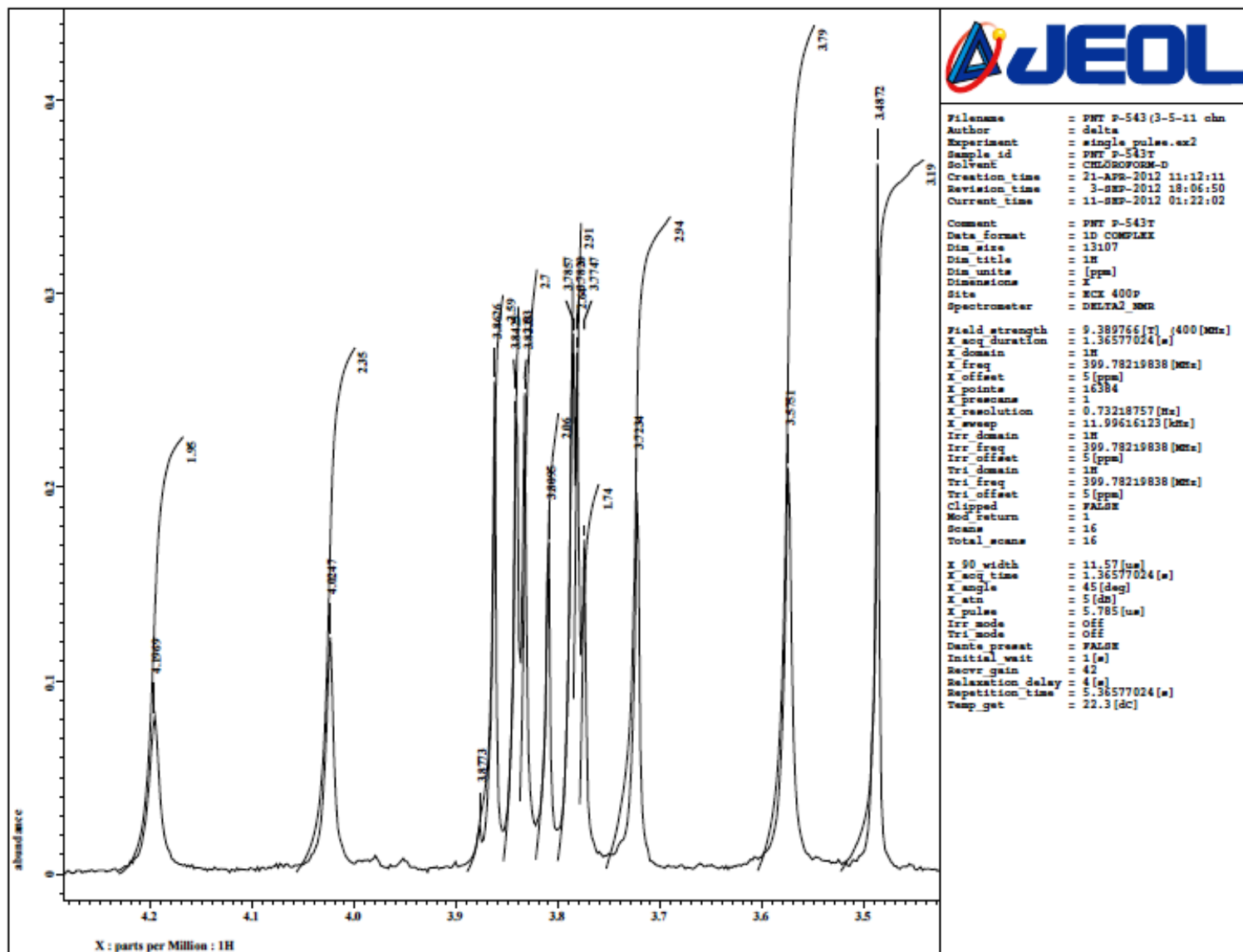


Fig. S18 Expansion of ^1H NMR spectrum of **5** (CDCl_3 , 400.0 MHz).

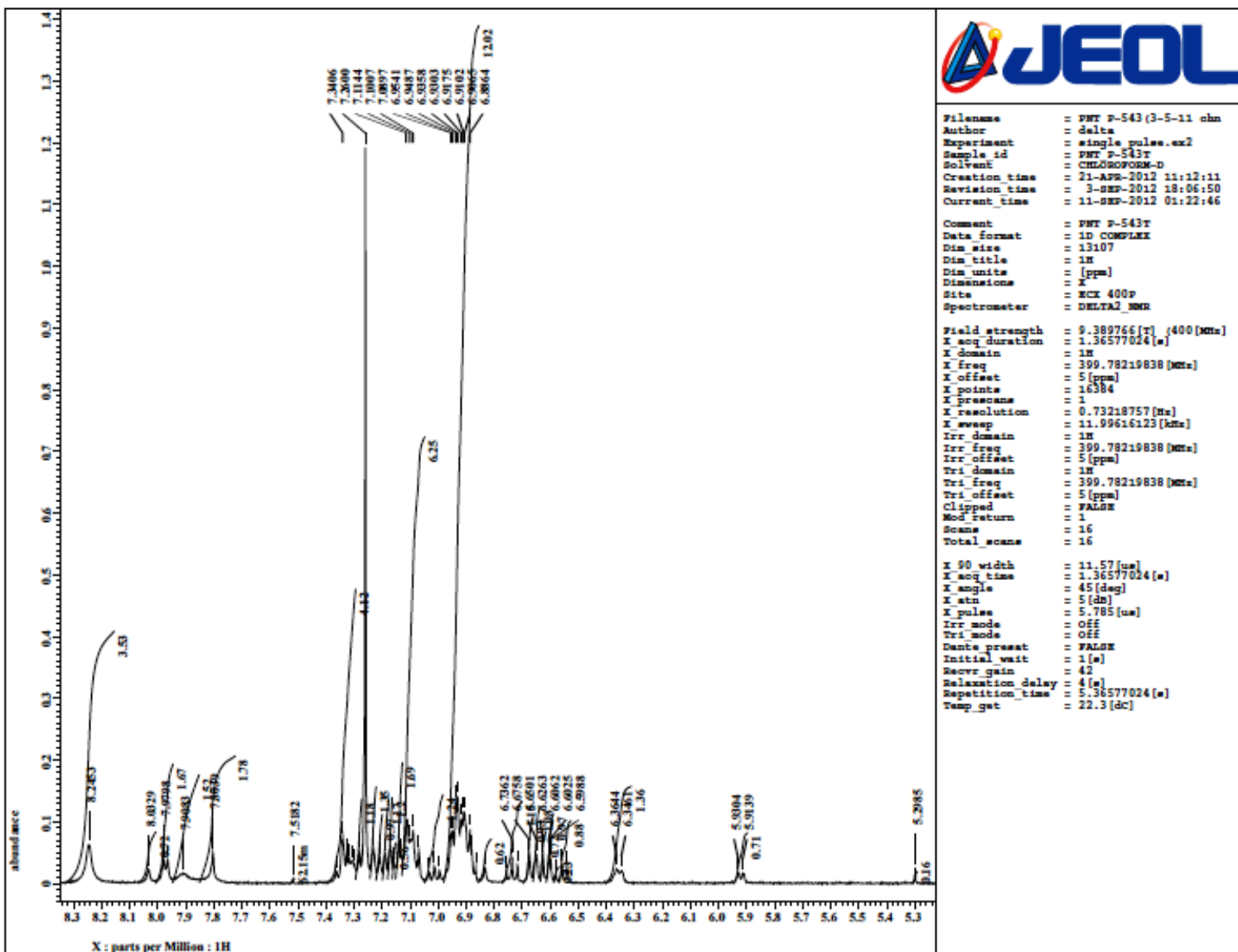


Fig. S19 Expansion of ^1H NMR spectrum of **5** (CDCl_3 , 400.0 MHz).

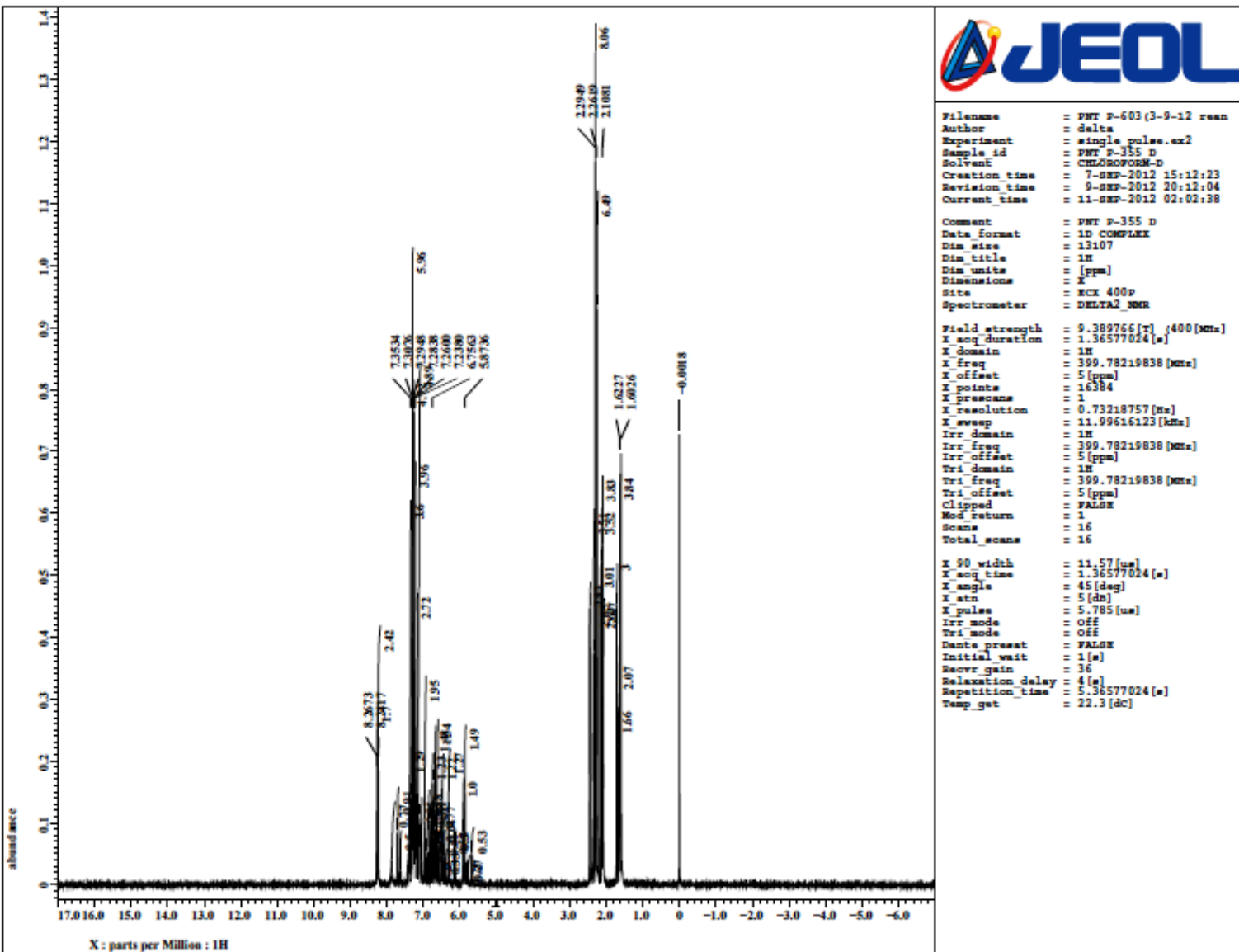


Fig. S20 ^1H NMR spectrum of **6** (CDCl_3 , 400.0 MHz).

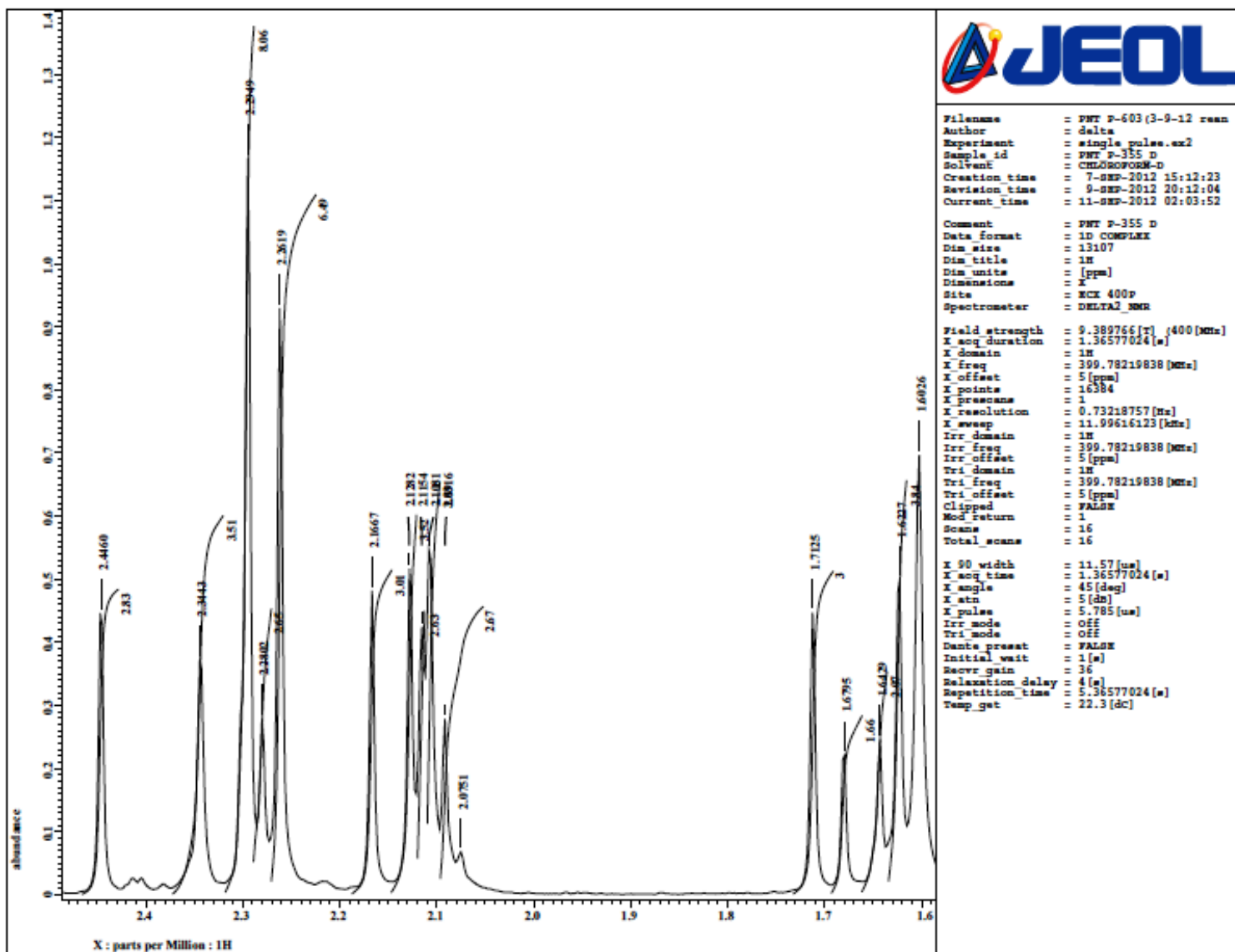


Fig. S21 Expansion of ^1H NMR spectrum of **6** (CDCl_3 , 400.0 MHz).

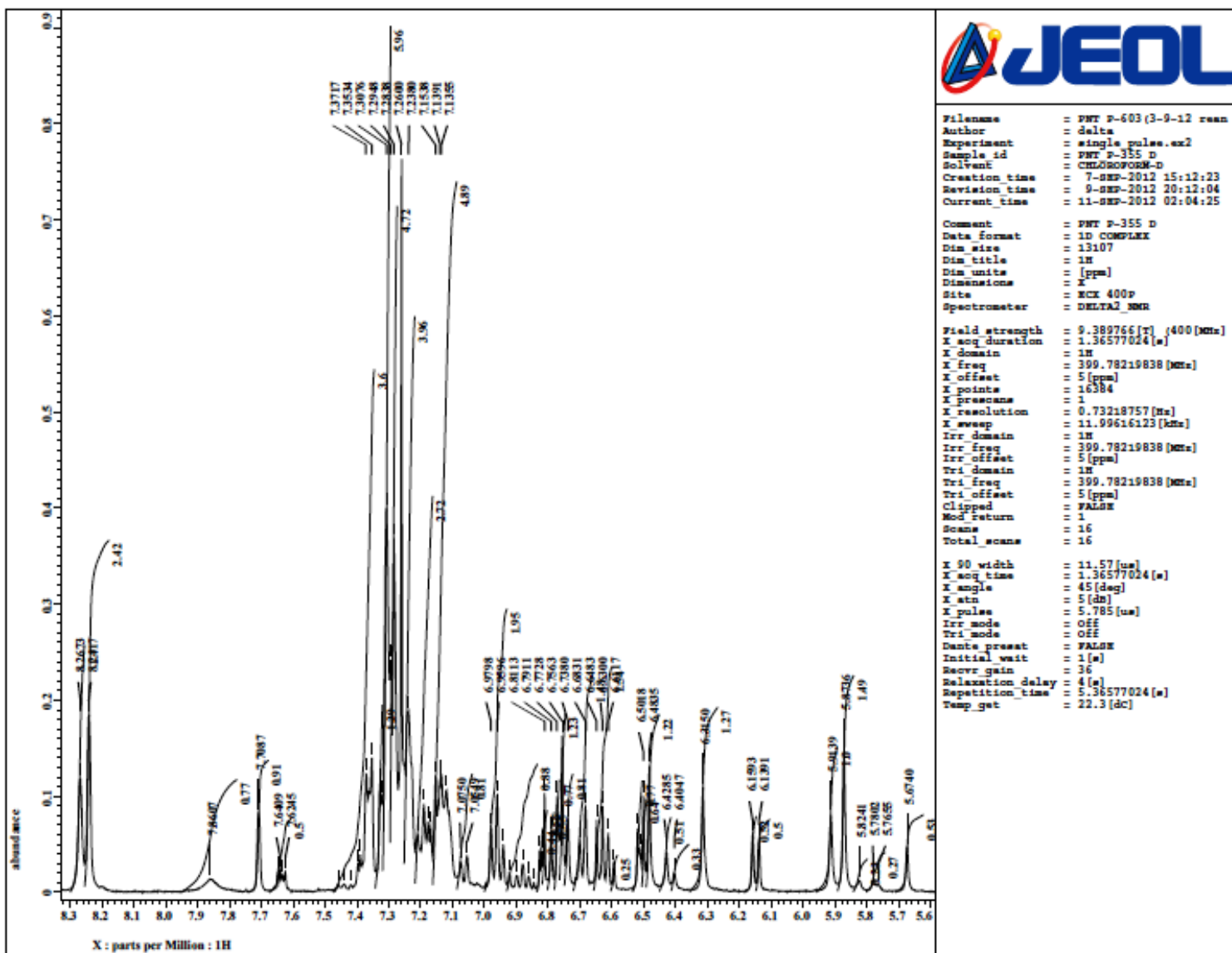


Fig. S22 Expansion of ^1H NMR spectrum of **6** (CDCl_3 , 400.0 MHz).

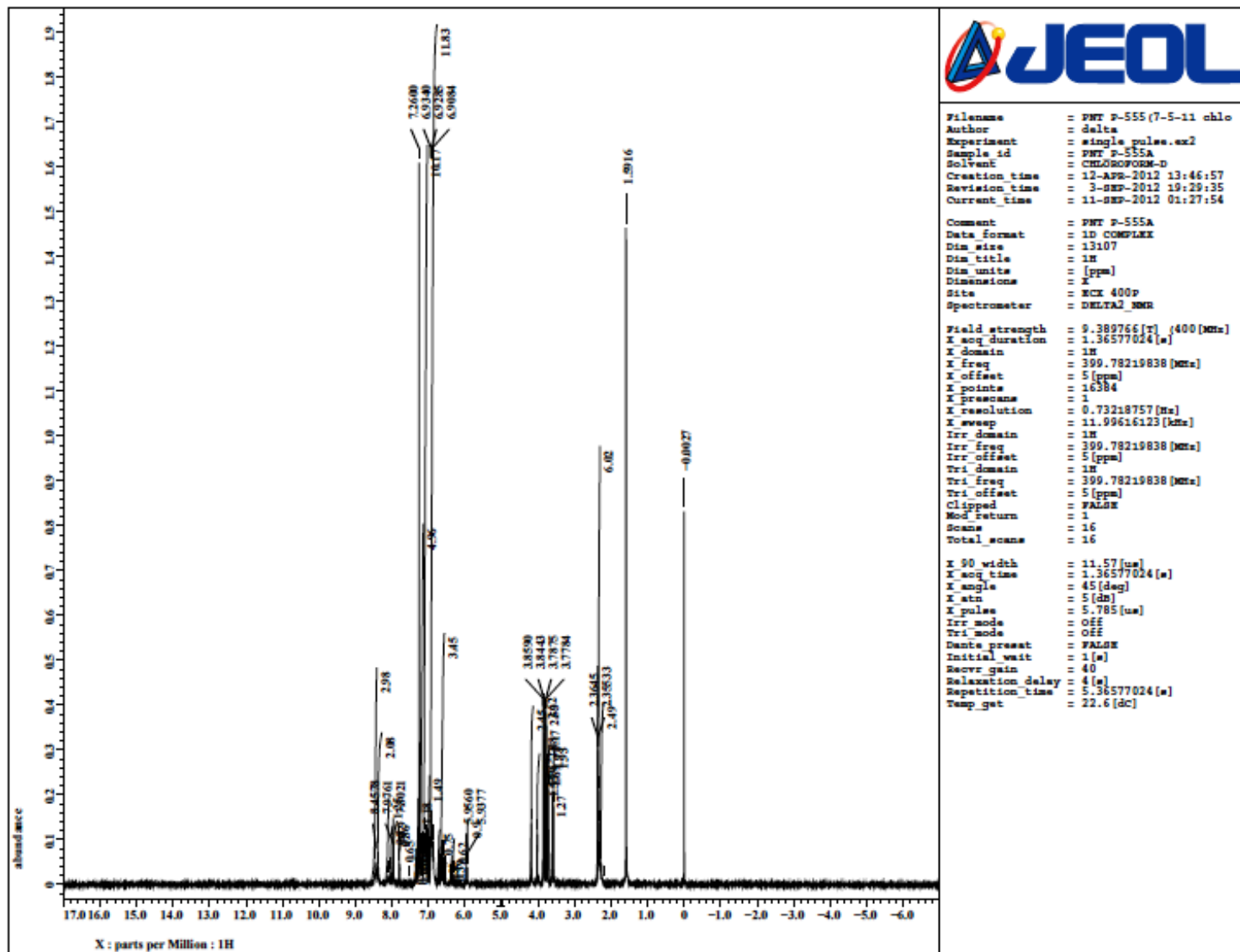


Fig. S23 ^1H NMR spectrum of **7** (CDCl_3 , 400.0 MHz).

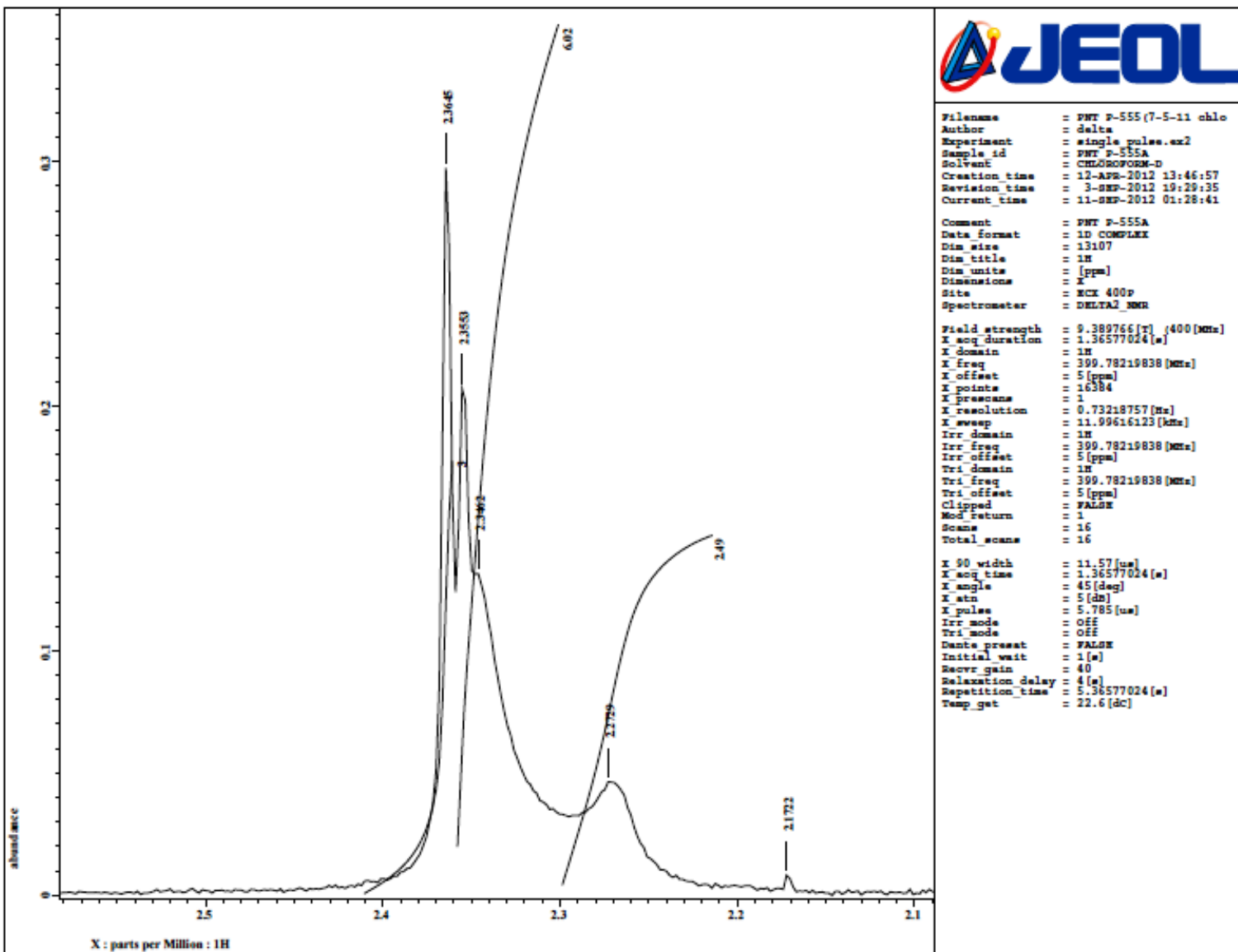


Fig. S24 Expansion of ¹H NMR spectrum of **7** (CDCl₃, 400.0 MHz).

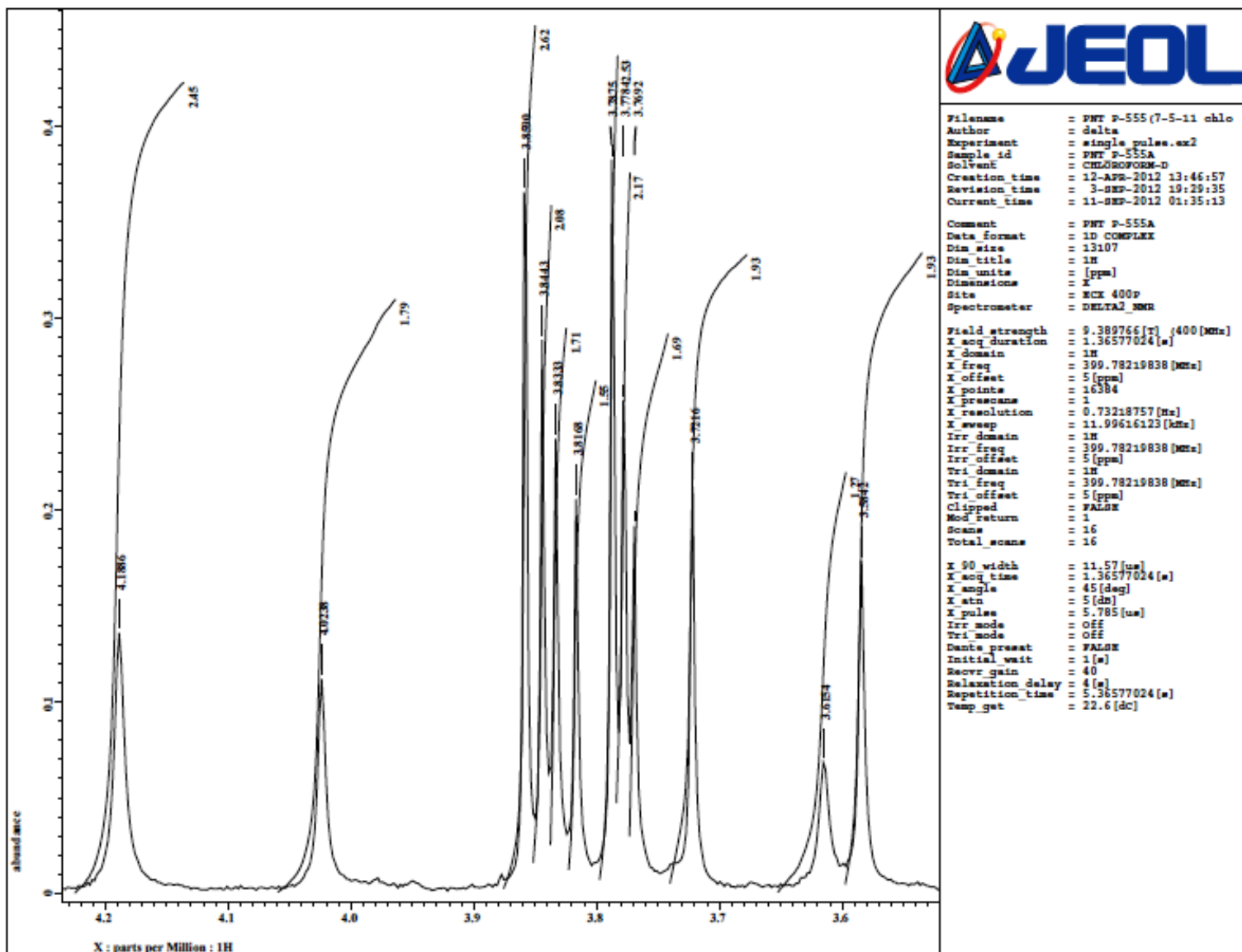


Fig. S25 Expansion of ¹H NMR spectrum of **7** (CDCl₃, 400.0 MHz).

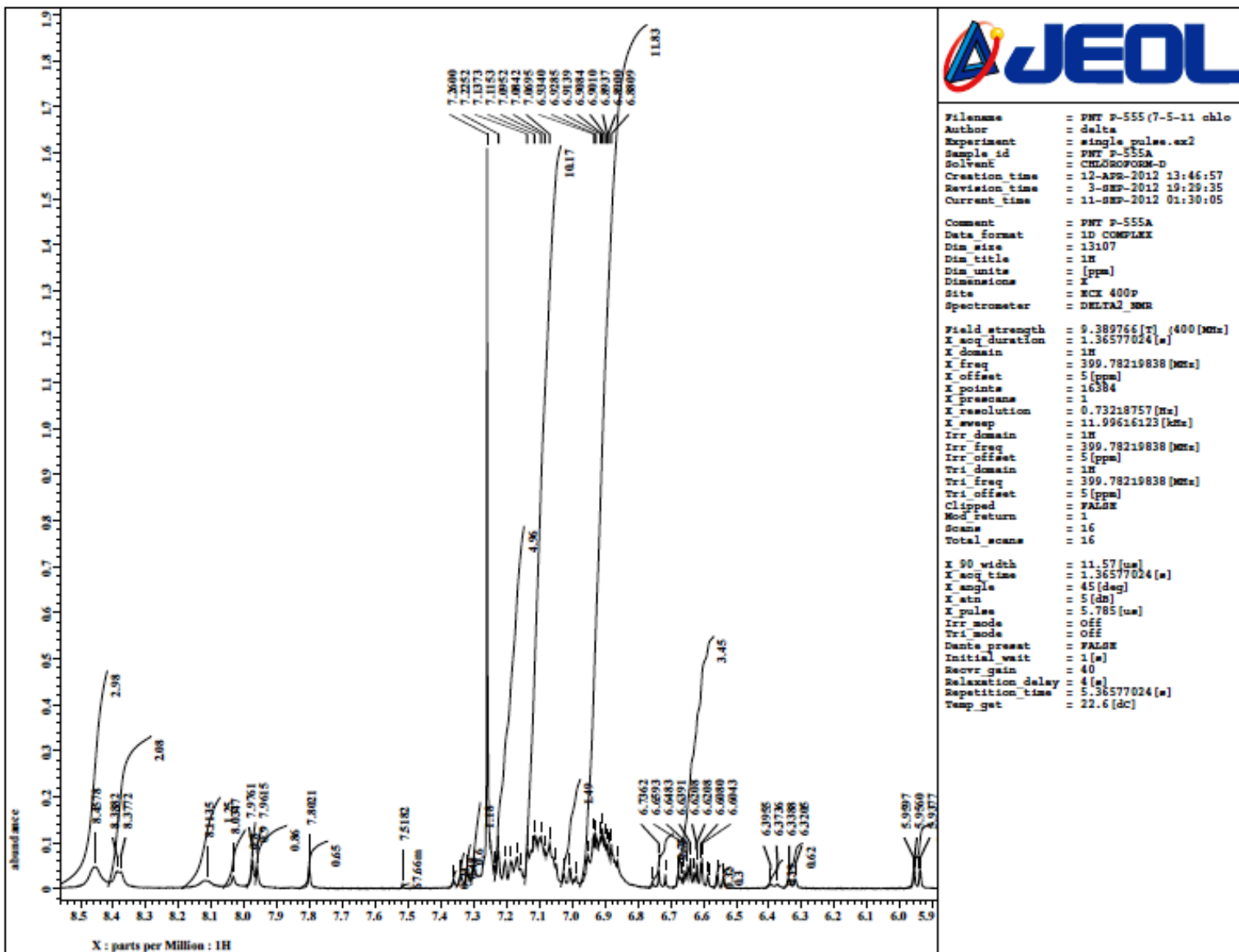


Fig. S26 Expansion of ^1H NMR spectrum of **7** (CDCl_3 , 400.0 MHz).

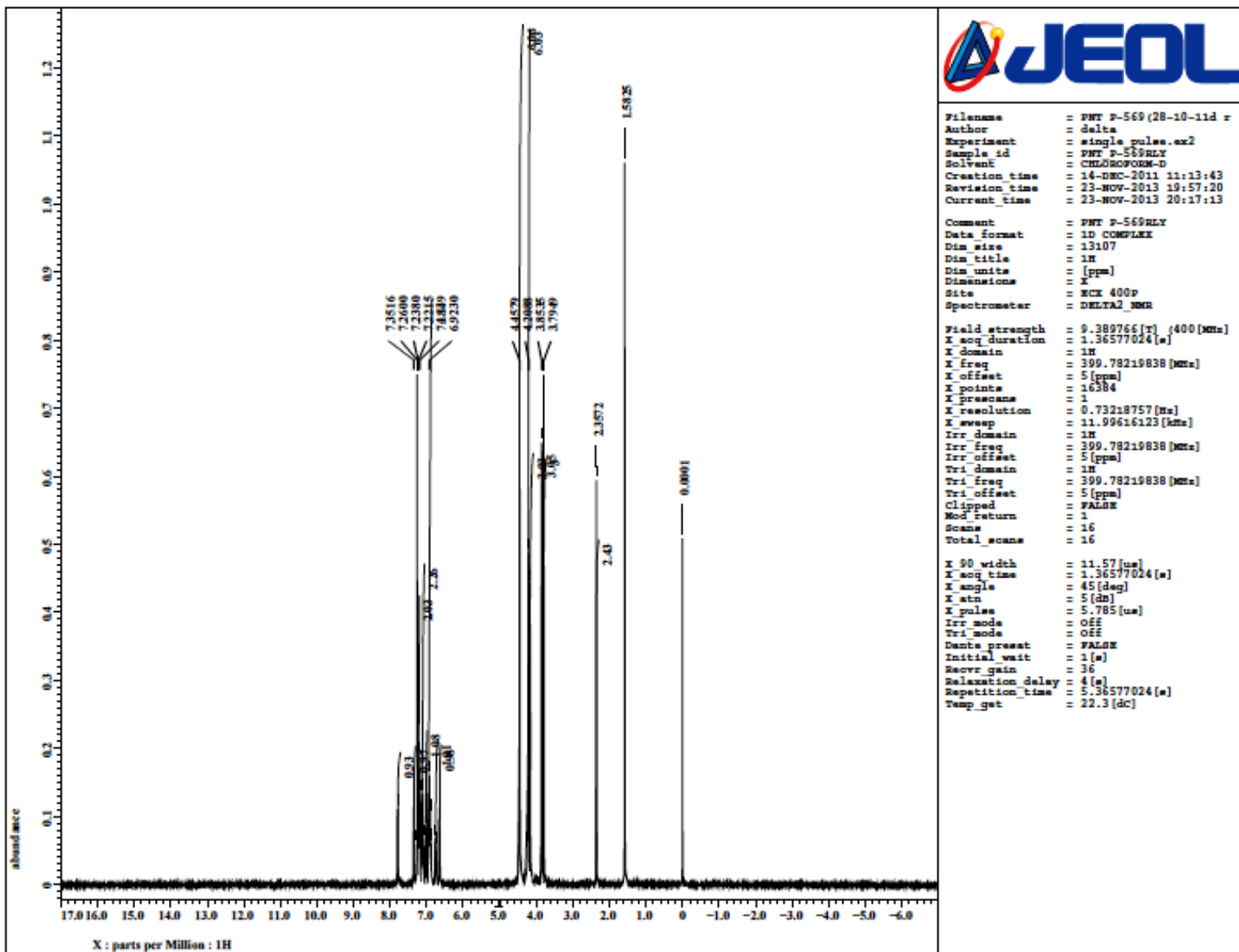


Fig. S27 ^1H NMR spectrum of **8/9** (CDCl_3 , 400.0 MHz).

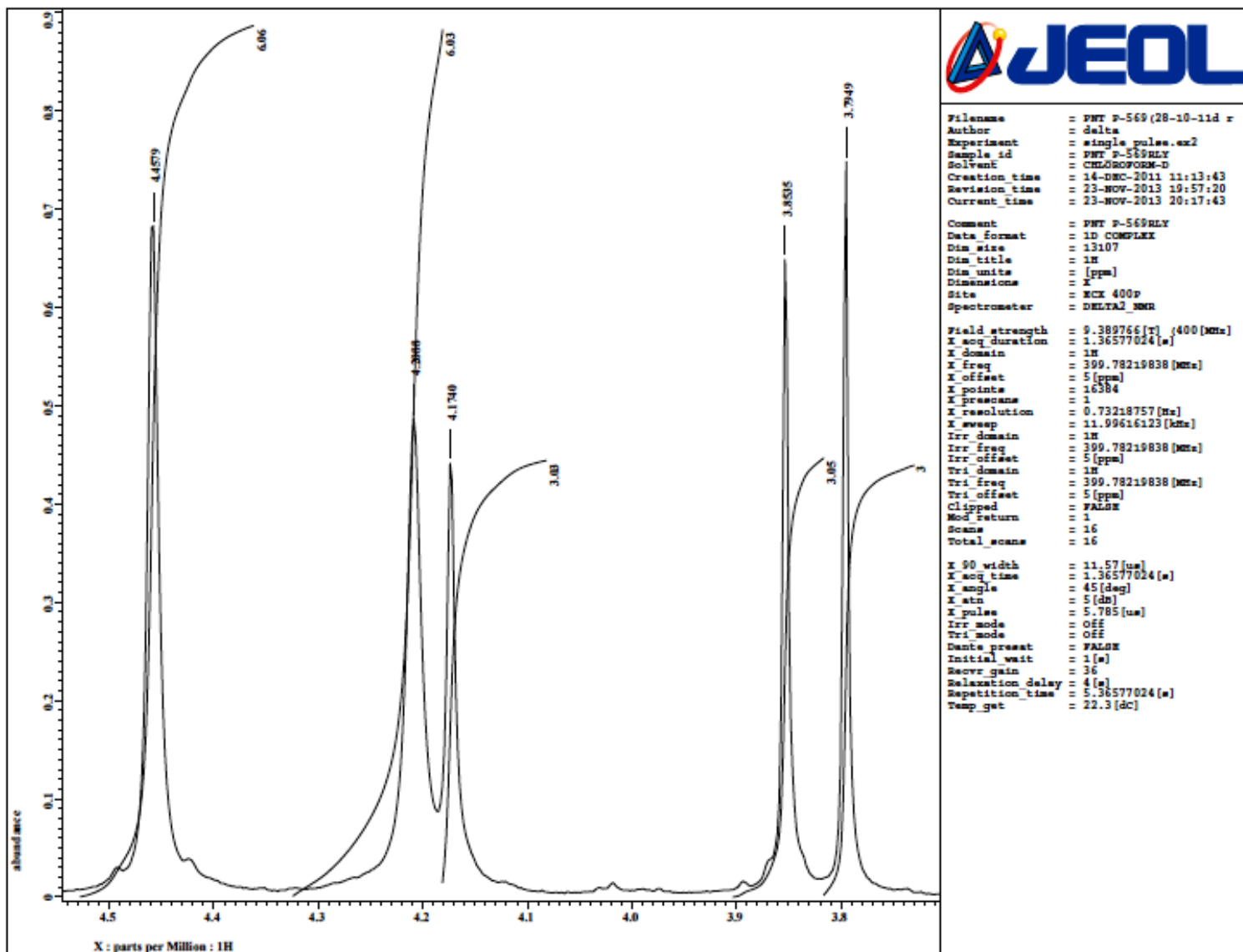


Fig. S28 Expansion of ^1H NMR spectrum of **8/9** (CDCl_3 , 400.0 MHz).

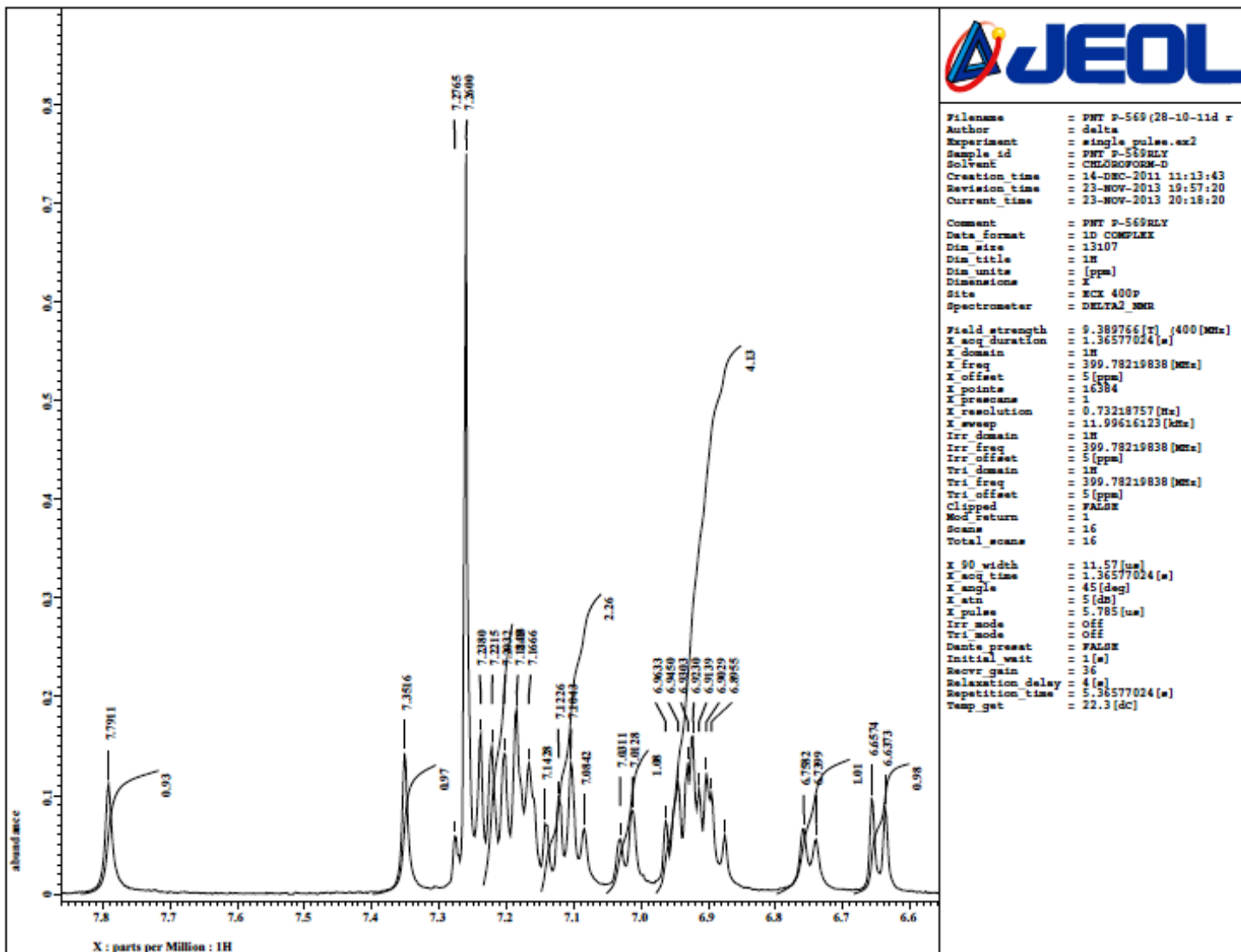


Fig. S29 Expansion of ^1H NMR spectrum of **8/9** (CDCl_3 , 400.0 MHz).

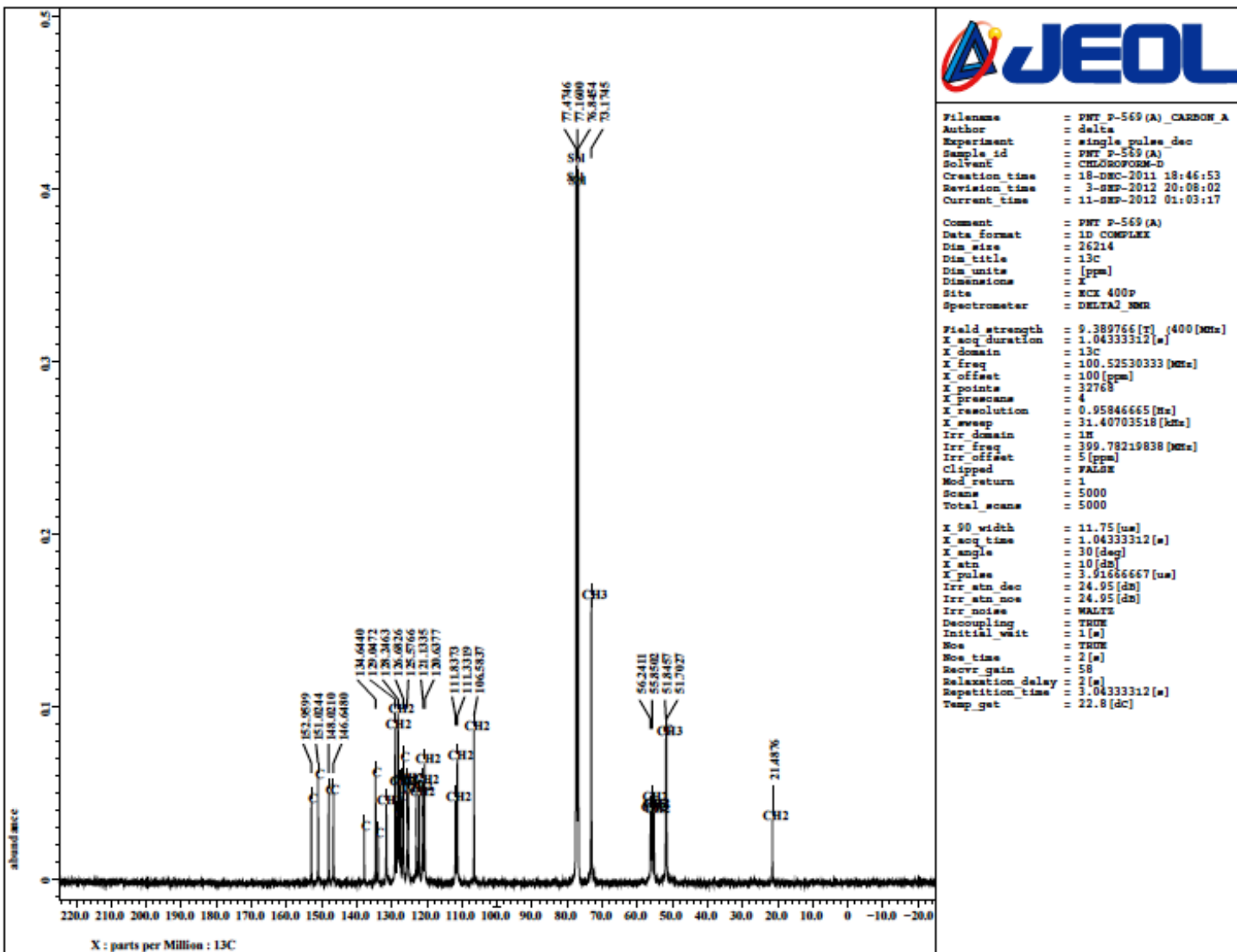


Fig. S30 ^{13}C NMR spectrum of 8/9 (CDCl_3 , 100.5 MHz).

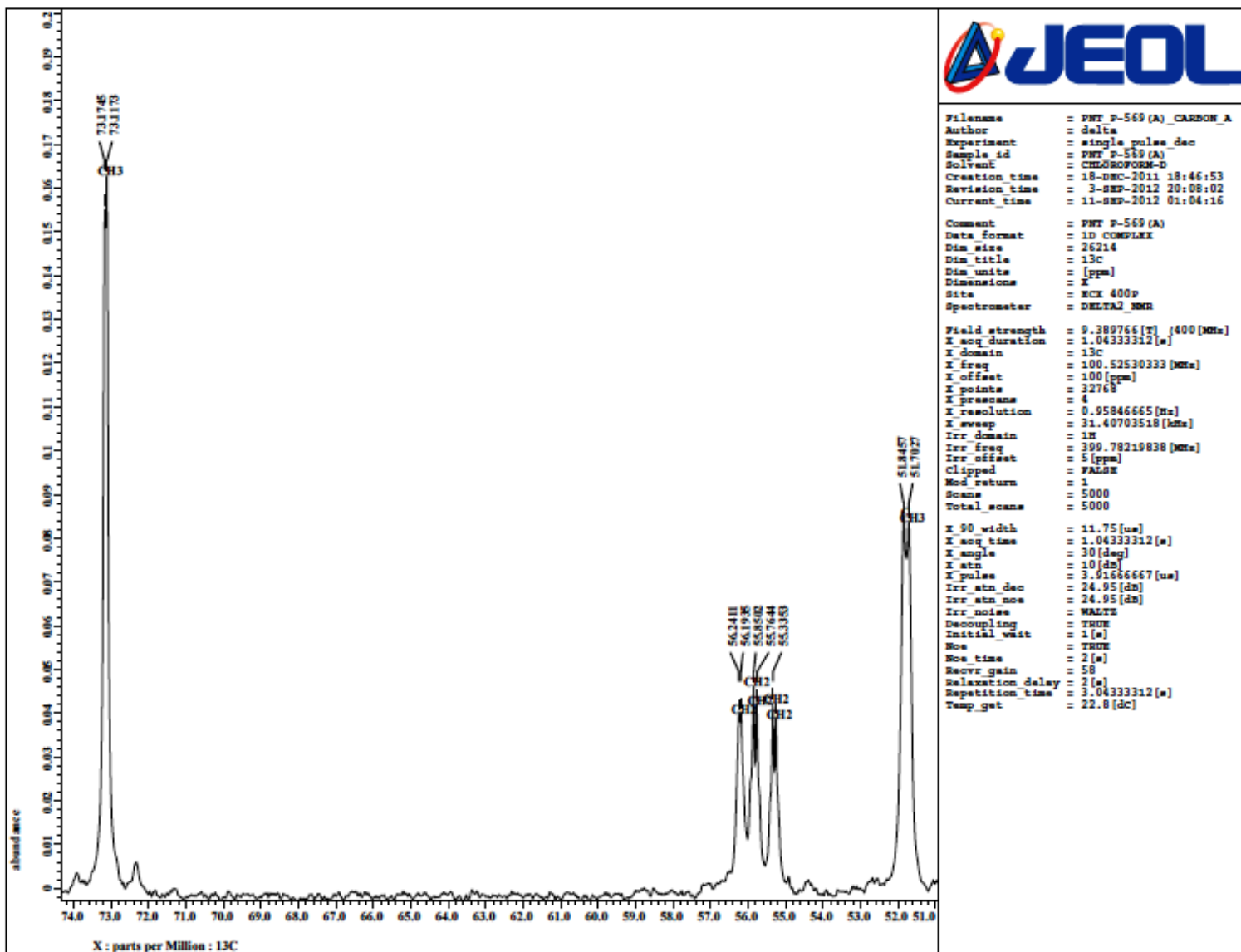


Fig. S31 Expansion of ^{13}C NMR spectrum of **8/9** (CDCl_3 , 100.5 MHz).

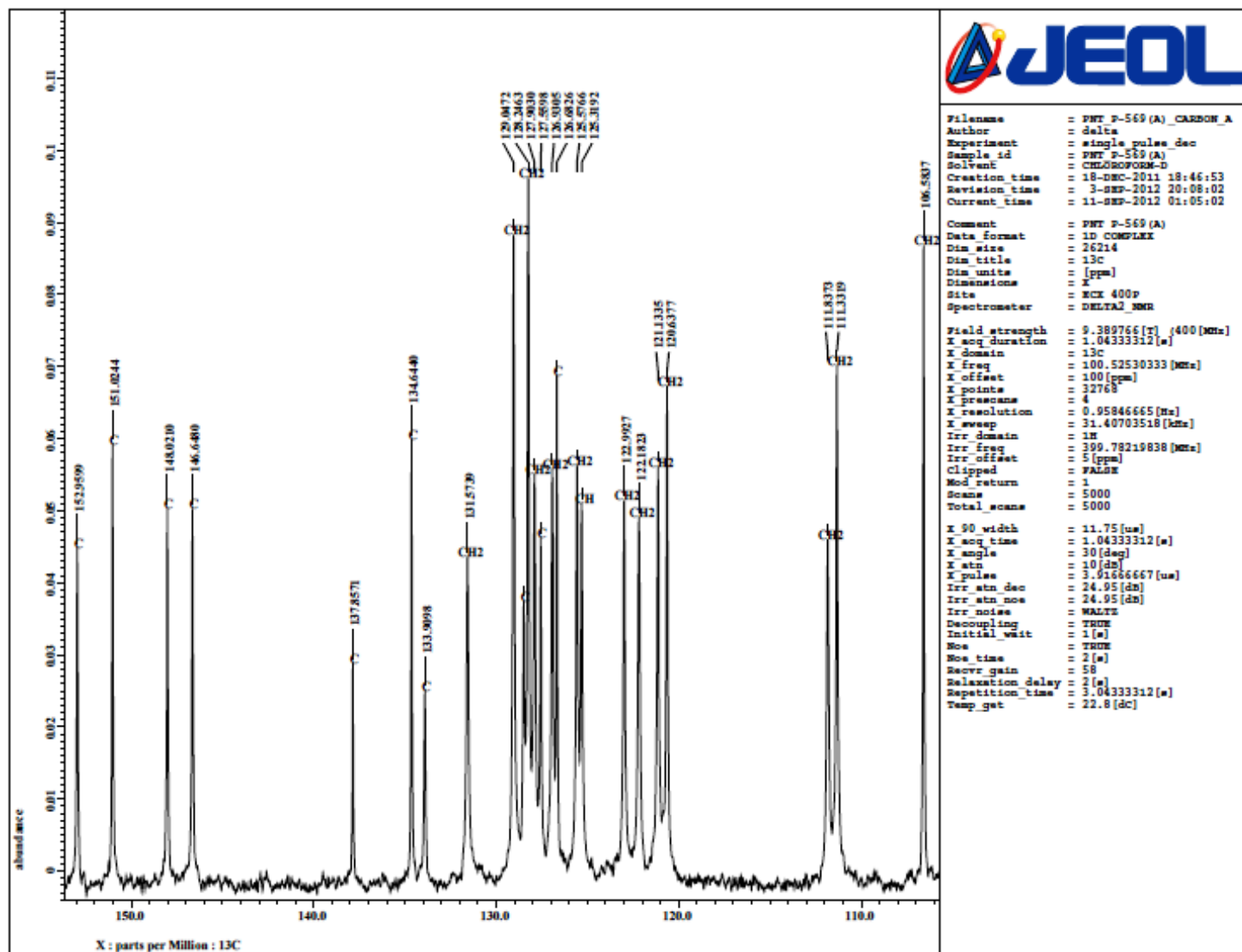


Fig. S32 Expansion of ^{13}C NMR spectrum of **8/9** (CDCl_3 , 100.5 MHz).

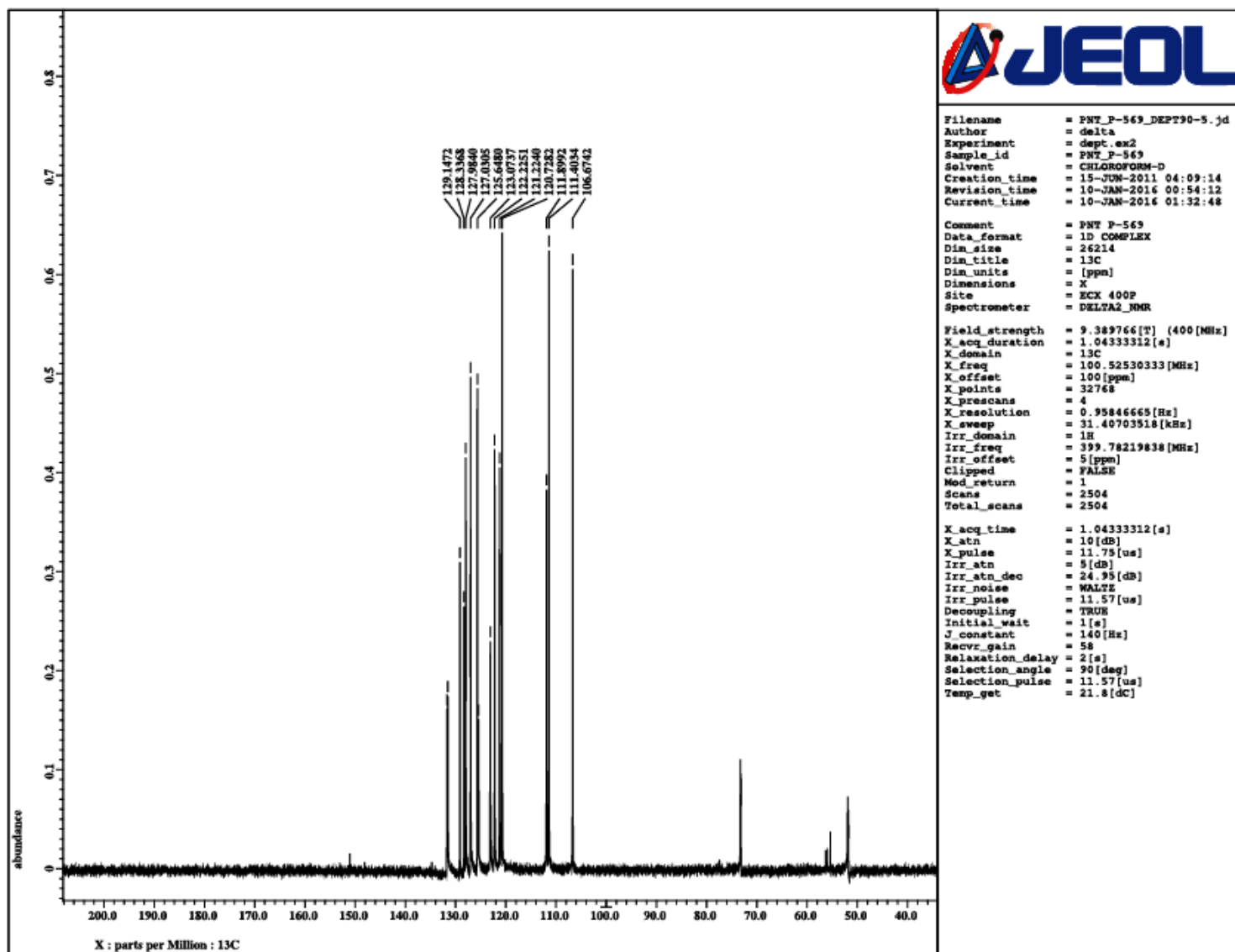


Fig. S33 DEPT 90 NMR spectrum of **8/9** (CDCl_3 , 100.5 MHz). The peaks around δ 50–56 and 73 correspond to residual peaks of CH_2 and OCH_3 carbons.

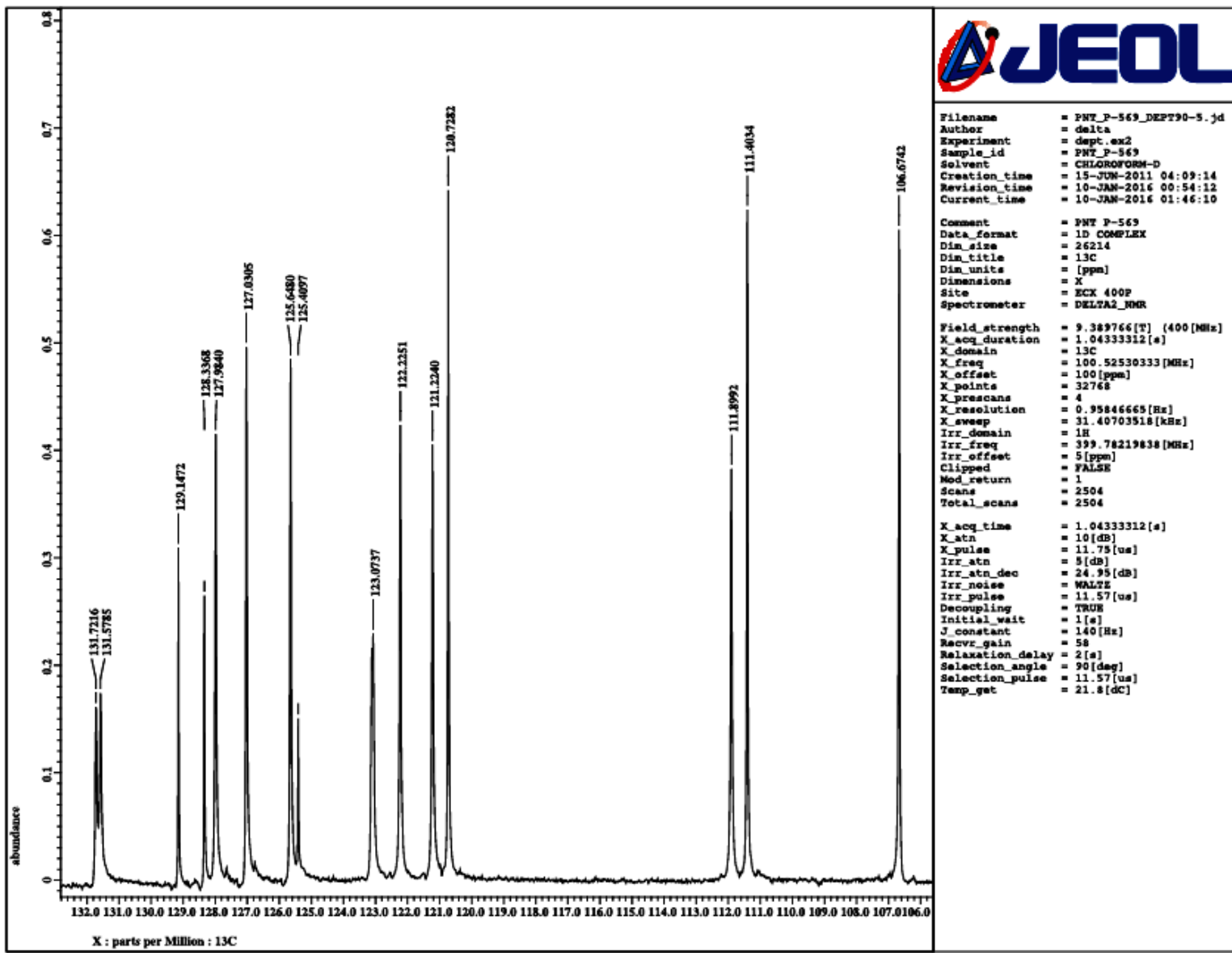


Fig. S34 Expansion of DEPT 90 NMR spectrum of **8/9**.

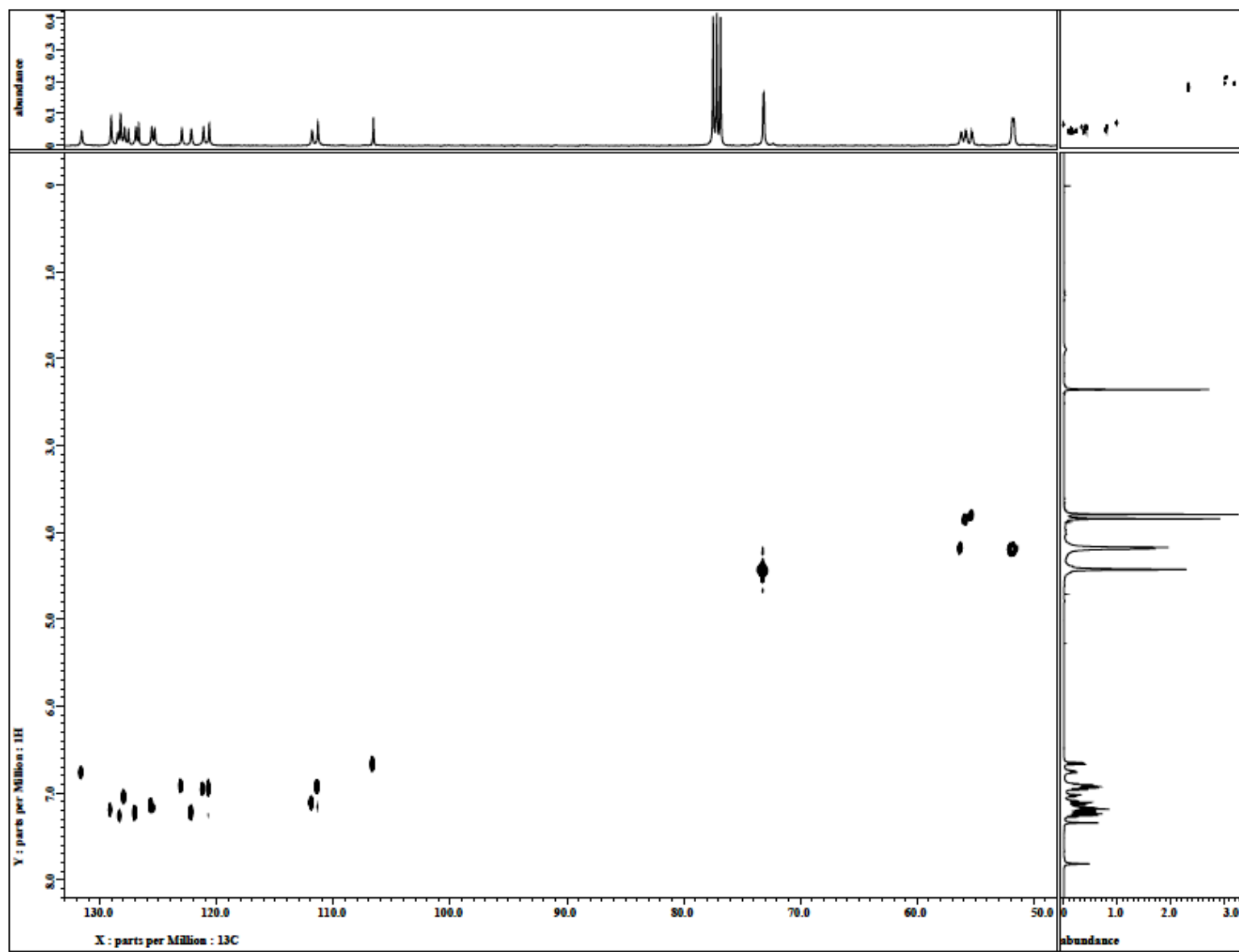


Fig. S35 The ^{13}C - ^1H HETCOR NMR spectrum of **8/9** (X-axis 100.5 MHz, Y-axis 400 MHz, CDCl_3).

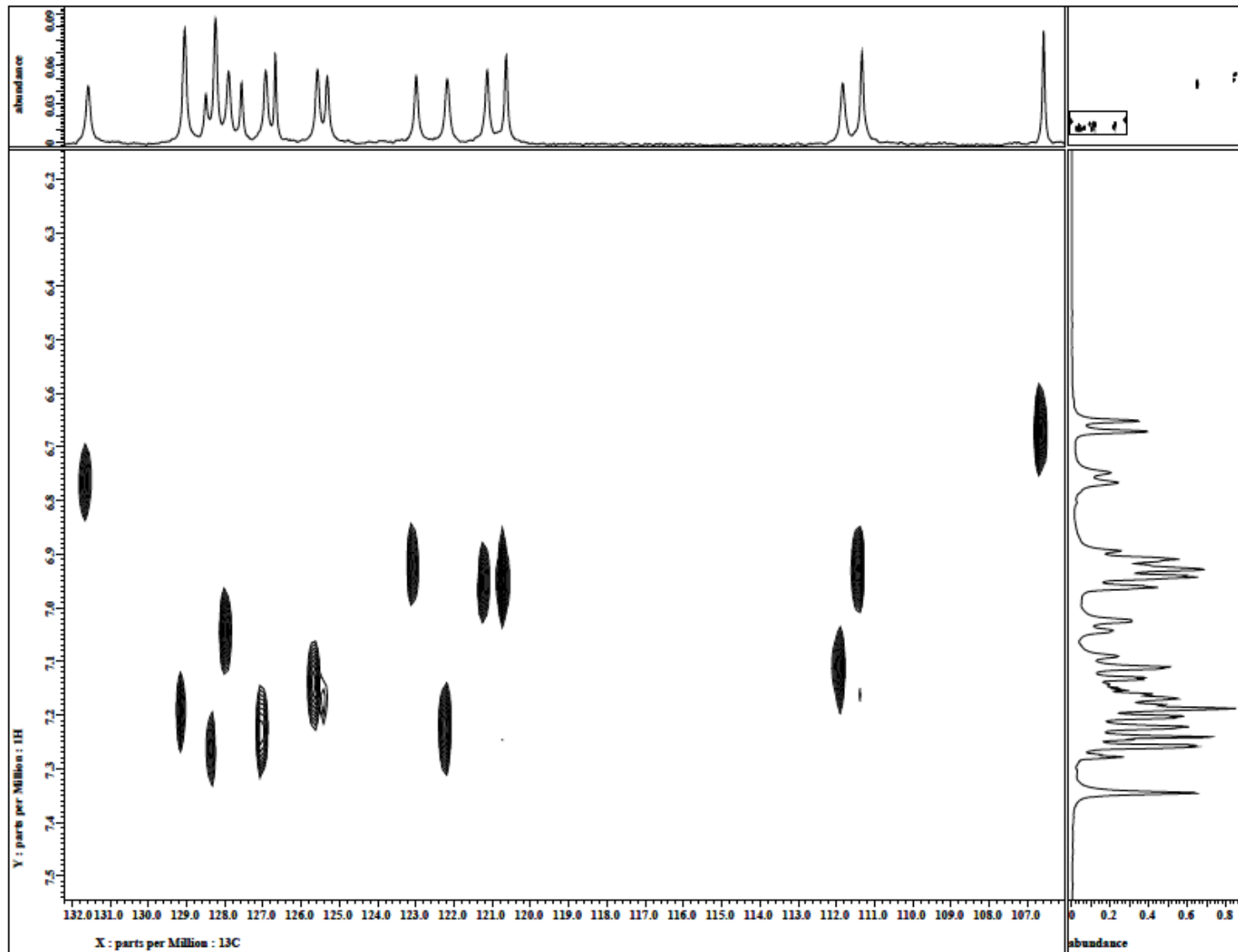


Fig. S36 The $^{13}\text{C}-^1\text{H}$ HETCOR NMR spectrum of **8/9** illustrated for the ArCH carbons (X-axis 100.5 MHz, Y-axis 400 MHz, CDCl_3).

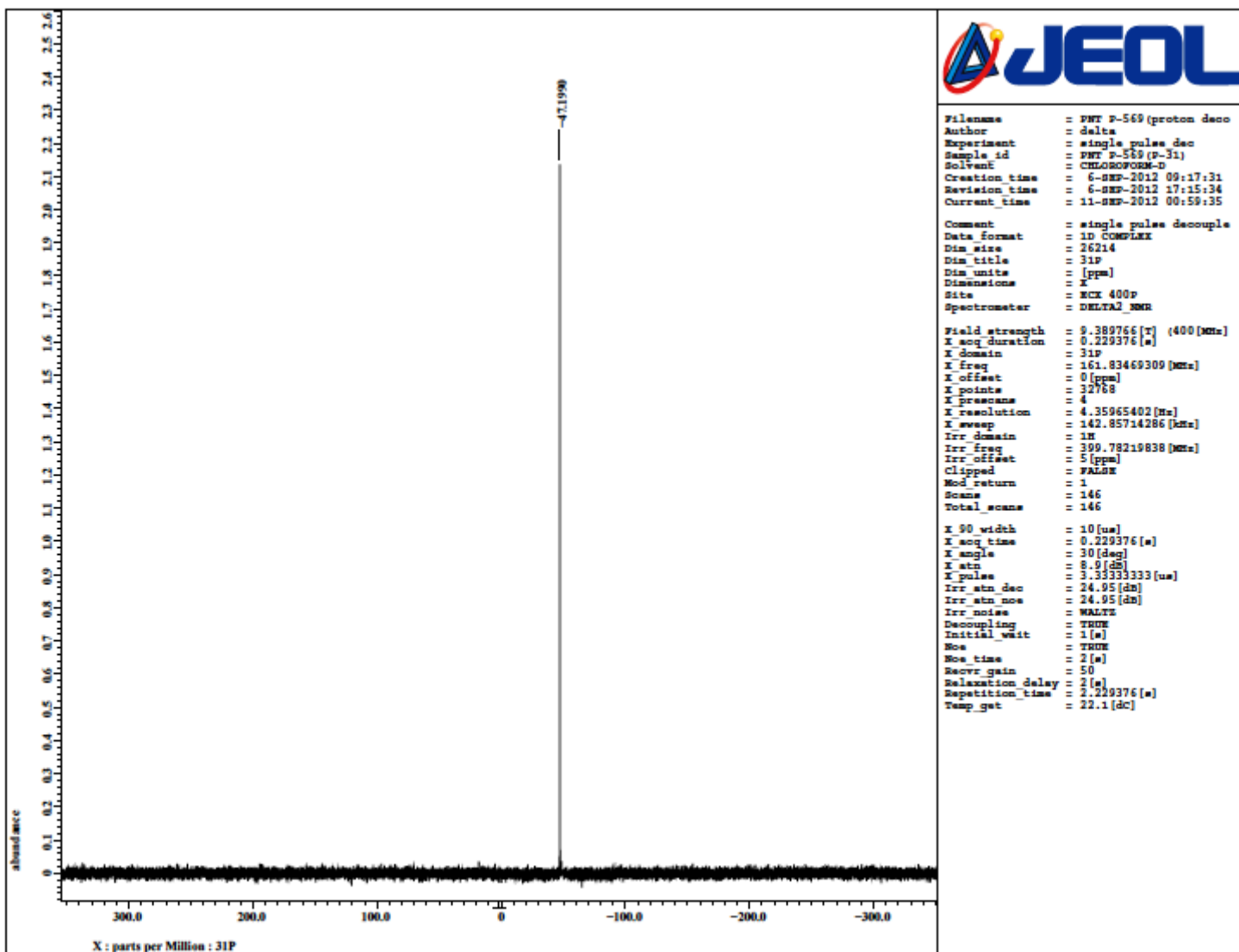


Fig. S37 $^{31}\text{P}\{\text{H}\}$ NMR spectrum of **8/9** (CDCl_3 , 161.8 MHz) at 35.8 μM concentration.

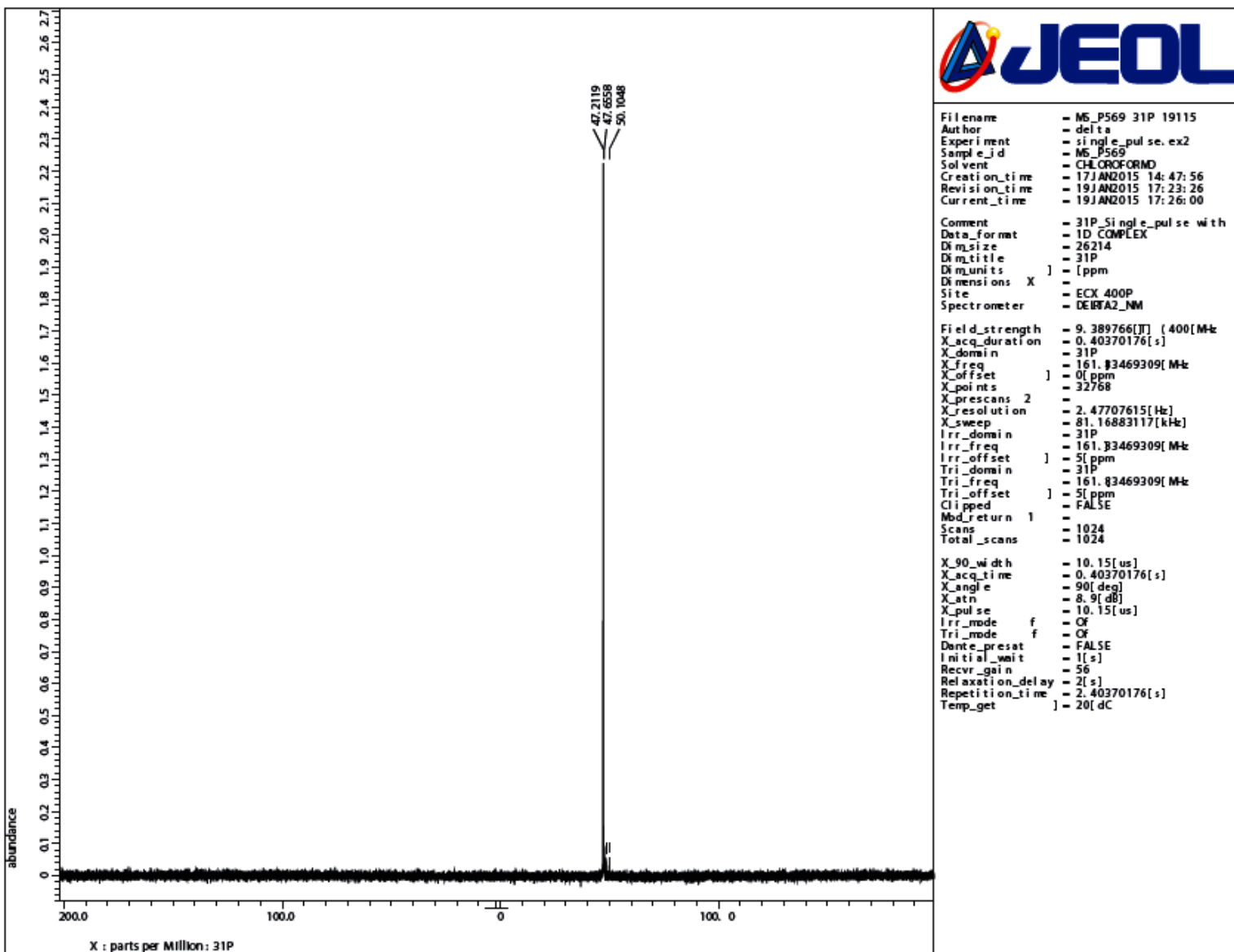


Fig. S38 $^{31}\text{P}\{\text{H}\}$ NMR spectrum of **8/9** (CDCl_3 , 161.8 MHz) at 7.16 μM concentration.

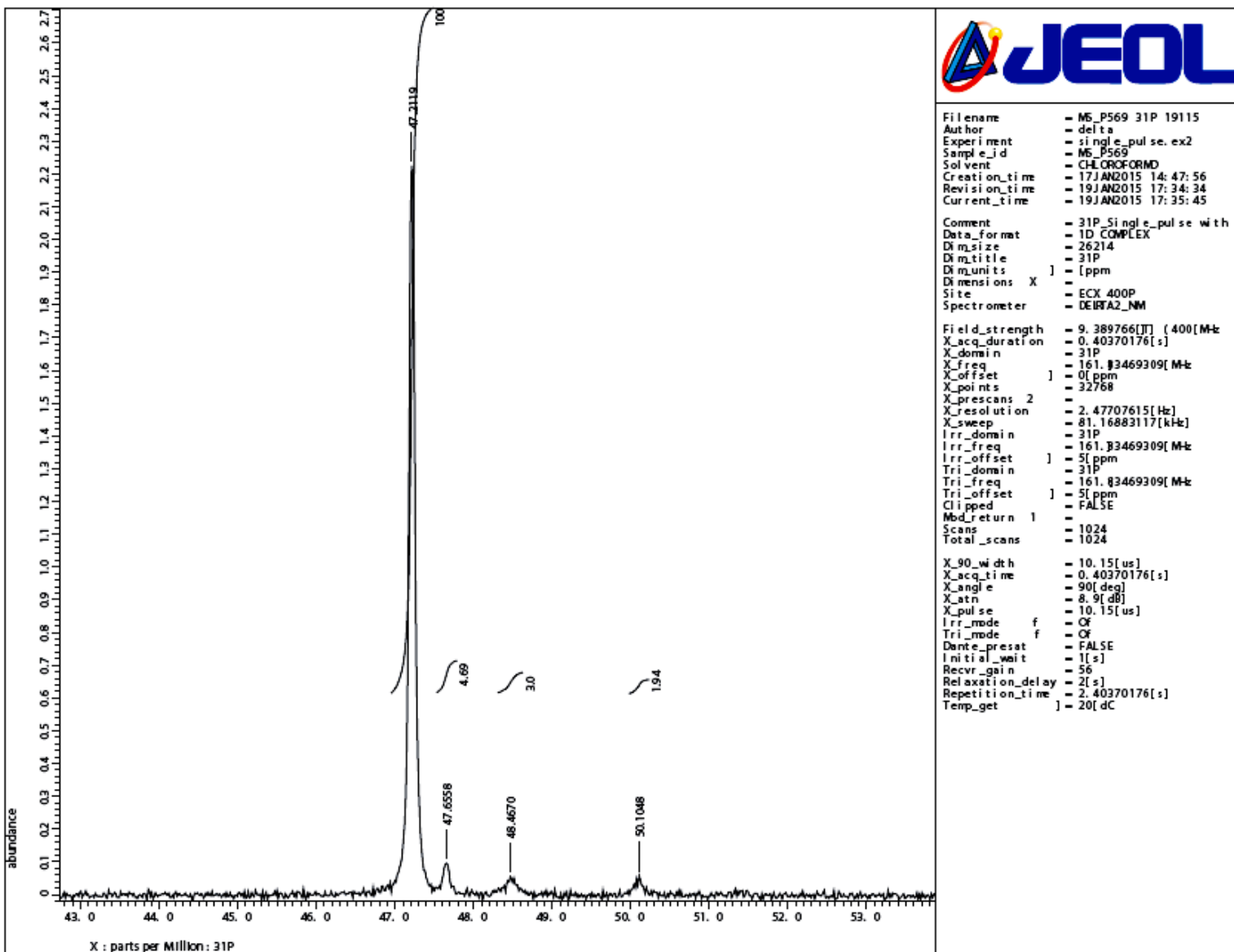


Fig. S39 Expansion of $^{31}\text{P}\{\text{H}\}$ NMR spectrum of **8/9** (CDCl_3 , 161.8 MHz) at 7.16 μM concentration.

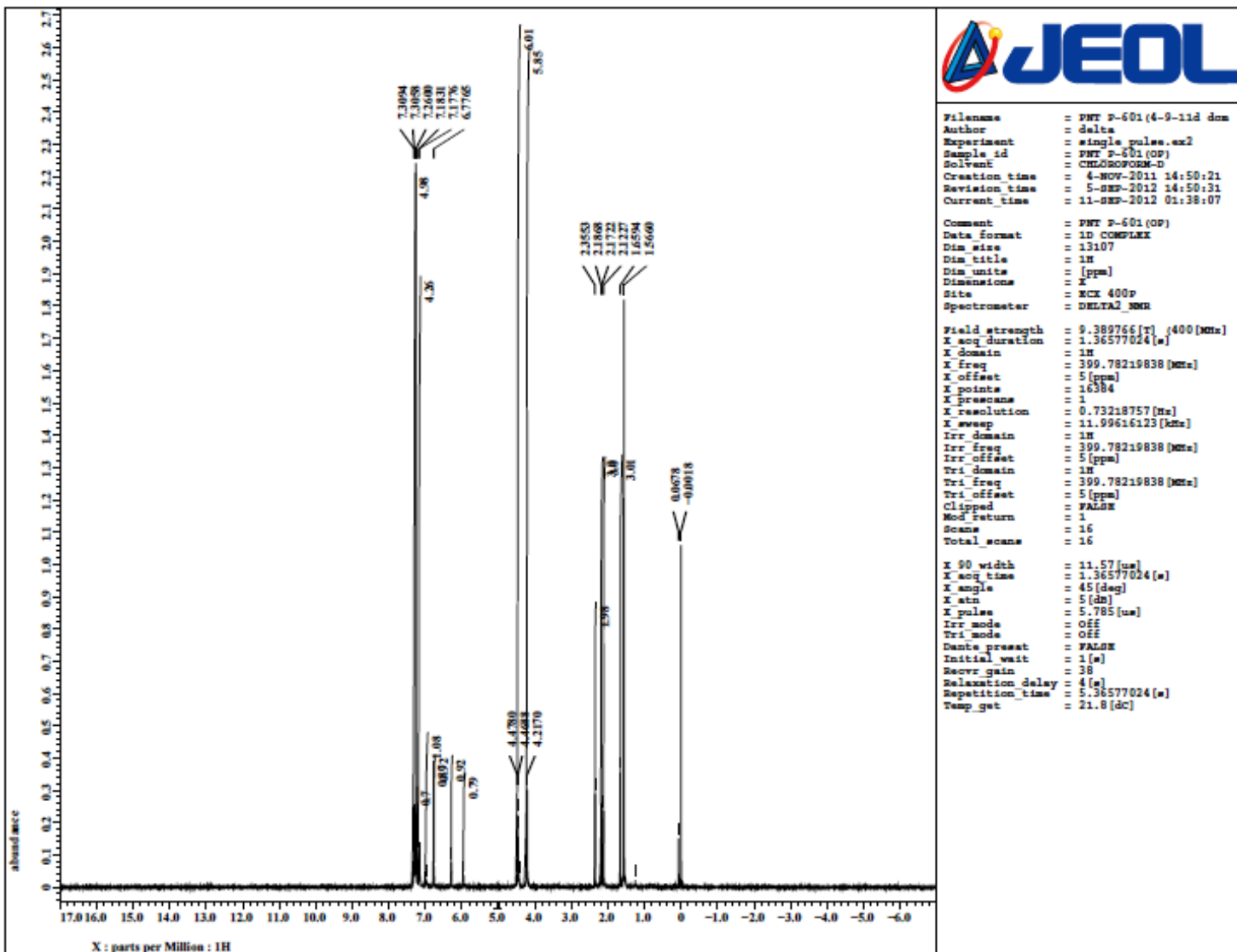


Fig. S40 ^1H NMR spectrum of **10** (CDCl_3 , 400.0 MHz).

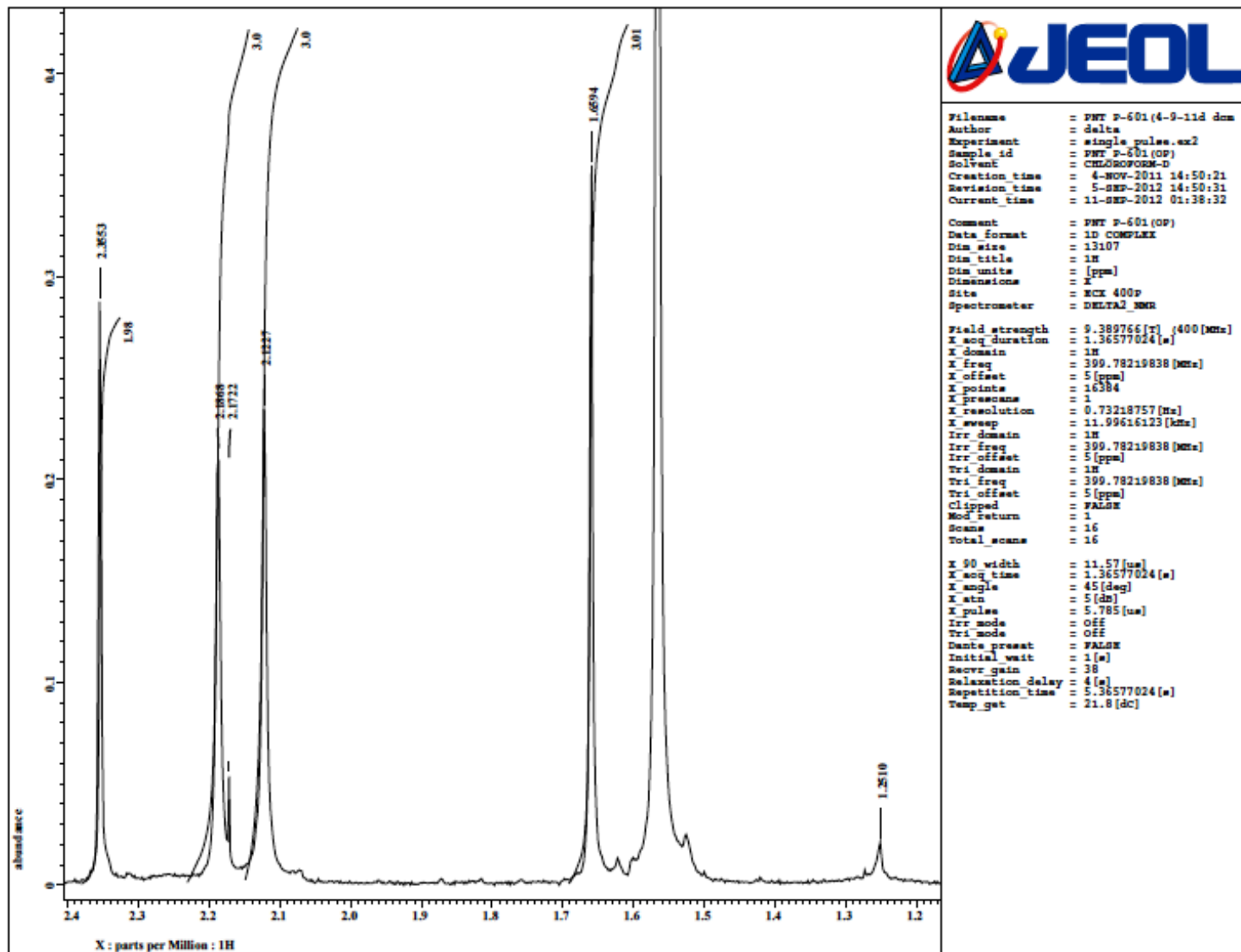


Fig. S41 Expansion of ^1H NMR spectrum of **10** (CDCl_3 , 400.0 MHz).

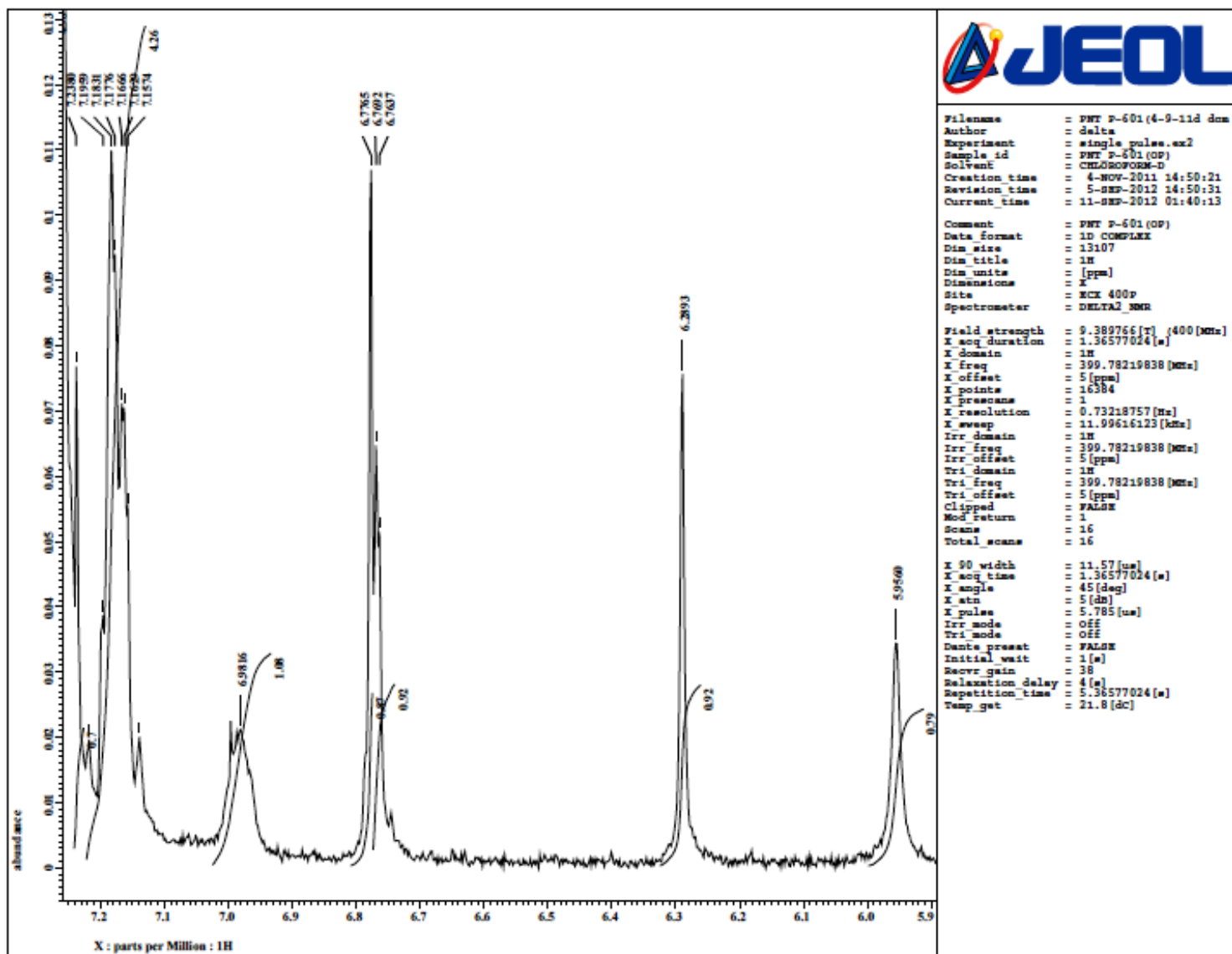


Fig. S42 Expansion of ^1H NMR spectrum of **10** (CDCl_3 , 400.0 MHz).

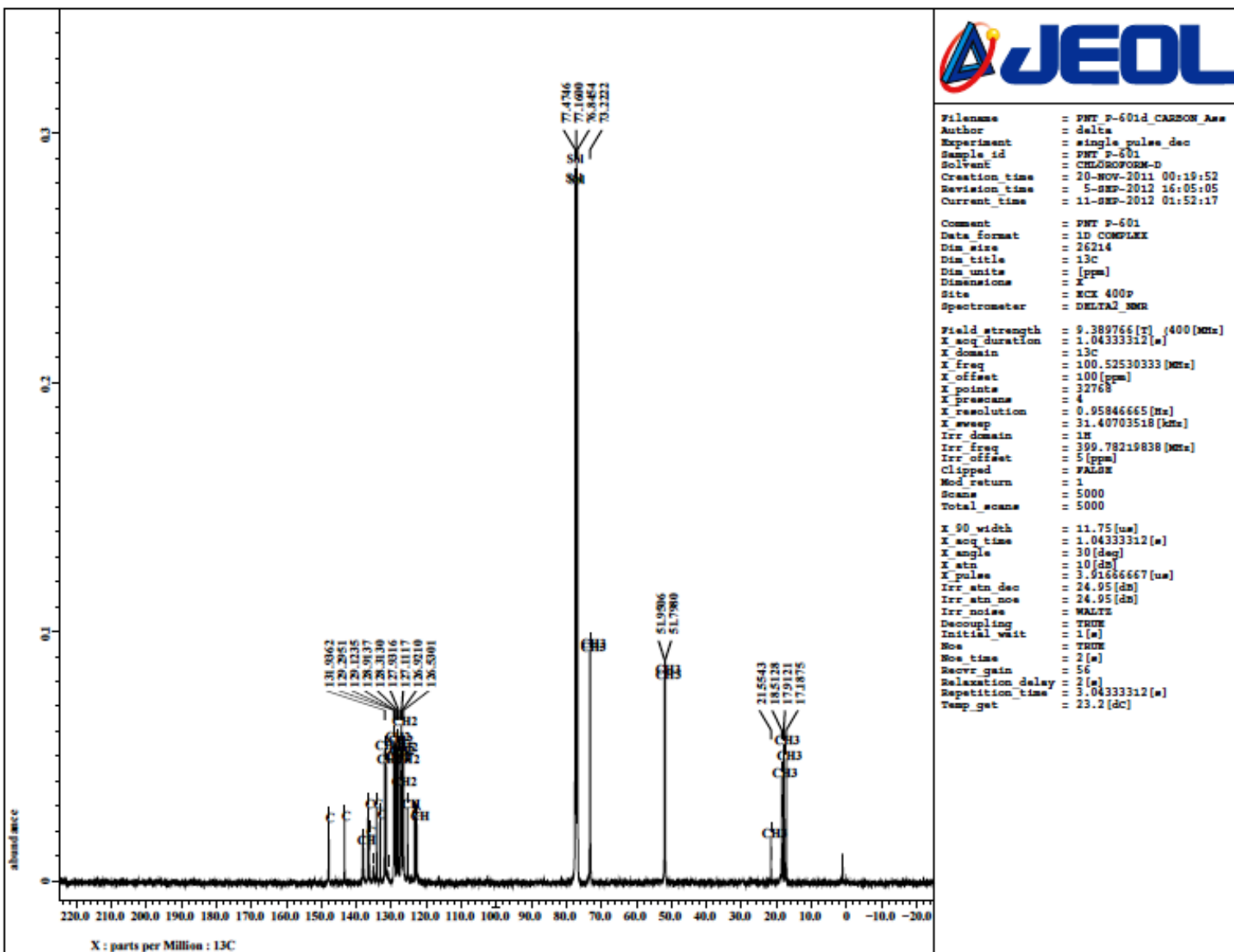


Fig. S43 ^{13}C NMR spectrum of **10** (CDCl_3 , 100.5 MHz).

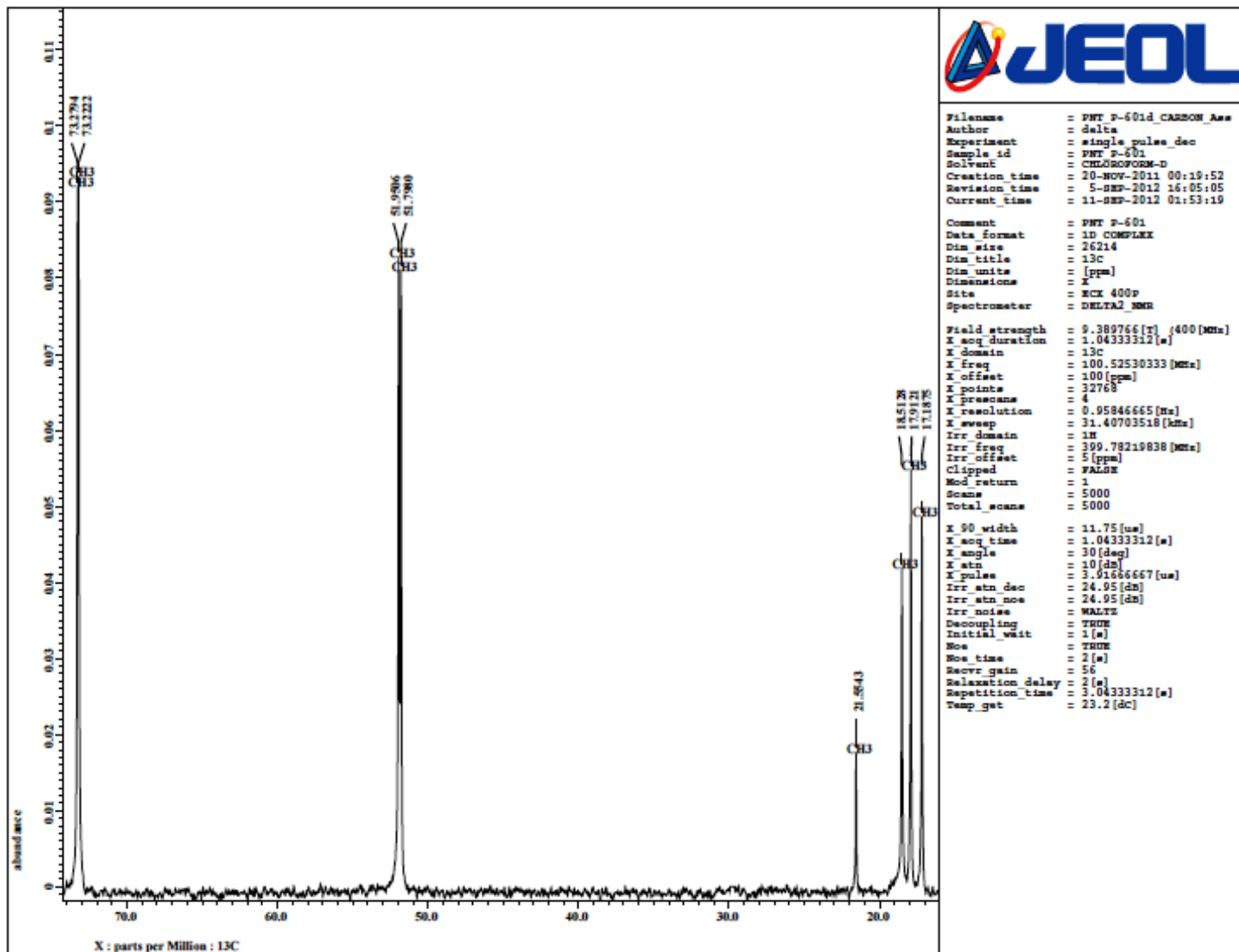


Fig. S44 Expansion of ^{13}C NMR spectrum of **10** (CDCl_3 , 100.5 MHz).

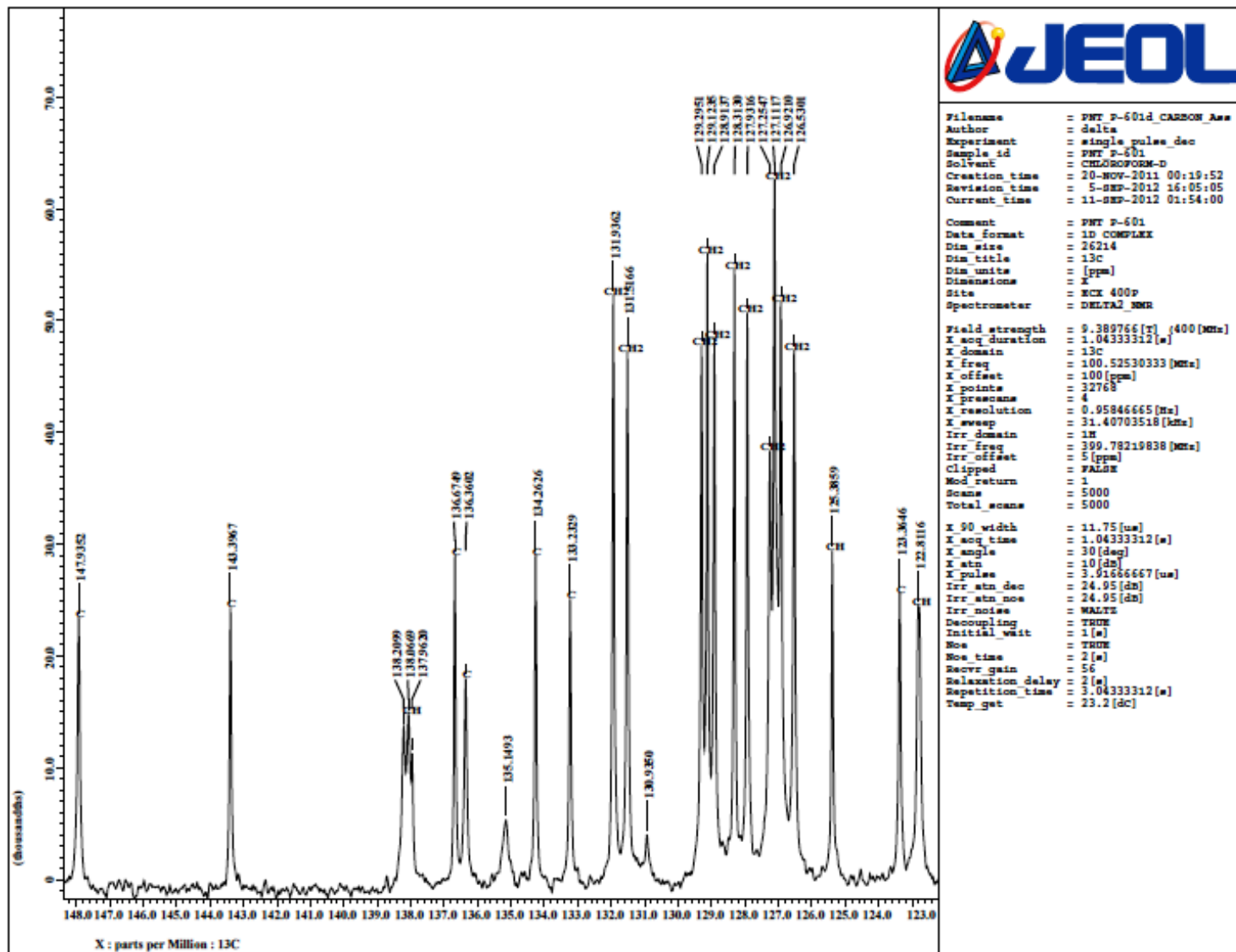


Fig. S45 Expansion of ^{13}C NMR spectrum of **10** (CDCl_3 , 100.5 MHz).

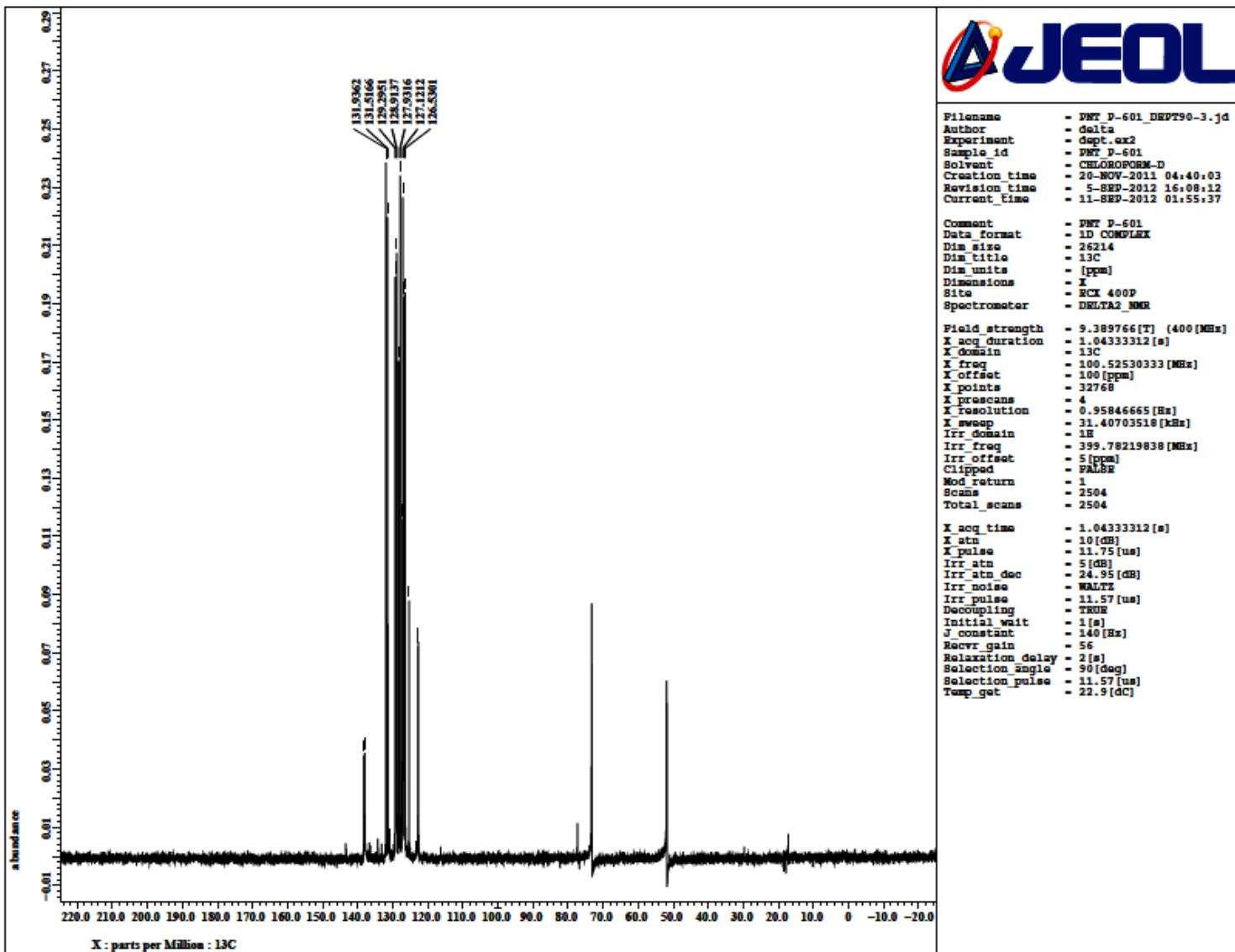


Fig. S46 DEPT 90 NMR spectrum of **10** (CDCl_3 , 100.5 MHz). The peaks around δ 15, 50 and 73 correspond to residual peaks of CH_3 and CH_2 carbons.

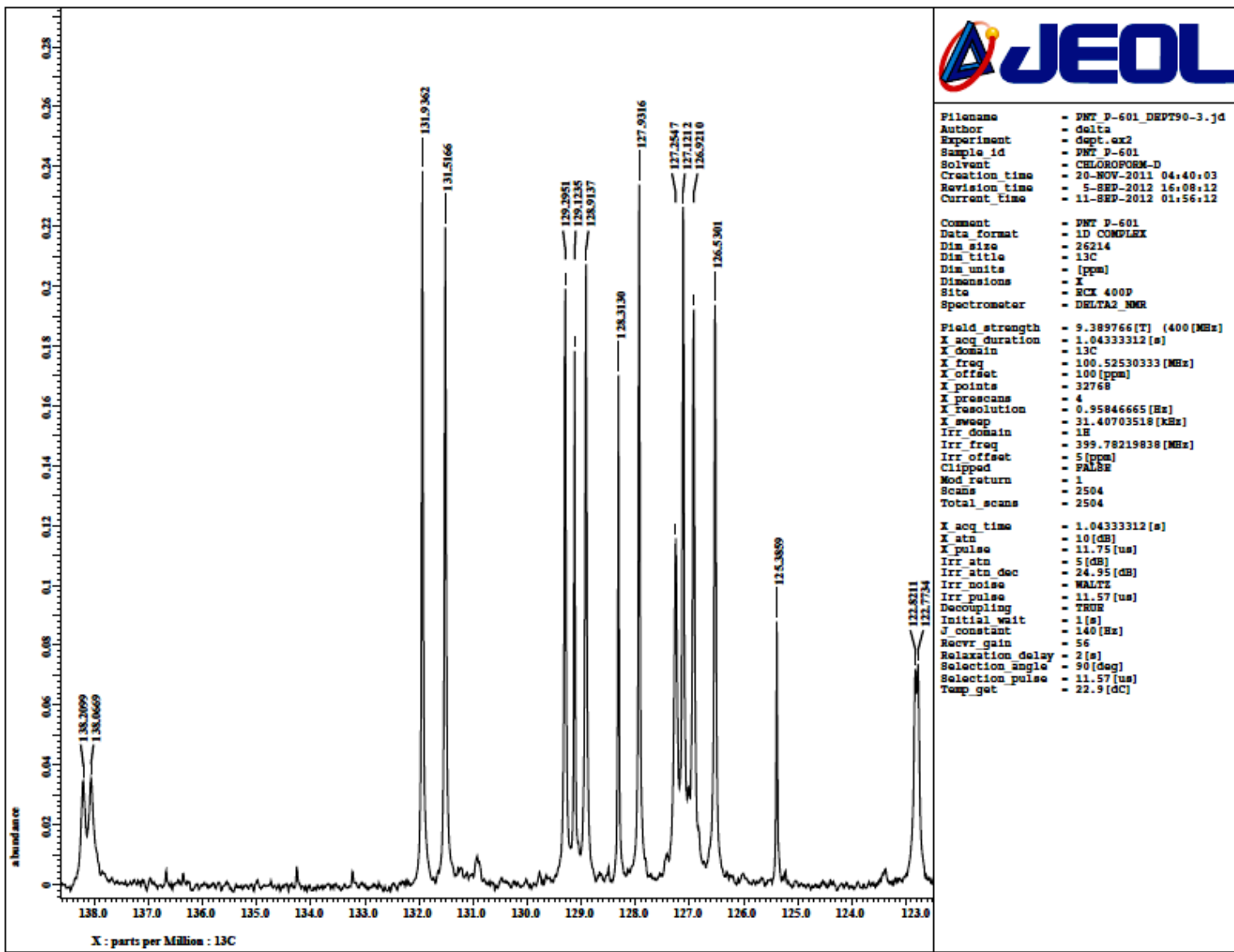


Fig. S47 Expansion of DEPT 90 NMR spectrum of **10**.

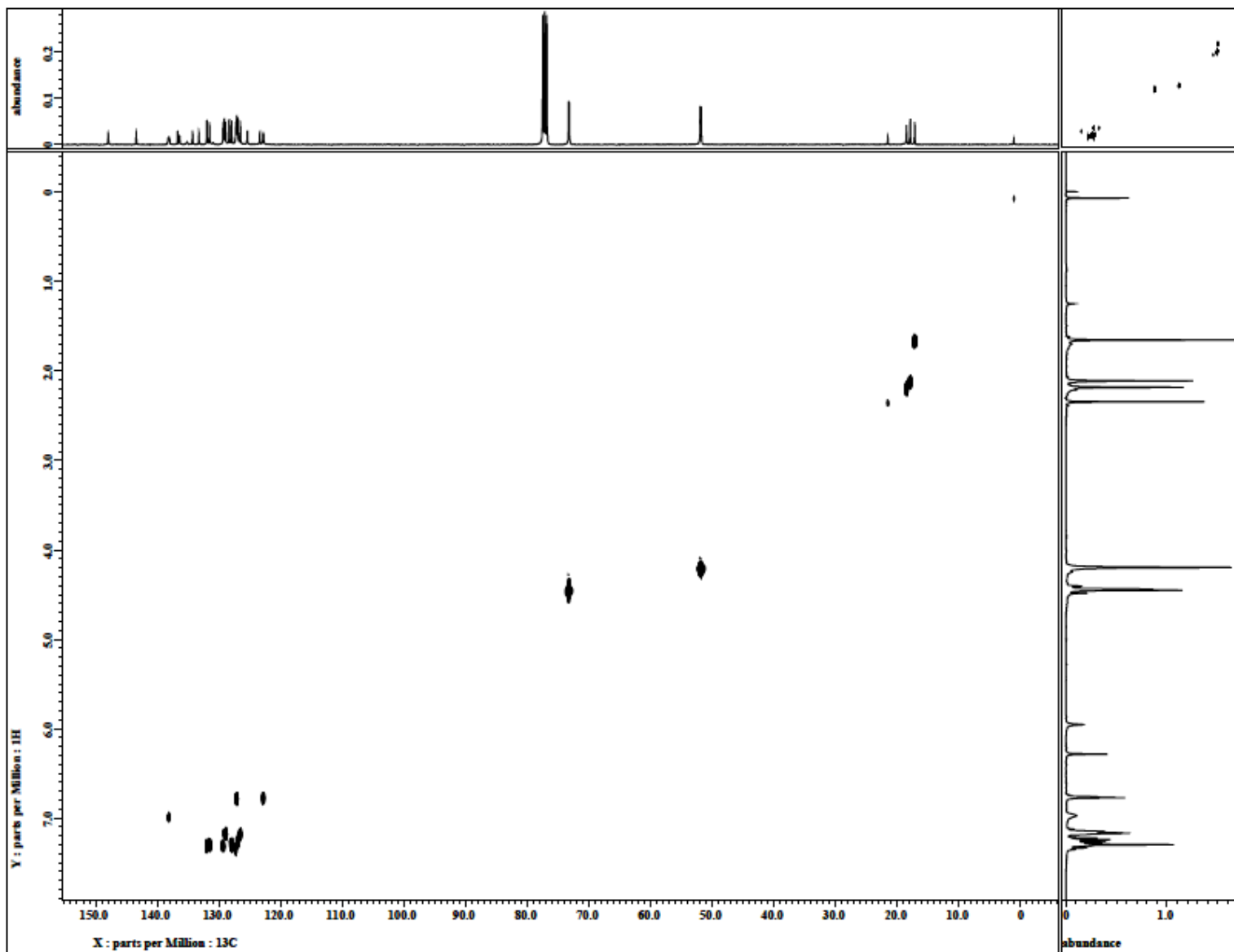


Fig. S48 The ^{13}C - ^1H HETCOR NMR spectrum of **10** (X-axis 100.5 MHz, Y-axis 400 MHz, CDCl_3).

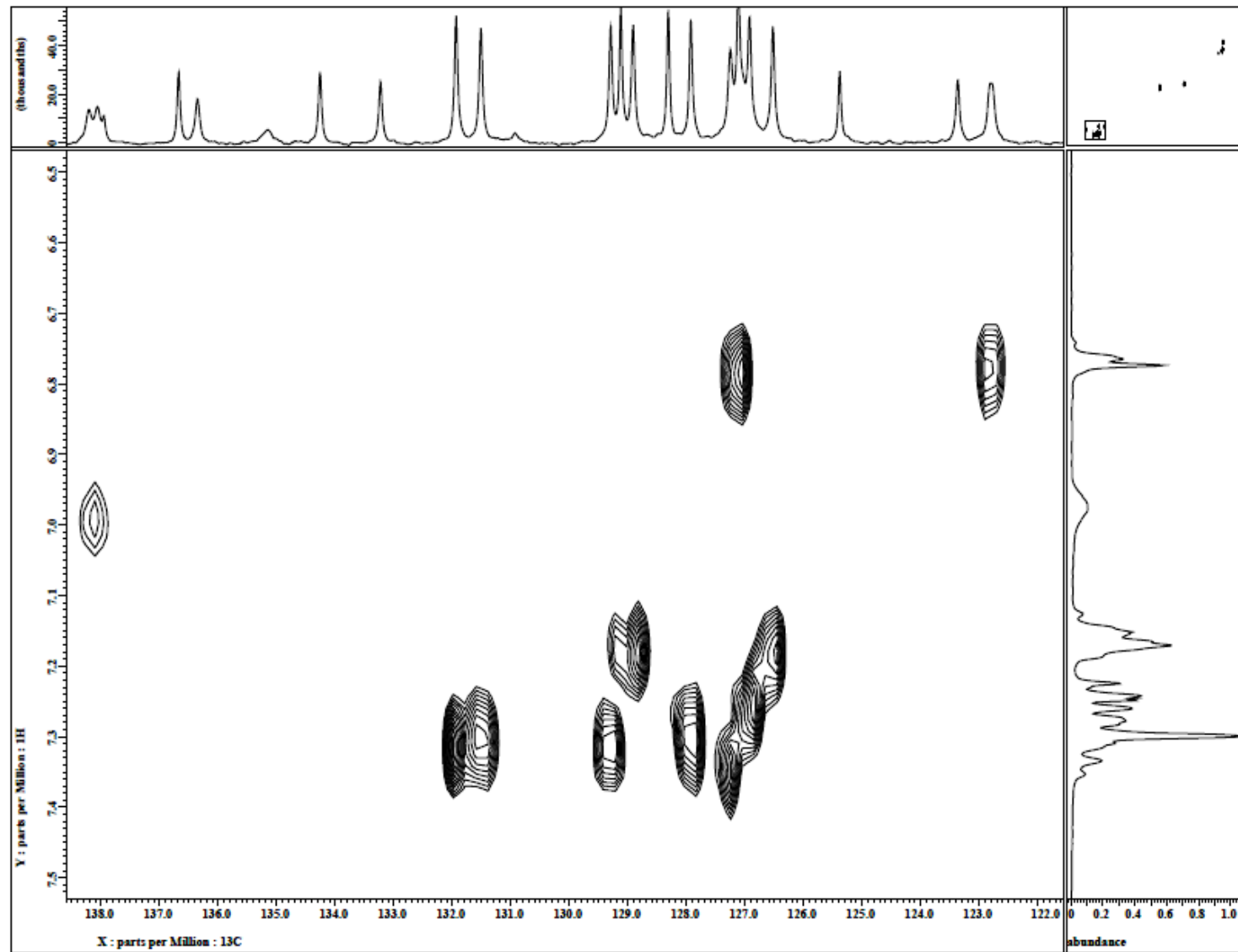


Fig. S49 The $^{13}\text{C}-^1\text{H}$ HETCOR NMR spectrum of **10** illustrated for the ArCH carbons (X-axis 100.5 MHz, Y-axis 400 MHz, CDCl_3).

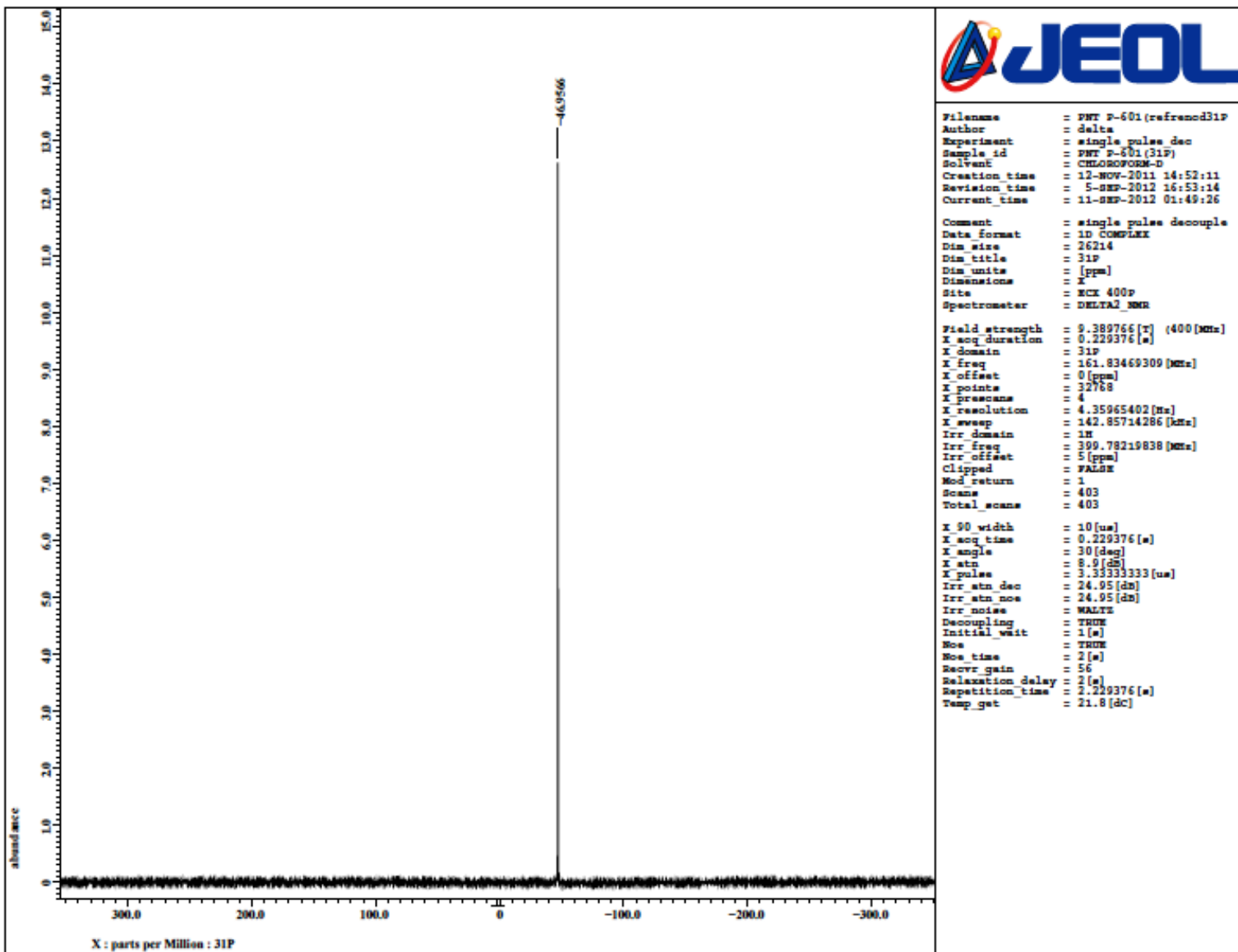


Fig. S50 ${}^3\text{P}\{{}^1\text{H}\}$ NMR spectrum of **10** (CDCl_3 , 161.8 MHz).

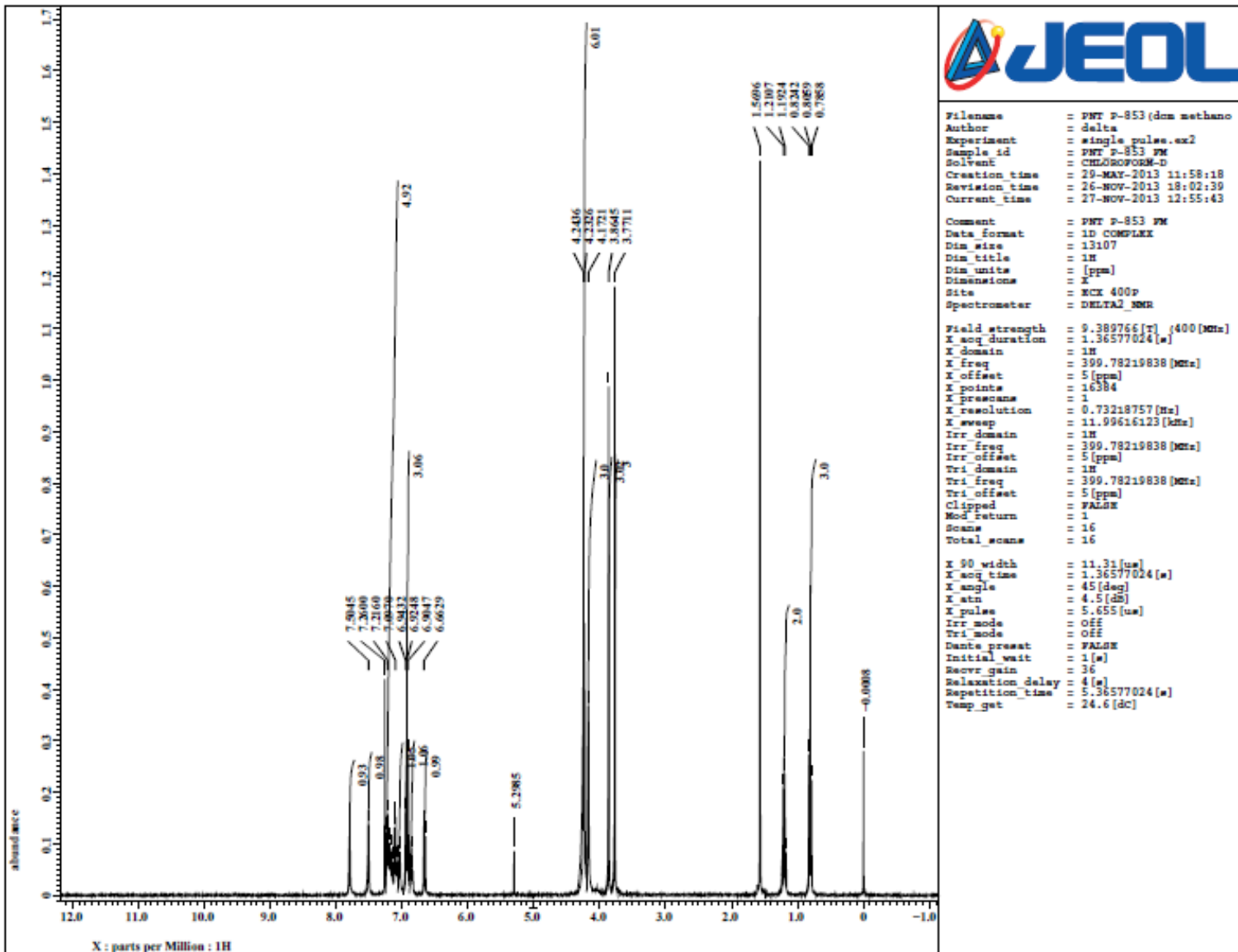


Fig. S51 ^1H NMR spectrum of **11** (CDCl_3 , 400.0 MHz).

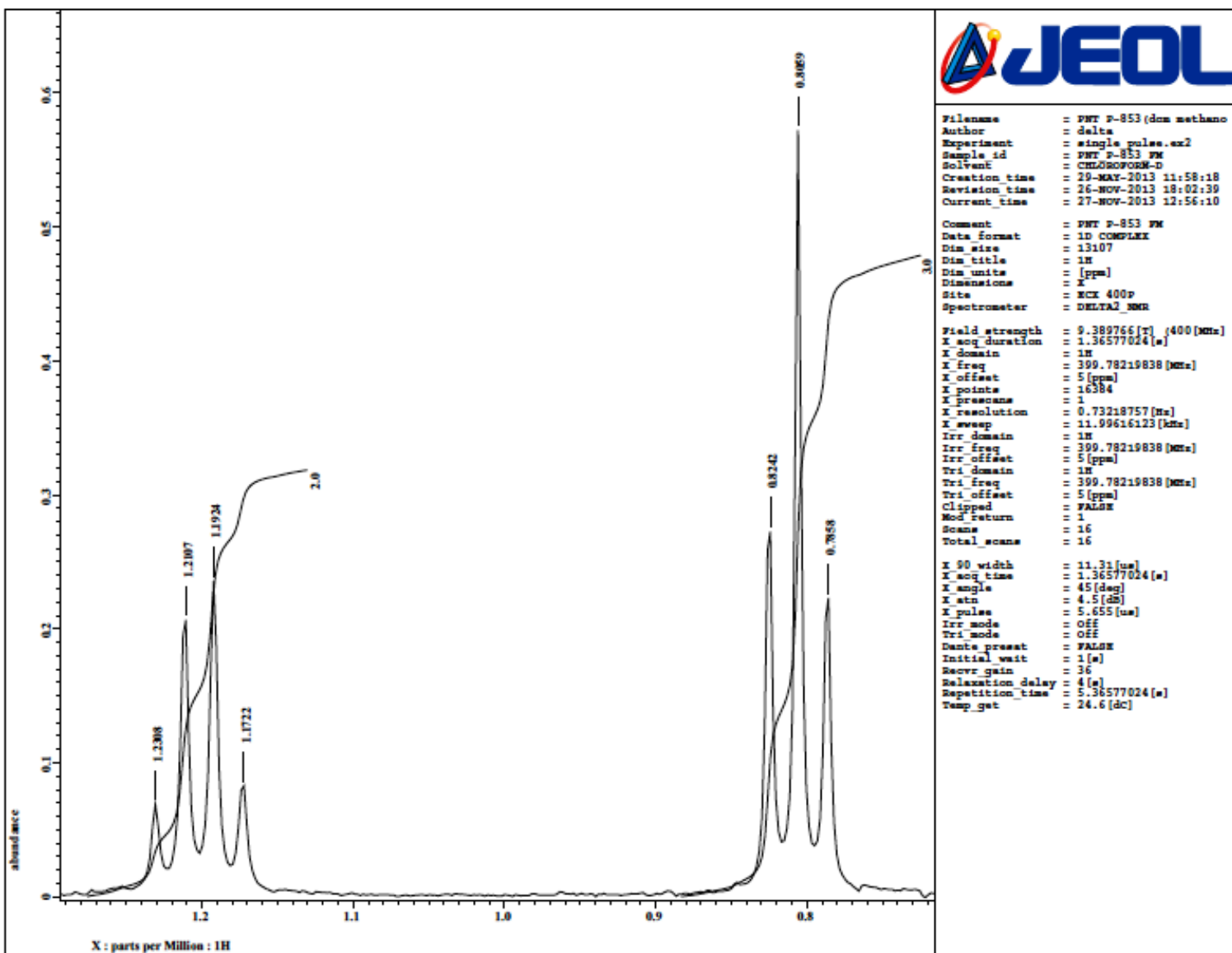


Fig. S52 Expansion of ^1H NMR spectrum of **11** (CDCl_3 , 400.0 MHz).

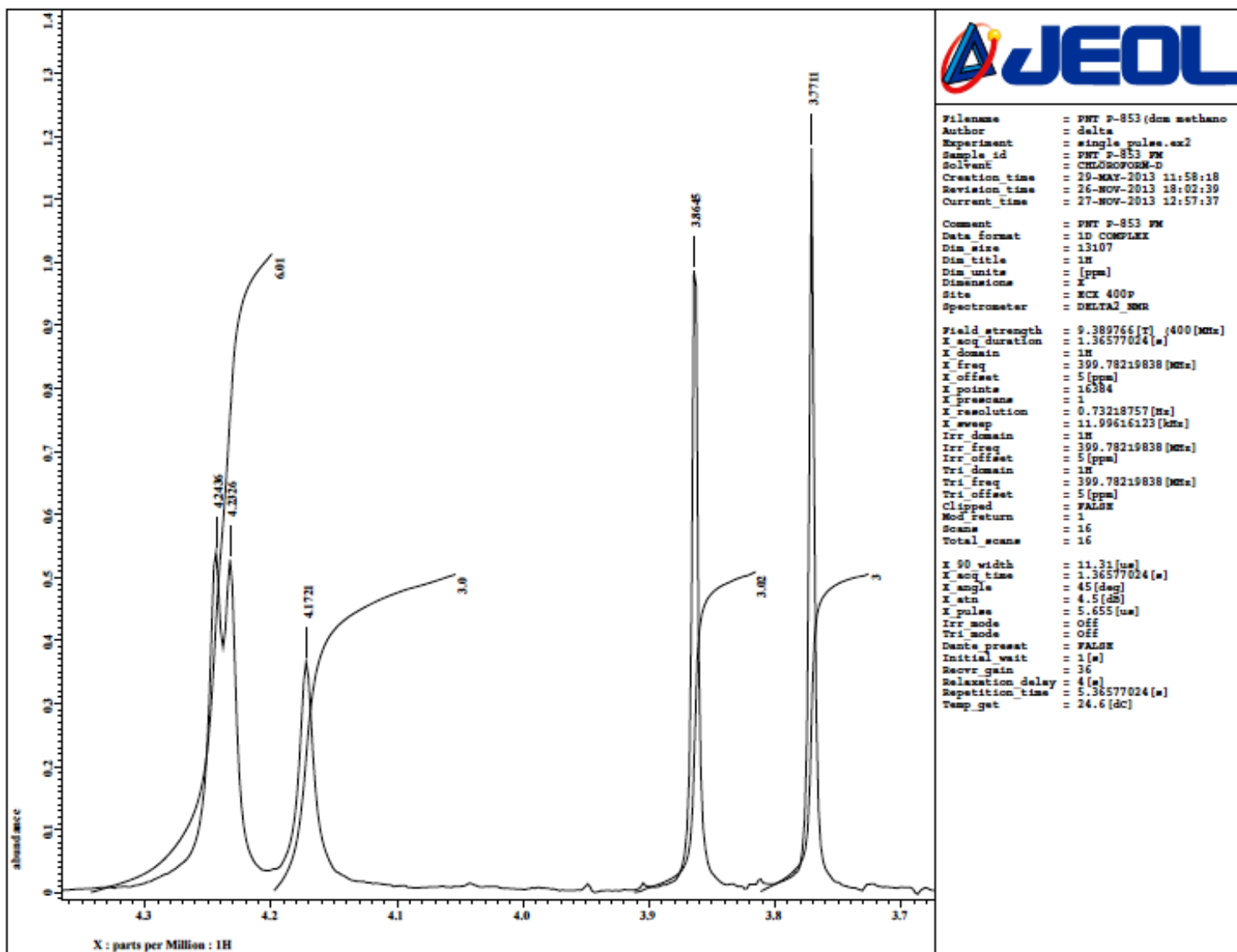


Fig. S53 Expansion of ¹H NMR spectrum of **11** (CDCl₃, 400.0 MHz).

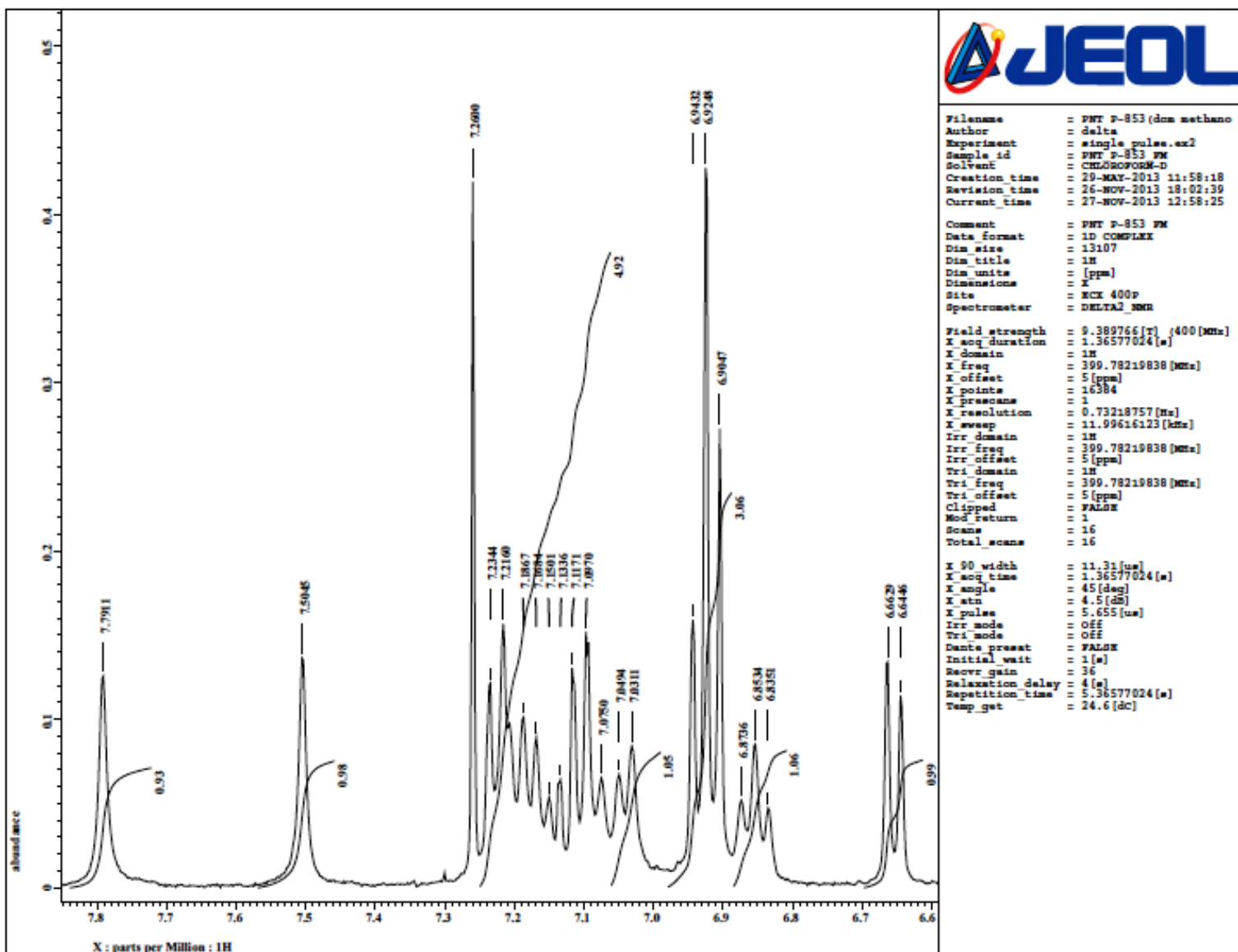


Fig. S54 Expansion of ^1H NMR spectrum of **11** (CDCl_3 , 400.0 MHz).

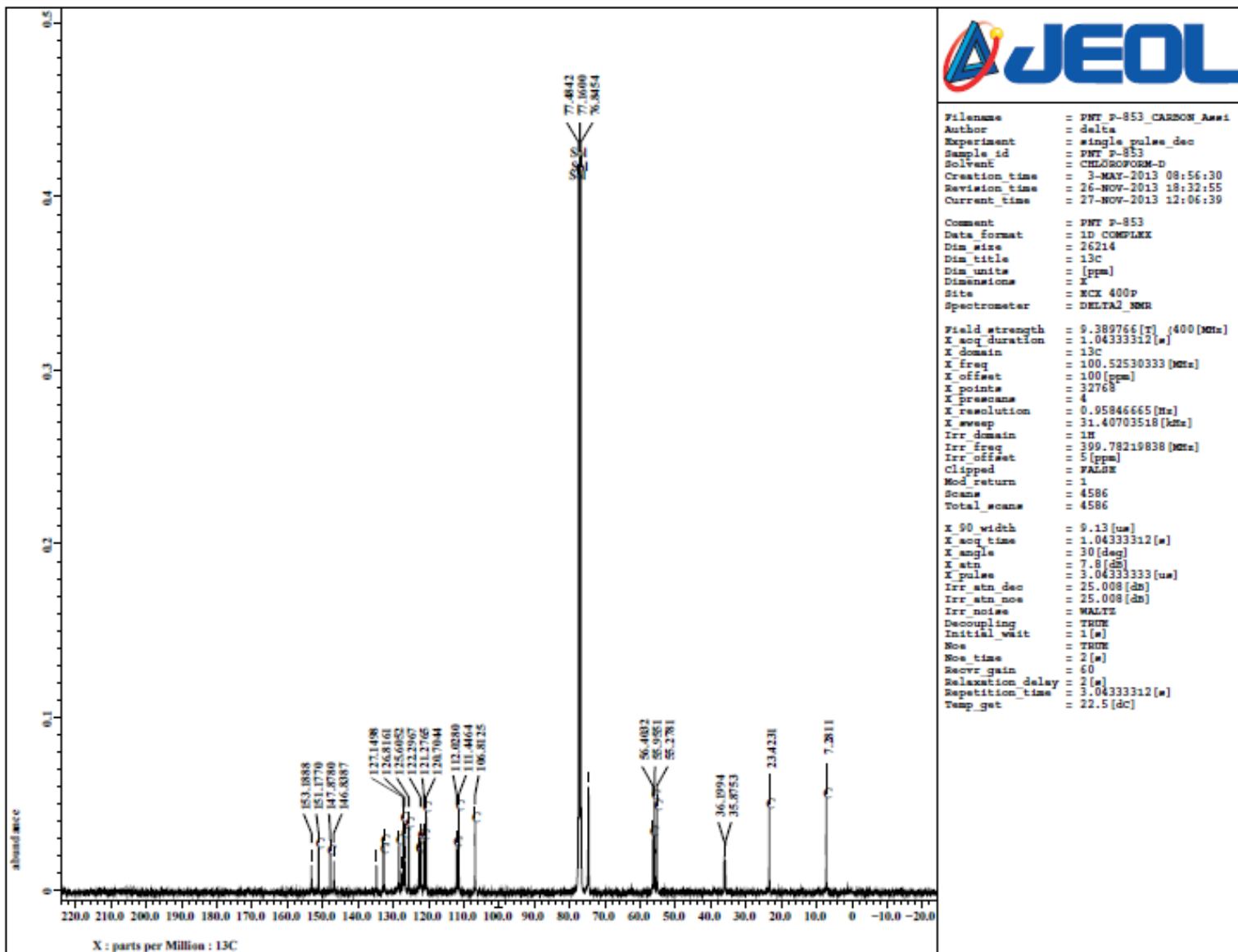


Fig. S55 ^{13}C NMR spectrum of **11** (CDCl_3 , 100.5 MHz).

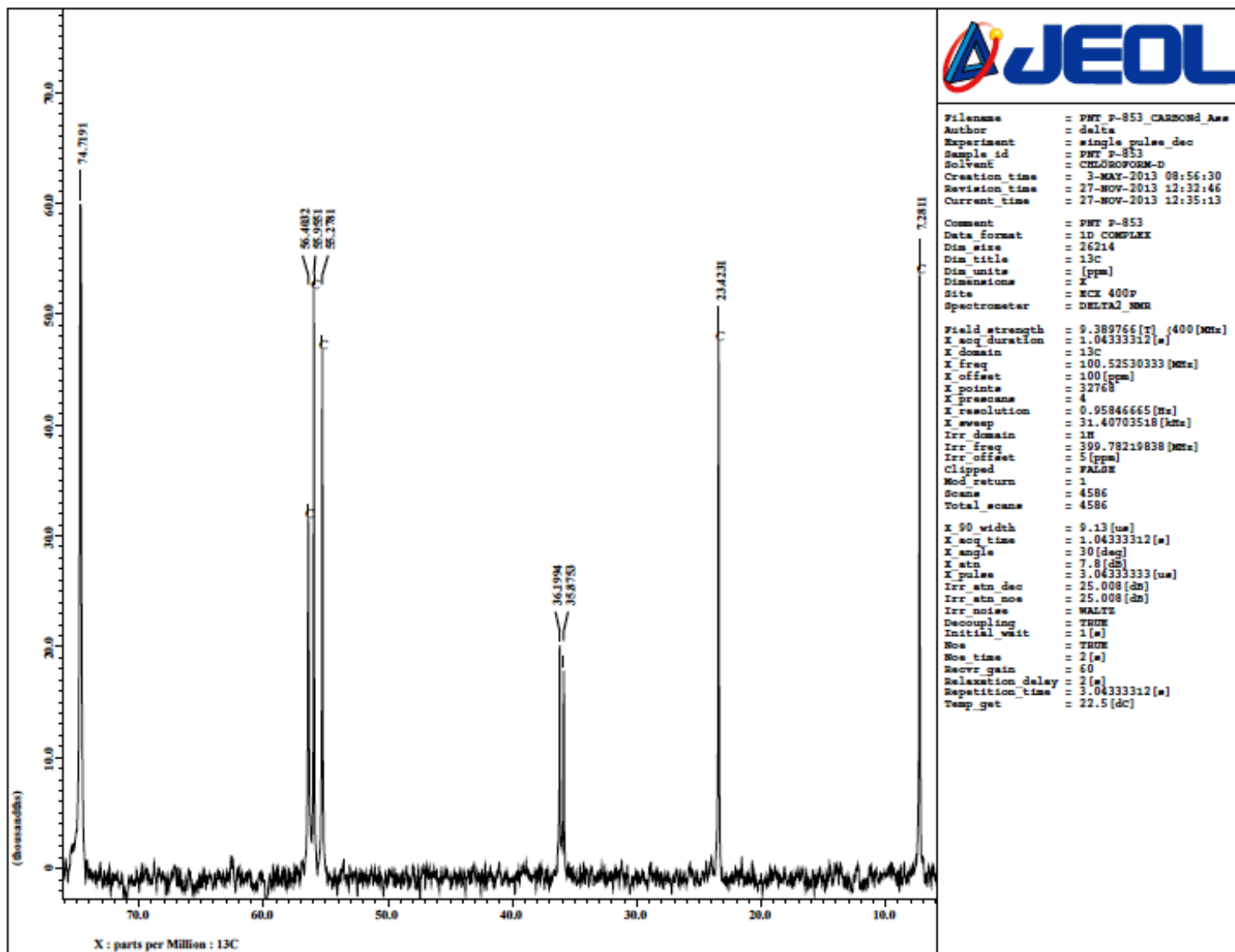


Fig. S56 Expansion of ^{13}C NMR spectrum of **11** (CDCl_3 , 100.5 MHz).

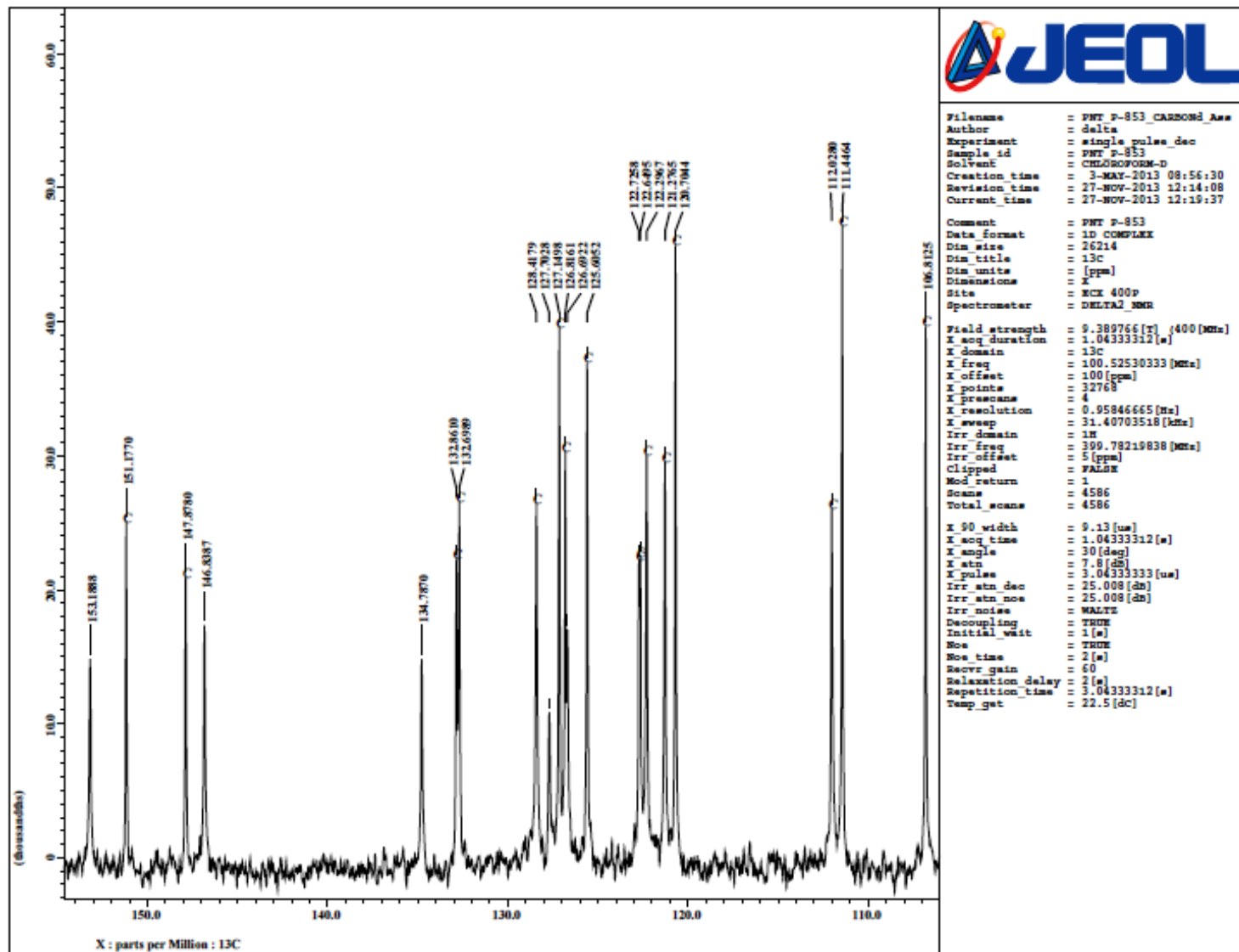


Fig. S57 Expansion of ^{13}C NMR spectrum of **11** (CDCl_3 , 100.5 MHz).

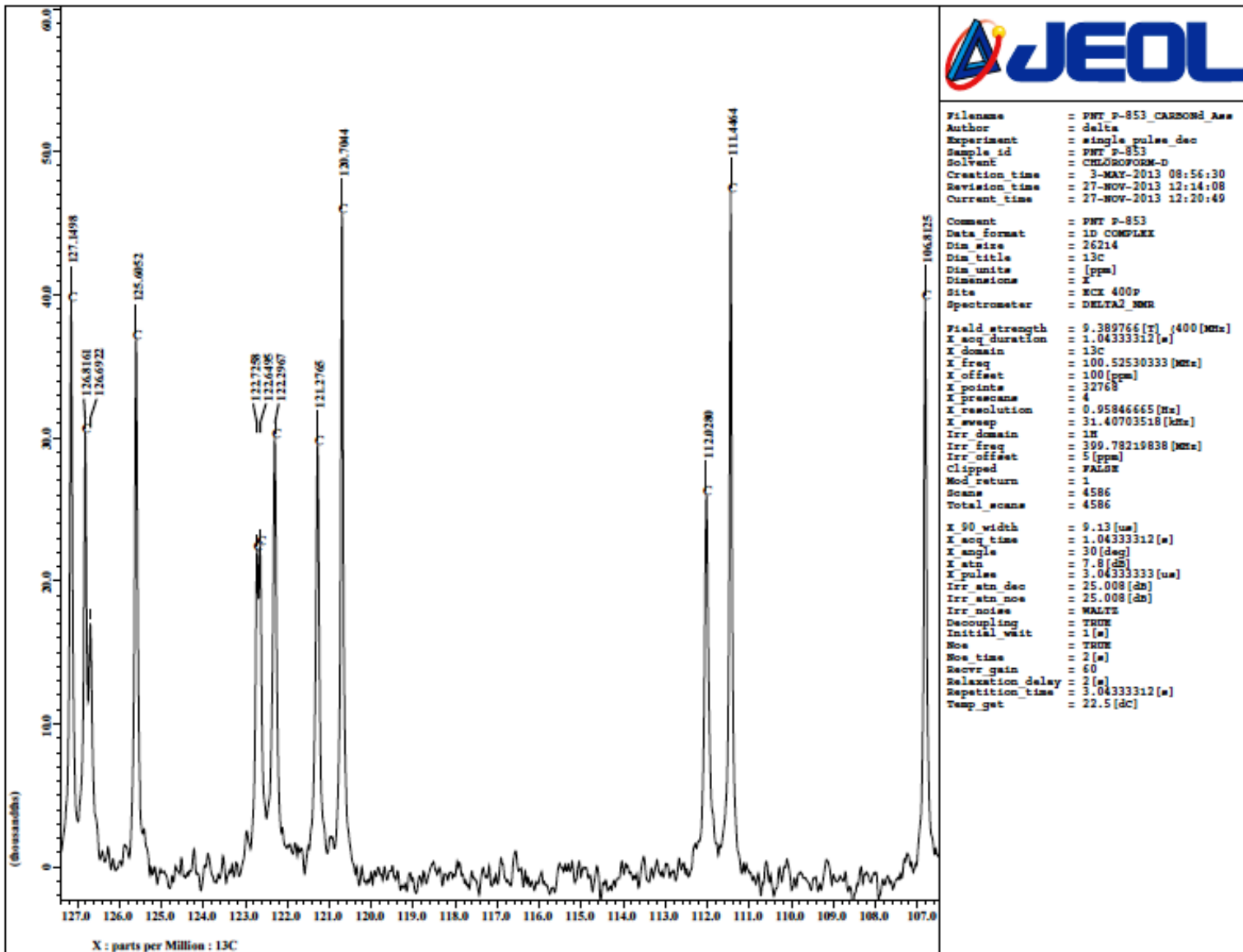


Fig. S58 Expansion of ^{13}C NMR spectrum of **11** (CDCl_3 , 100.5 MHz).

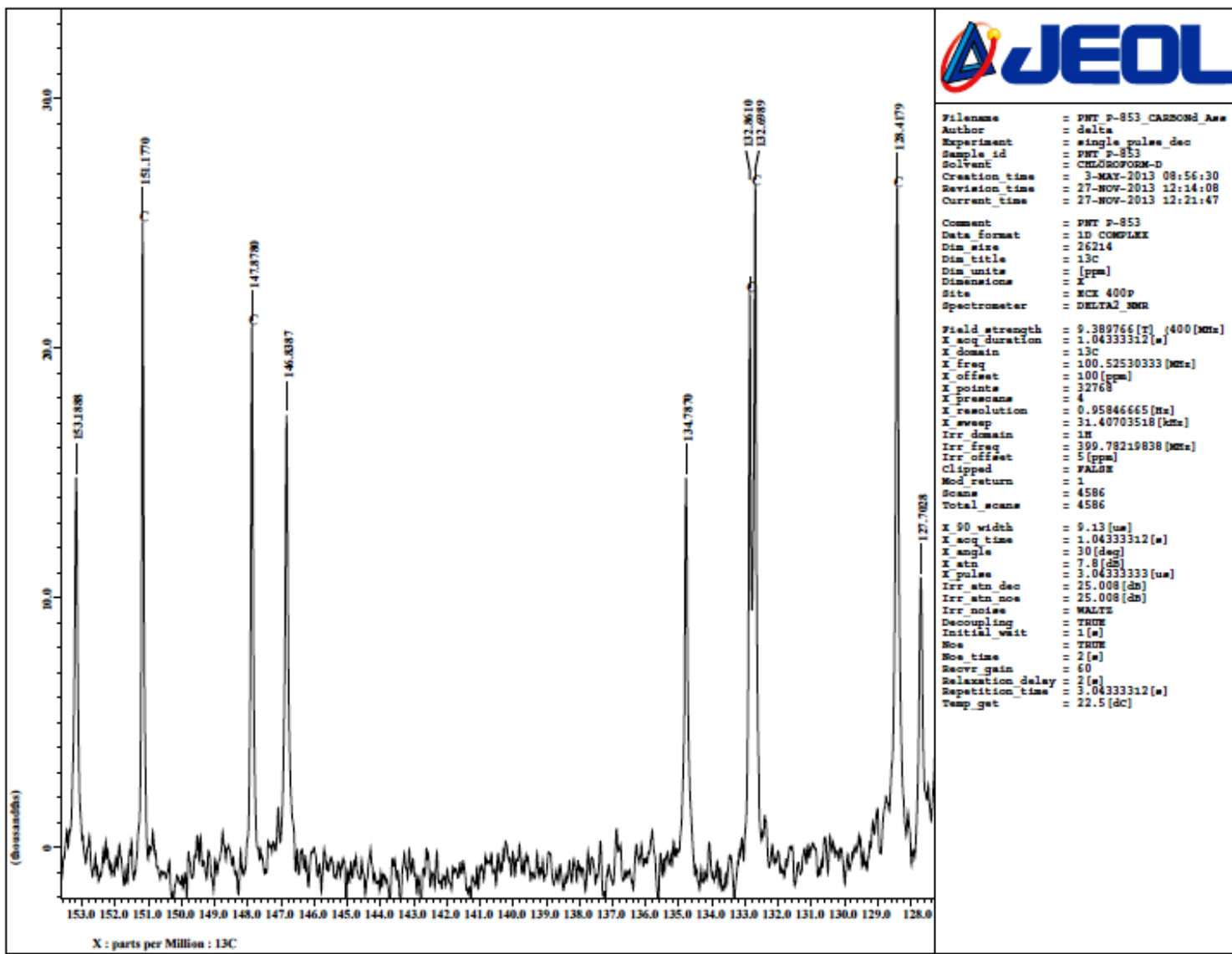


Fig. S59 Expansion of ^{13}C NMR spectrum of **11** (CDCl_3 , 100.5 MHz).

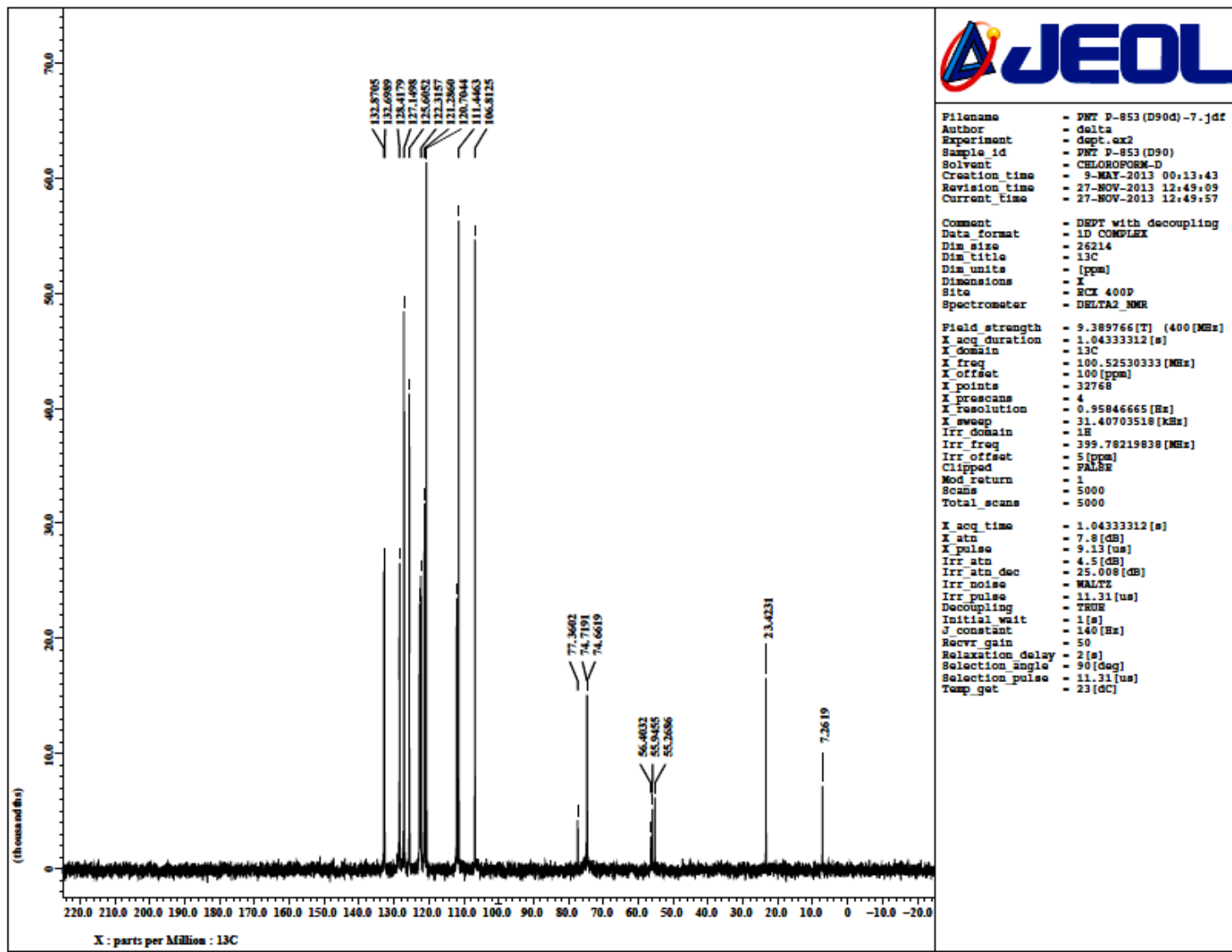


Fig. S60 DEPT 90 NMR spectrum of **11** (CDCl_3 , 100.5 MHz). The peaks around δ 7–75 correspond to residual peaks of C, CH_2 , CH_3 , OCH_2 or OCH_3 carbons.

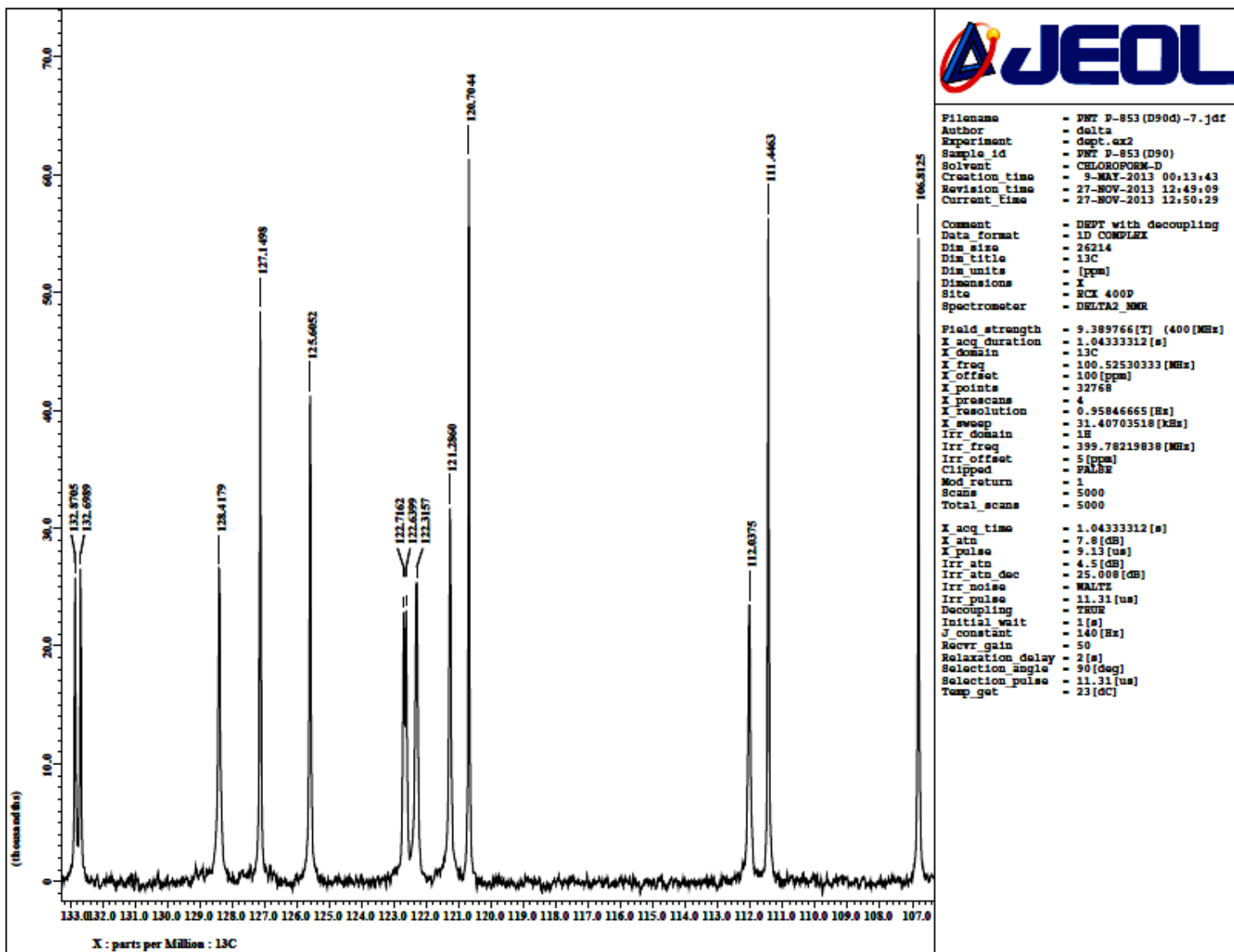


Fig. S61 Expansion of DEPT 90 NMR spectrum of **11**.

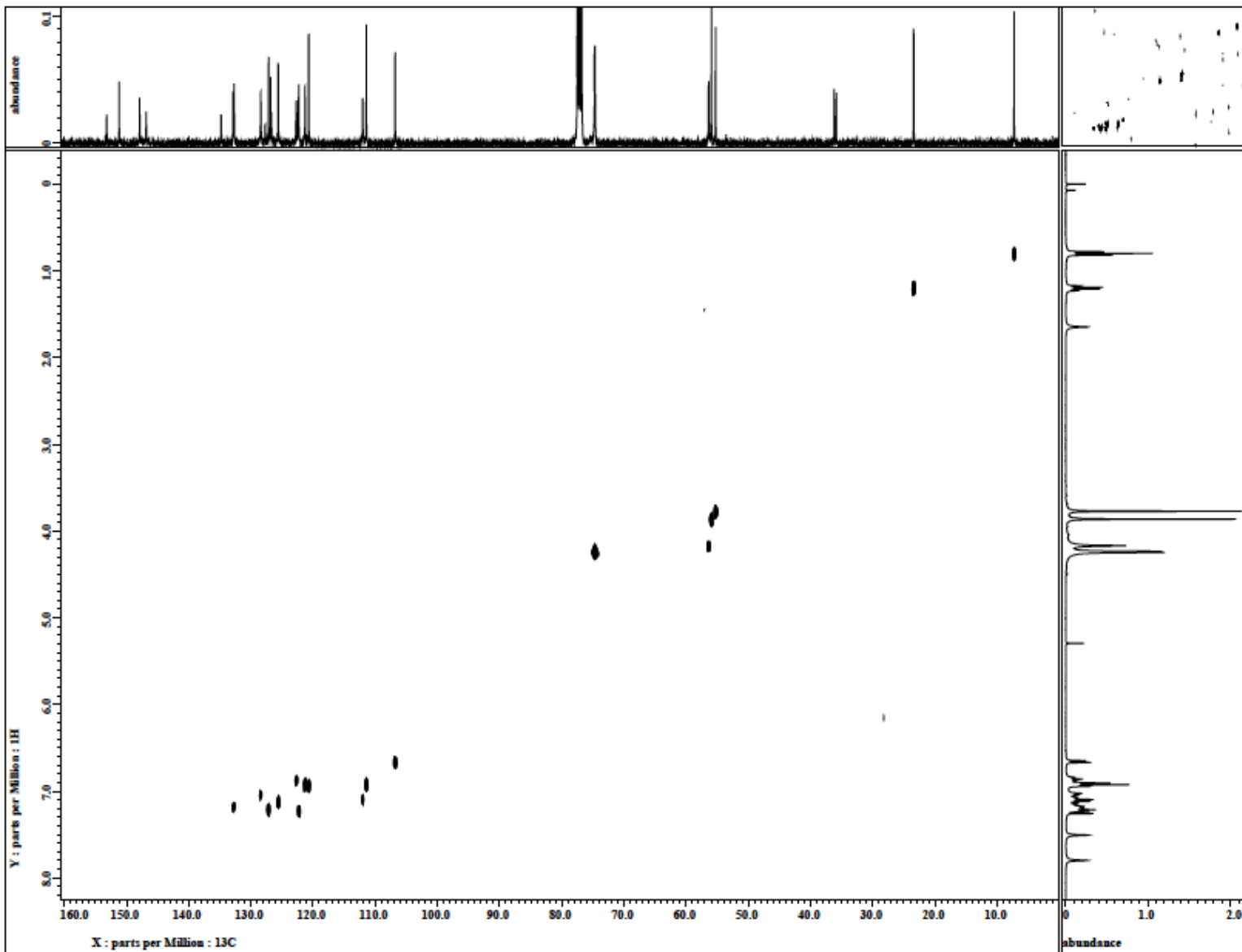


Fig. S62 The ^{13}C - ^1H HETCOR NMR spectrum of **11** (X-axis 100.5 MHz, Y-axis 400 MHz, CDCl_3).

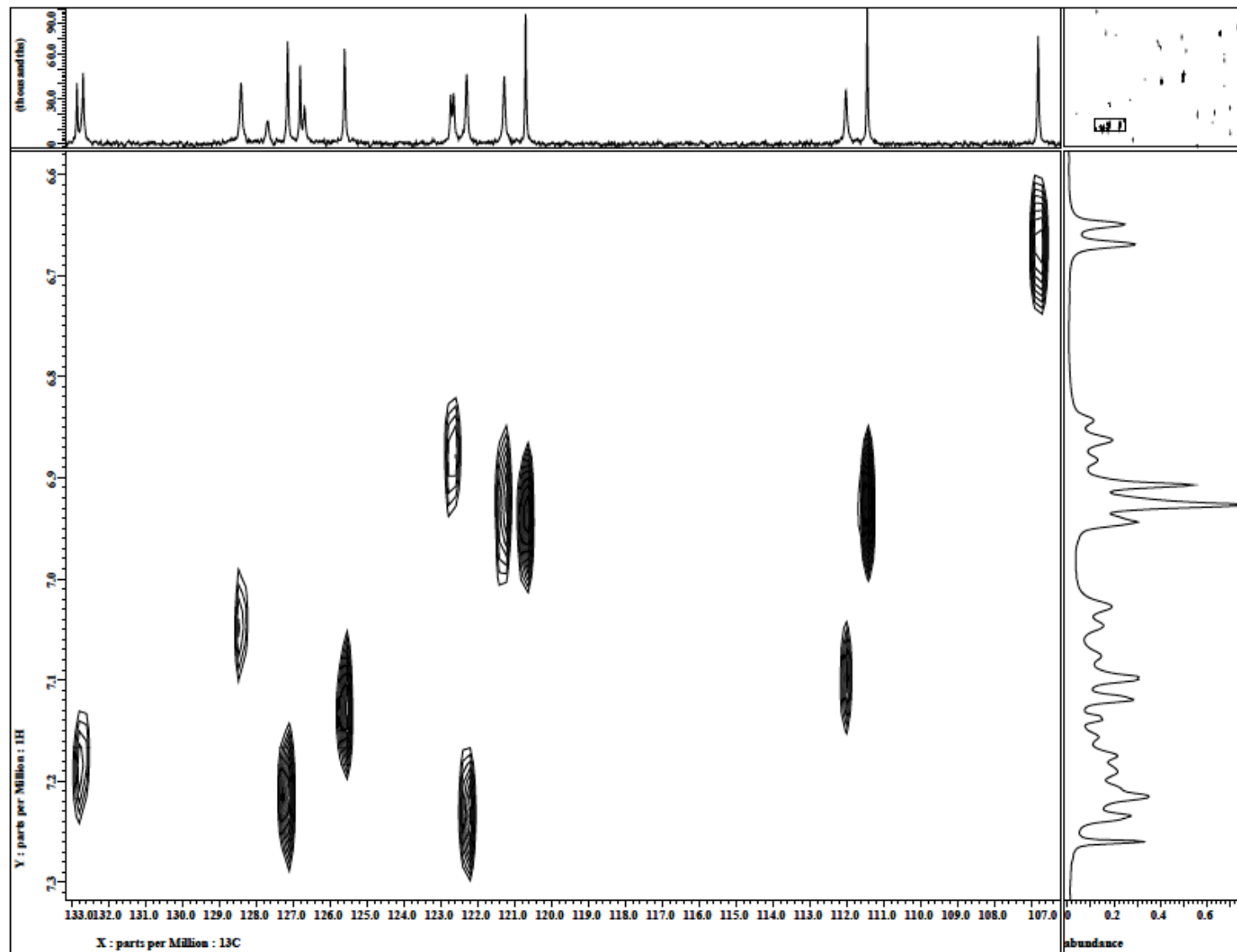


Fig. S63 The ^{13}C - ^1H HETCOR NMR spectrum of **11** illustrated for the ArCH carbons (X-axis 100.5 MHz, Y-axis 400 MHz, CDCl_3).

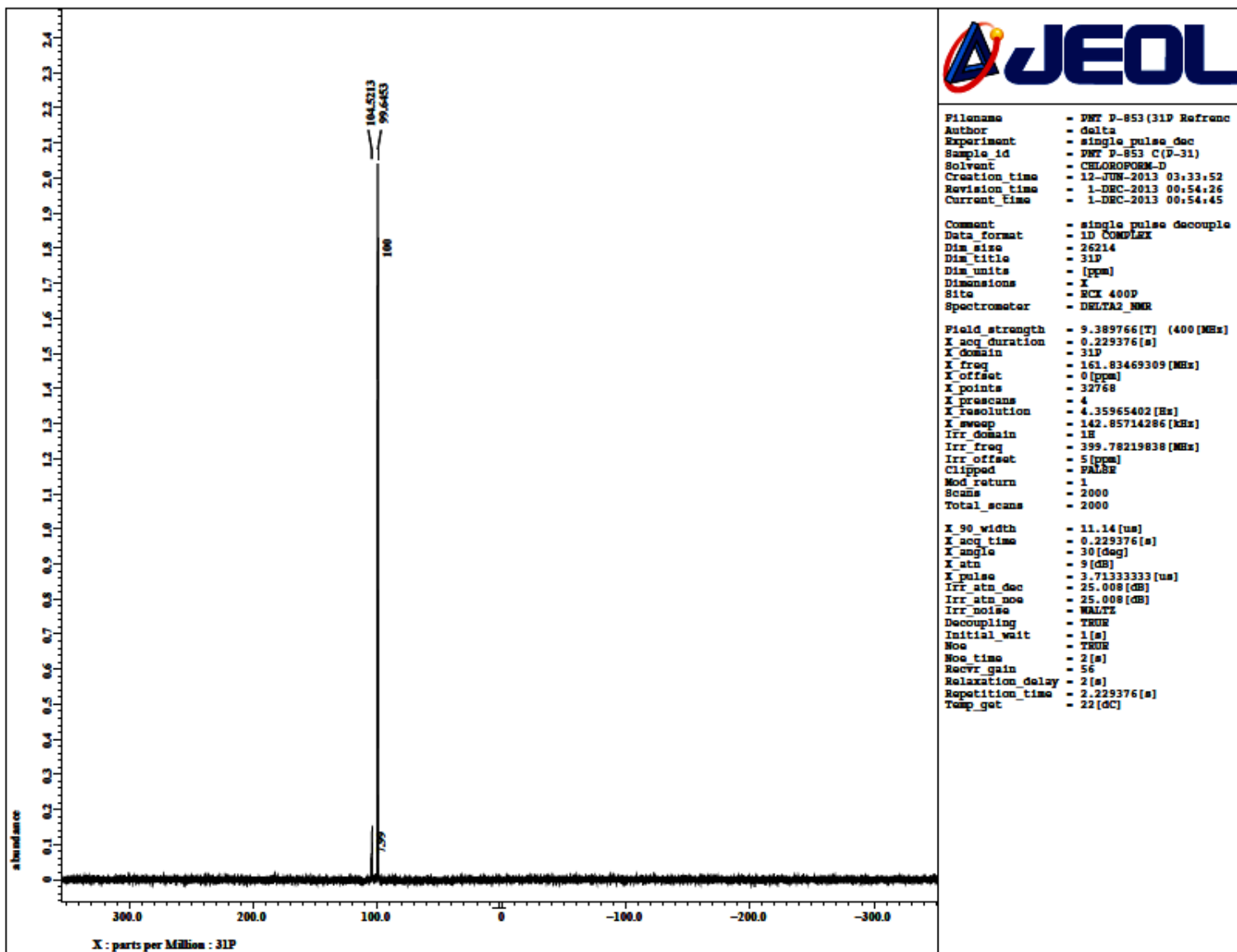


Fig. S64 $^{31}\text{P}\{\text{H}\}$ NMR spectrum of **11** (CDCl_3 , 161.8 MHz).

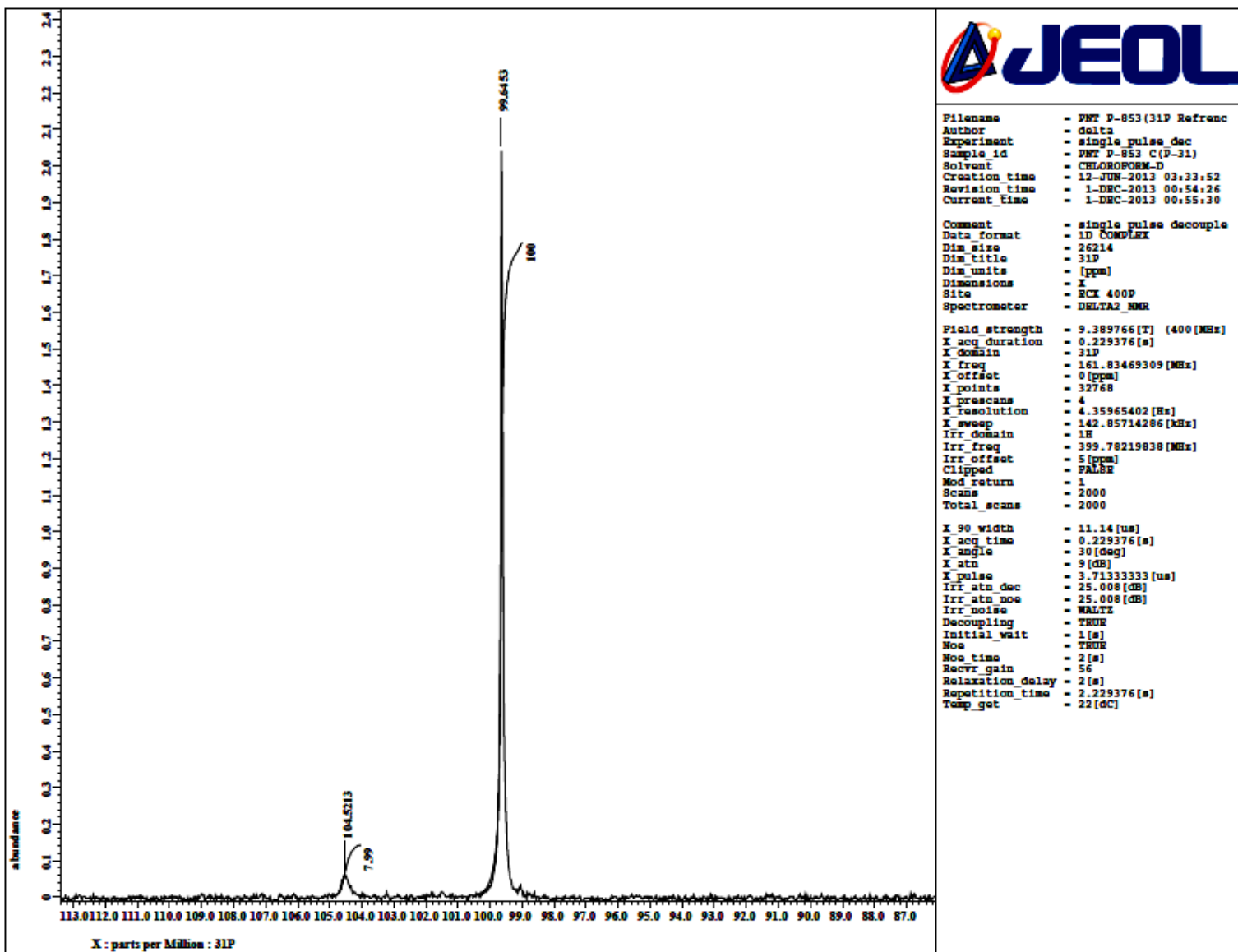


Fig. S65 Expansion of $^{31}\text{P}\{\text{H}\}$ NMR spectrum of **11** (CDCl_3 , 161.8 MHz).

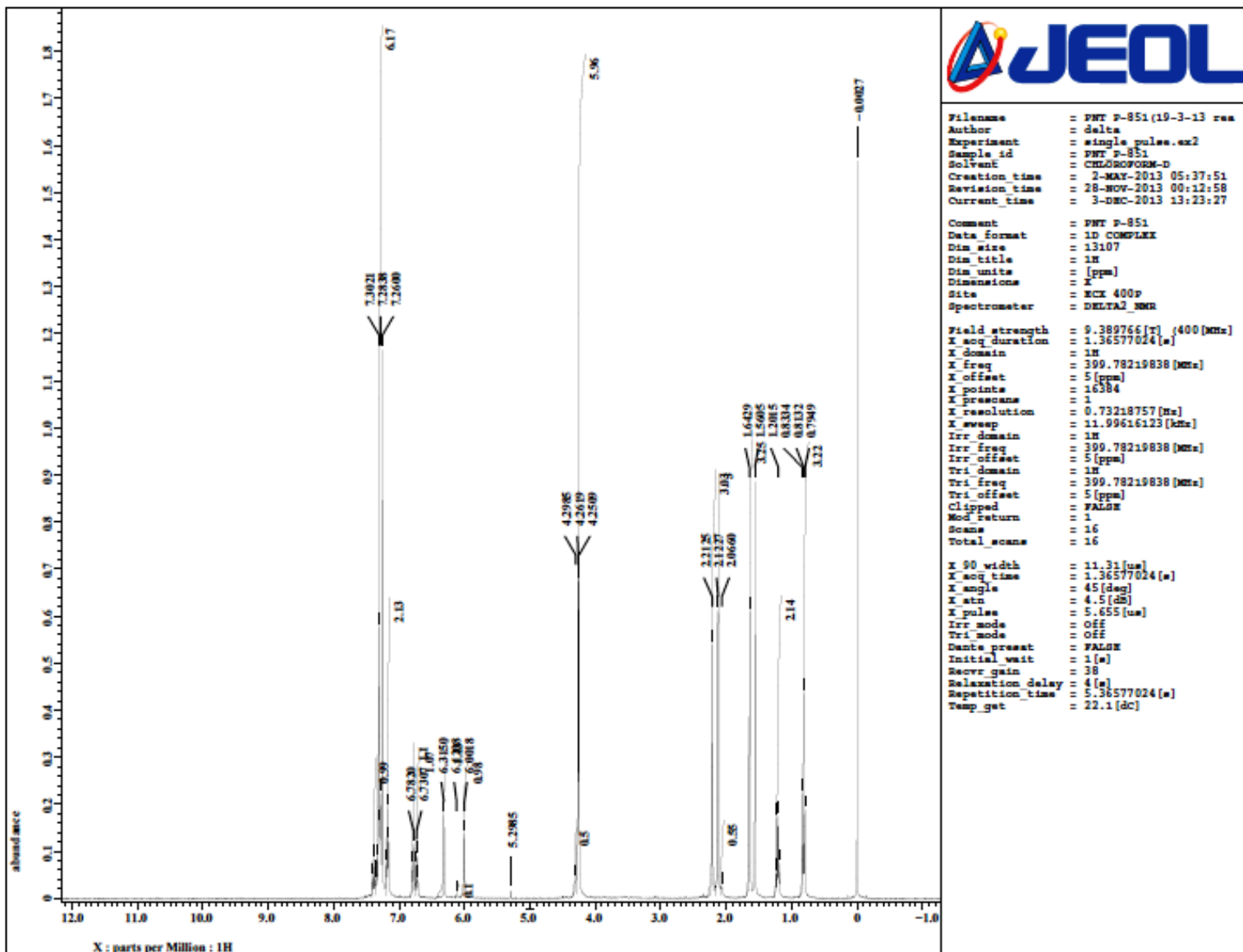


Fig. S66 ^1H NMR spectrum of **12** (CDCl_3 , 400.0 MHz).

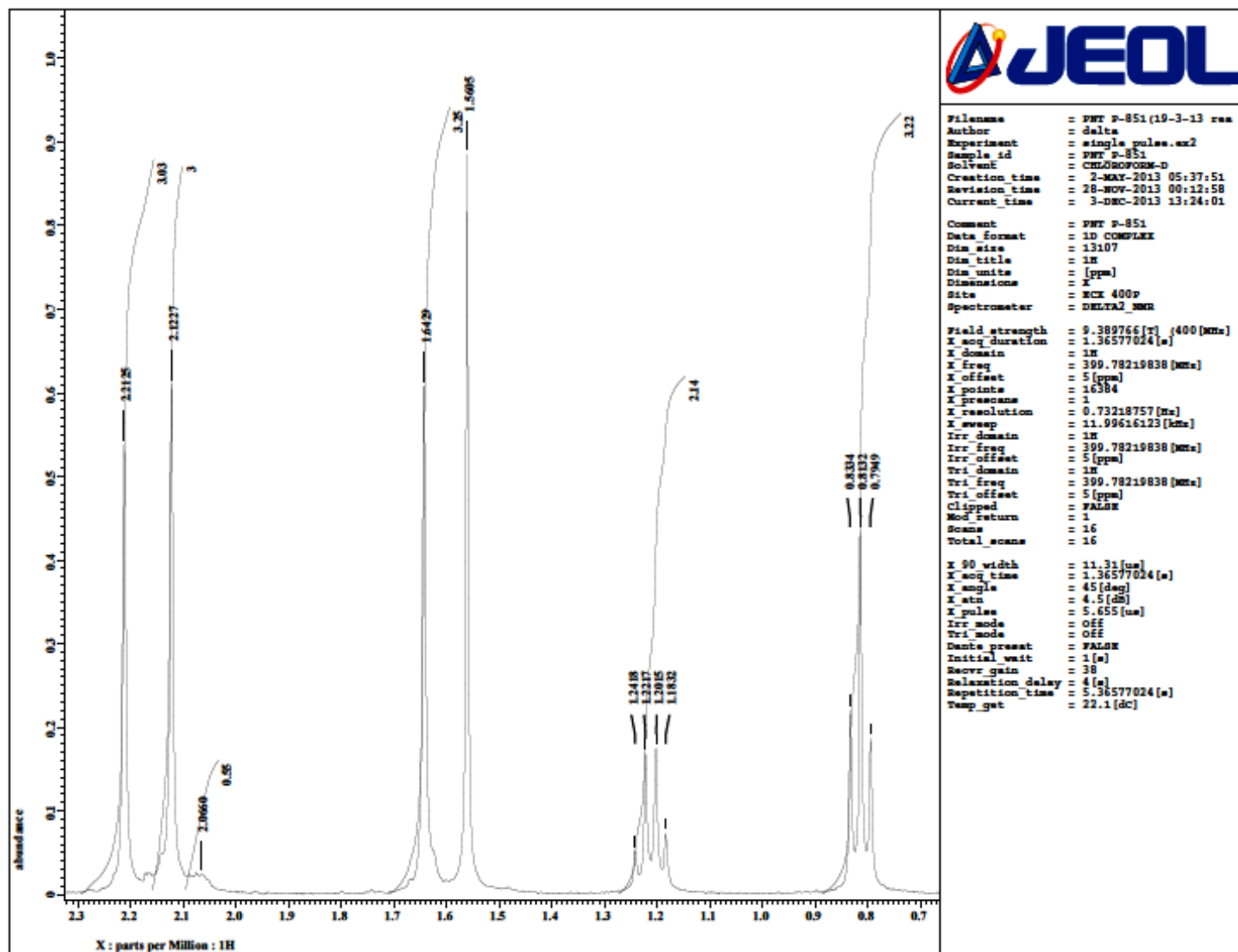


Fig. S67 Expansion of ^1H NMR spectrum of **12** (CDCl_3 , 400.0 MHz).

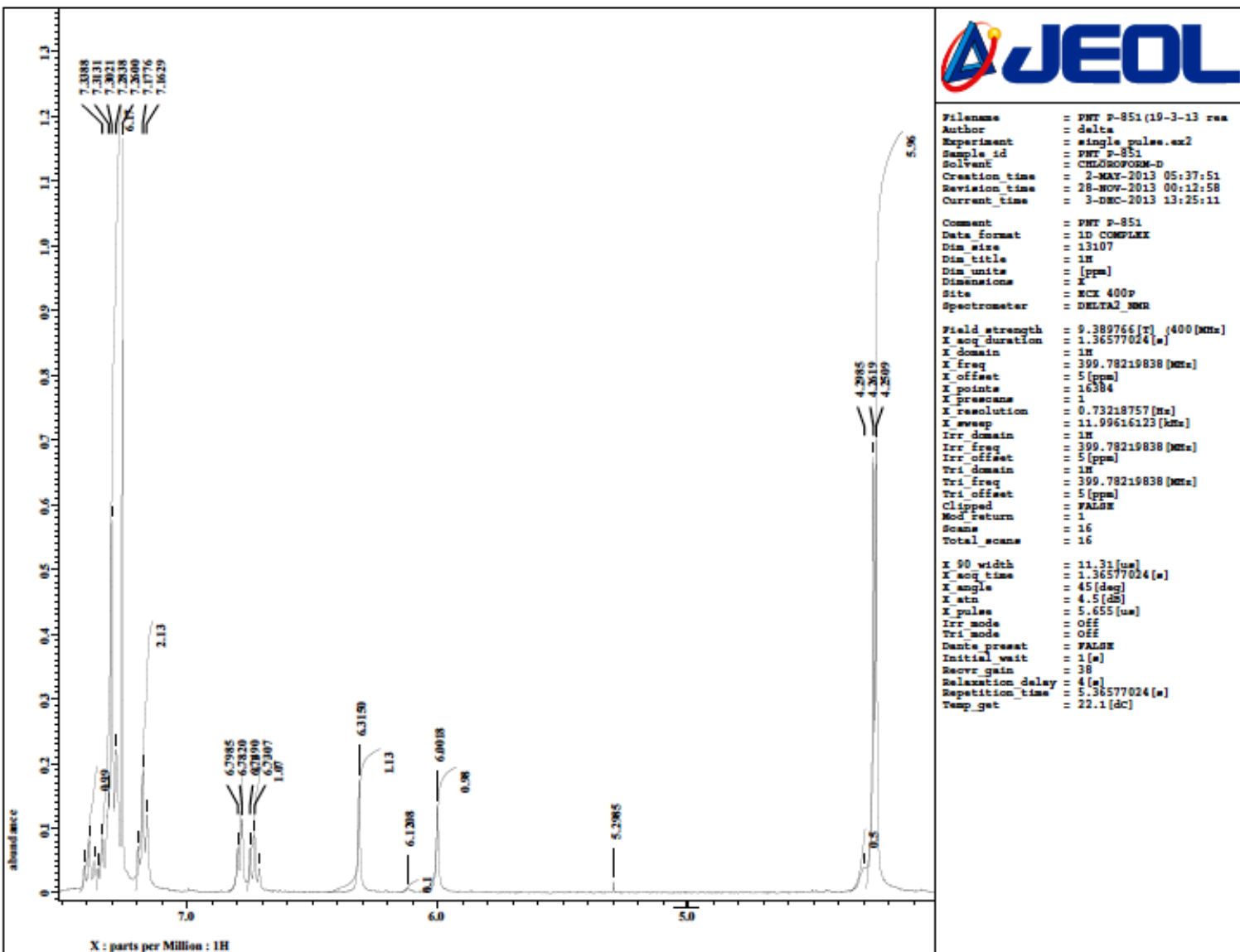


Fig. S68 Expansion of ^1H NMR spectrum of **12** (CDCl_3 , 400.0 MHz).

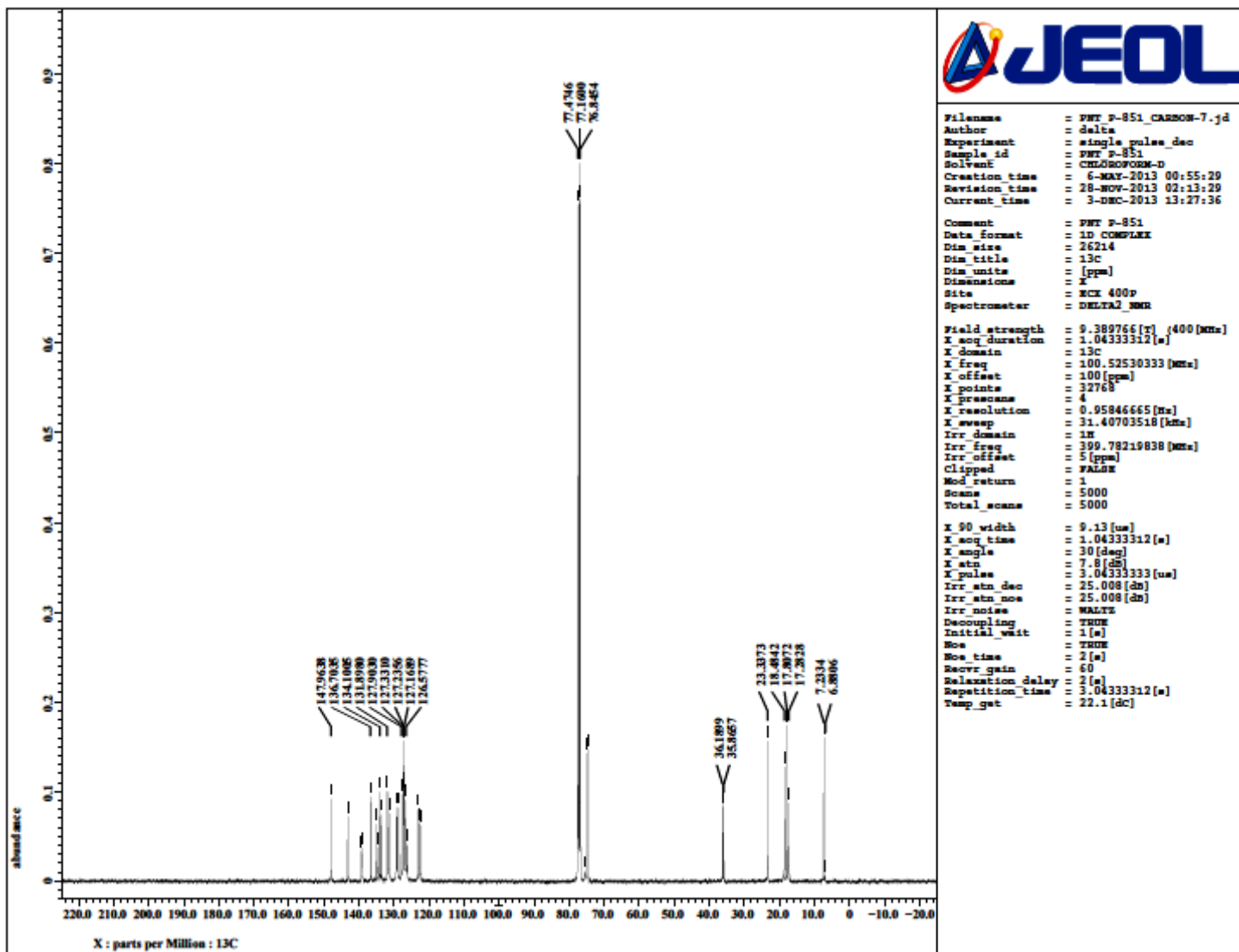


Fig. S69 ^{13}C NMR spectrum of **12** (CDCl_3 , 100.5 MHz).

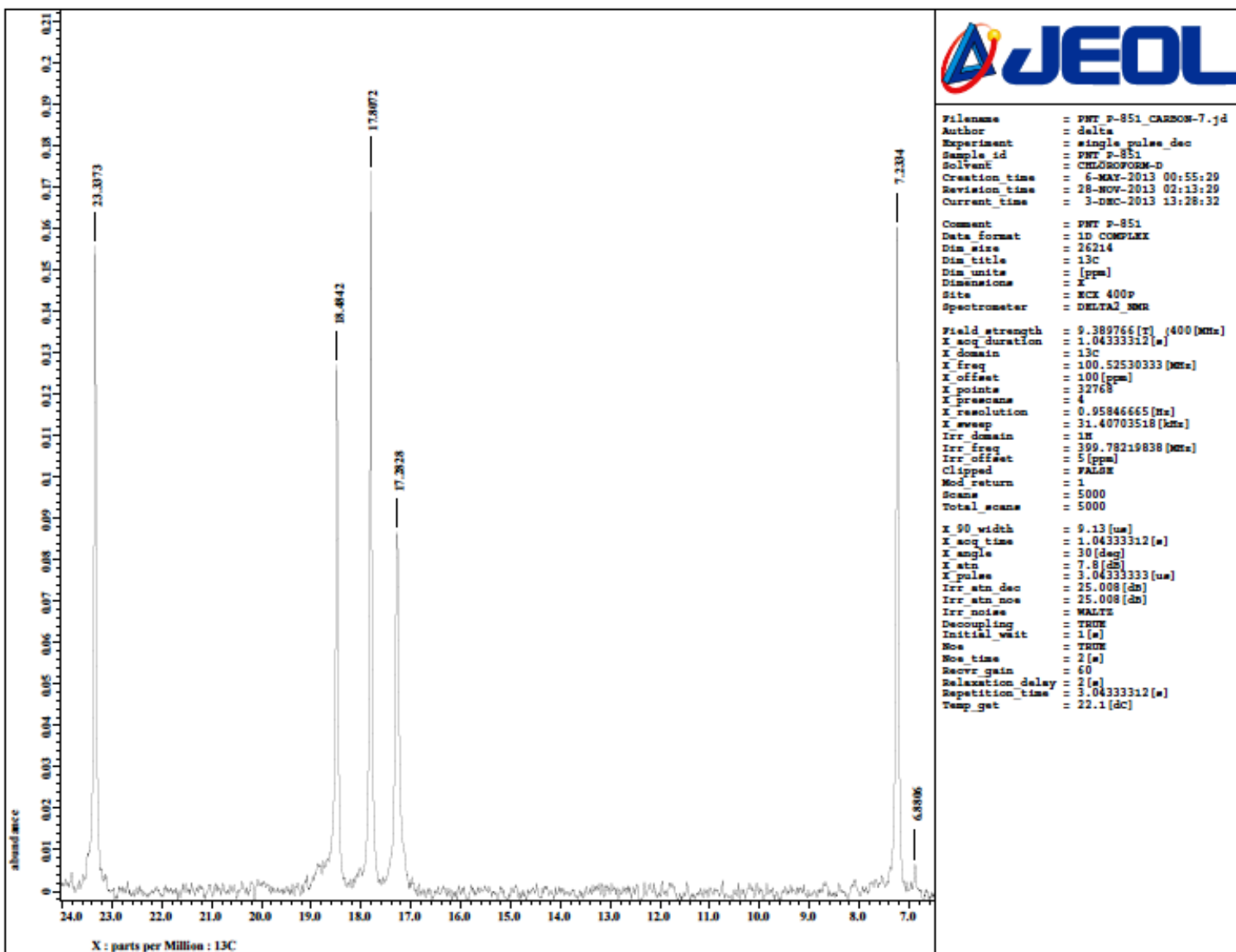


Fig. S70 Expansion of ^{13}C NMR spectrum of **12** (CDCl_3 , 100.5 MHz).

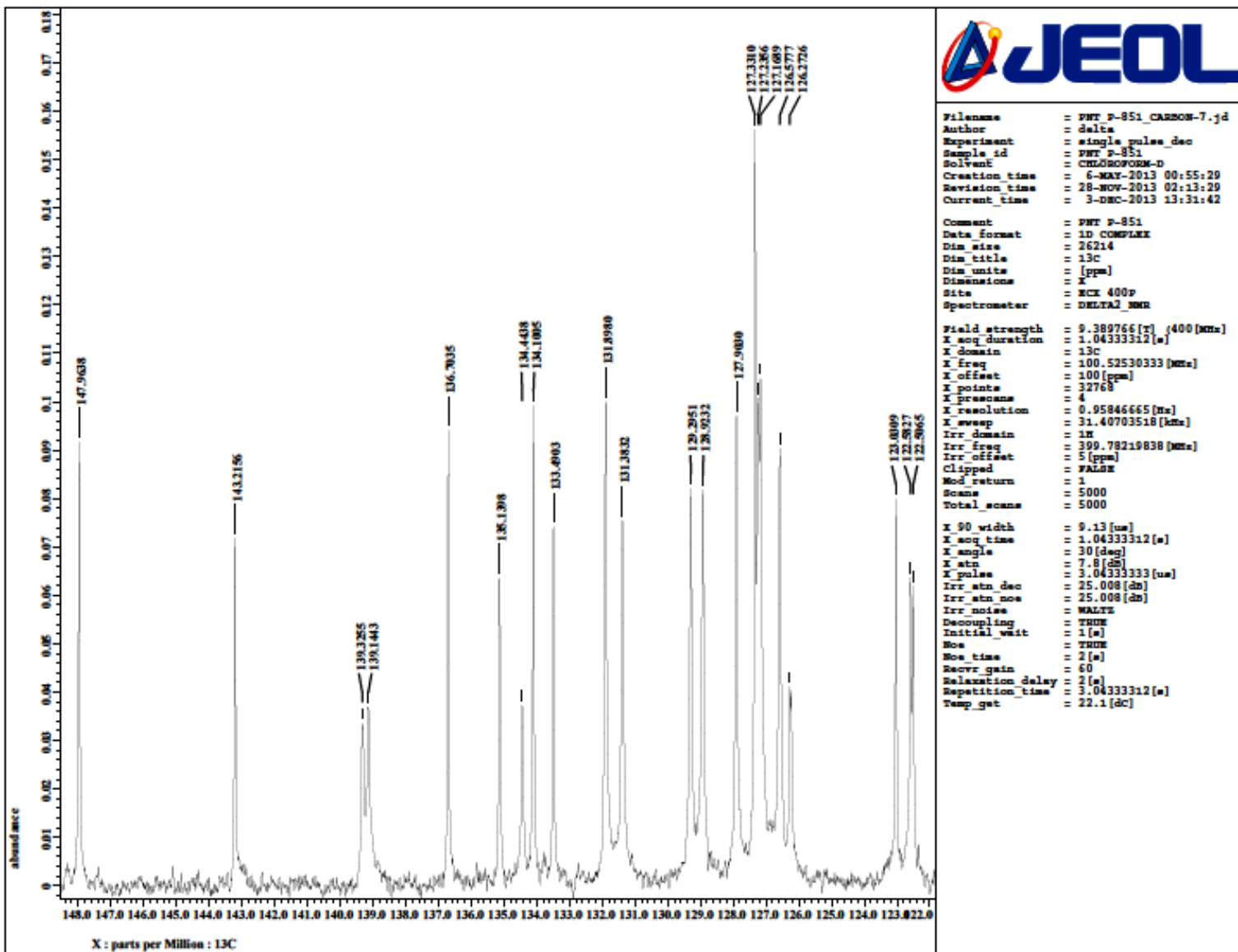


Fig. S71 Expansion of ^{13}C NMR spectrum of **12** (CDCl_3 , 100.5 MHz).

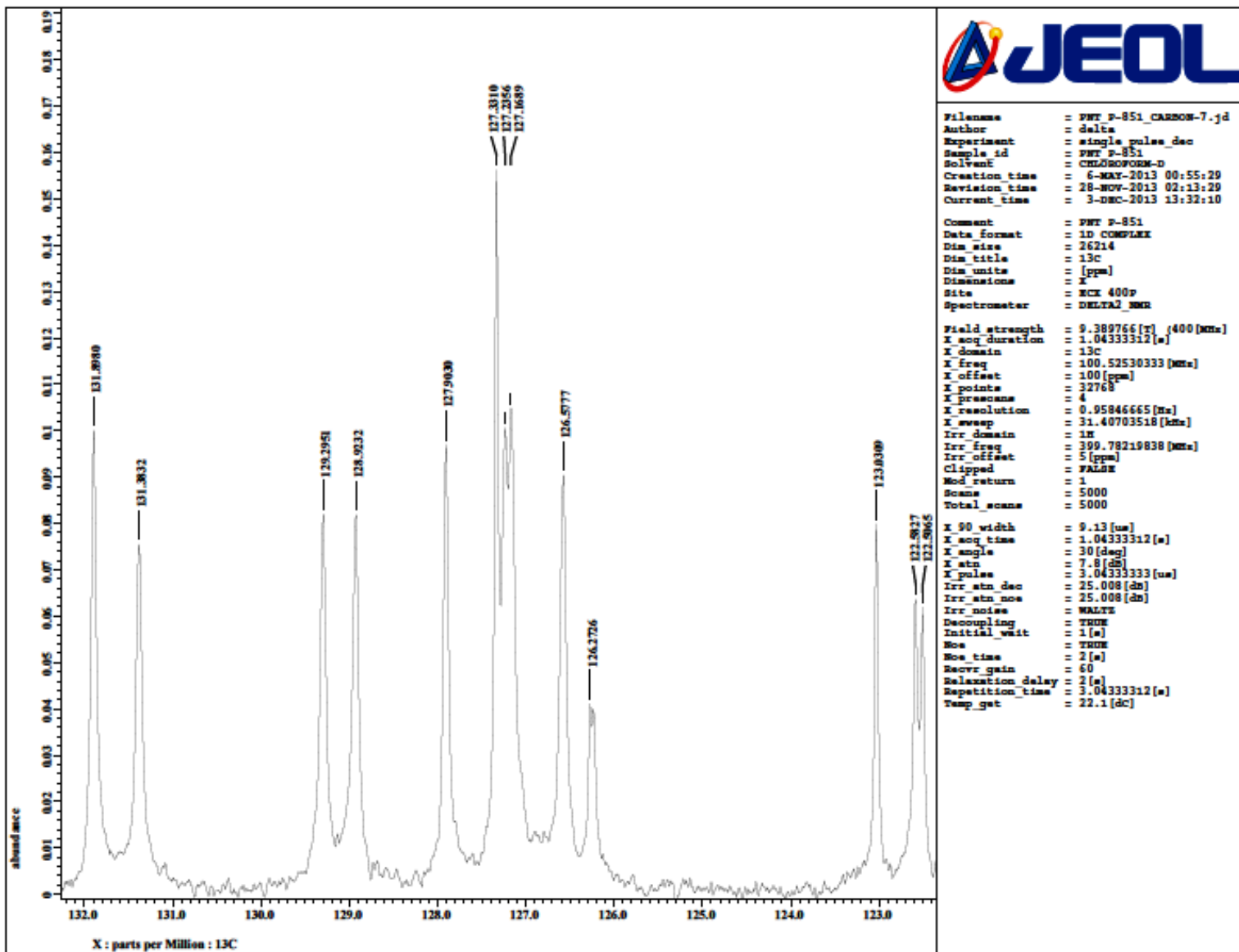


Fig. S72 Expansion of ^{13}C NMR spectrum of **12** (CDCl_3 , 100.5 MHz).

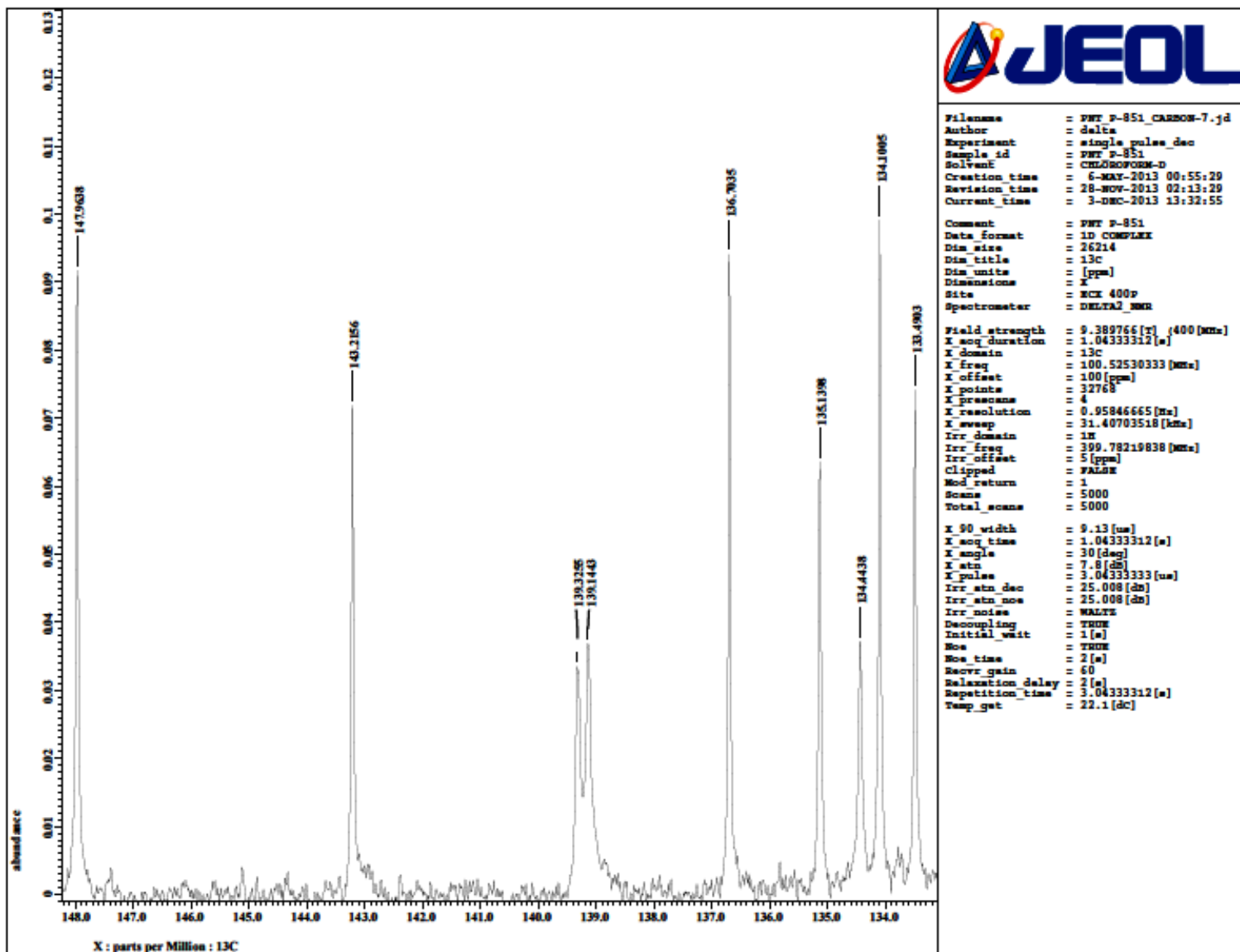


Fig. S73 Expansion of ^{13}C NMR spectrum of **12** (CDCl_3 , 100.5 MHz).

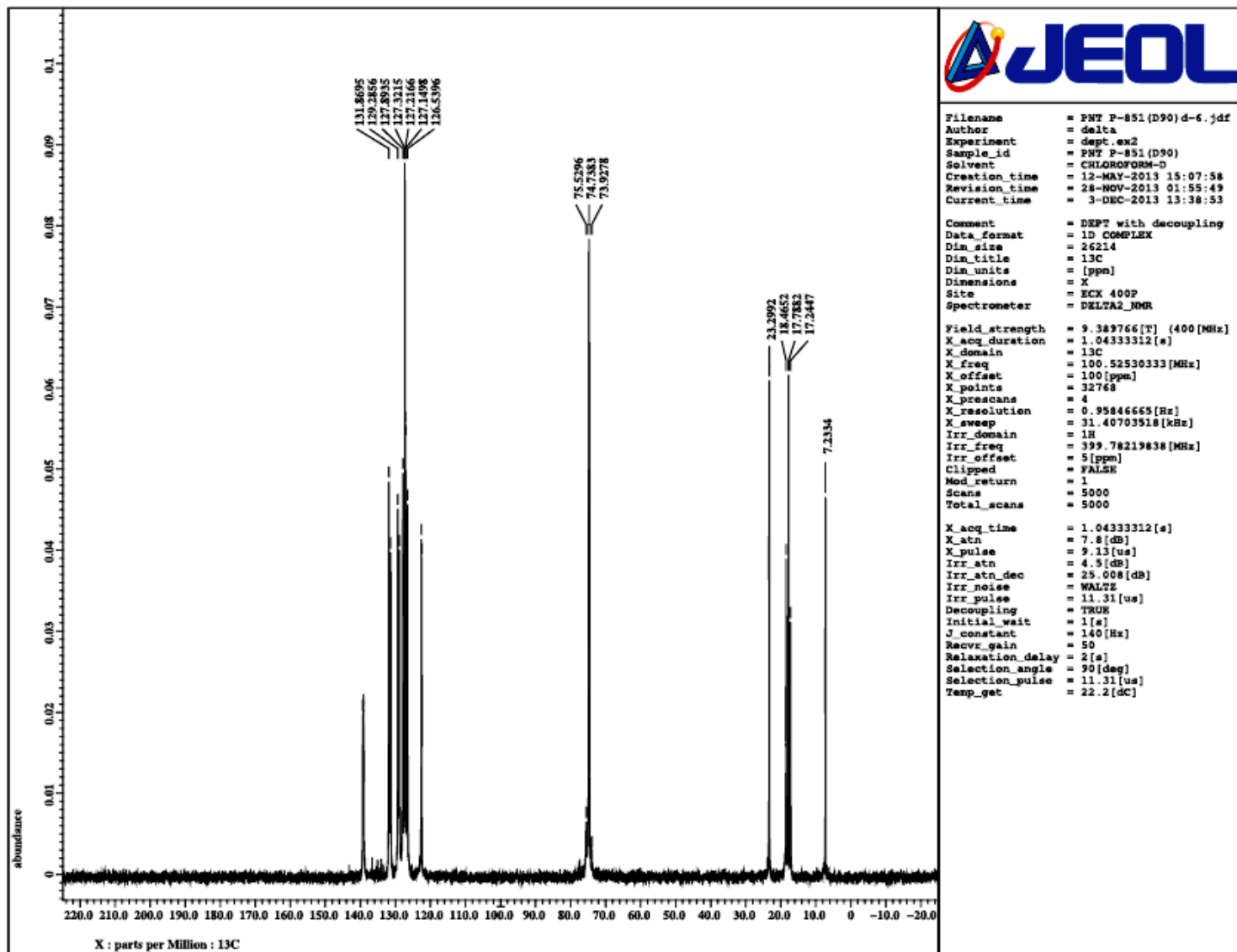


Fig. S74 DEPT 90 NMR spectrum of **12** (CDCl_3 , 100.5 MHz). The peaks around δ 7–75 correspond to residual peaks of C, CH_2 , OCH_2 or CH_3 carbons.

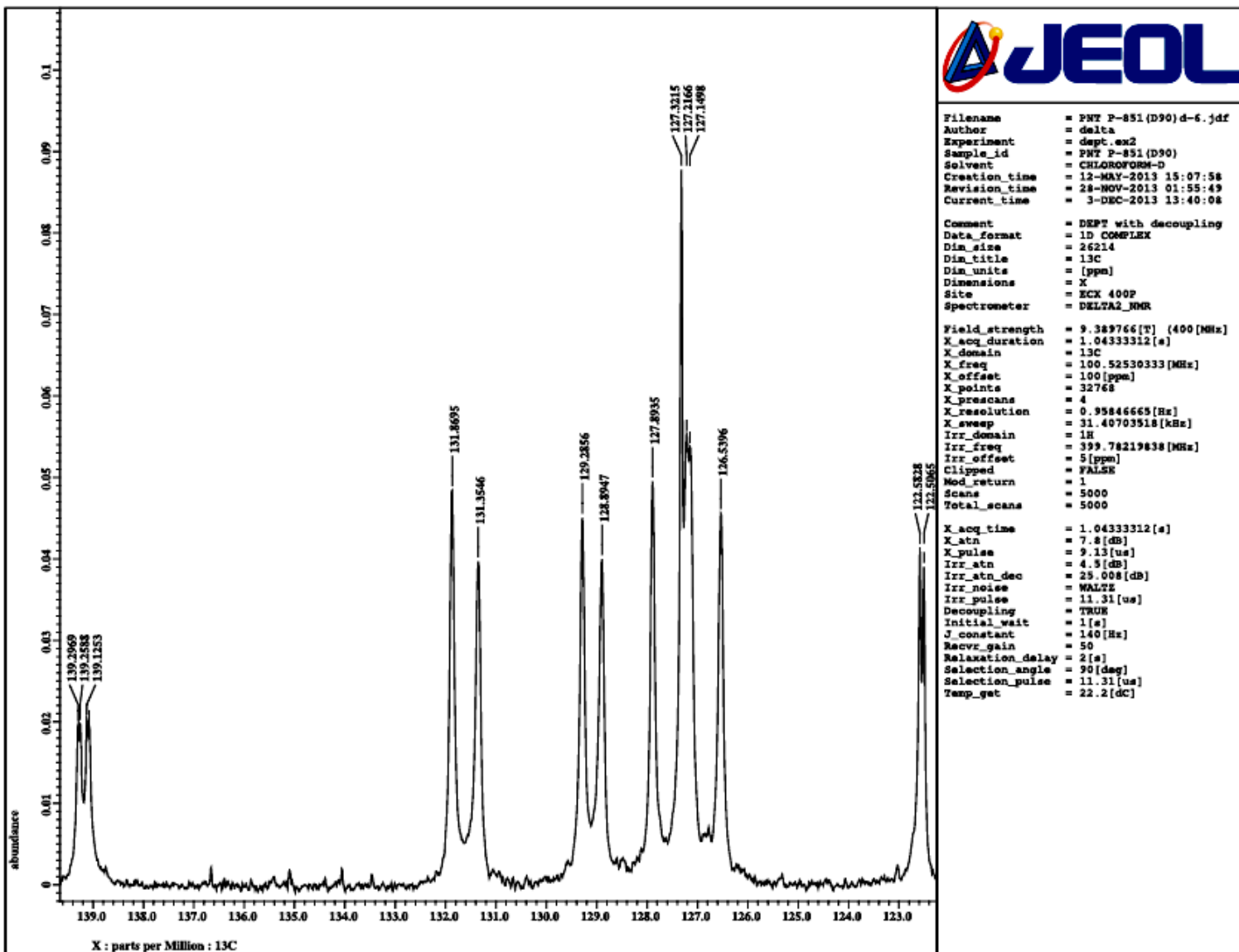


Fig. S75 Expansion of DEPT 90 NMR spectrum of **12**.

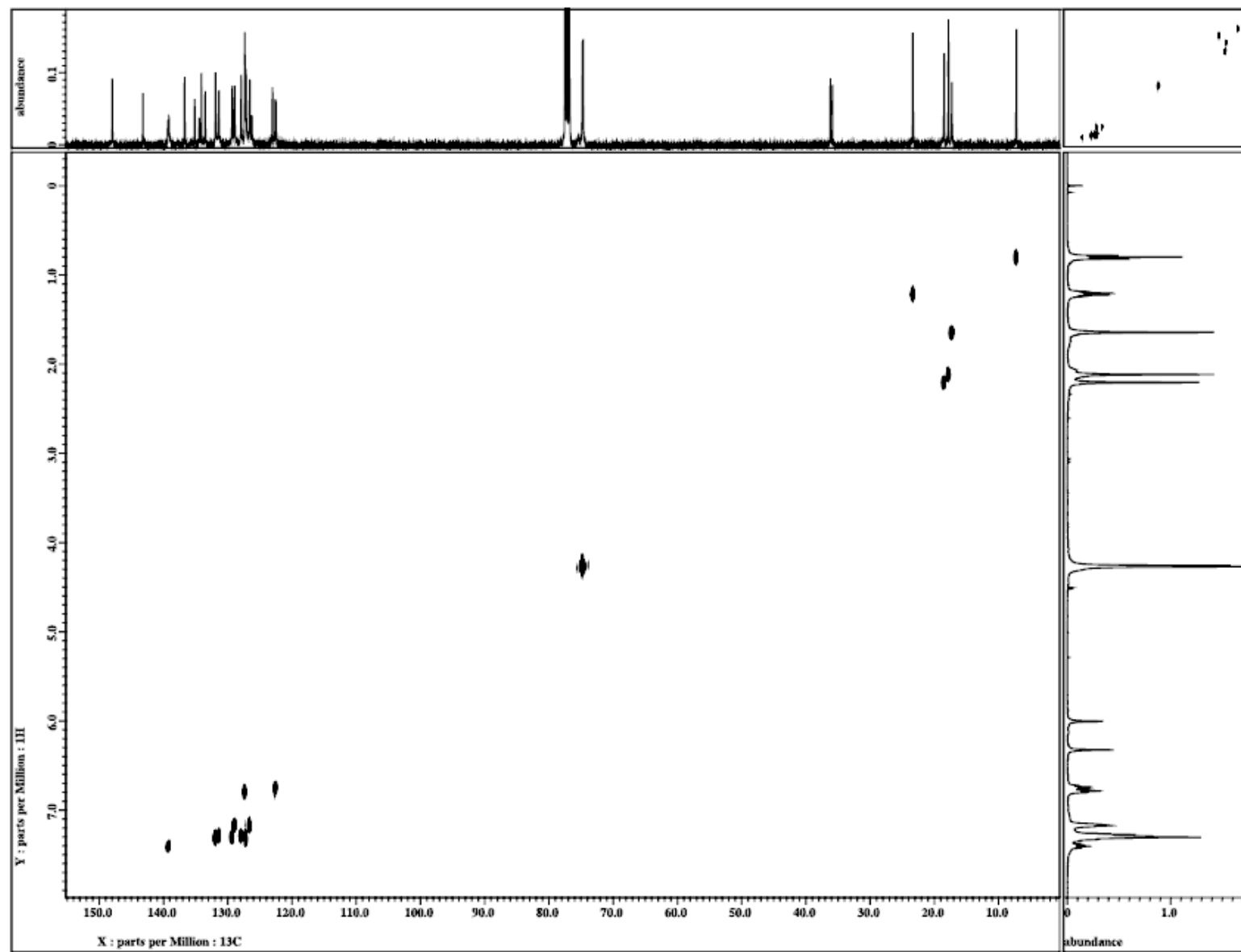


Fig. S76 The ^{13}C - ^1H HETCOR NMR spectrum of **12** (X-axis 100.5 MHz, Y-axis 400 MHz, CDCl_3).

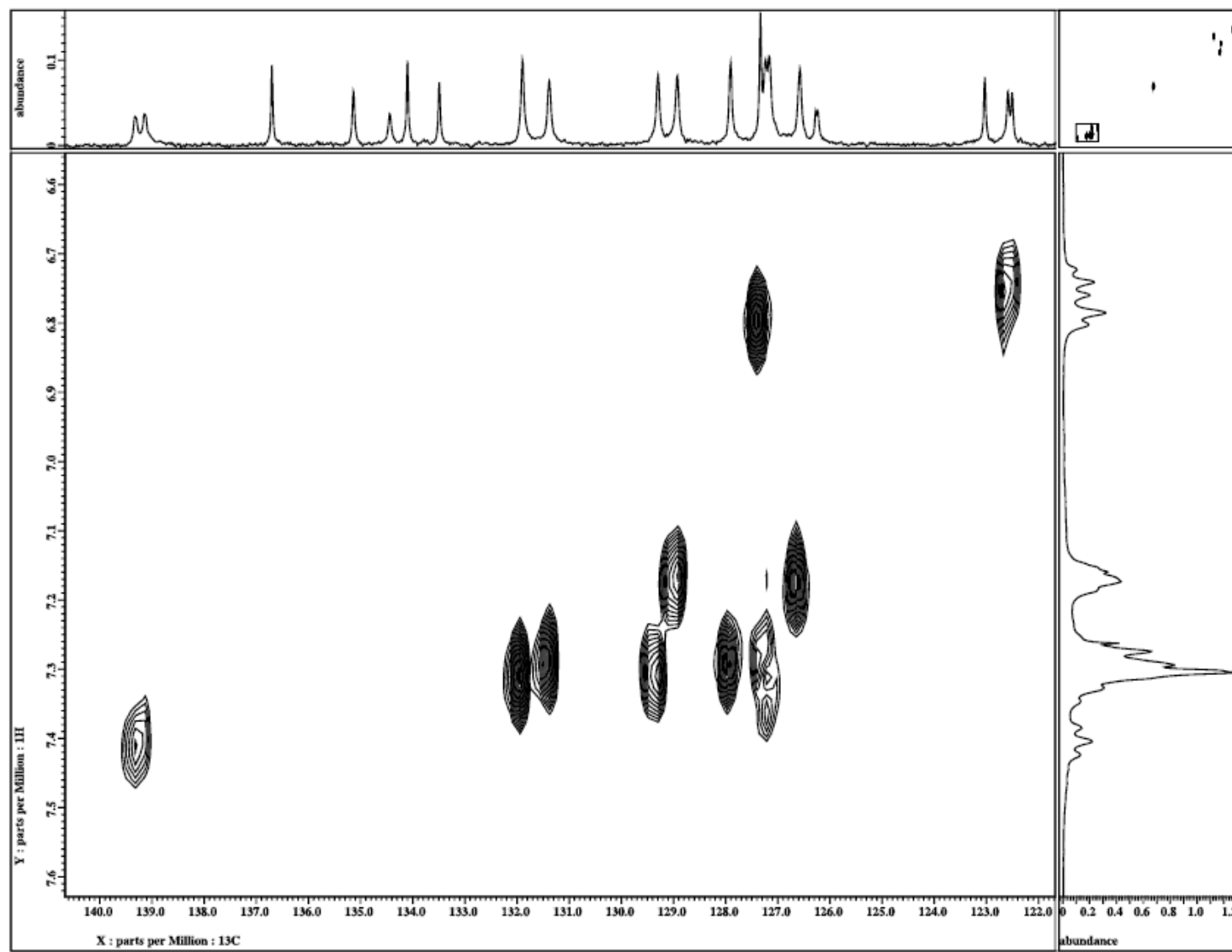


Fig. S77 The ^{13}C - ^1H HETCOR NMR spectrum of **12** illustrated for the ArCH carbons (X-axis 100.5 MHz, Y-axis 400 MHz, CDCl_3).

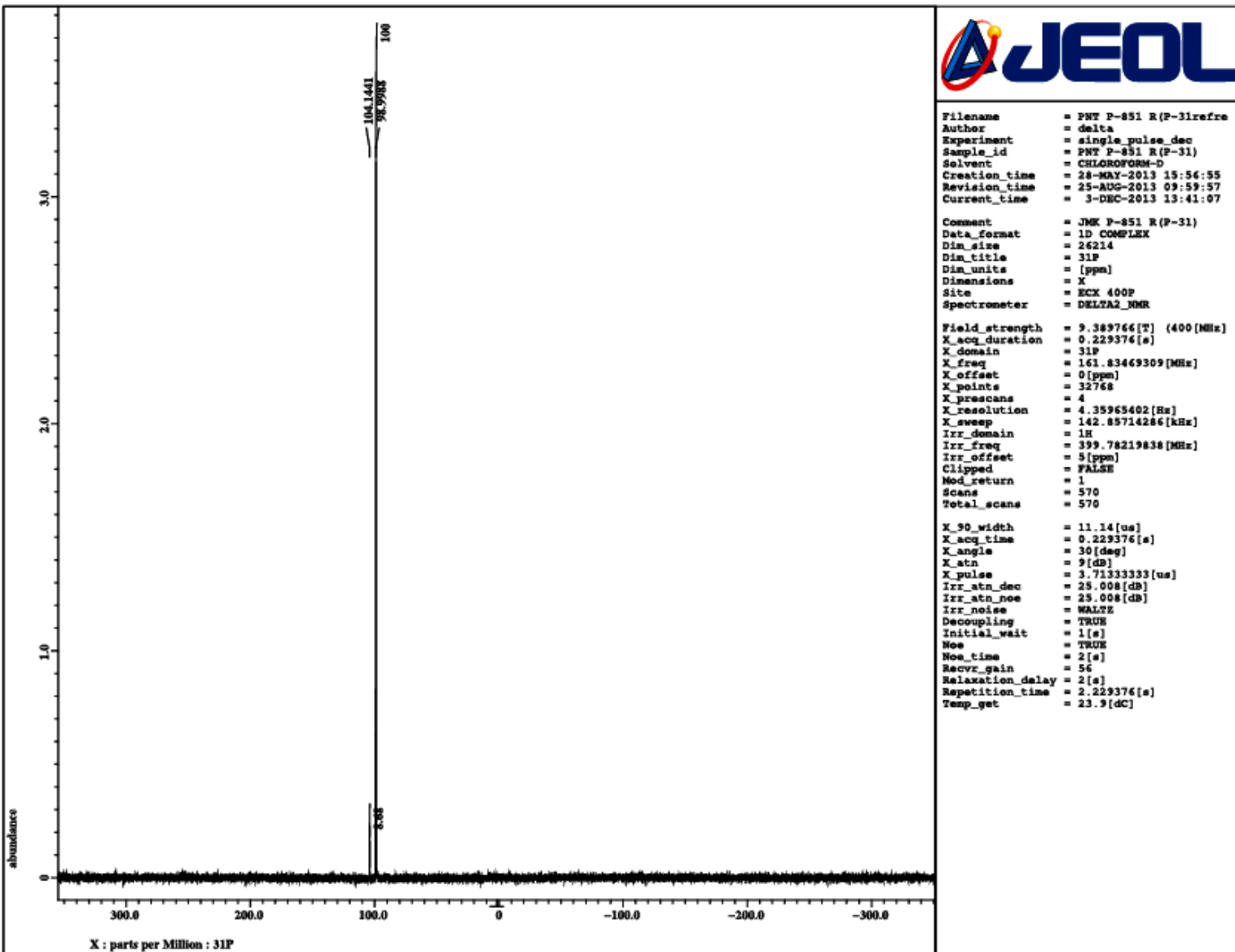


Fig. S78 $^{31}\text{P}\{\text{H}\}$ NMR spectrum of **12** (CDCl_3 , 161.8 MHz).

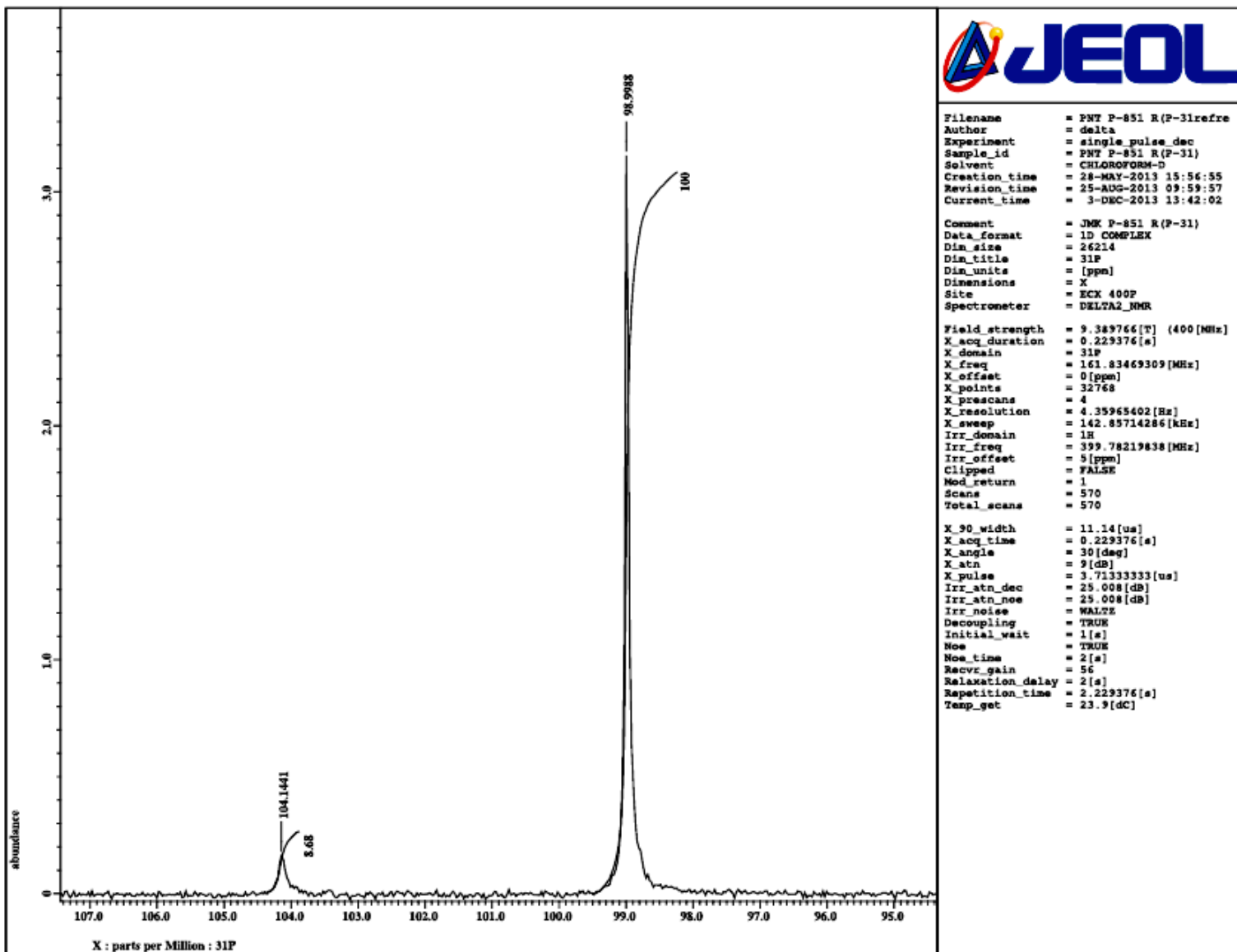


Fig. S79 Expansion of ${}^3\text{P}\{{}^1\text{H}\}$ NMR spectrum of **12** (CDCl_3 , 161.8 MHz).

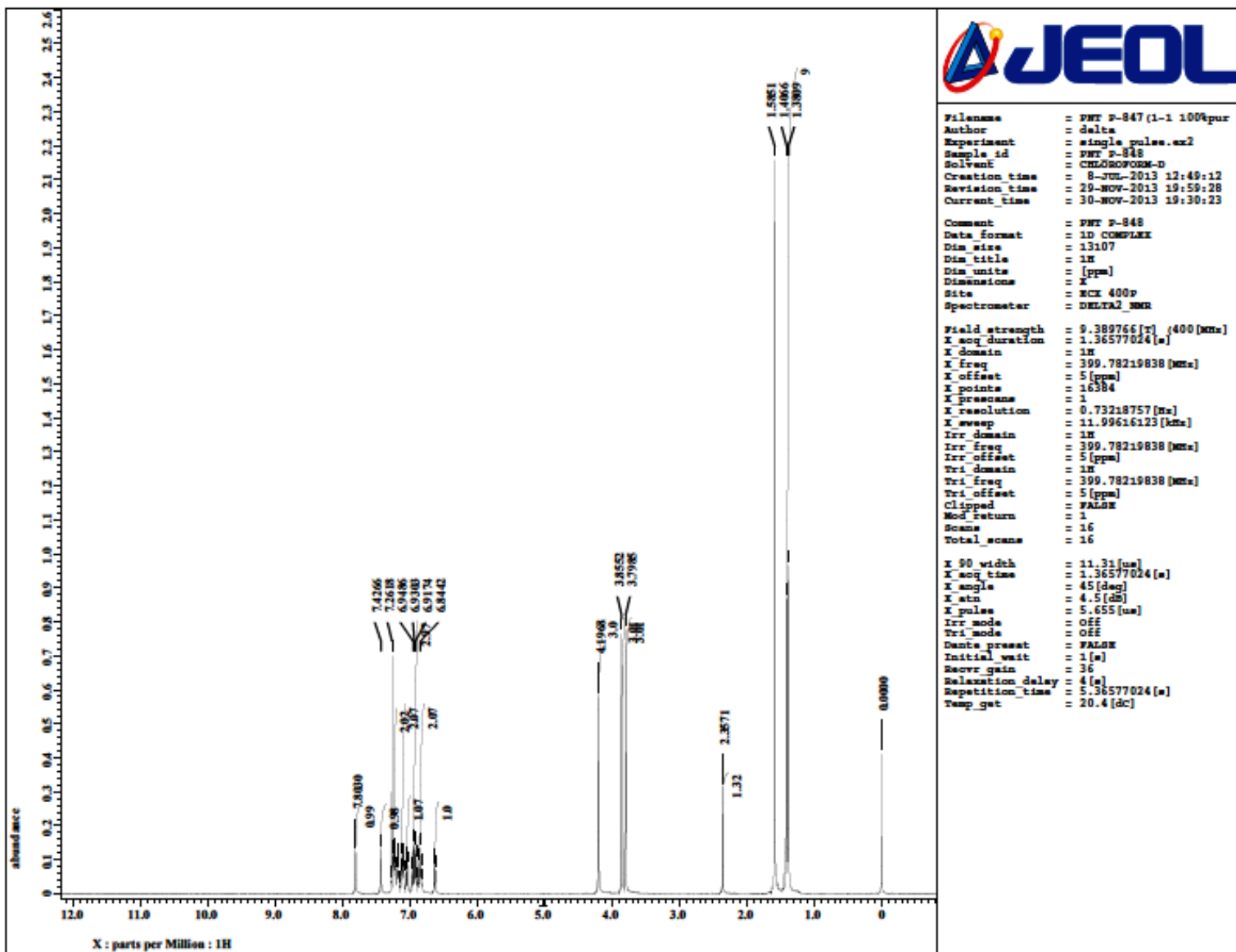


Fig. S80 ^1H NMR spectrum of **13** (CDCl_3 , 400.0 MHz).

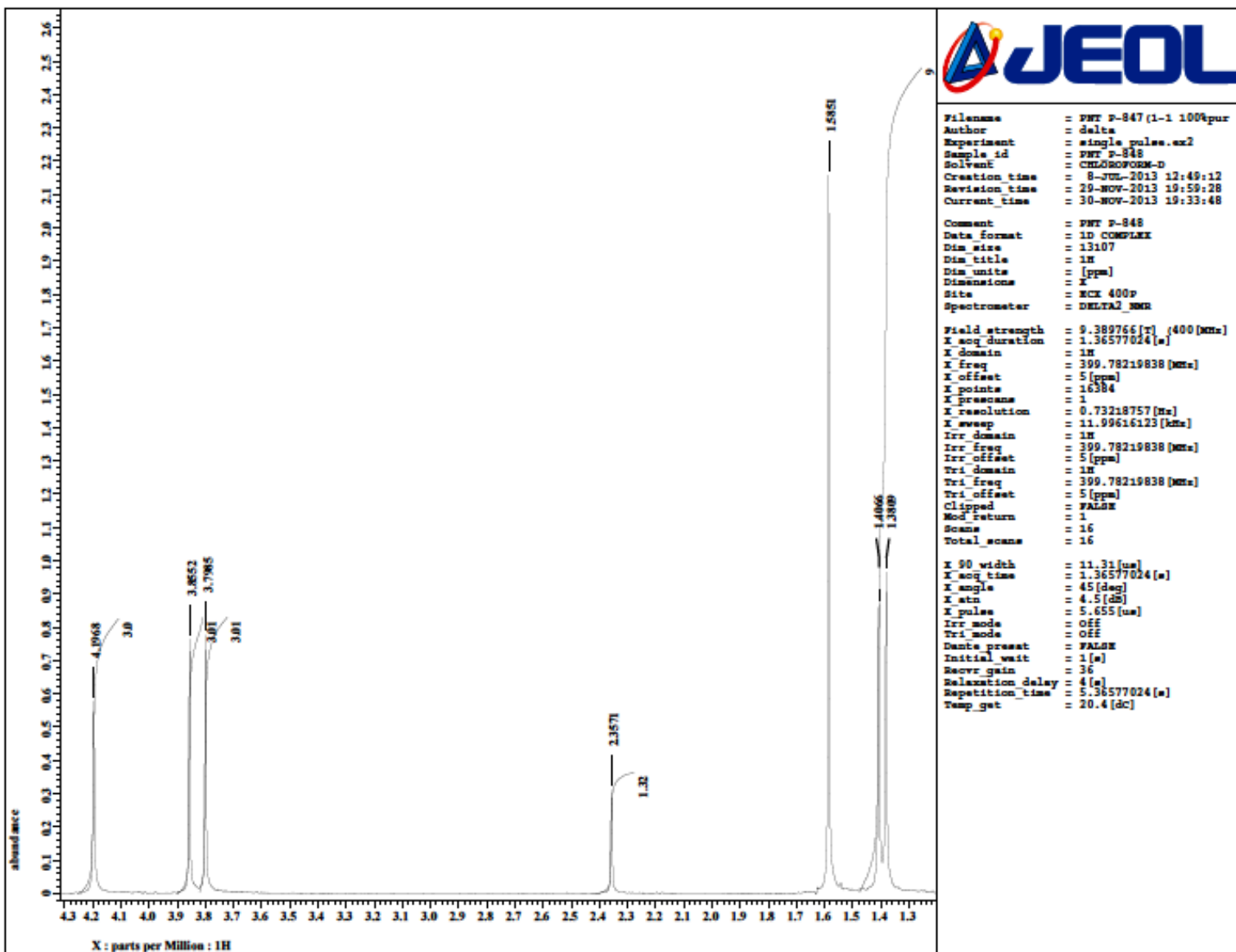


Fig. S81 Expansion of ^1H NMR spectrum of **13** (CDCl_3 , 400.0 MHz).

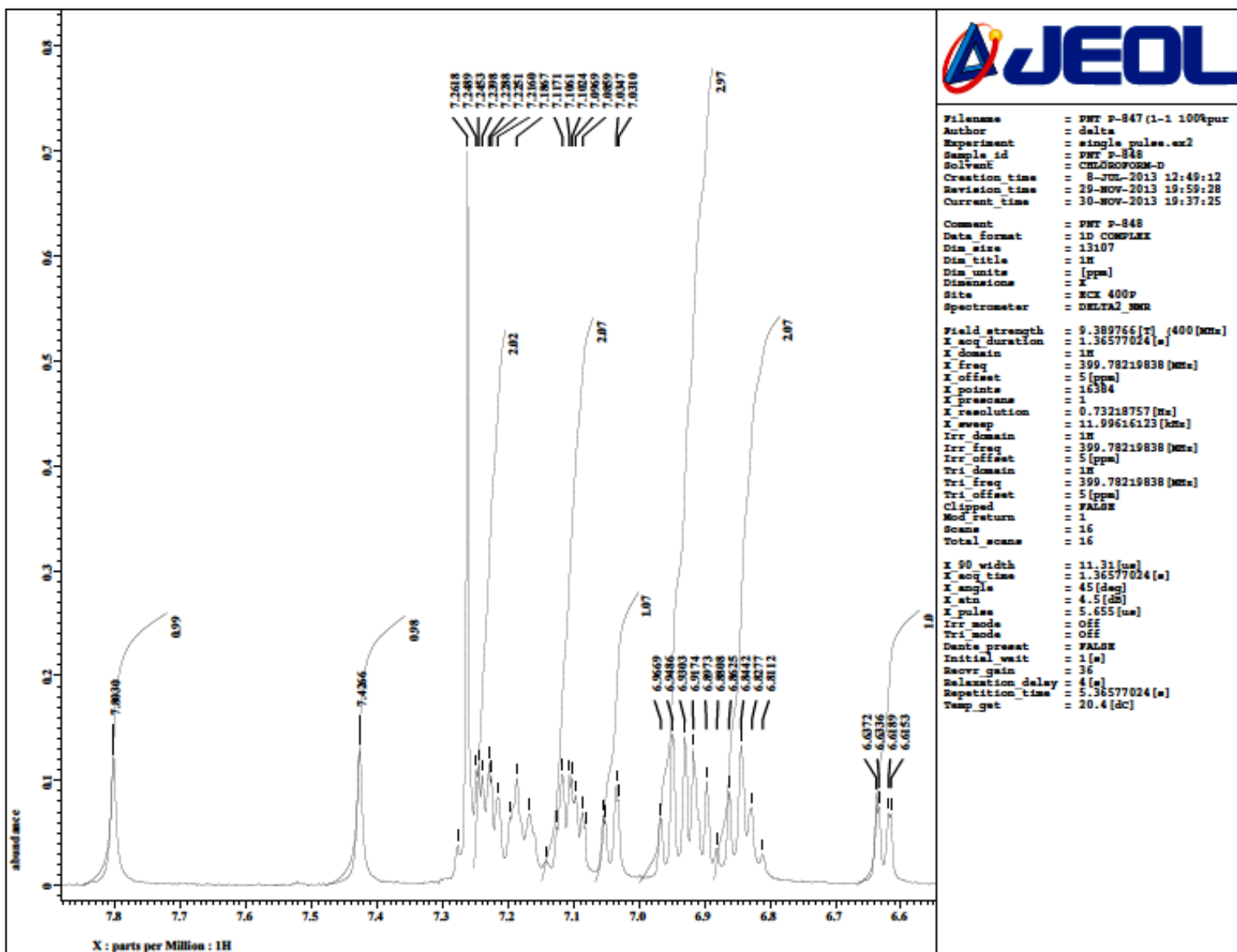


Fig. S82 Expansion of ^1H NMR spectrum of **13** (CDCl_3 , 400.0 MHz).

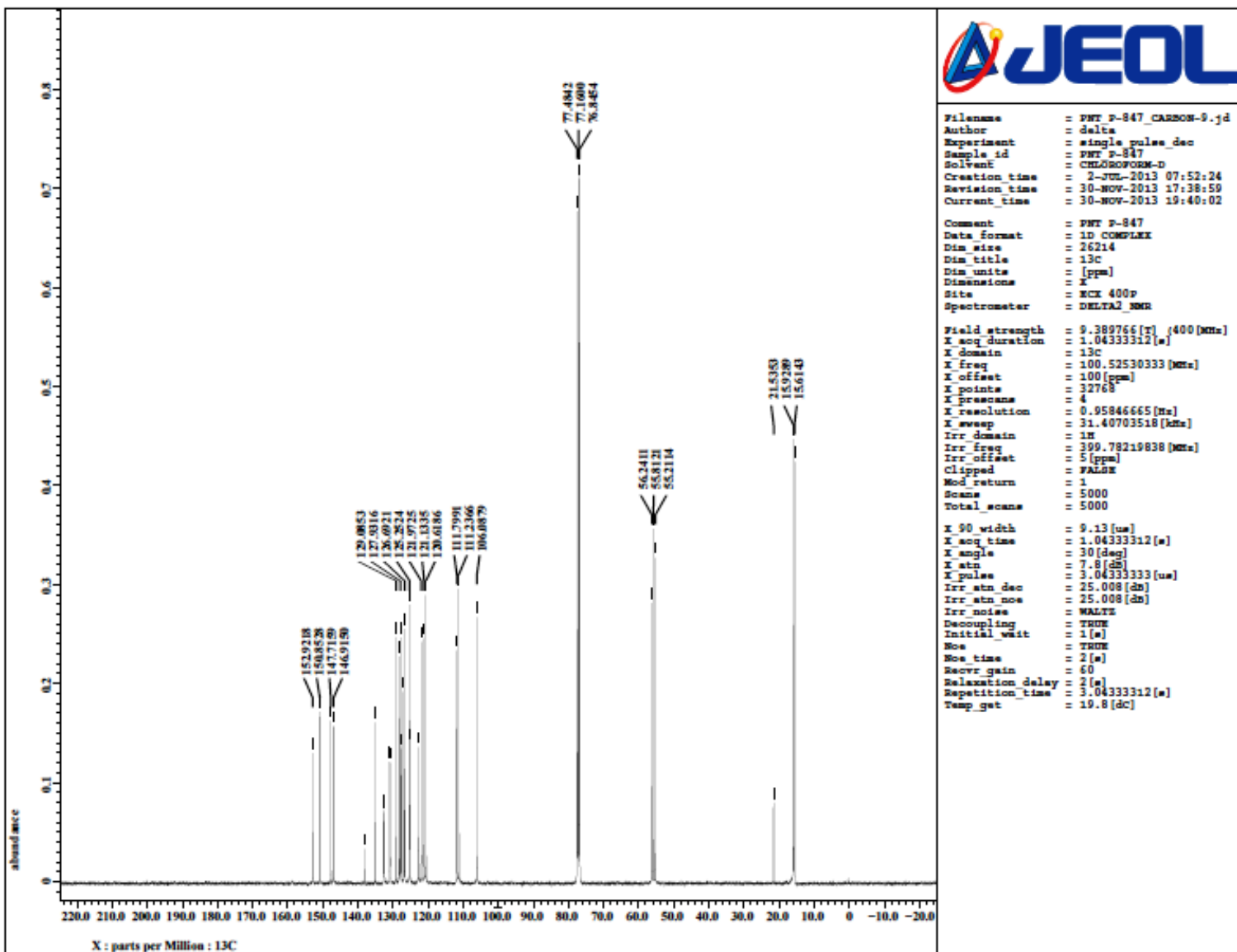


Fig. S83 ^{13}C NMR spectrum of **13** (CDCl_3 , 100.5 MHz).

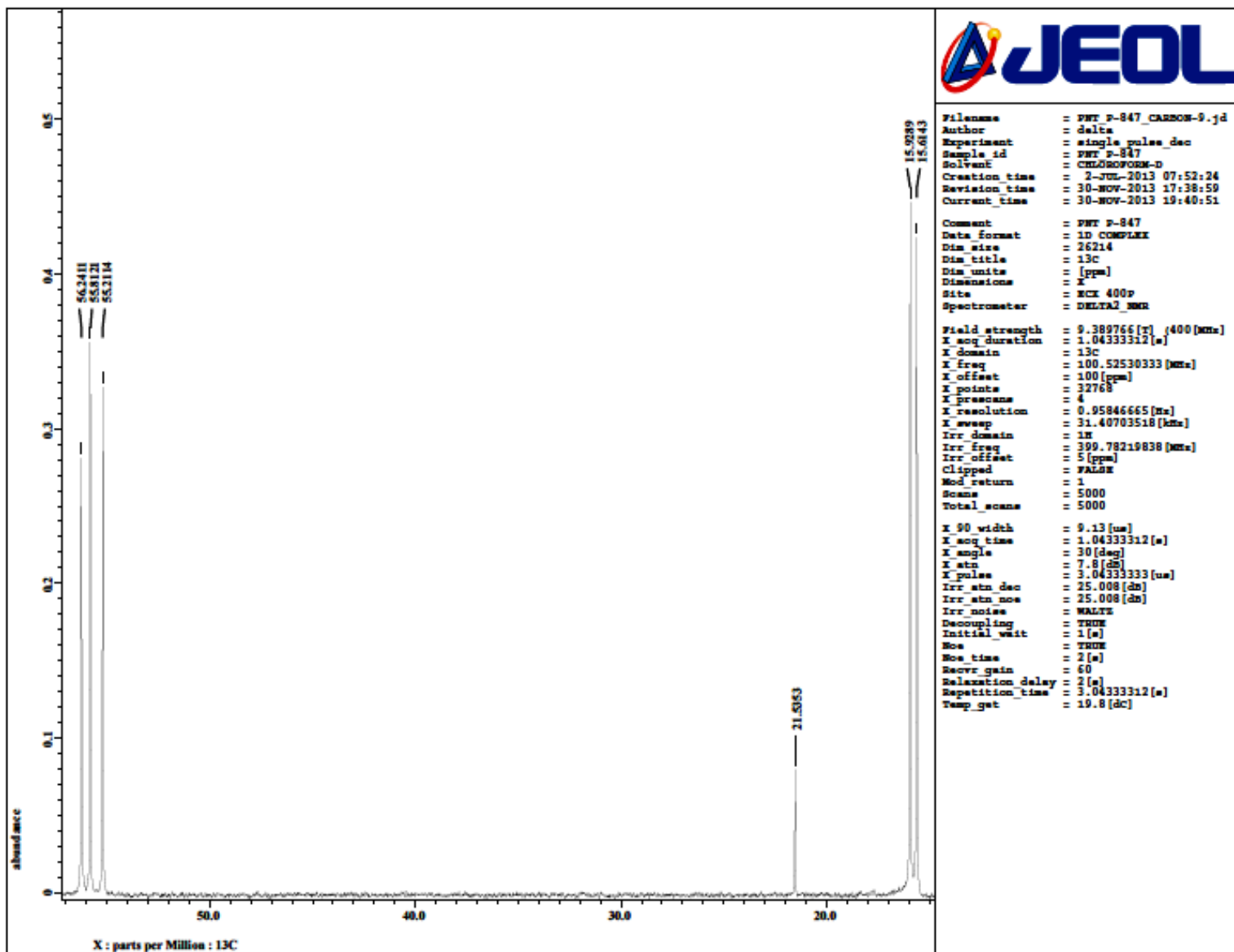


Fig. S84 Expansion of ^{13}C NMR spectrum of **13** (CDCl_3 , 100.5 MHz).

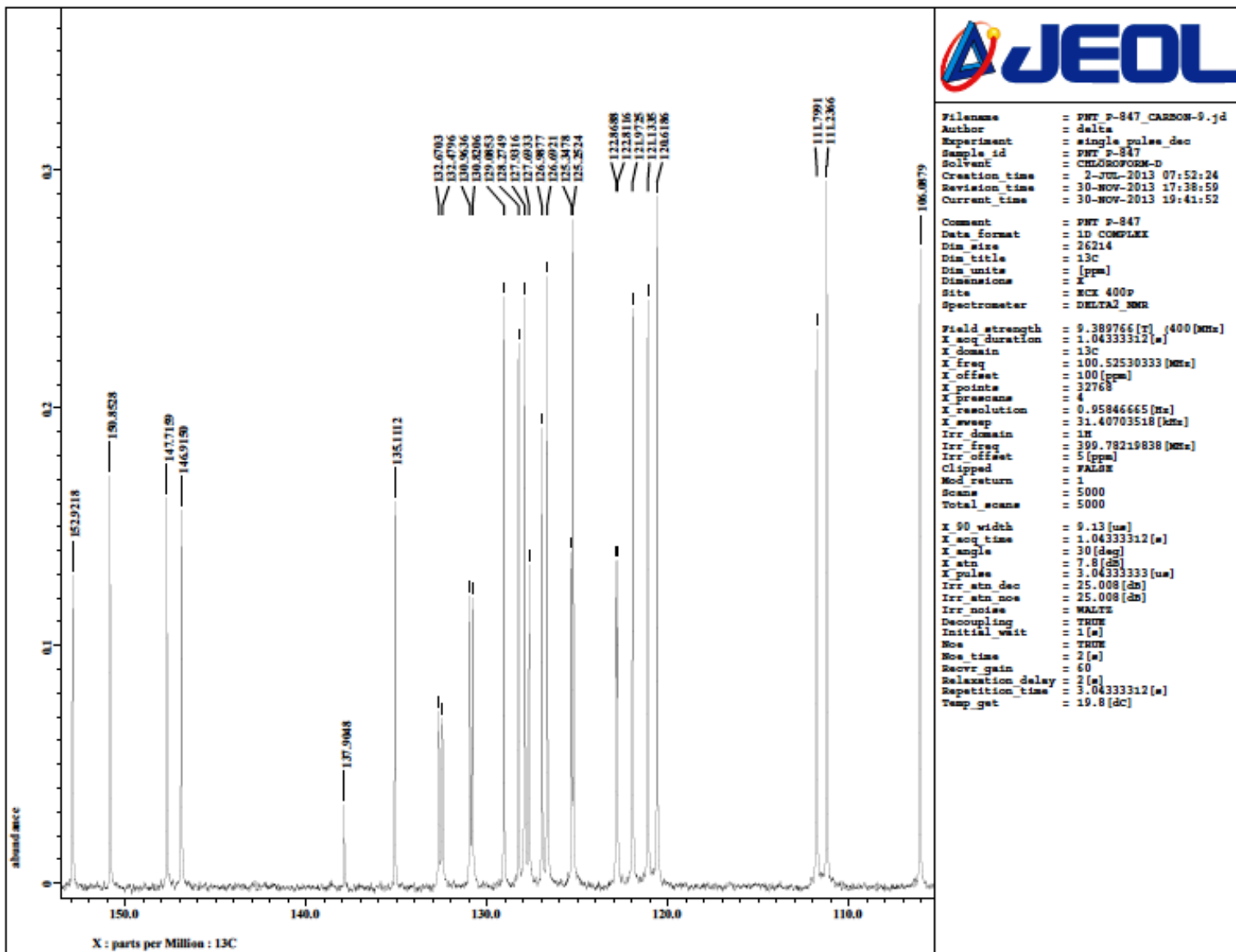


Fig. S85 Expansion of ^{13}C NMR spectrum of **13** (CDCl_3 , 100.5 MHz).

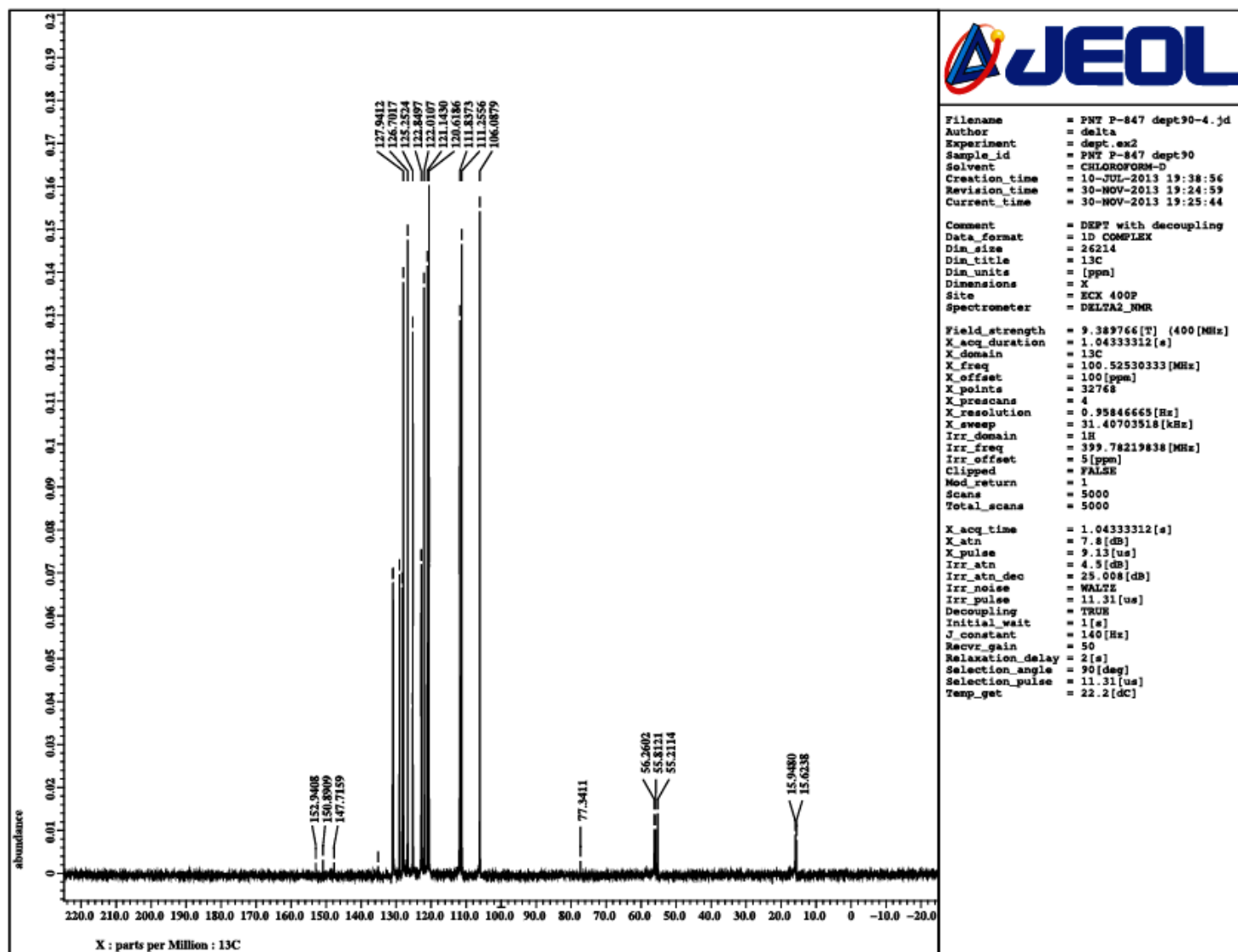


Fig. S86 DEPT 90 NMR spectrum of **13** (CDCl_3 , 100.5 MHz). The peaks around δ 15 and 56 correspond to residual peaks of CH_3 and OCH_3 carbons.

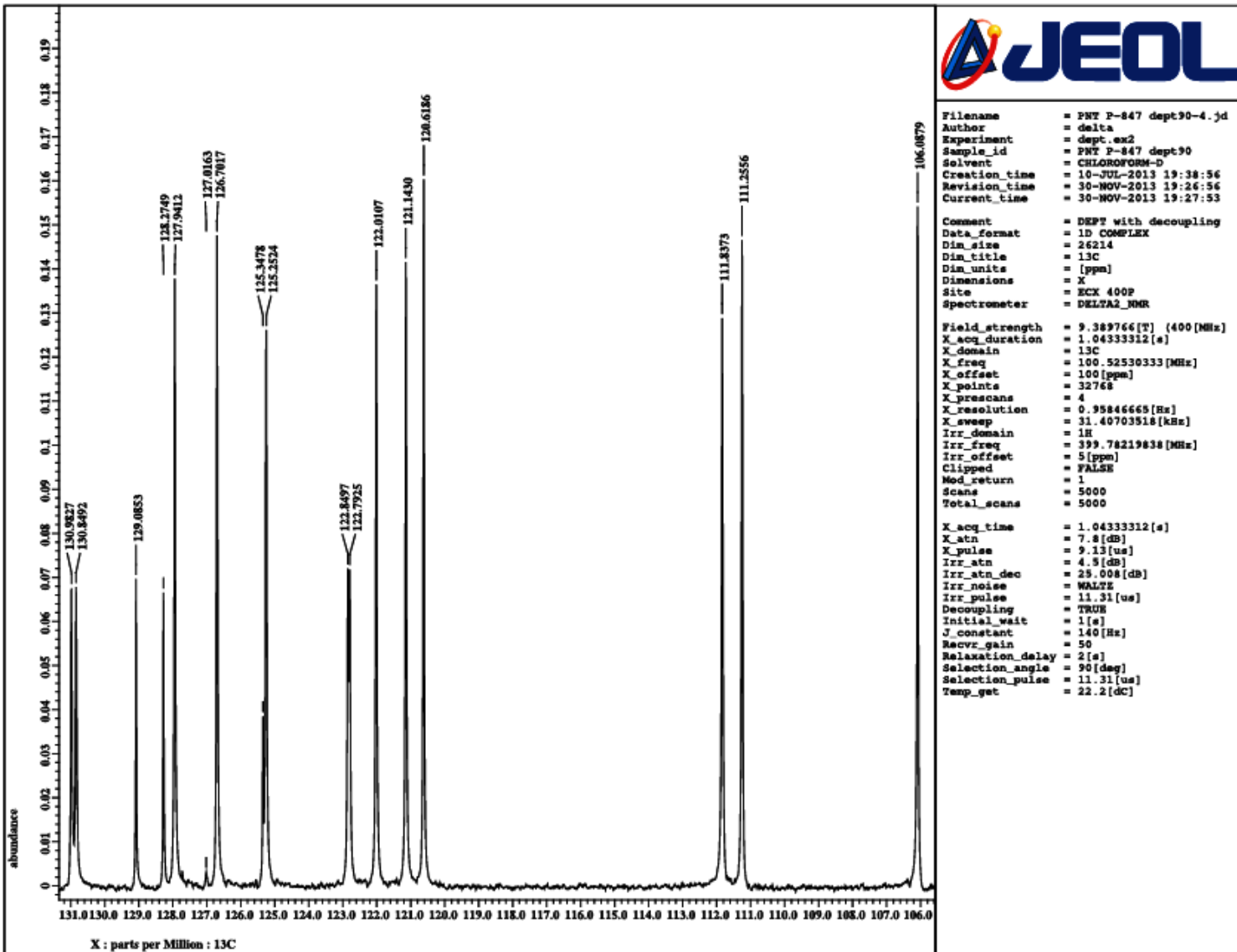


Fig. S87 Expansion of DEPT 90 NMR spectrum of 13.

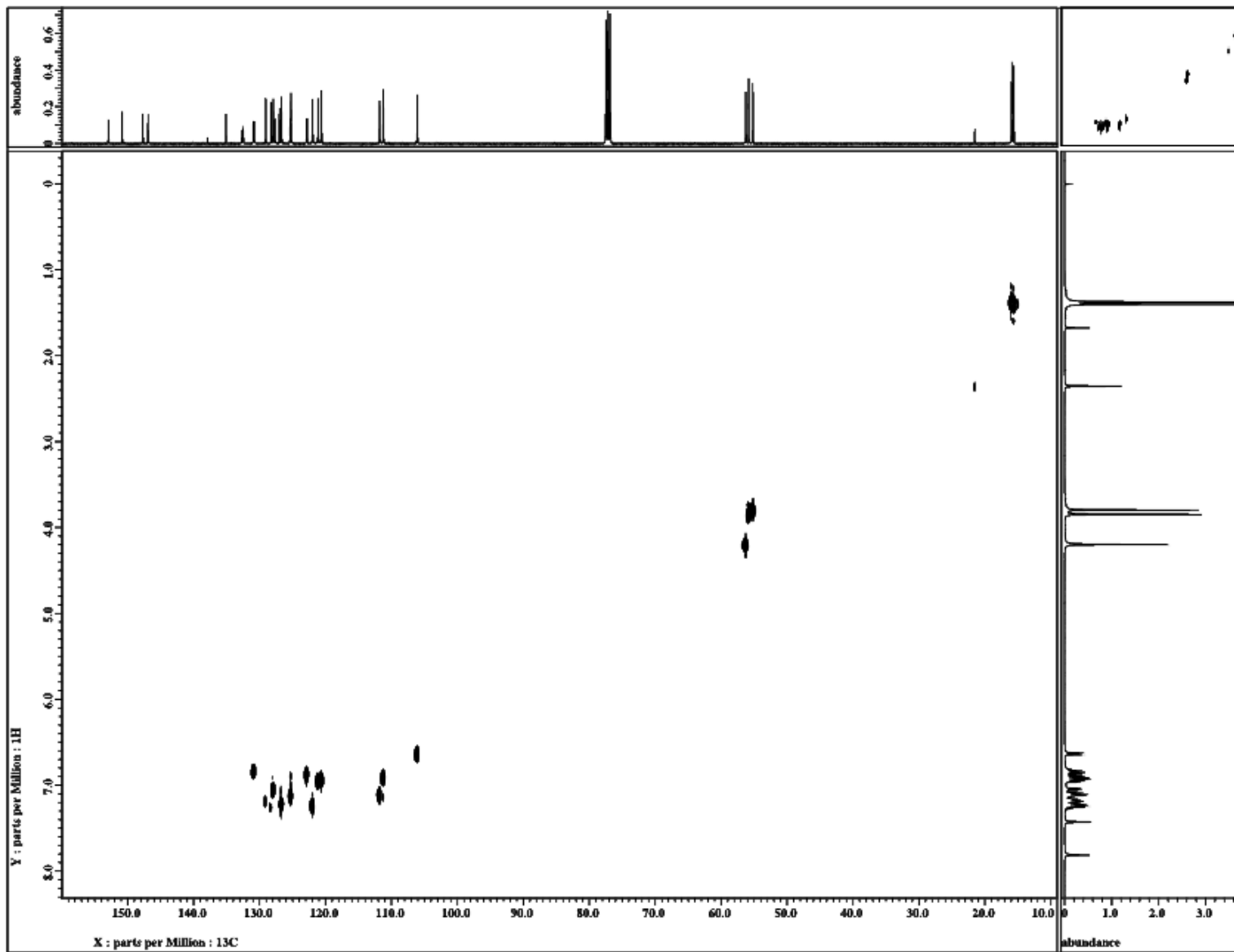


Fig. S88 The ^{13}C - ^1H HETCOR NMR spectrum of **13** (X-axis 100.5 MHz, Y-axis 400 MHz, CDCl_3).

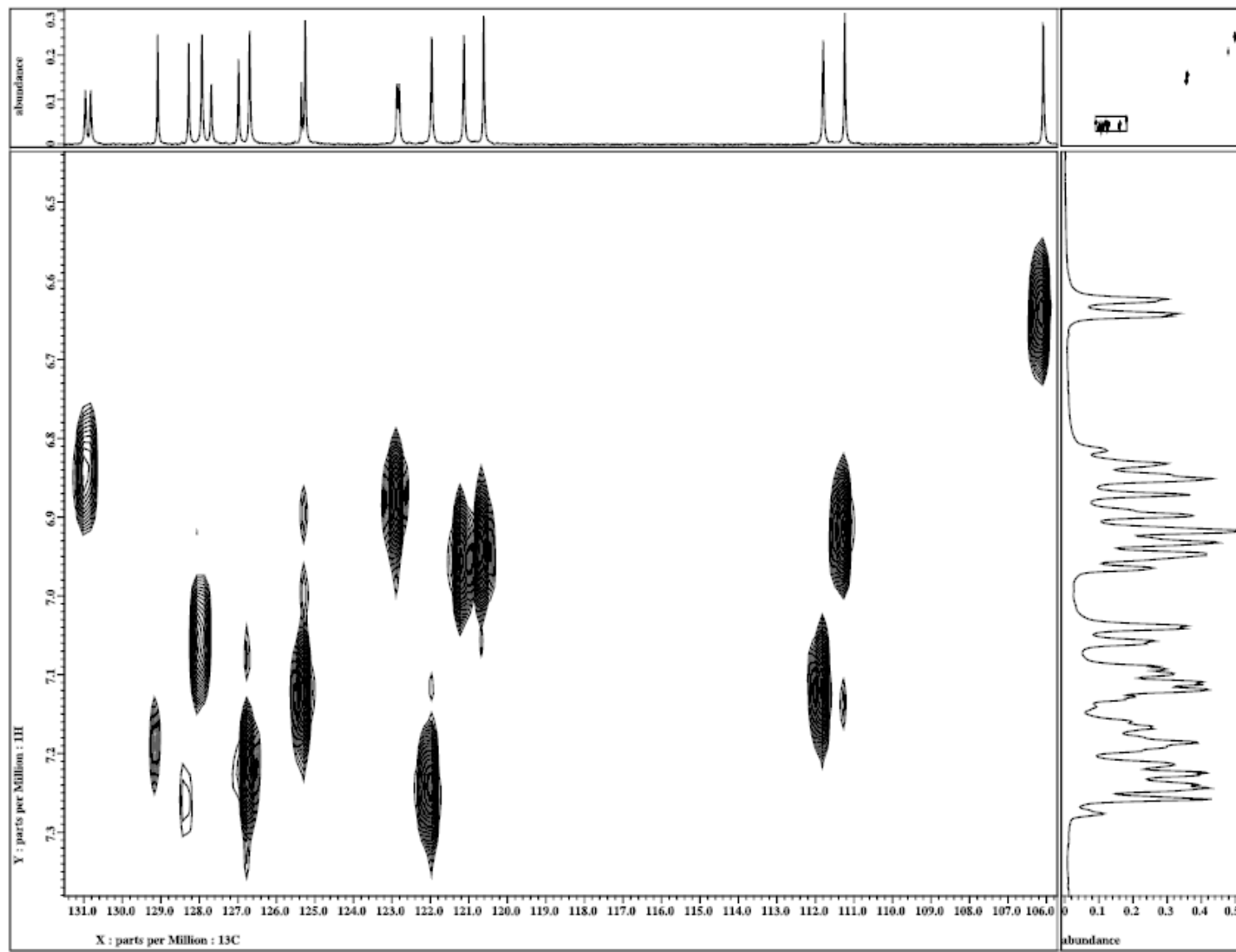


Fig. S89 The ¹³C-¹H HETCOR NMR spectrum of **13** illustrated for the ArCH carbons (X-axis 100.5 MHz, Y-axis 400 MHz, CDCl₃).

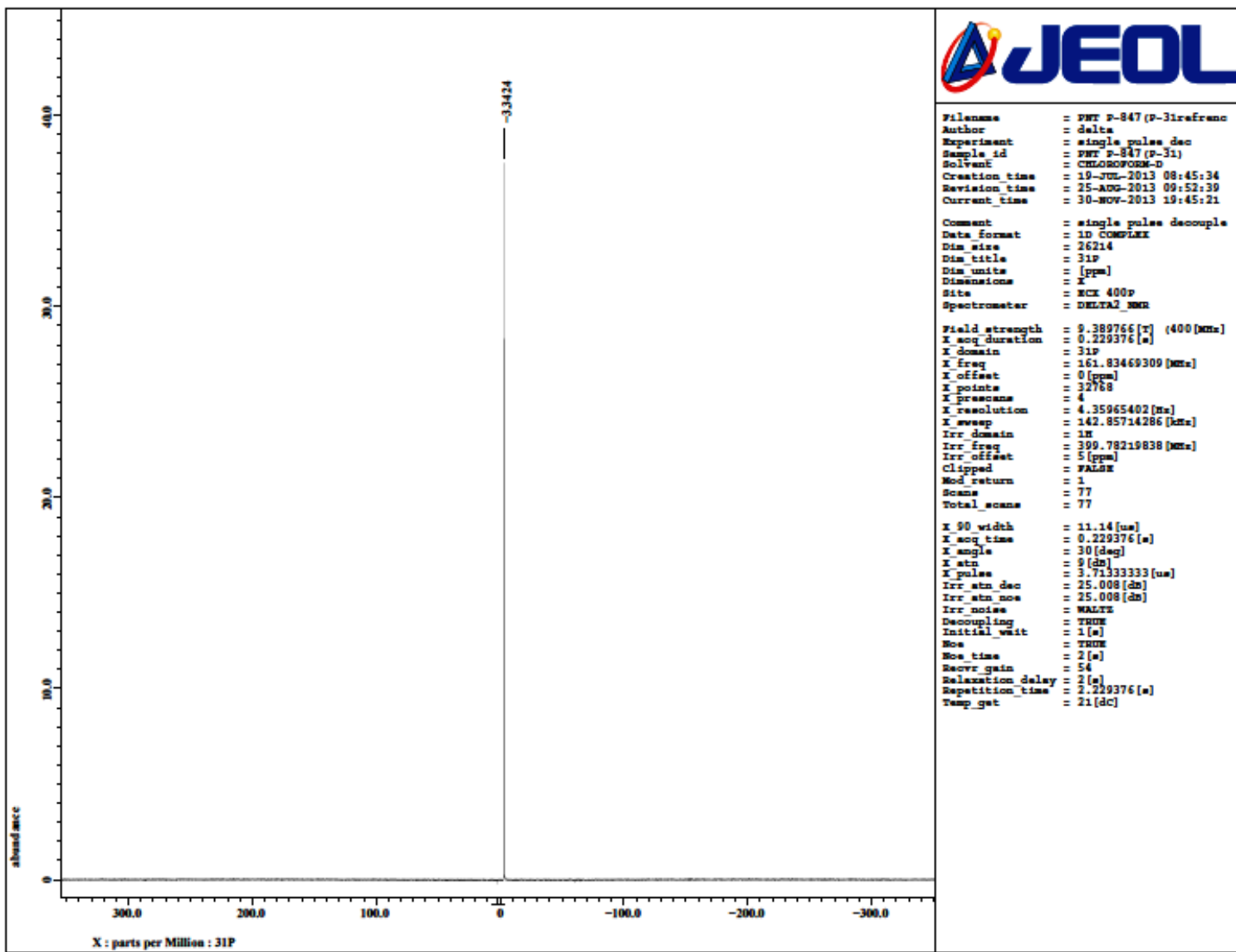


Fig. S90 $^{31}\text{P}\{\text{H}\}$ NMR spectrum of **13** (CDCl_3 , 161.8 MHz).

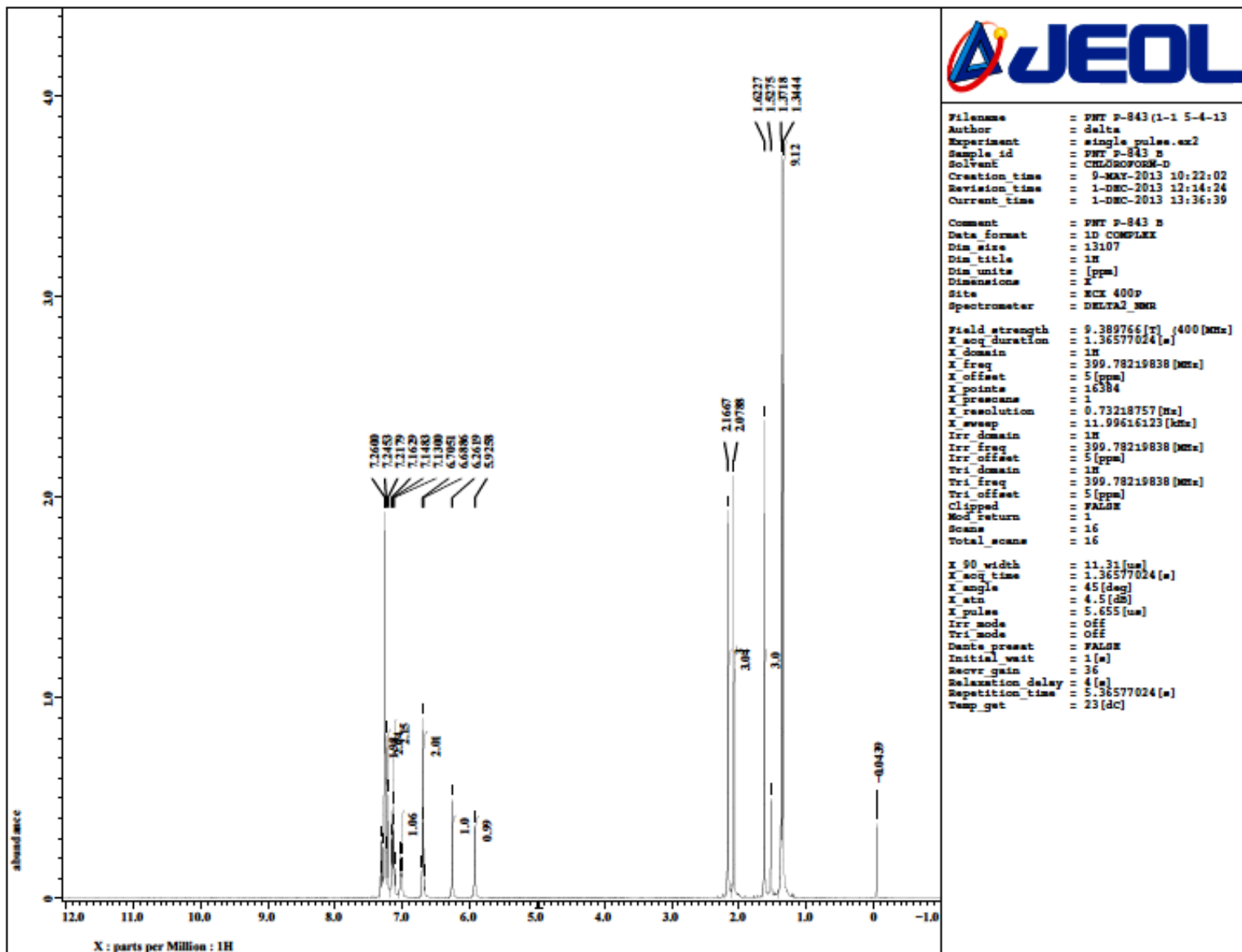


Fig. S91 ^1H NMR spectrum of **14** (CDCl_3 , 400.0 MHz).

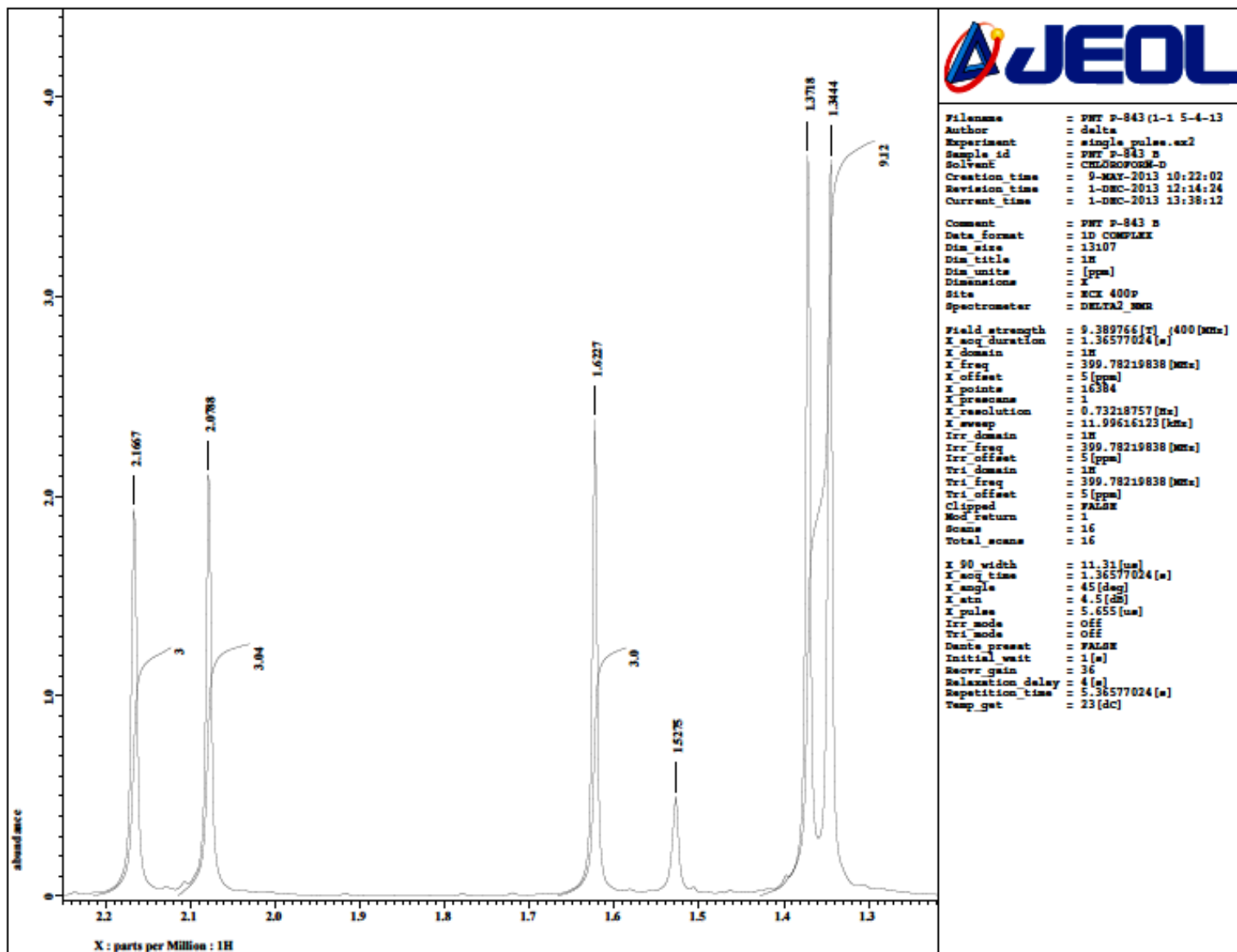


Fig. S92 Expansion of ^1H NMR spectrum of **14** (CDCl_3 , 400.0 MHz).

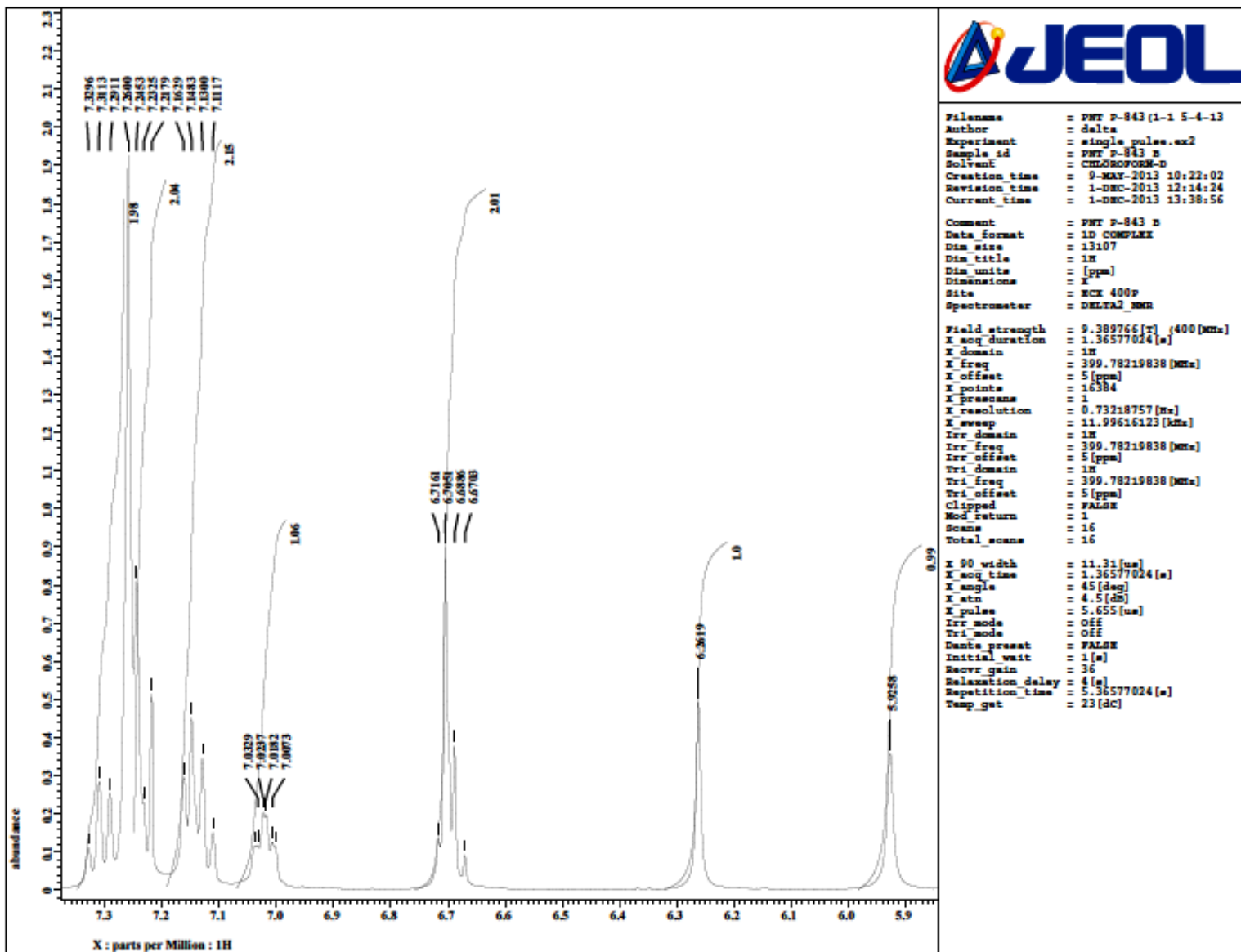


Fig. S93 Expansion of ^1H NMR spectrum of **14** (CDCl_3 , 400.0 MHz).

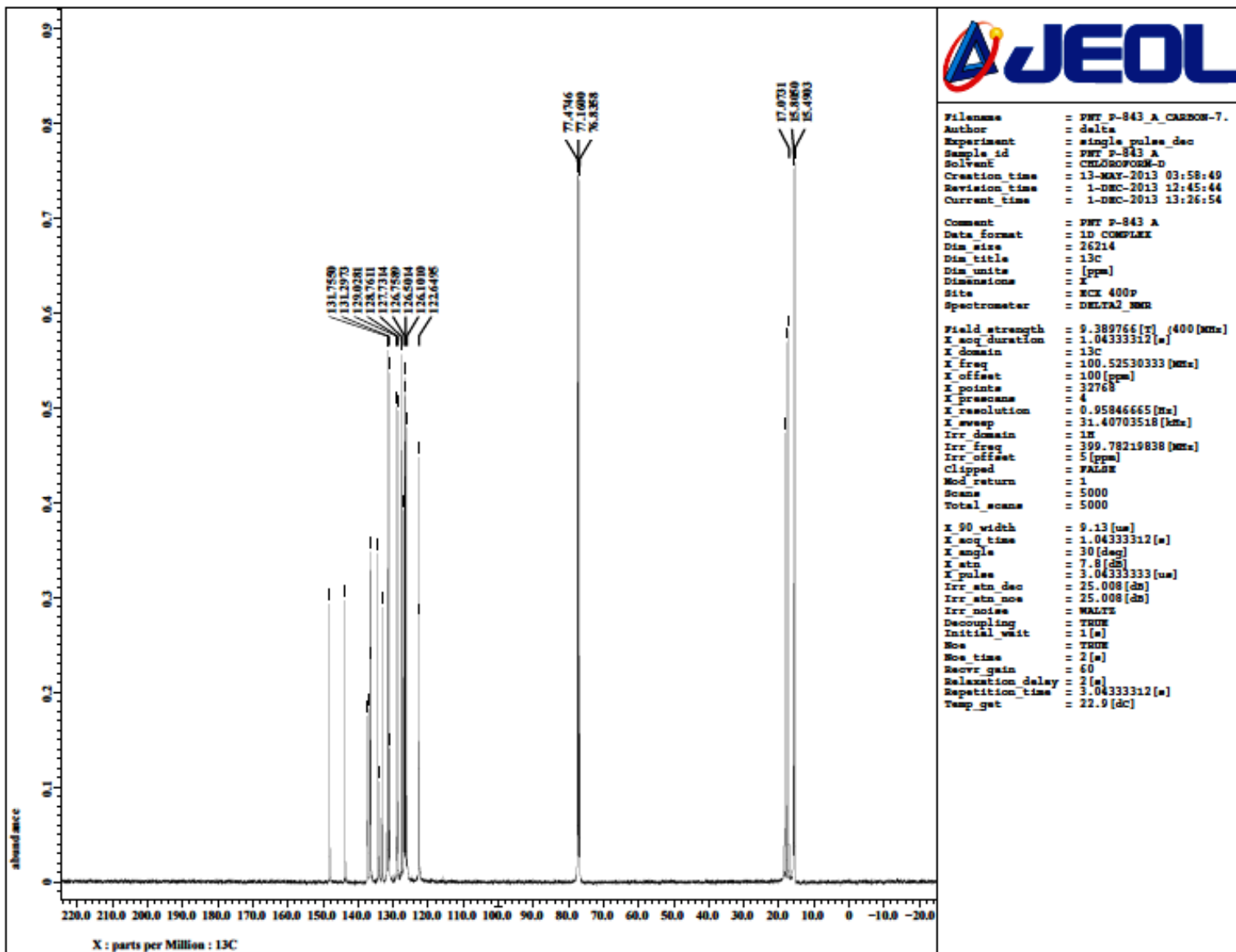


Fig. S94 ^{13}C NMR spectrum of **14** (CDCl_3 , 100.5 MHz).

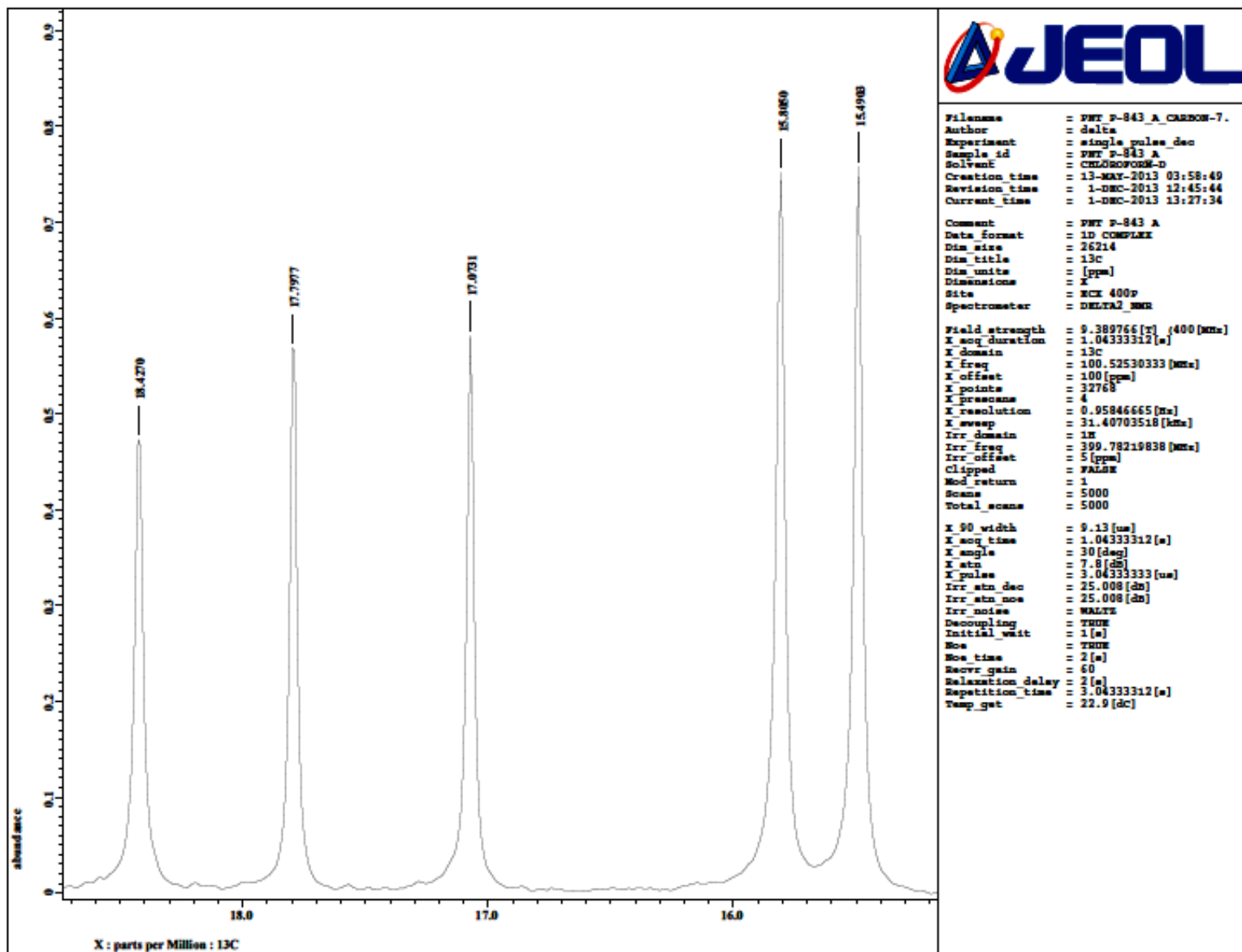


Fig. S95 Expansion of ^{13}C NMR spectrum of **14** (CDCl_3 , 100.5 MHz).

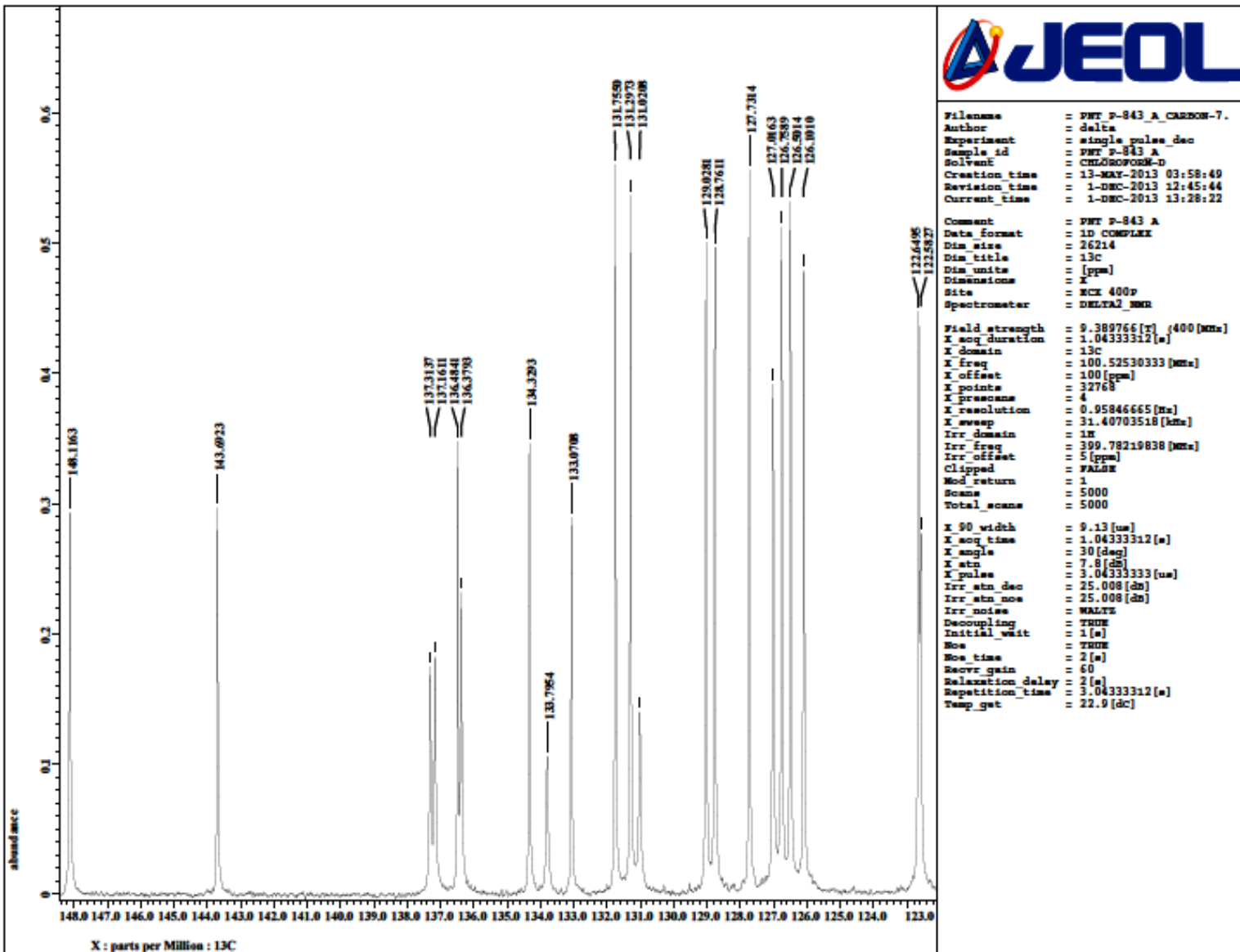


Fig. S96 Expansion of ^{13}C NMR spectrum of **14** (CDCl_3 , 100.5 MHz).

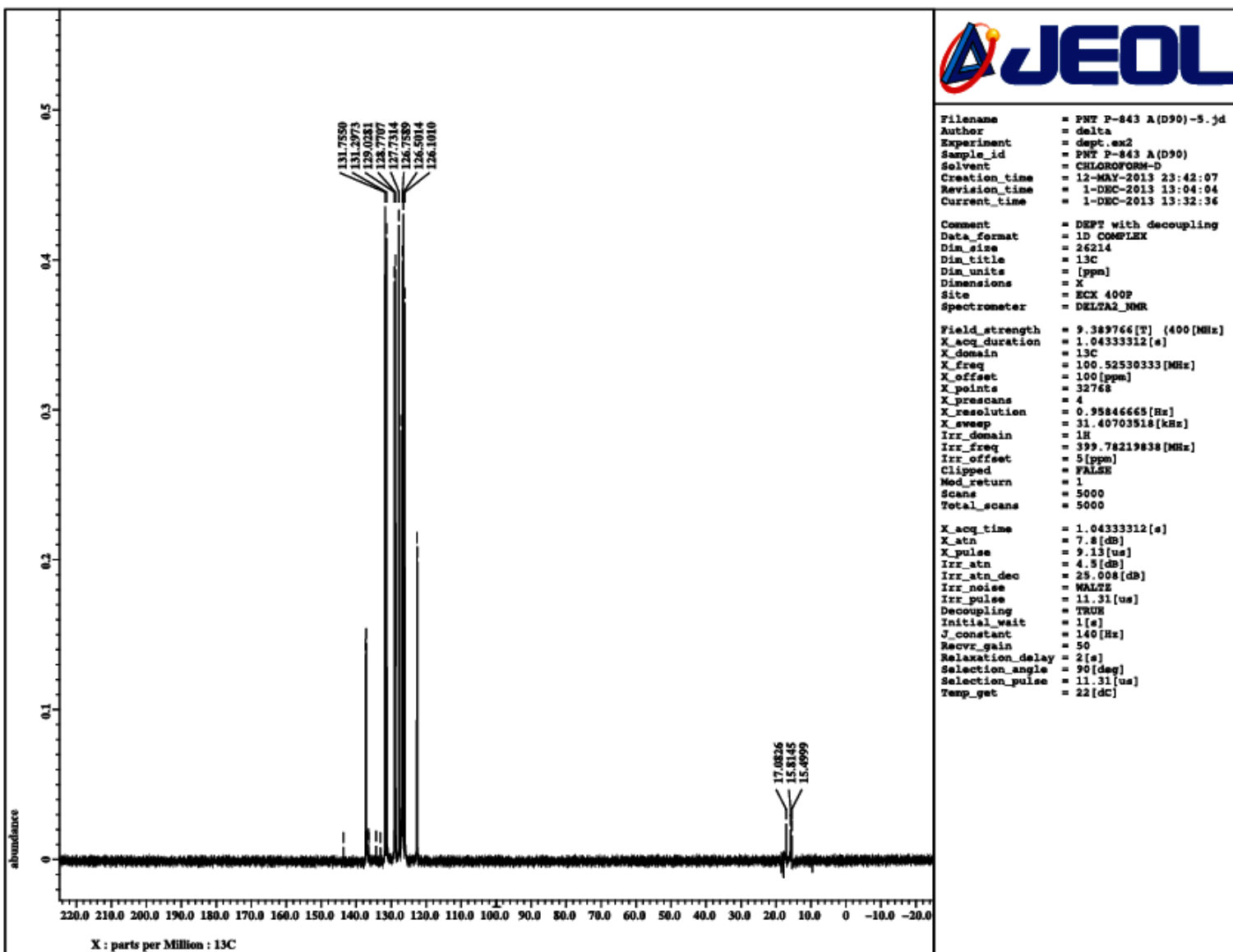


Fig. S97 DEPT 90 NMR spectrum of **14** (CDCl_3 , 100.5 MHz). The peaks around δ 15 correspond to residual peaks of CH_3 carbons.

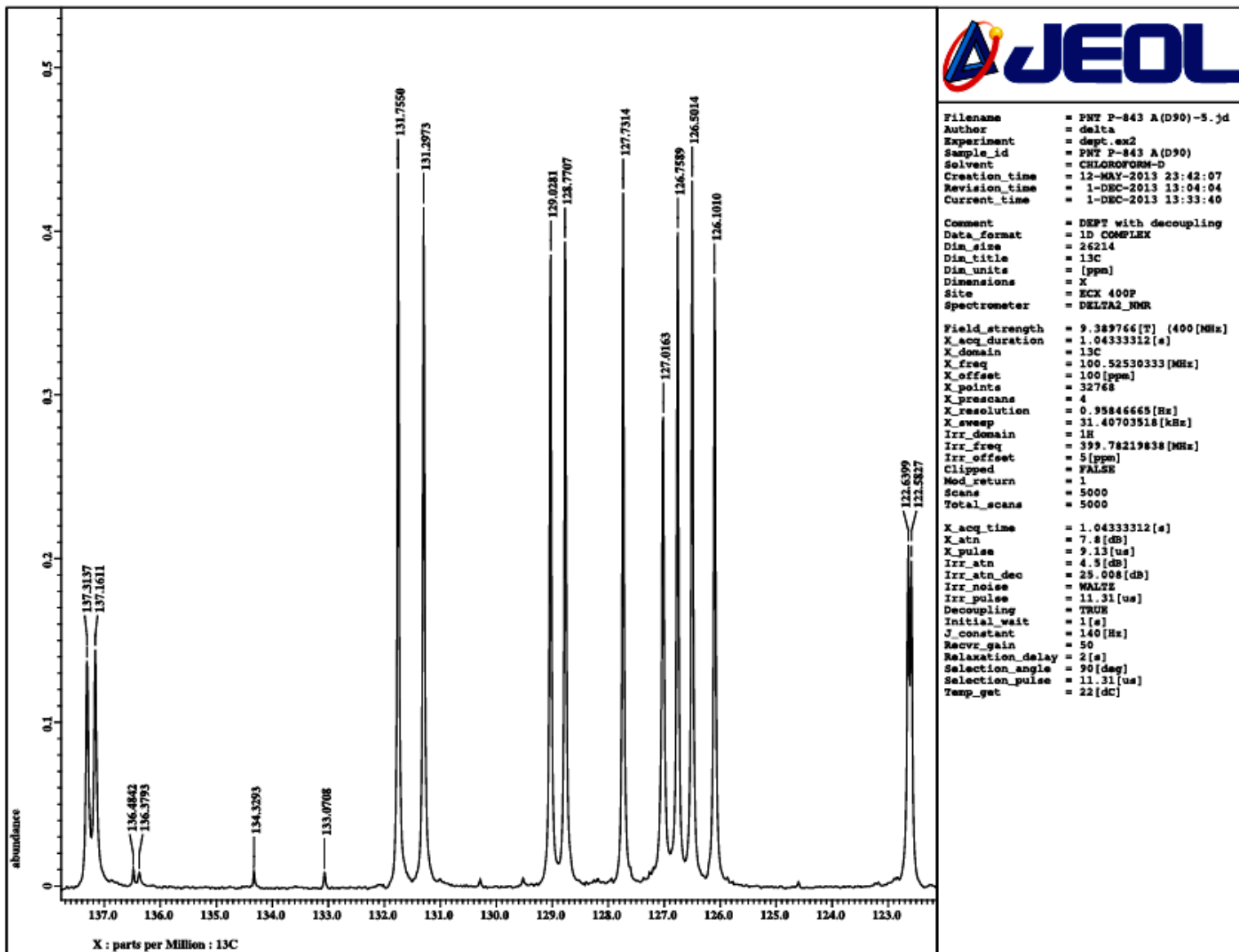


Fig. S98 Expansion of DEPT 90 NMR spectrum of **14**.

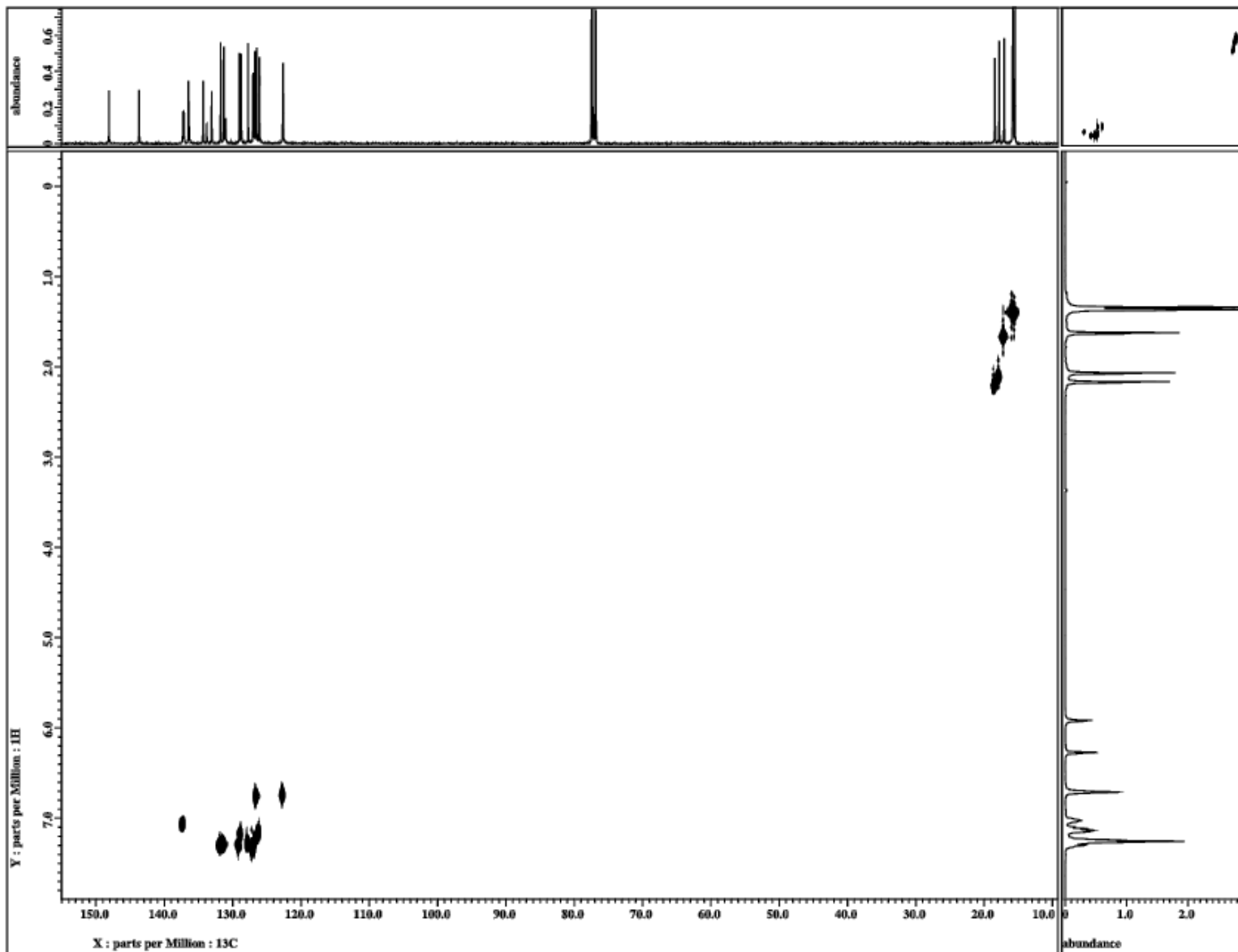


Fig. S99 The ^{13}C - ^1H HETCOR NMR spectrum of **14** (X-axis 100.5 MHz, Y-axis 400 MHz, CDCl_3).

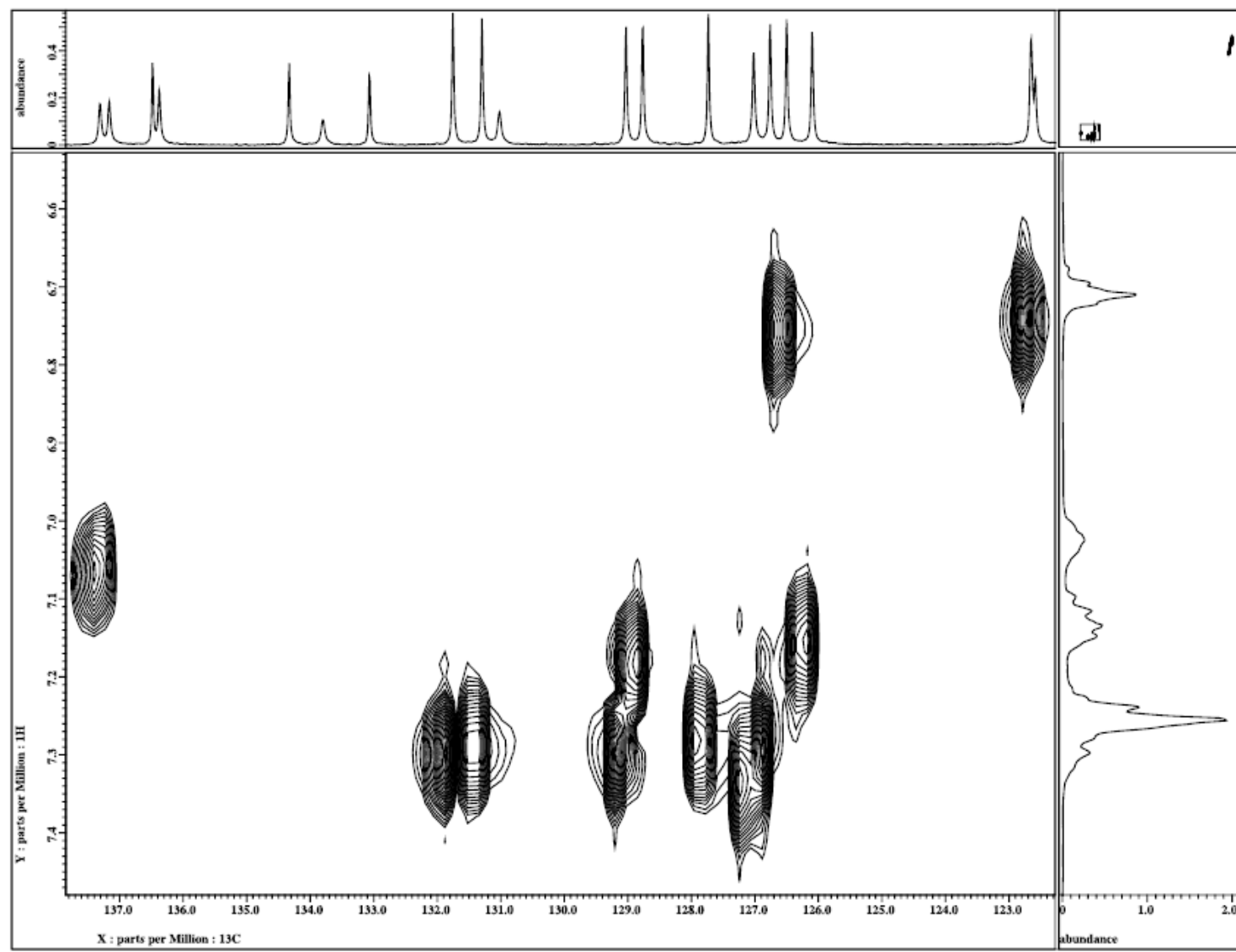


Fig. S100 The $^{13}\text{C}-^1\text{H}$ HETCOR NMR spectrum of **14** illustrated for the ArCH carbons (X-axis 100.5 MHz, Y-axis 400 MHz, CDCl_3).

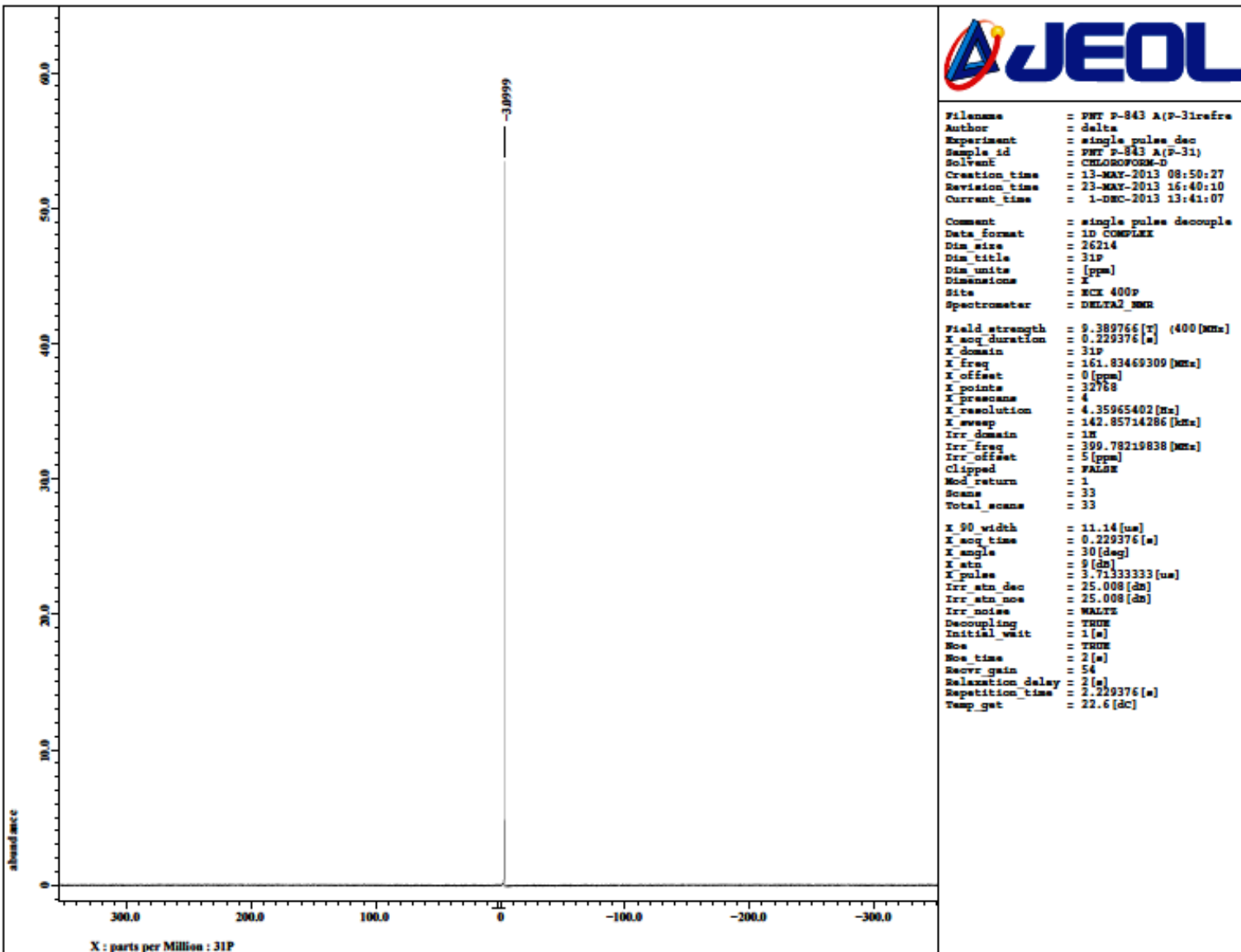


Fig. S101 $^{31}\text{P}\{\text{H}\}$ NMR spectrum of **14** (CDCl_3 , 161.8 MHz).

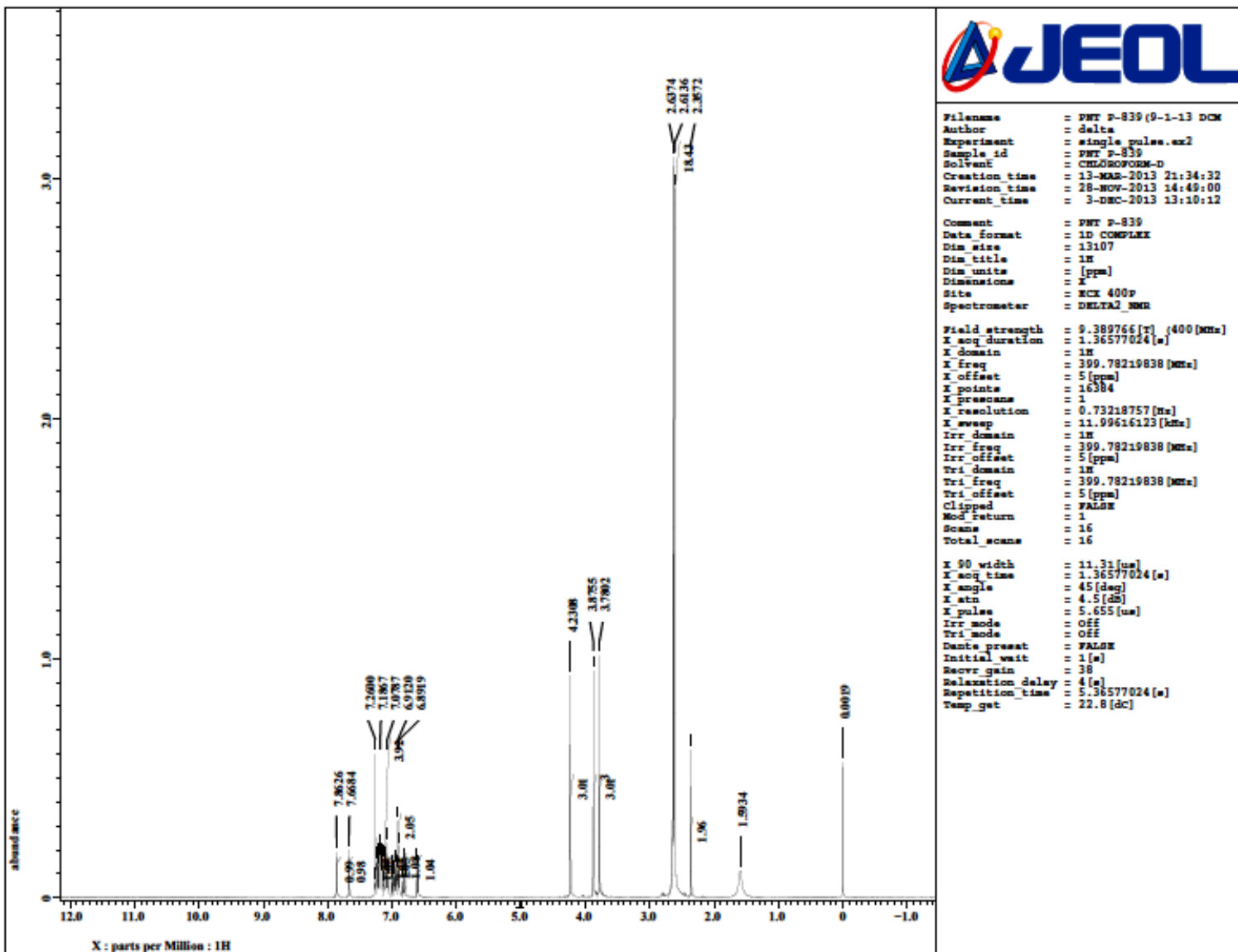


Fig. S102 ^1H NMR spectrum of **15** (CDCl_3 , 400.0 MHz).

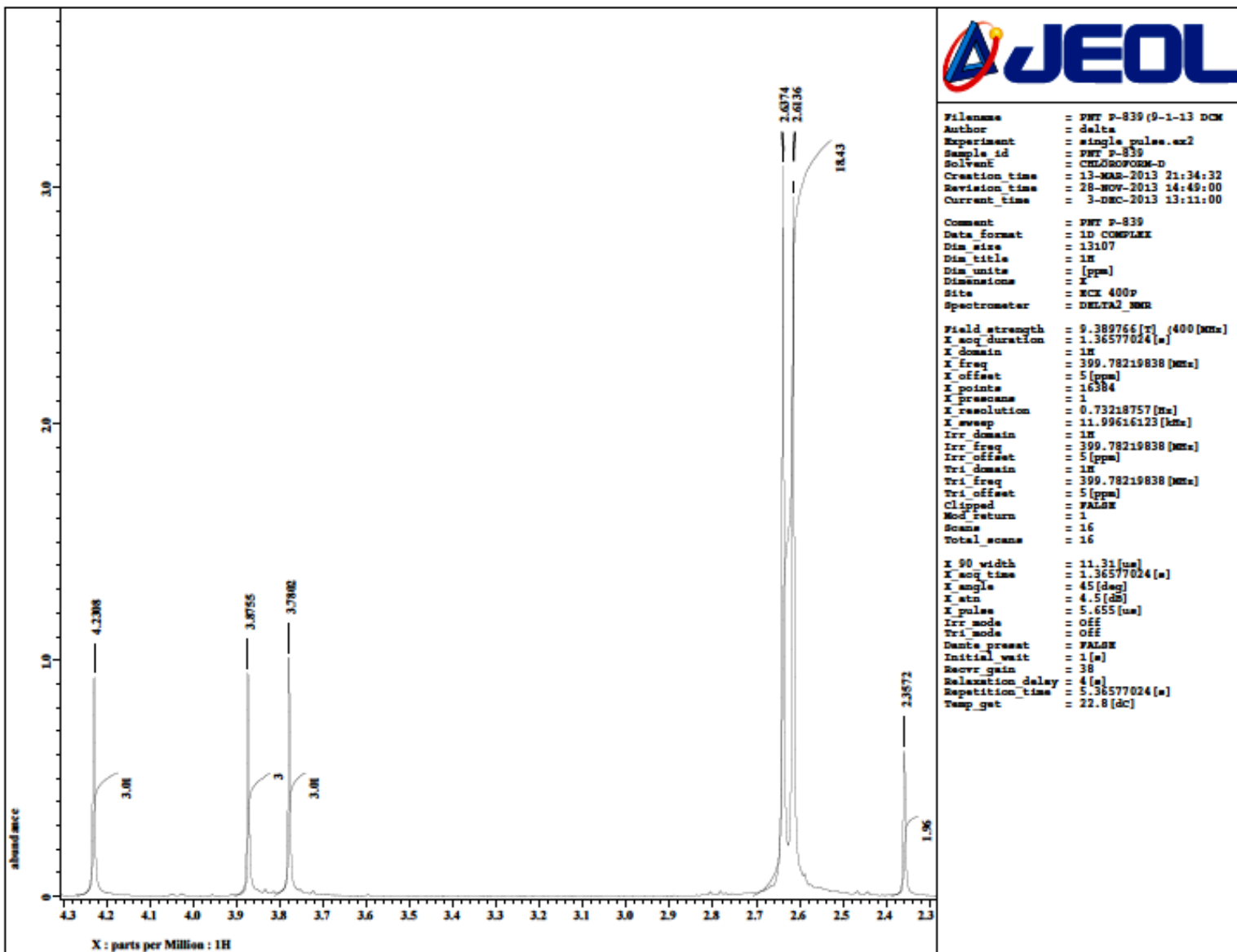


Fig. S103 Expansion of ^1H NMR spectrum of **15** (CDCl_3 , 400.0 MHz).

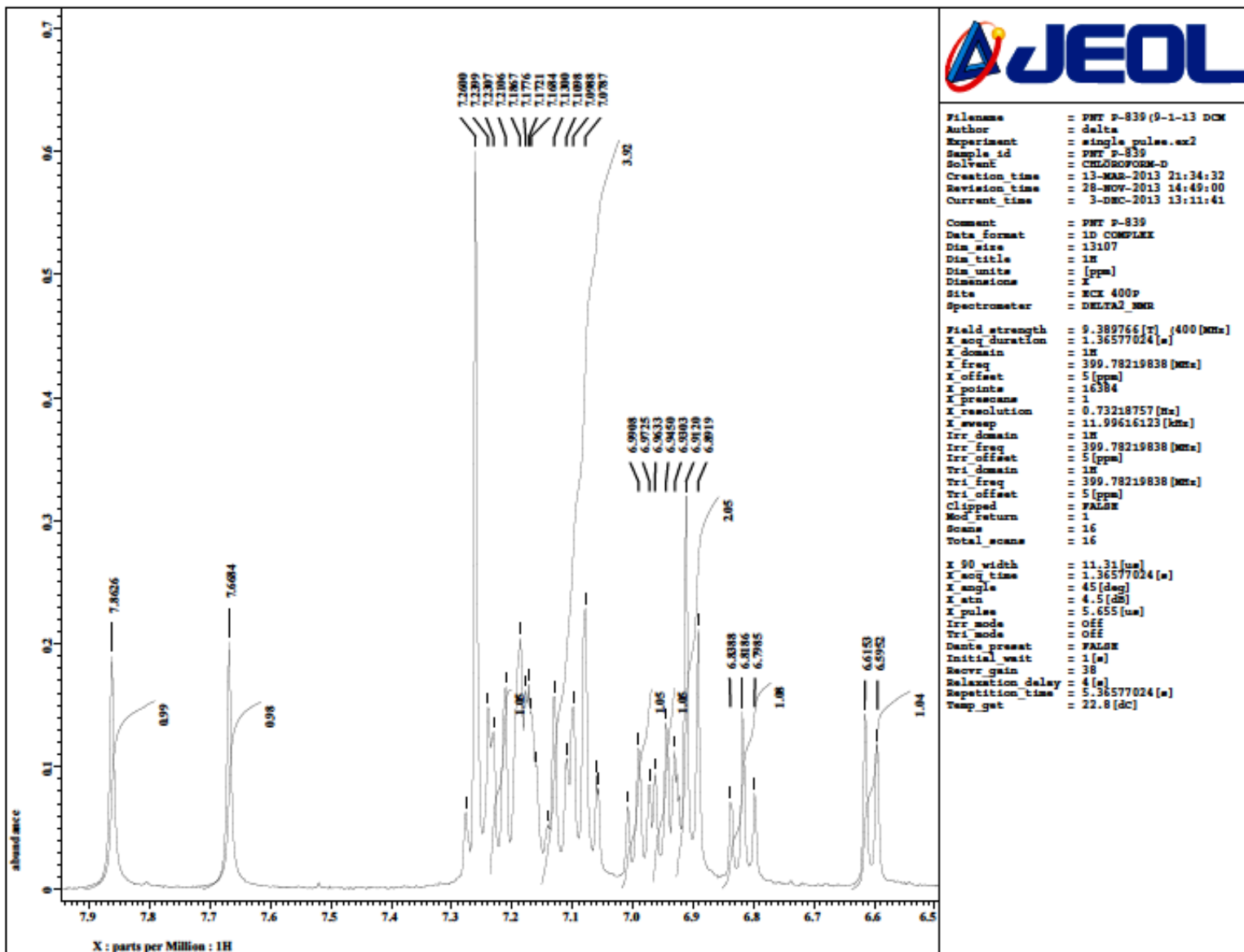


Fig. S104 Expansion of ^1H NMR spectrum of **15** (CDCl_3 , 400.0 MHz).

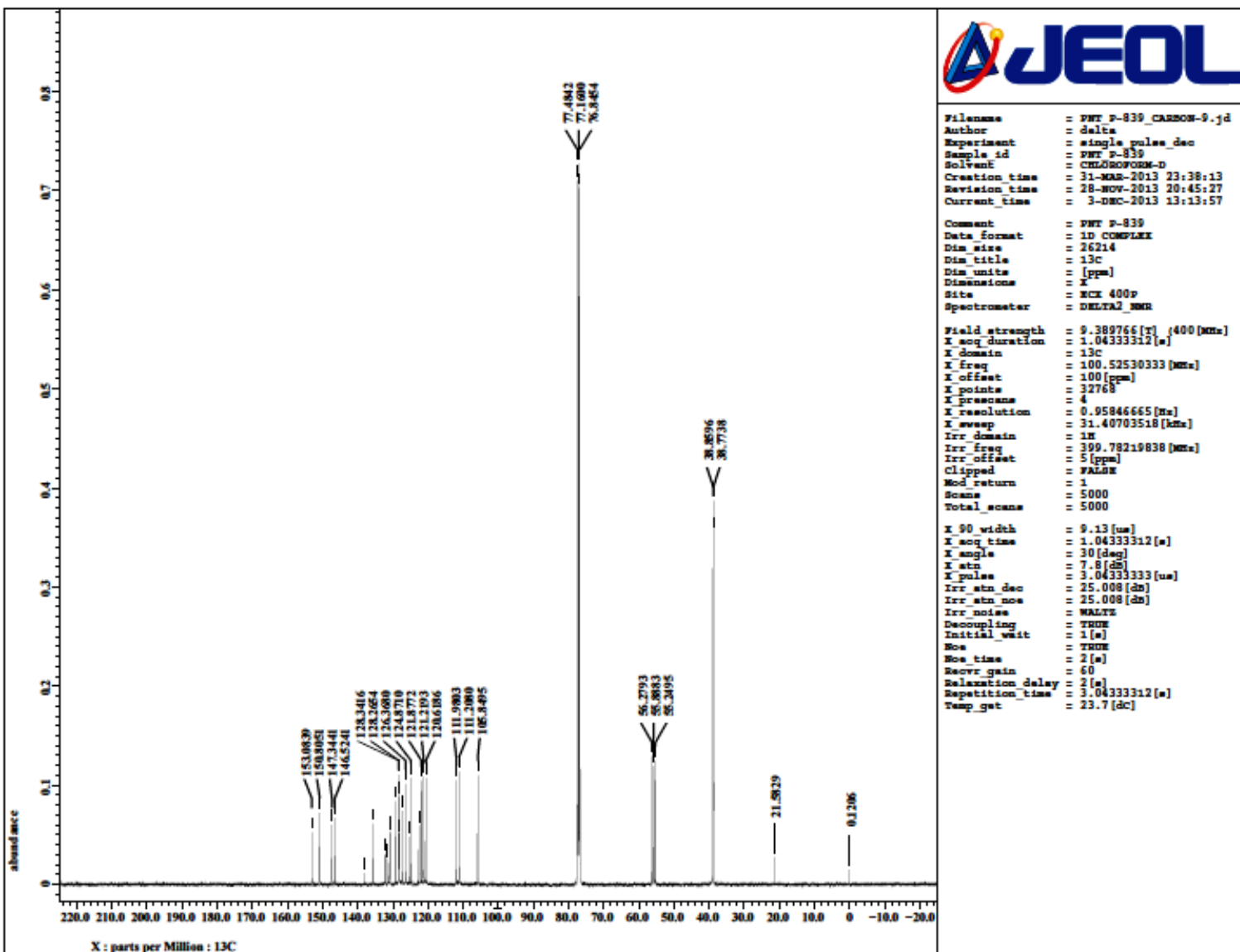


Fig. S105 ^{13}C NMR spectrum of **15** (CDCl_3 , 100.5 MHz).

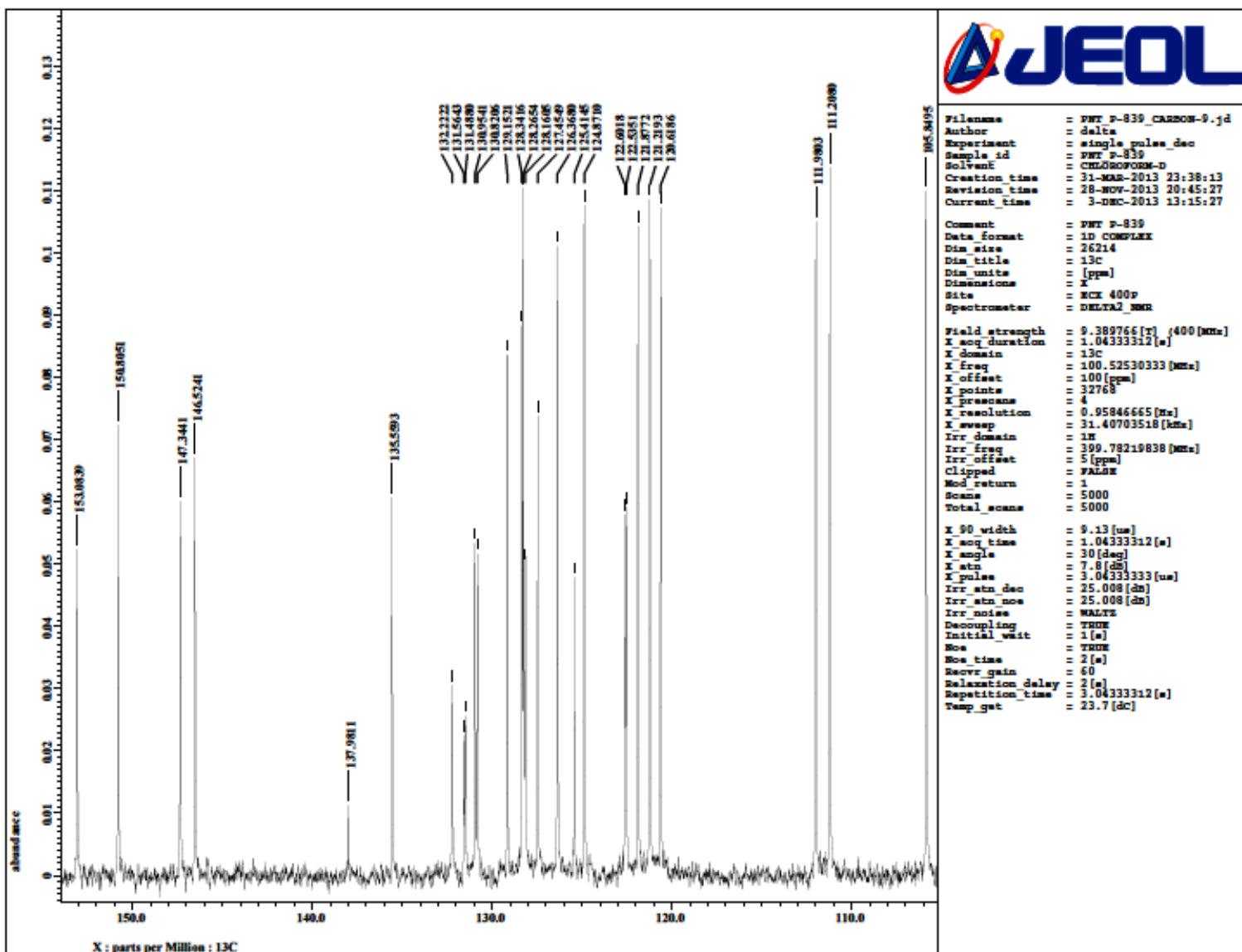


Fig. S106 Expansion of ^{13}C NMR spectrum of **15** (CDCl_3 , 100.5 MHz).

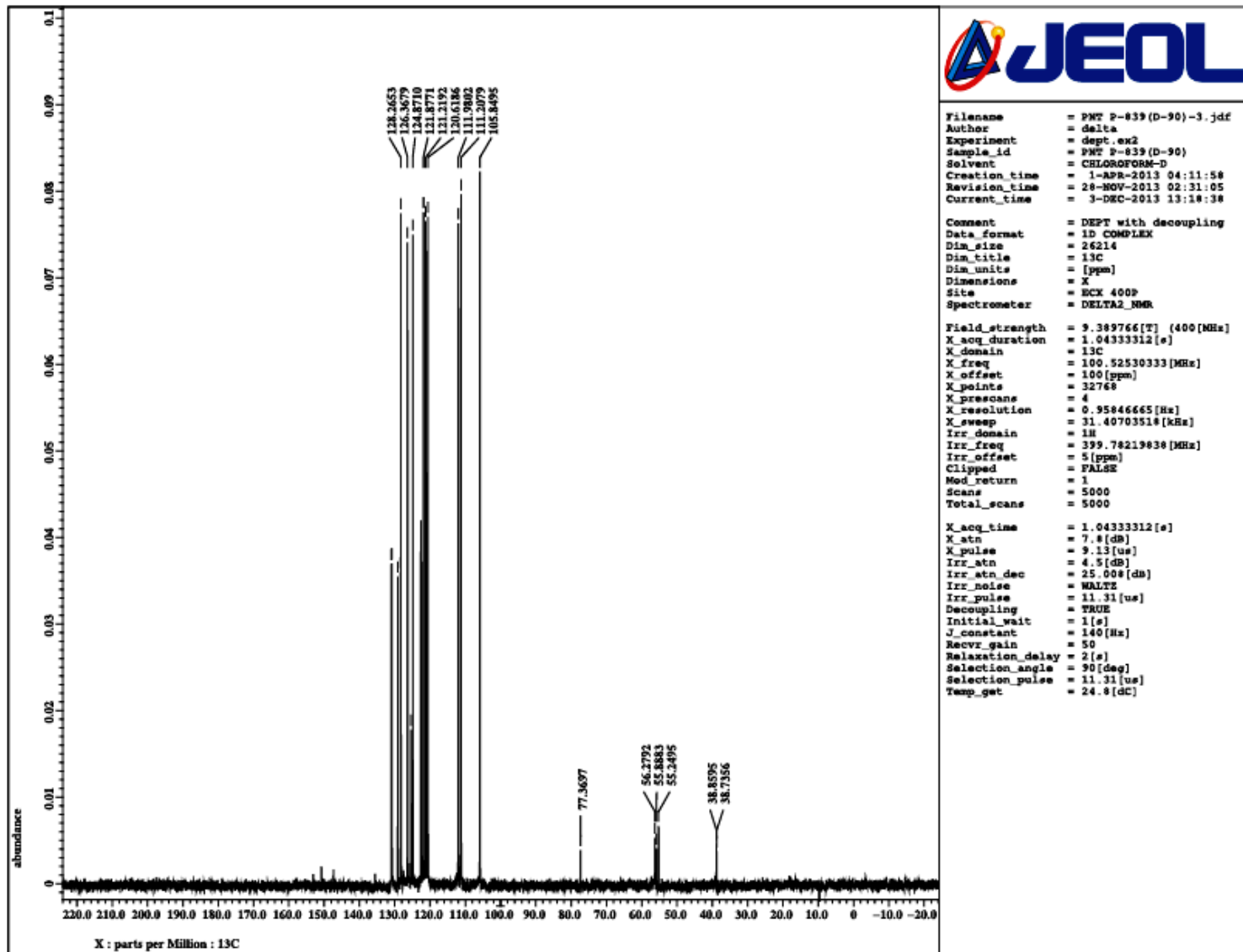


Fig. S107 DEPT 90 NMR spectrum of **15** (CDCl_3 , 100.5 MHz). The peaks around δ 38 and 56 correspond to residual peaks of CH_3 and OCH_3 carbons.

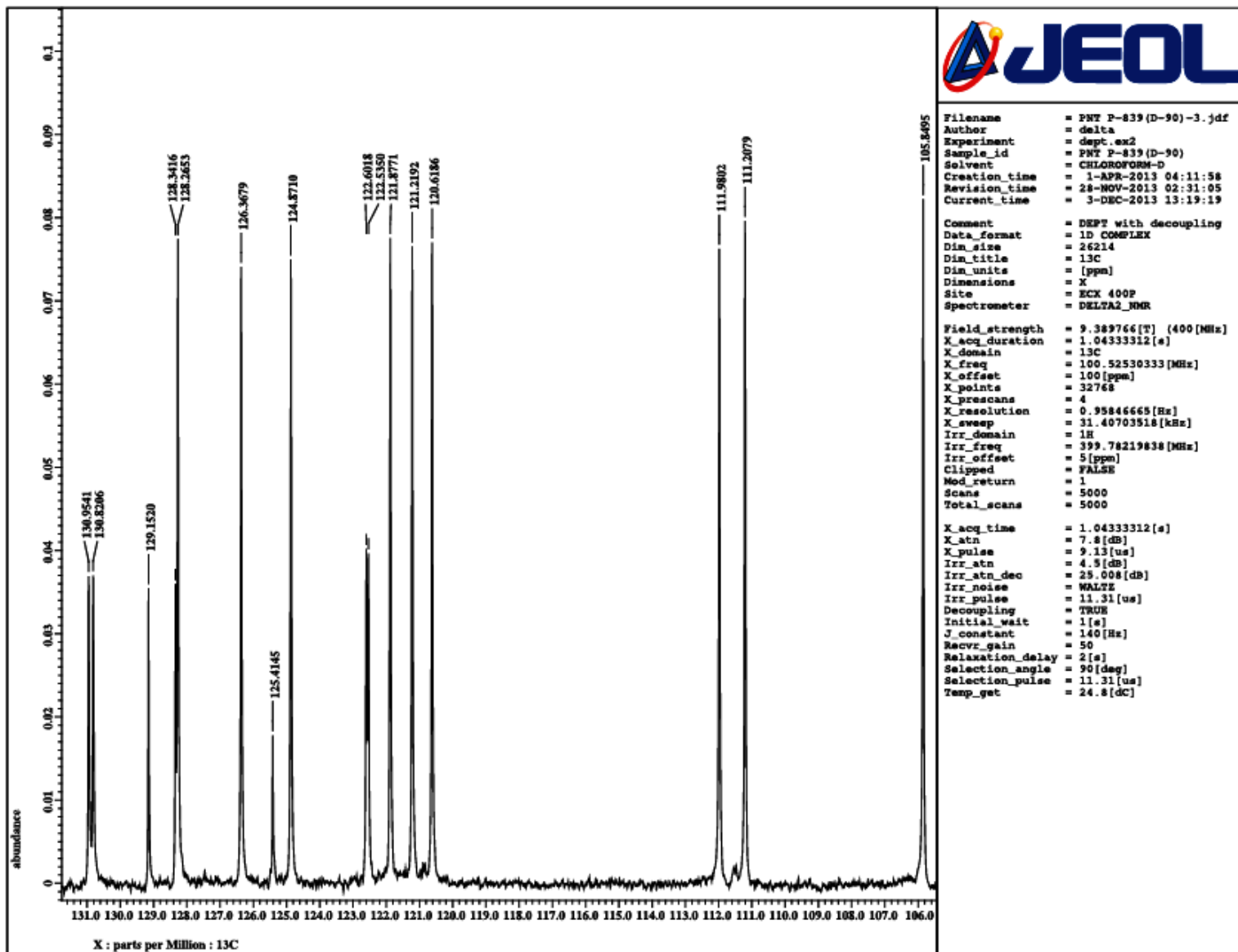


Fig. S108 Expansion of DEPT 90 NMR spectrum of 15.

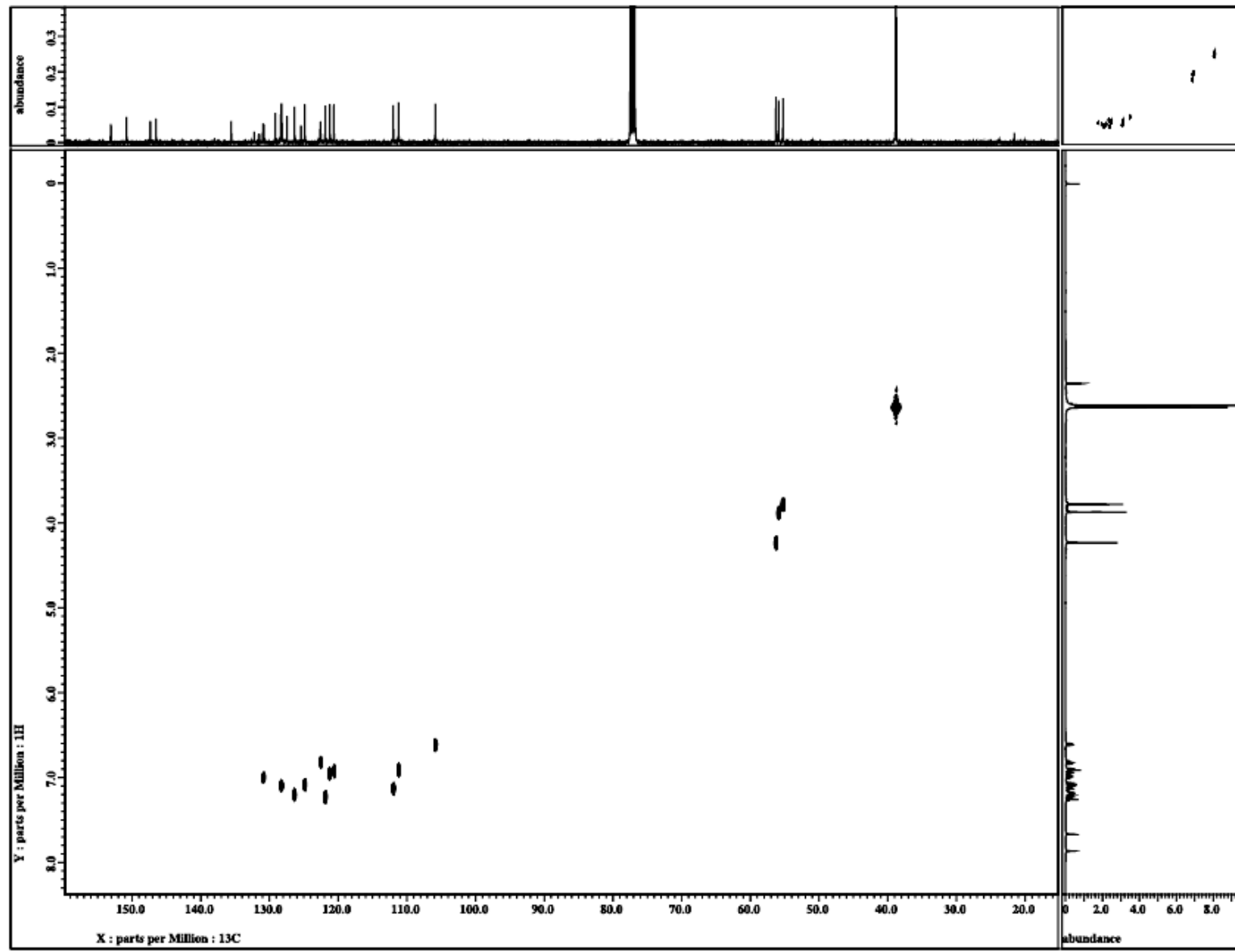


Fig. S109 The ^{13}C - ^1H HETCOR NMR spectrum of **15** (X-axis 100.5 MHz, Y-axis 400 MHz, CDCl_3).

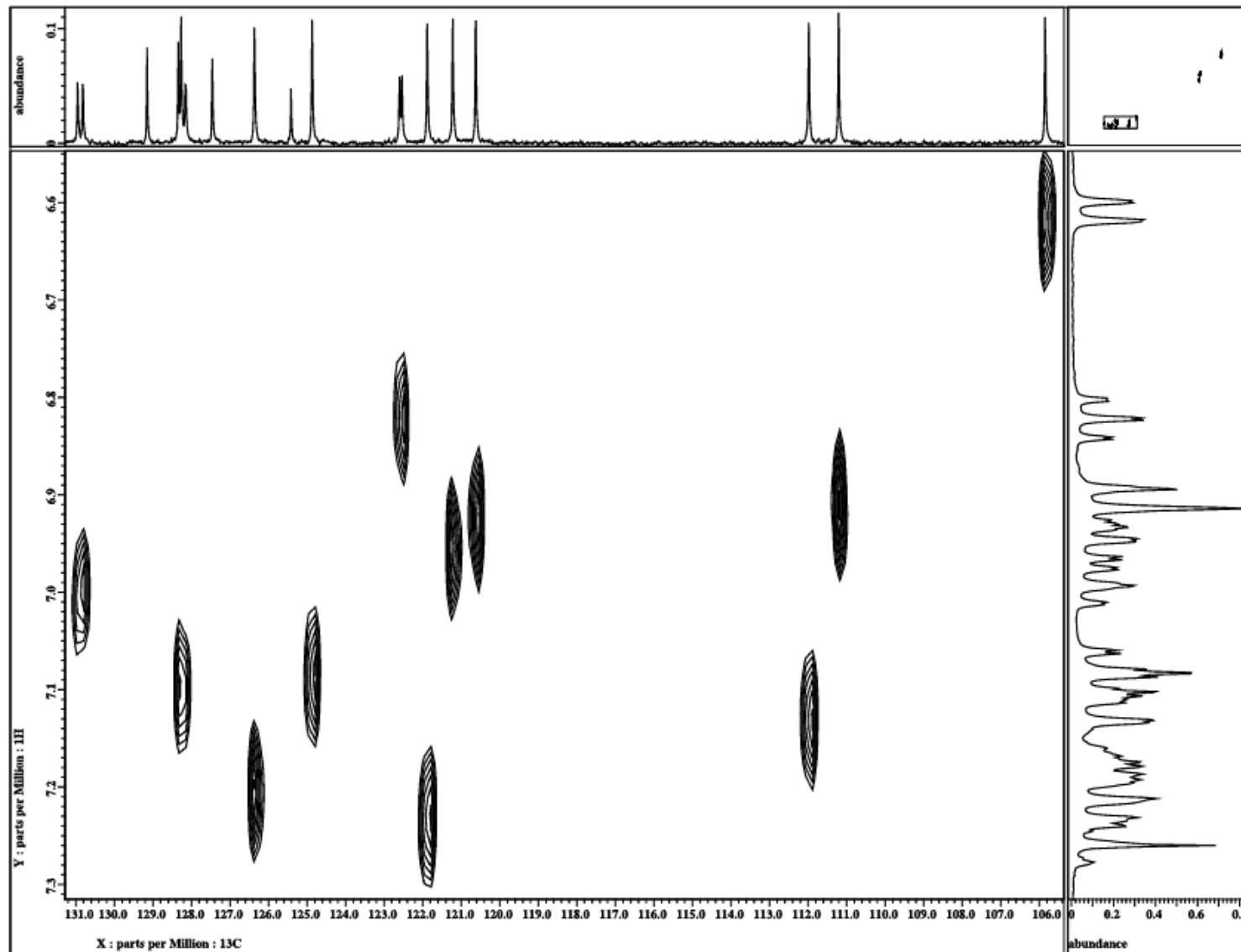


Fig. S110 The ^{13}C - ^1H HETCOR NMR spectrum of **15** illustrated for the ArCH carbons (X-axis 100.5 MHz, Y-axis 400 MHz, CDCl_3).

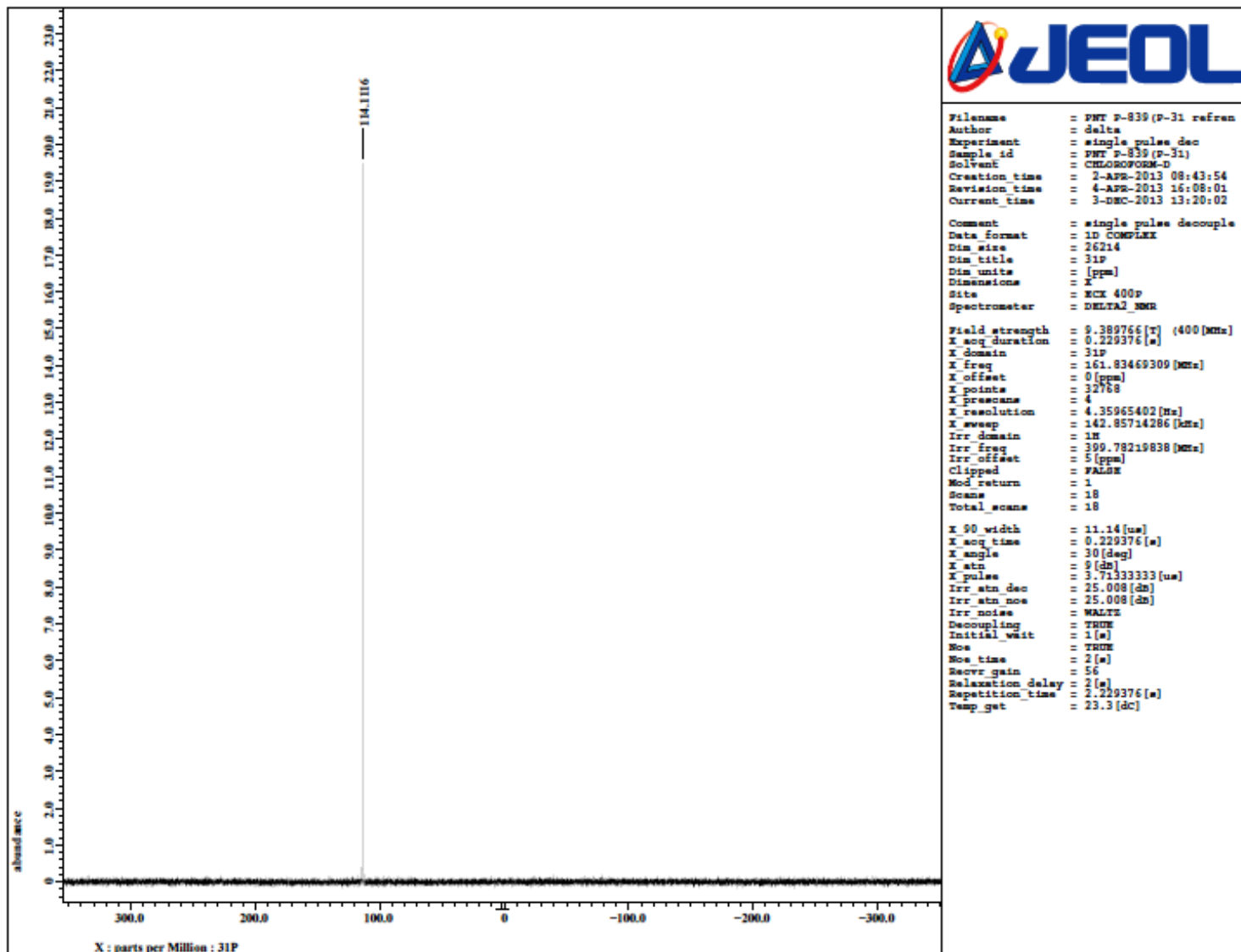


Fig. S111 $^{31}\text{P}\{\text{H}\}$ NMR spectrum of **15** (CDCl₃, 161.8 MHz).

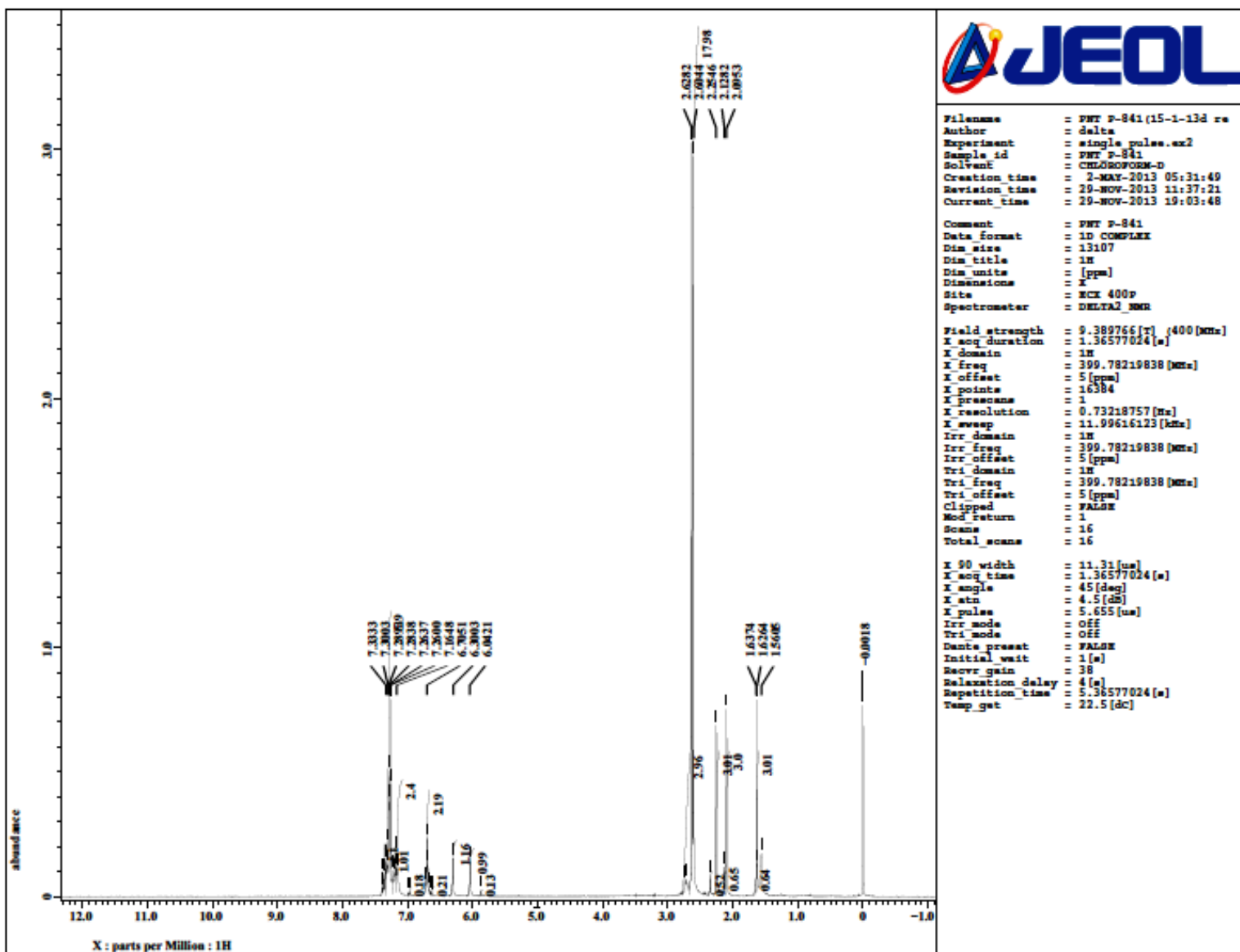


Fig. S112 ^1H NMR spectrum of **16** (CDCl_3 , 400.0 MHz).

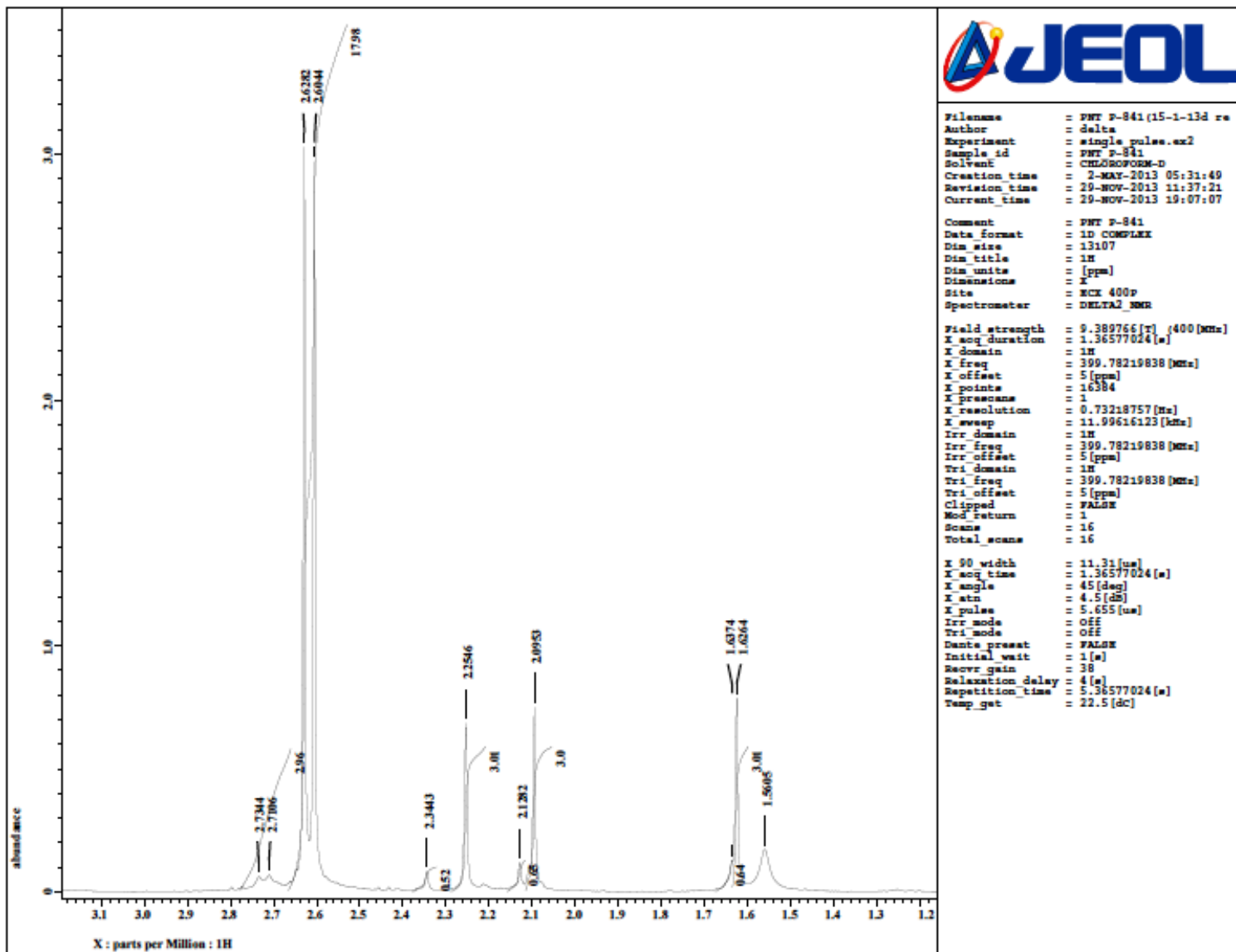


Fig. S113 Expansion of ^1H NMR spectrum of **16** (CDCl_3 , 400.0 MHz).

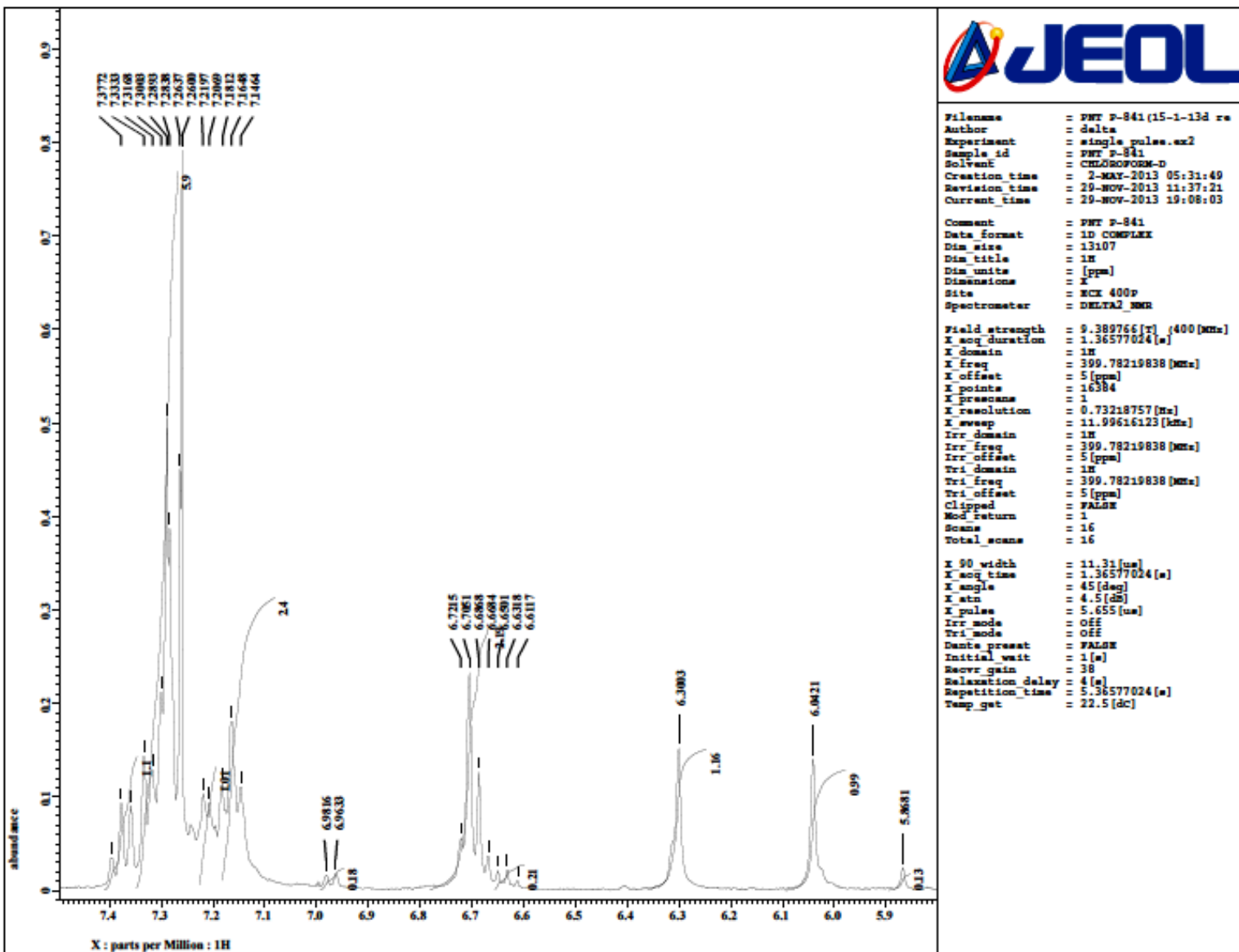


Fig. S114 Expansion of ^1H NMR spectrum of **16** (CDCl_3 , 400.0 MHz).

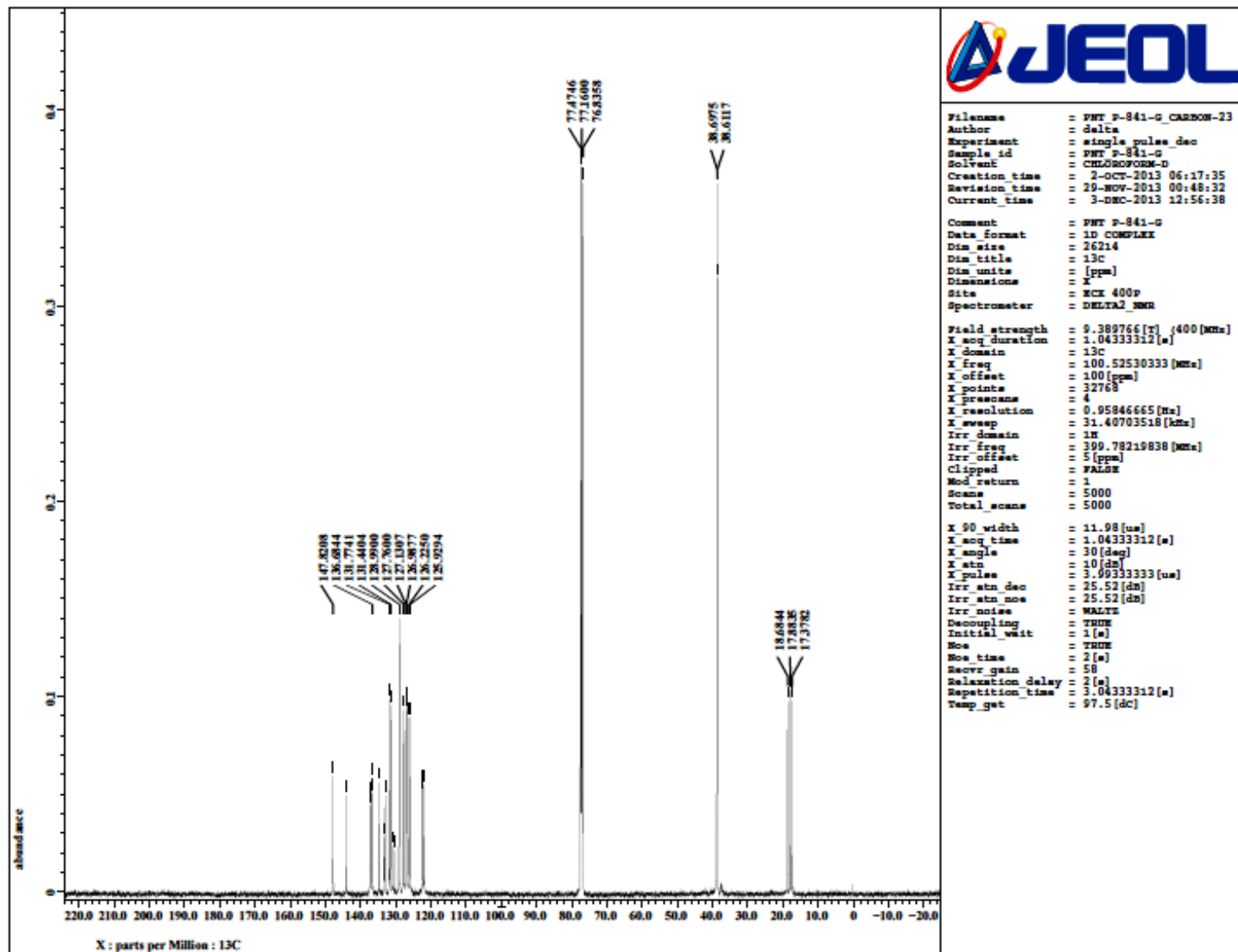


Fig. S115 ^{13}C NMR spectrum of **16** (CDCl_3 , 100.5 MHz).

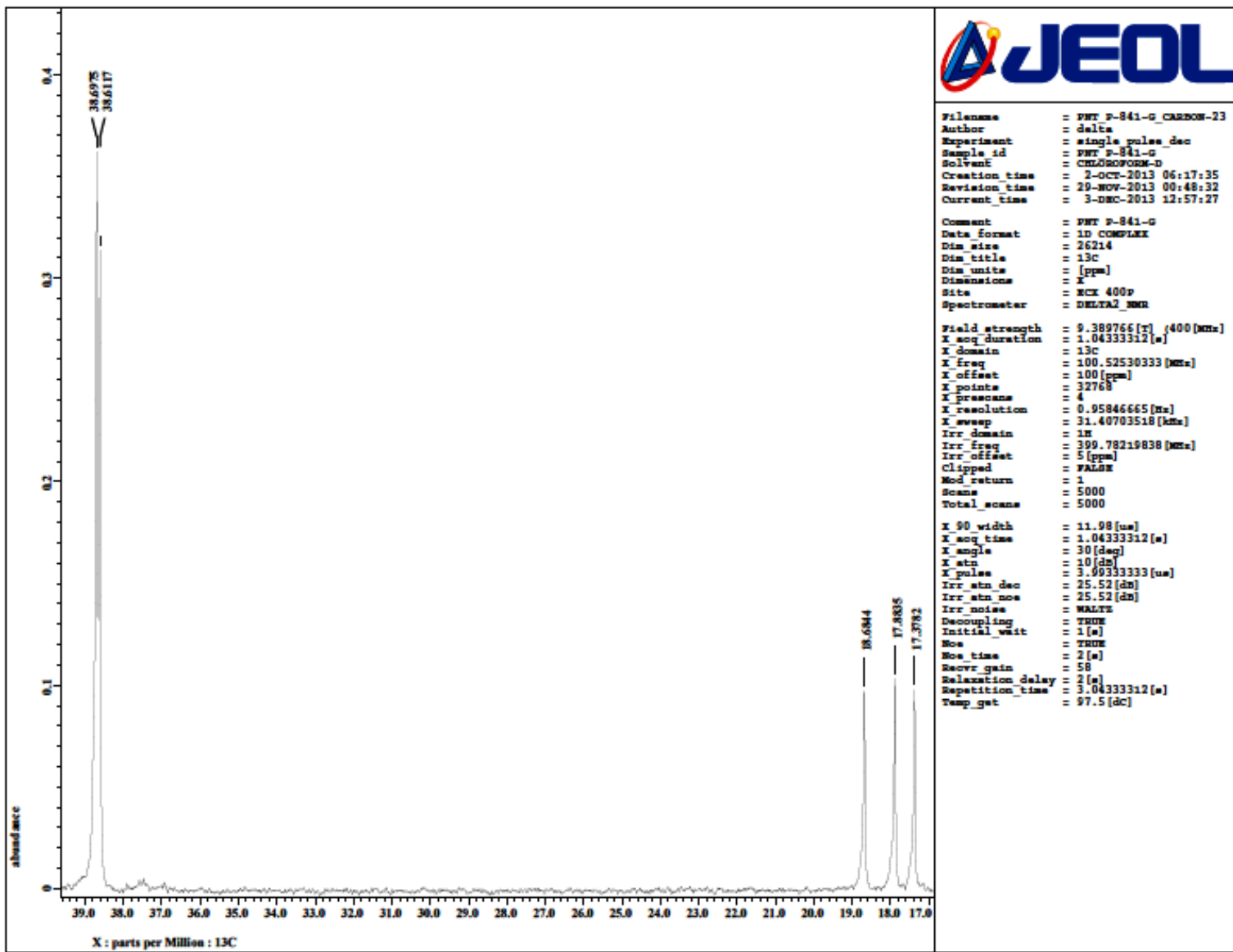


Fig. S116 Expansion of ^{13}C NMR spectrum of **16** (CDCl_3 , 100.5 MHz).

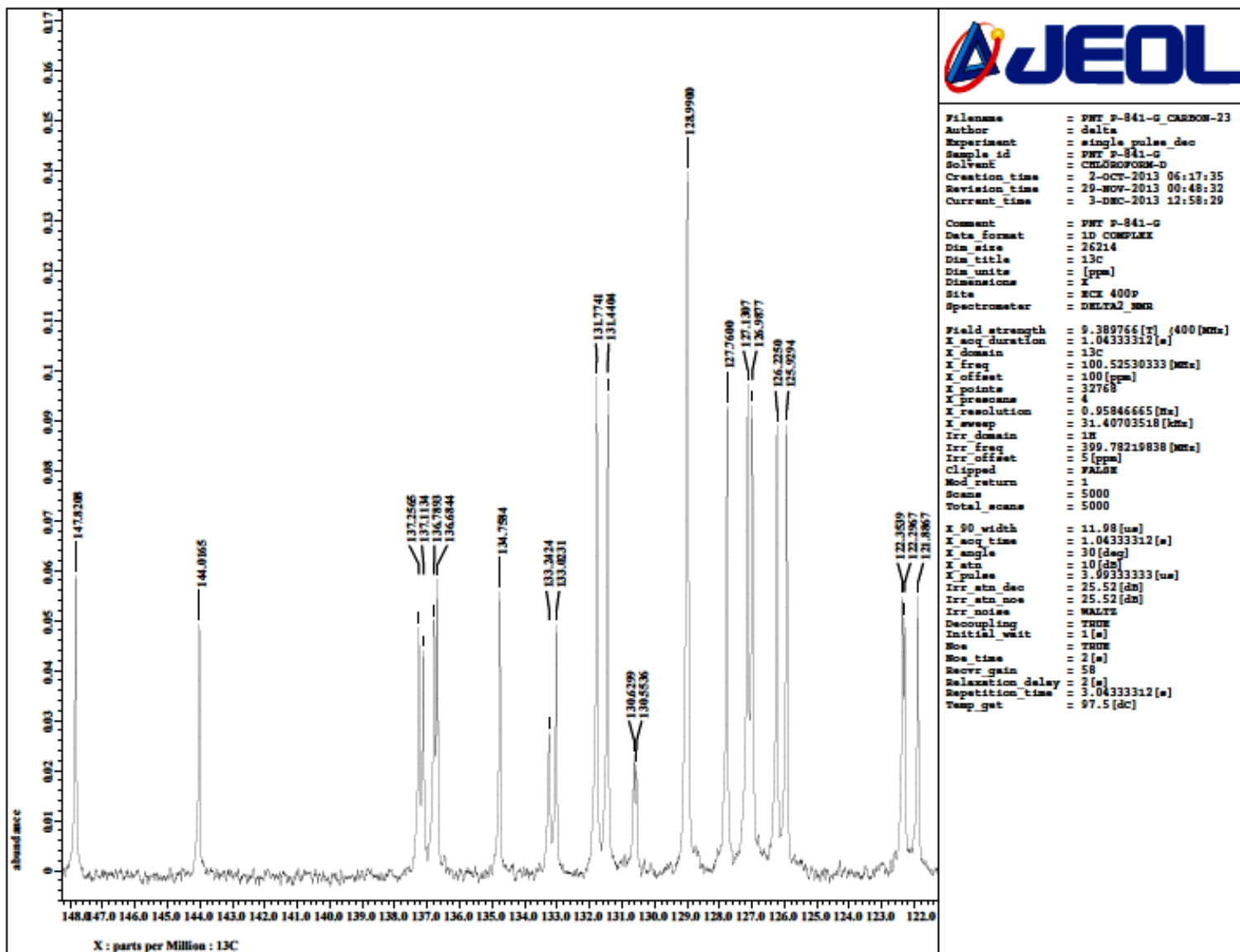


Fig. S117 Expansion of ^{13}C NMR spectrum of **16** (CDCl_3 , 100.5 MHz).

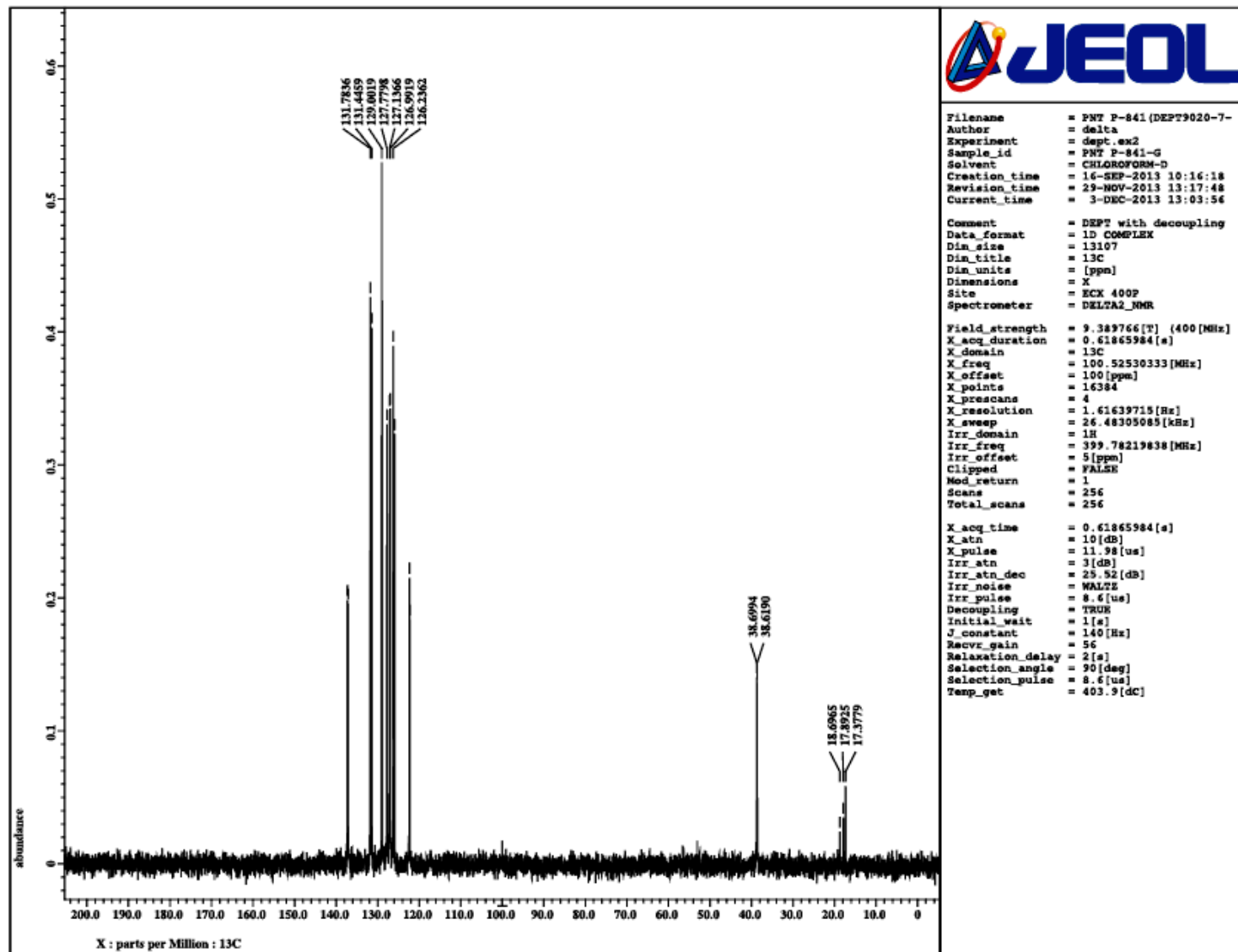


Fig. S118 DEPT 90 NMR spectrum of **16** (CDCl_3 , 100.5 MHz). The peaks around δ 17 and 38 correspond to residual peaks of CH_3 carbons.

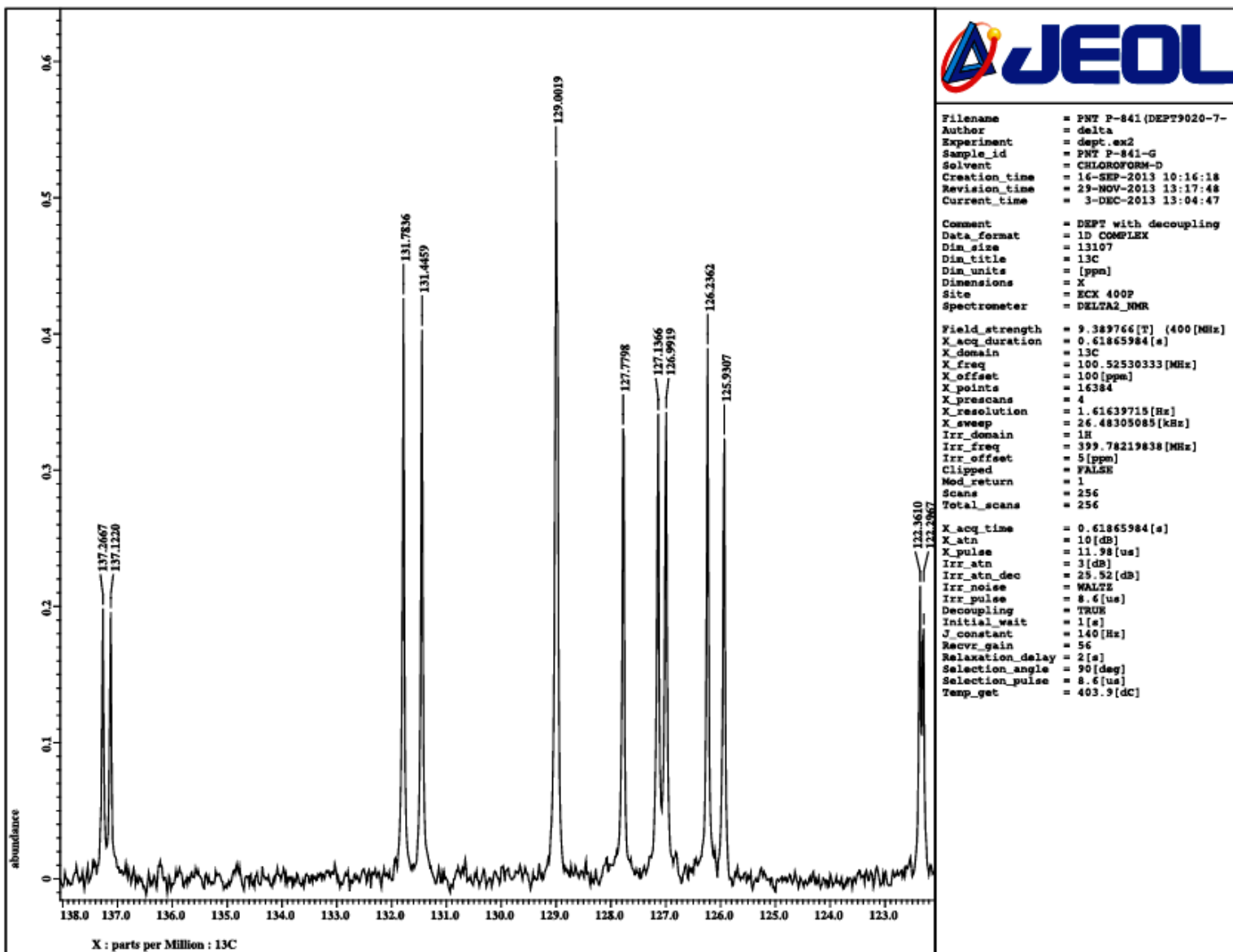


Fig. S119 Expansion of DEPT 90 NMR spectrum of **16**.

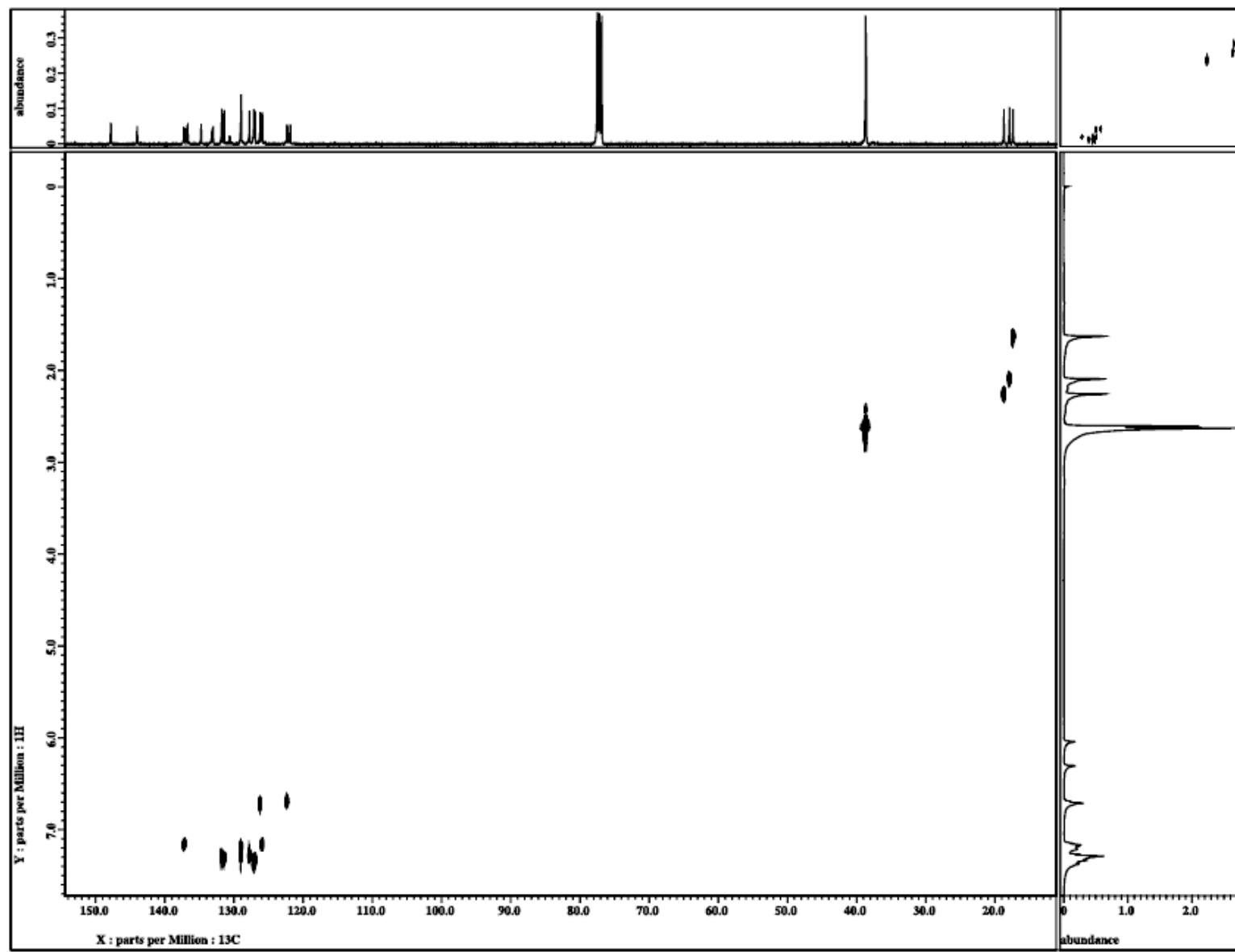


Fig. S120 The ^{13}C - ^1H HETCOR NMR spectrum of **16** (X-axis 100.5 MHz, Y-axis 400 MHz, CDCl_3).

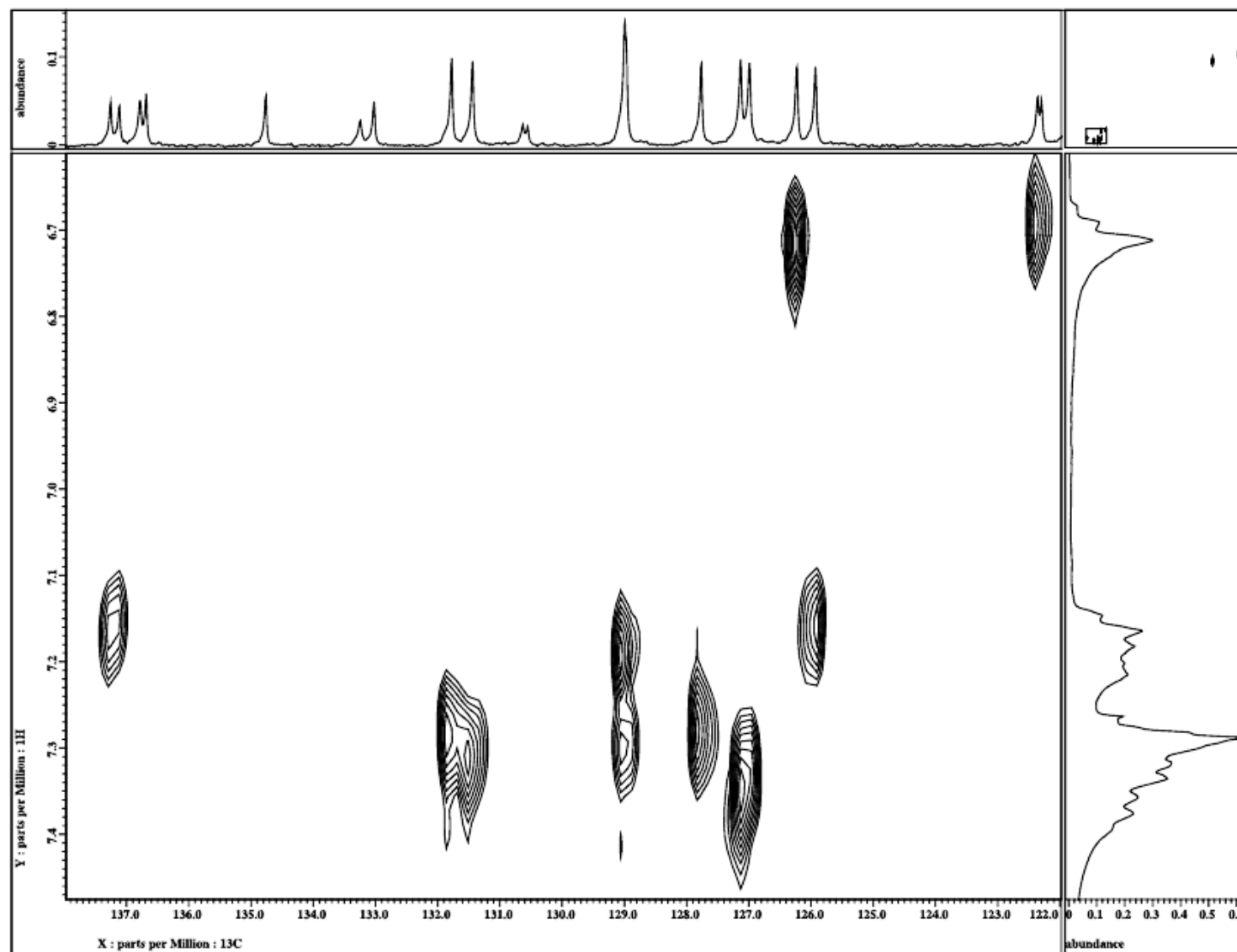


Fig. S121 The ^{13}C - ^1H HETCOR NMR spectrum of **16** illustrated for the ArCH carbons (X-axis 100.5 MHz, Y-axis 400 MHz, CDCl_3).

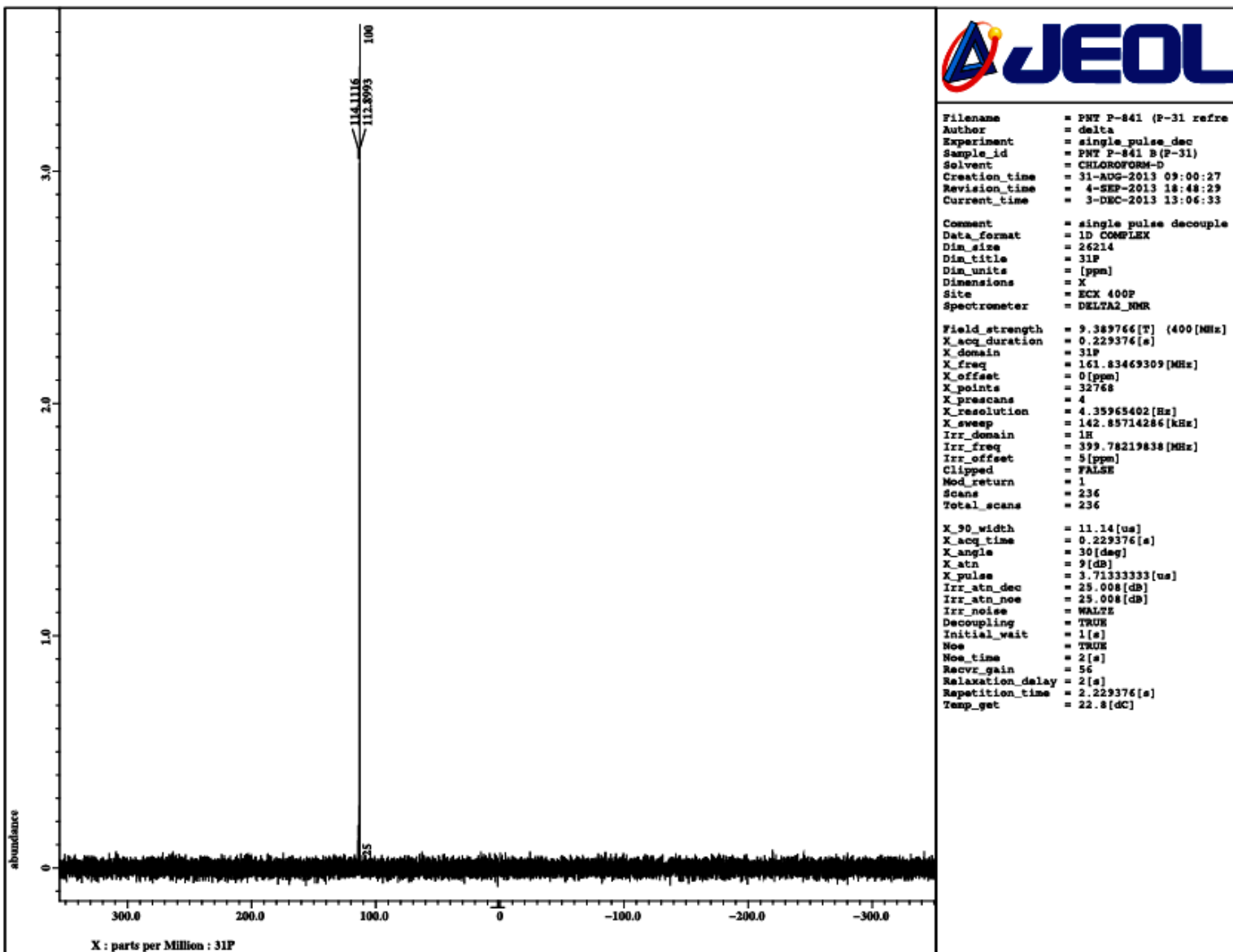


Fig. S122 $^{31}\text{P}\{\text{H}\}$ NMR spectrum of **16** (CDCl_3 , 161.8 MHz).

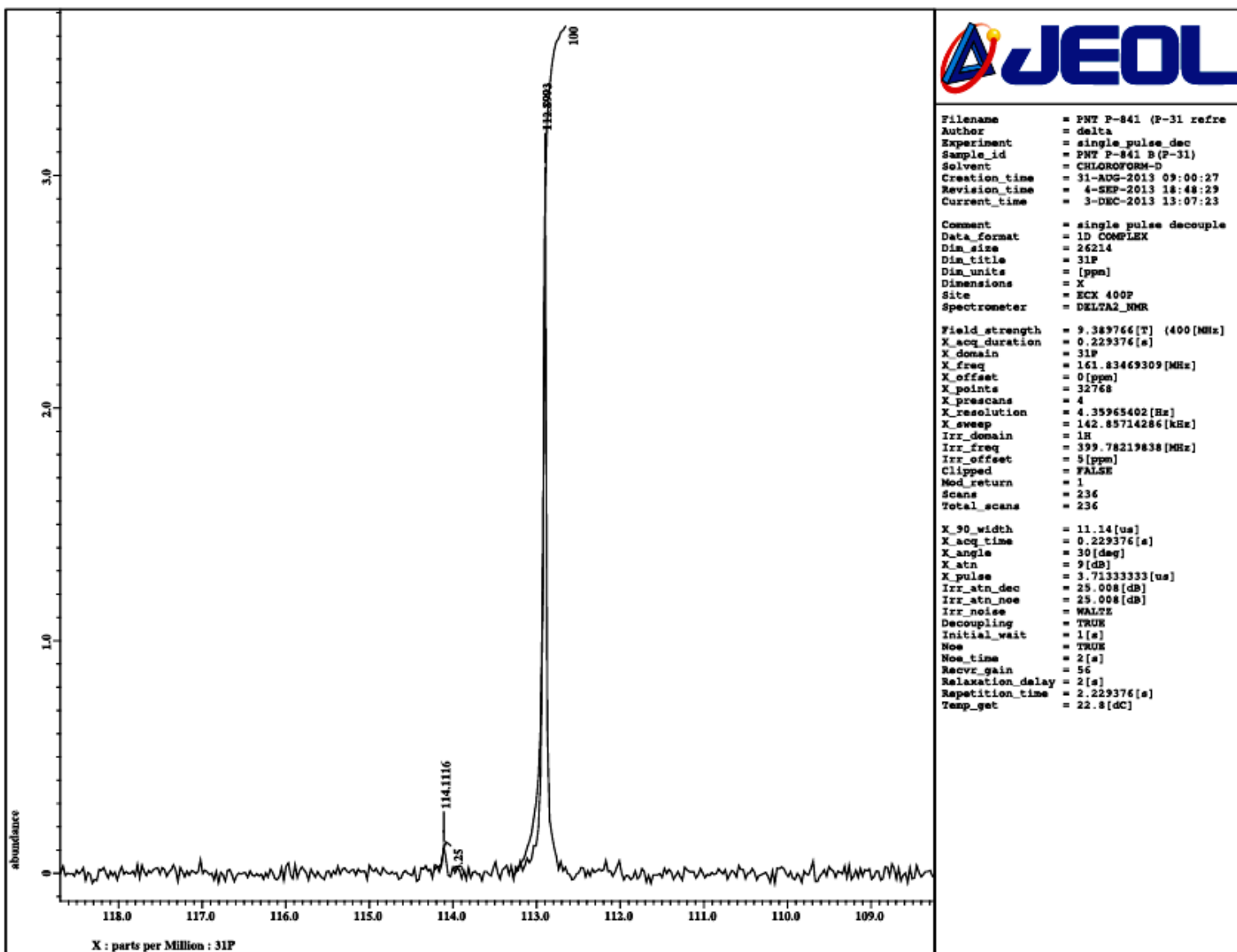


Fig. S123 Expansion of $^{31}\text{P}\{^1\text{H}\}$ NMR spectrum of **16** (CDCl_3 , 161.8 MHz).

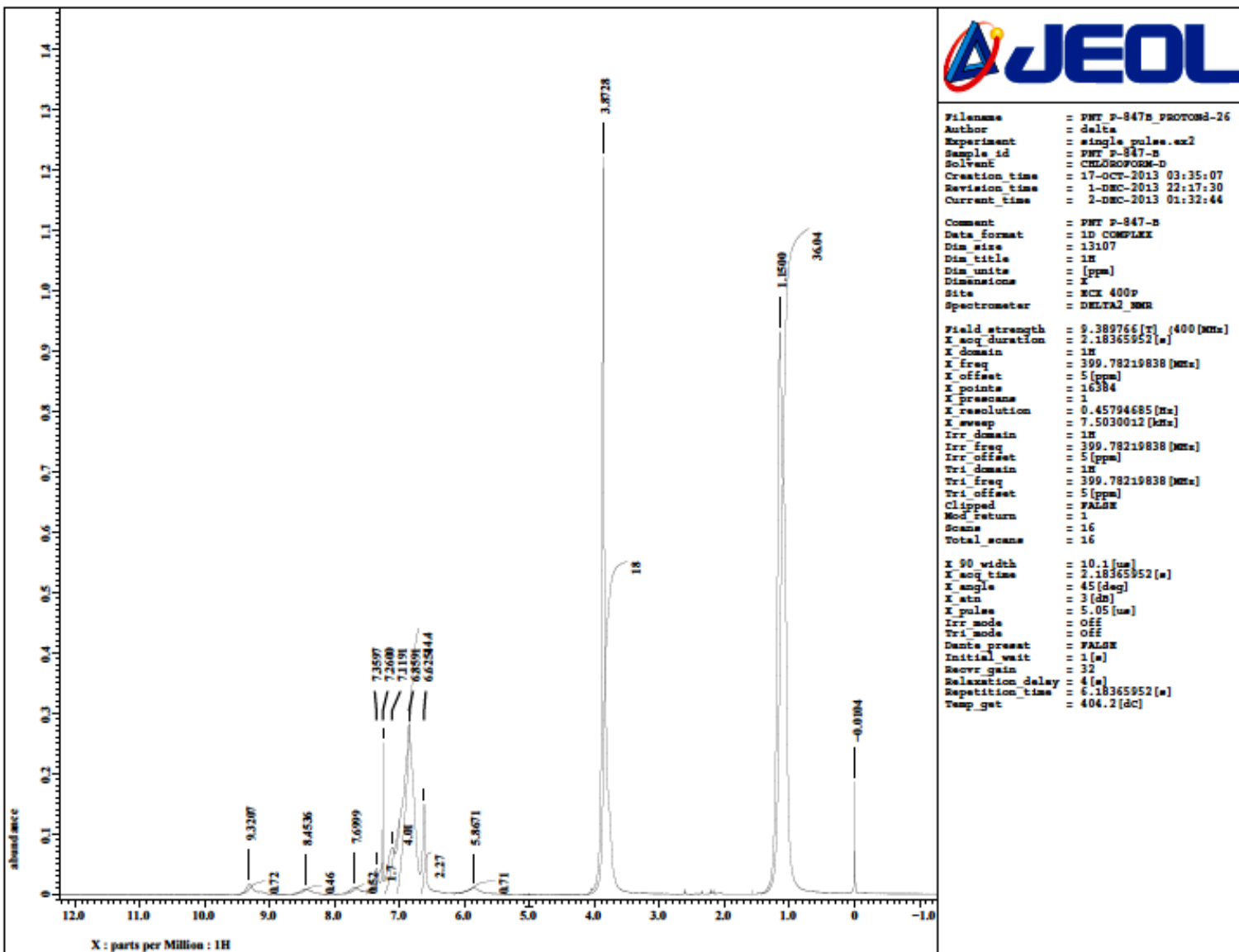


Fig. S124 ^1H NMR spectrum of **17** (CDCl_3 , 400.0 MHz).

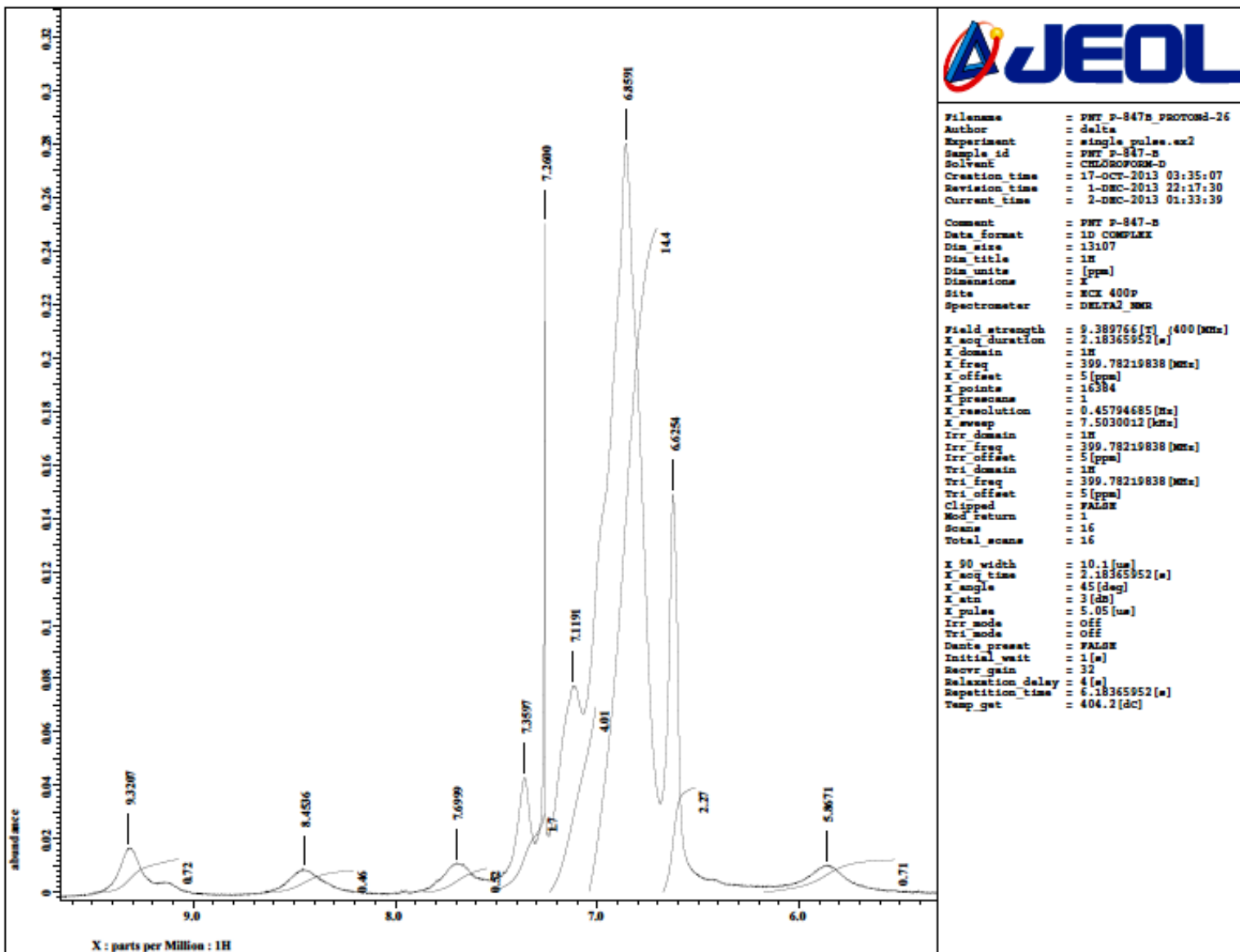


Fig. S125 Expansion of ^1H NMR spectrum of **17** (CDCl_3 , 400.0 MHz).

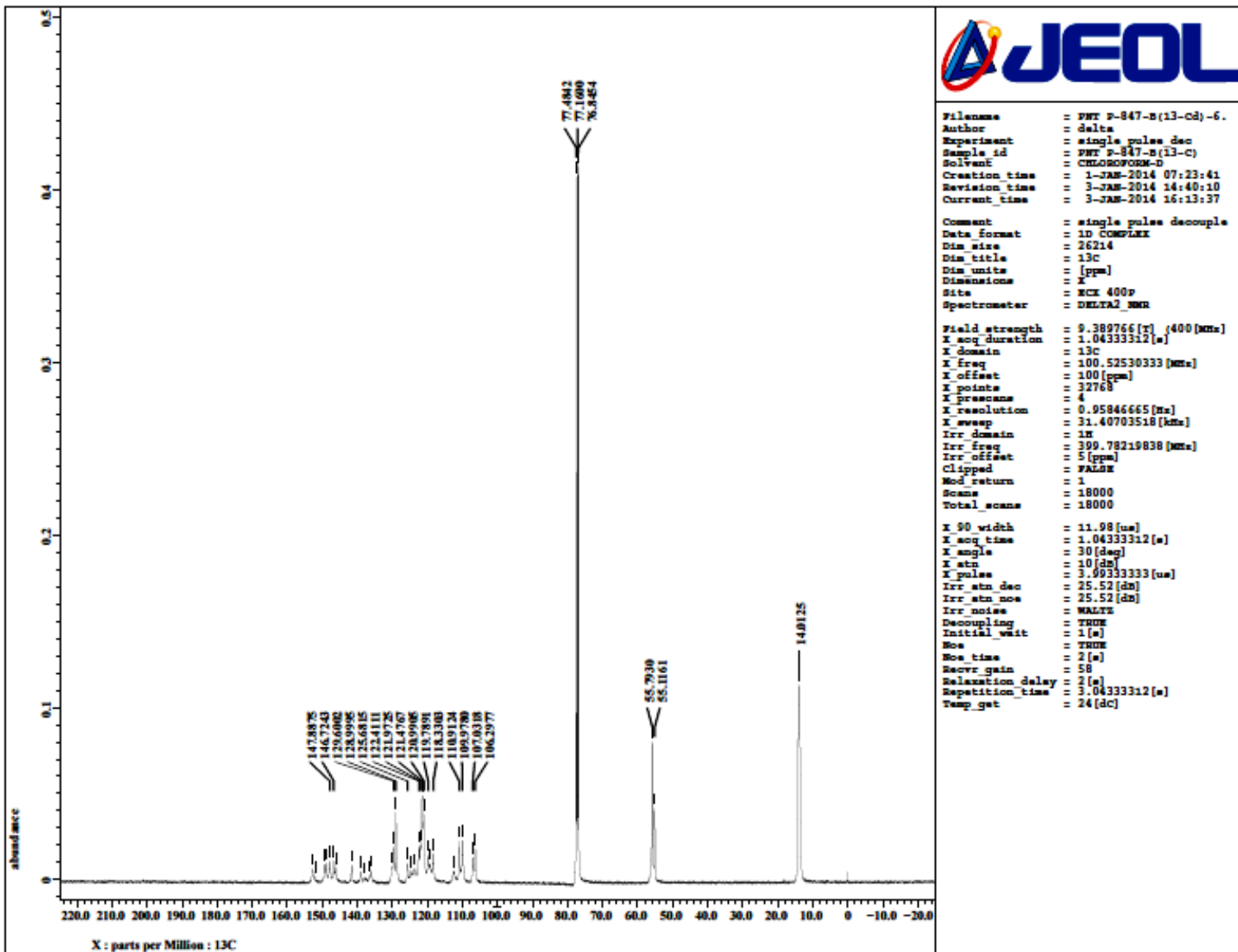


Fig. S126 ^{13}C NMR spectrum of **17** (CDCl_3 , 100.5 MHz).

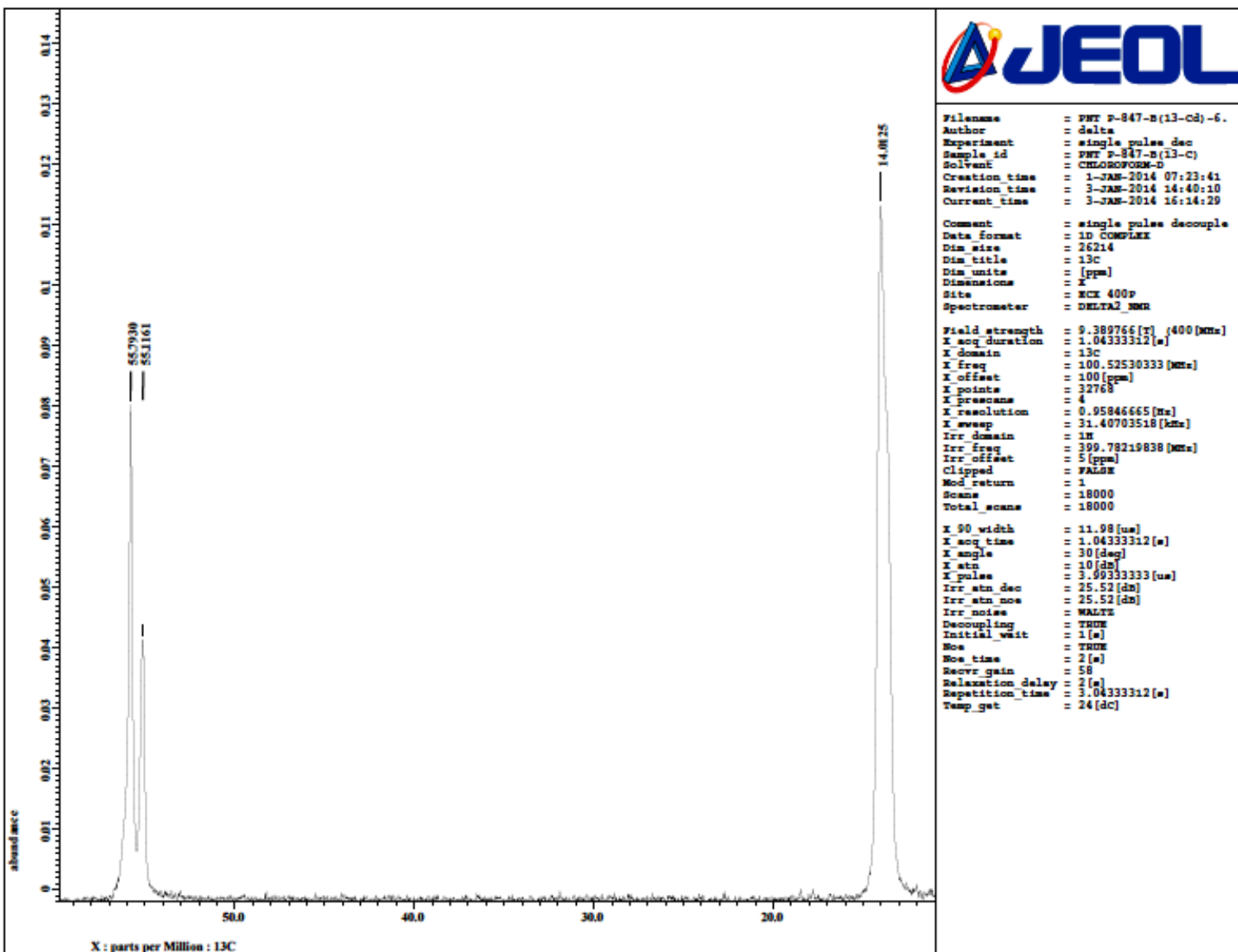


Fig. S127 Expansion of ^{13}C NMR spectrum of **17** (CDCl_3 , 100.5 MHz).

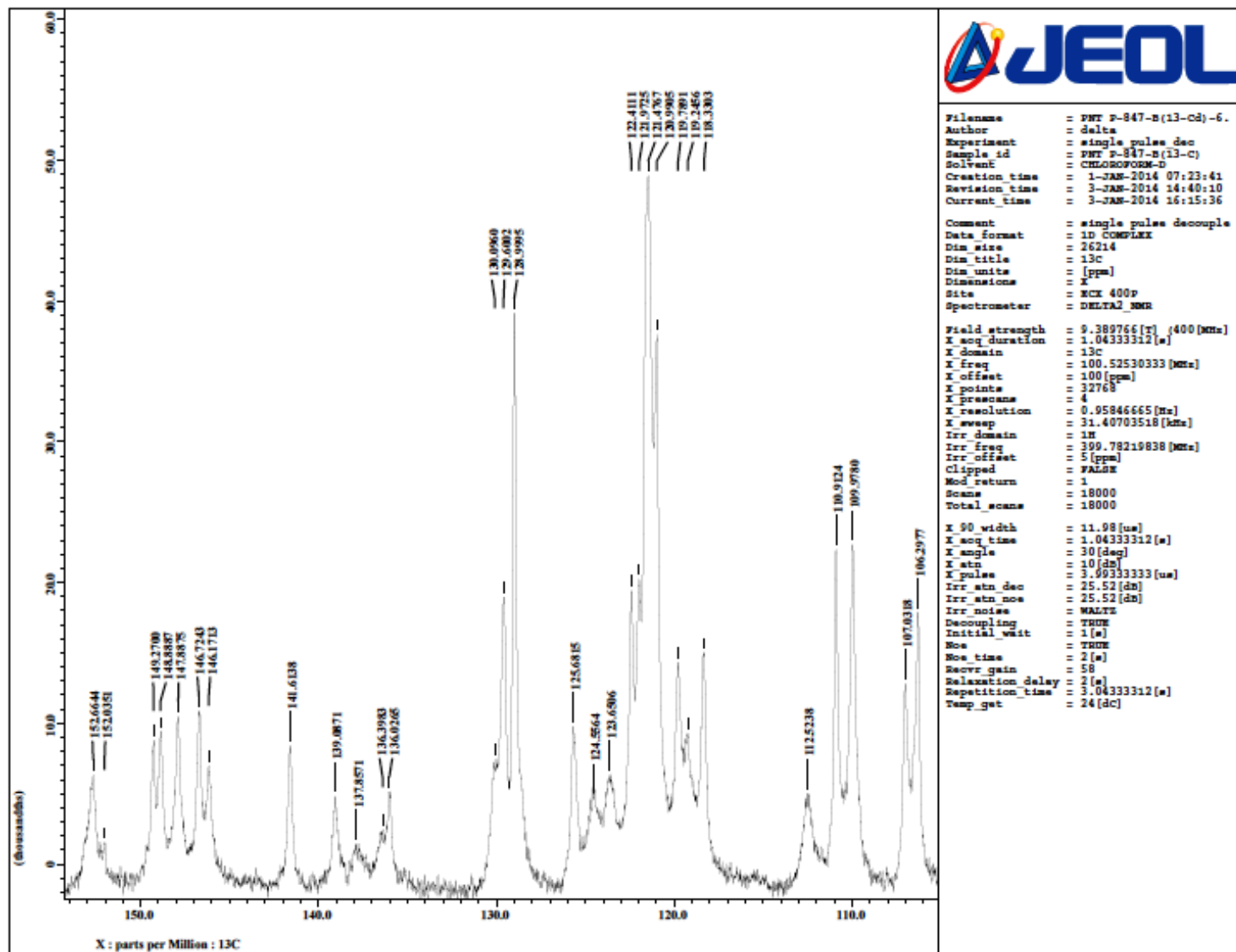


Fig. S128 Expansion of ^{13}C NMR spectrum of **17** (CDCl_3 , 100.5 MHz).

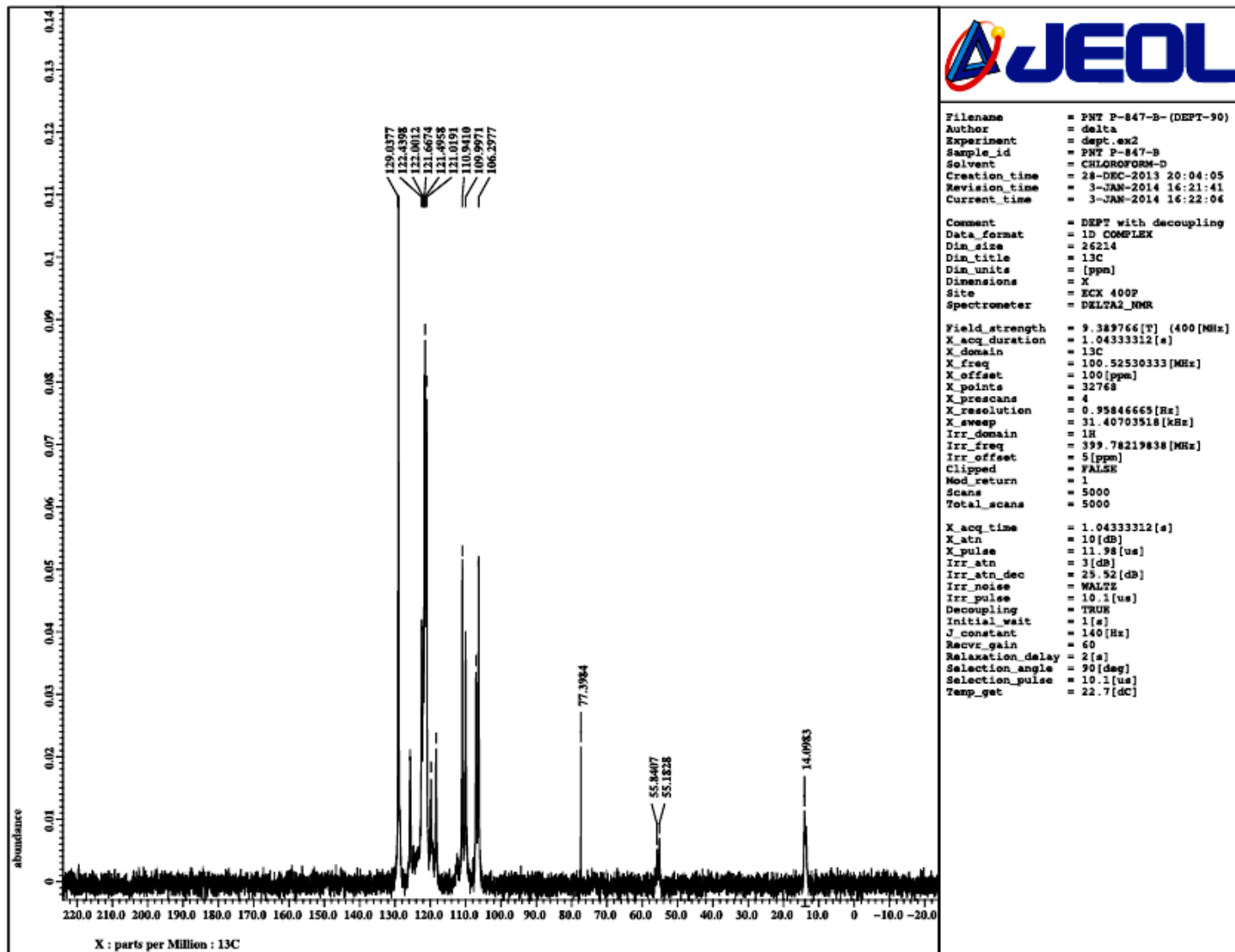


Fig. S129 DEPT 90 NMR spectrum of **17** (CDCl_3 , 100.5 MHz). The peaks around δ 14 and 55 correspond to residual peaks of CH_3 and OCH_3 carbons.

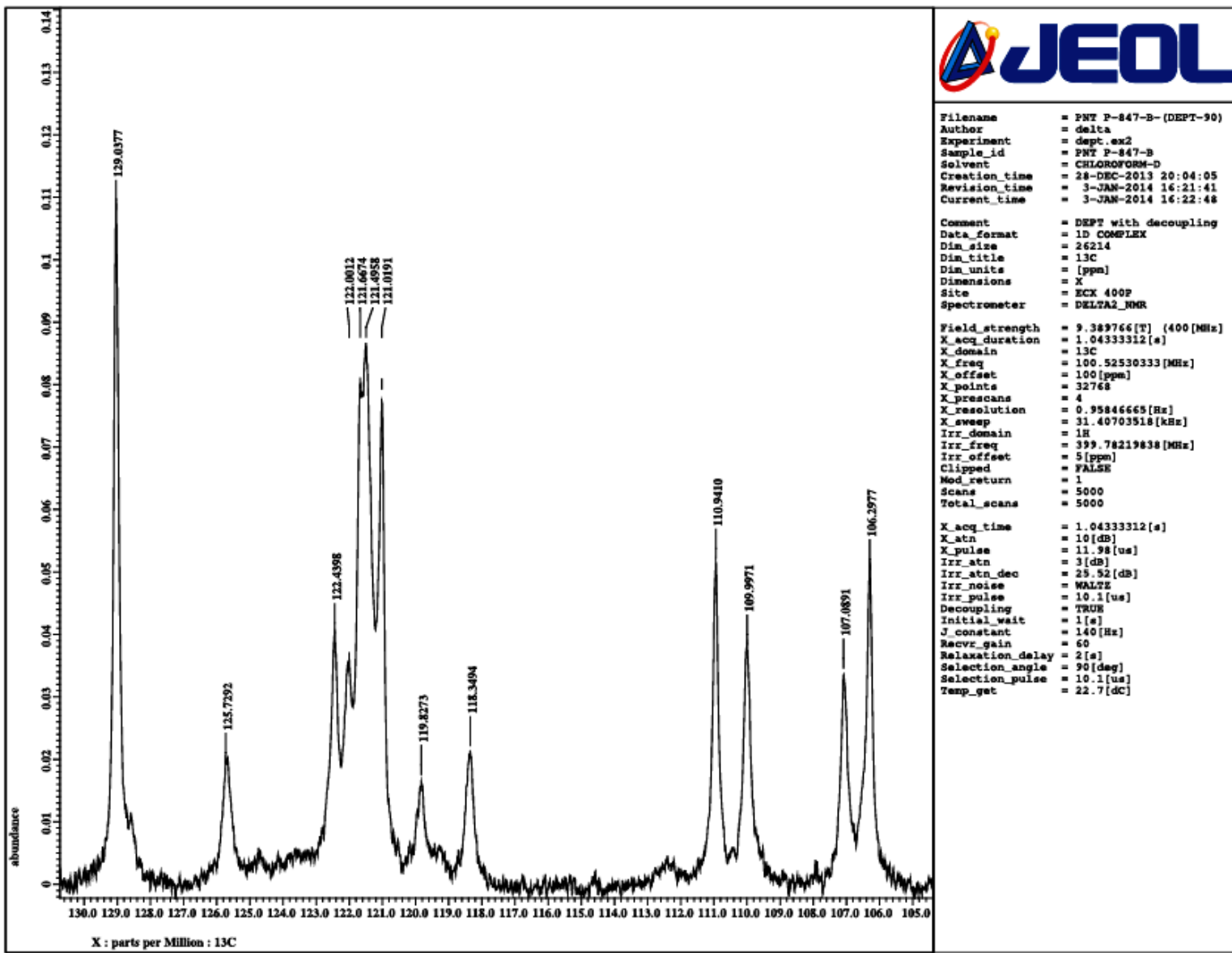


Fig. S130 Expansion of DEPT 90 NMR spectrum of **17**.

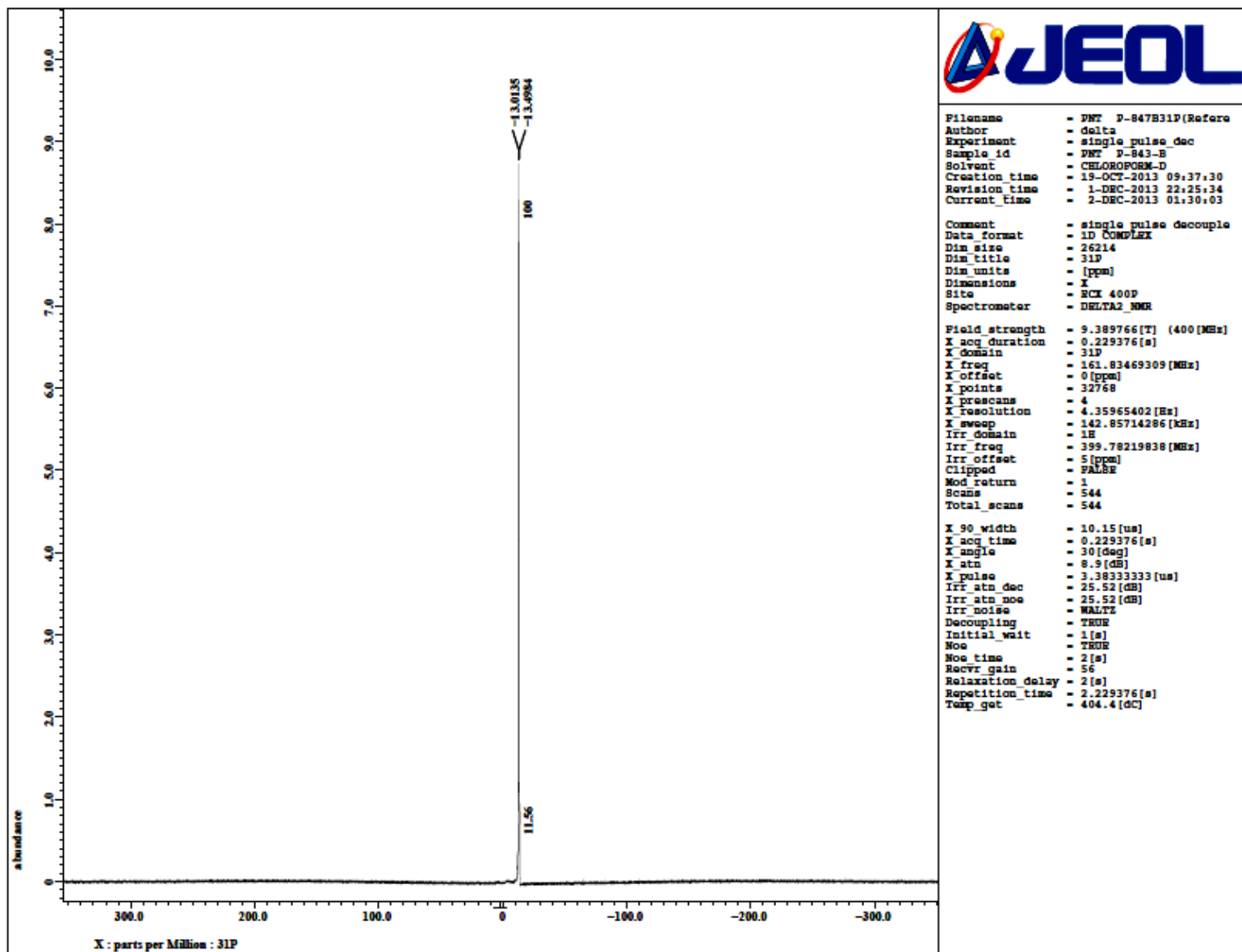


Fig. S131 $^{31}\text{P}\{\text{H}\}$ NMR spectrum of **17** (CDCl_3 , 161.8 MHz).

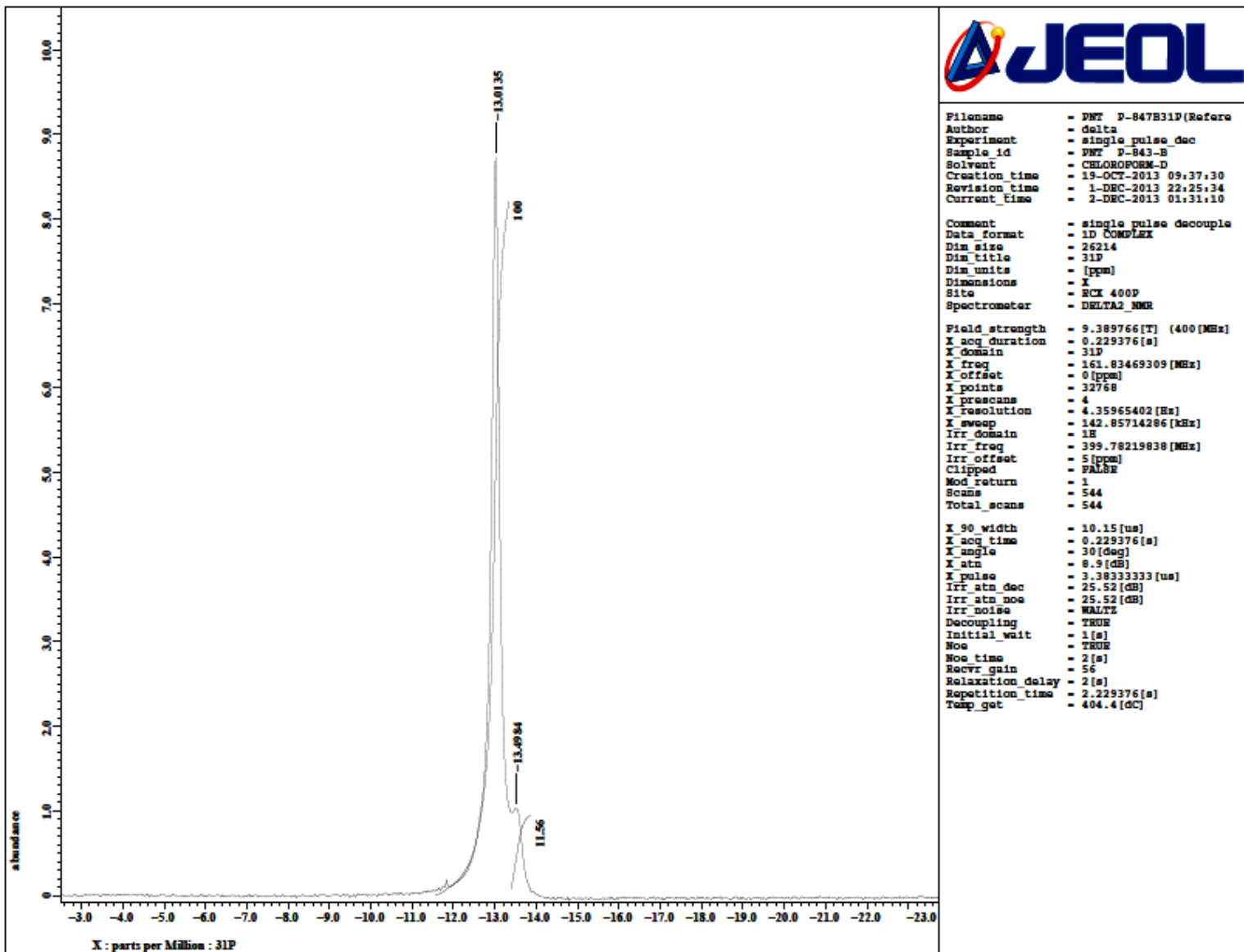


Fig. S132 Expansion of $^{31}\text{P}\{\text{H}\}$ NMR spectrum of **17** (CDCl_3 , 161.8 MHz).

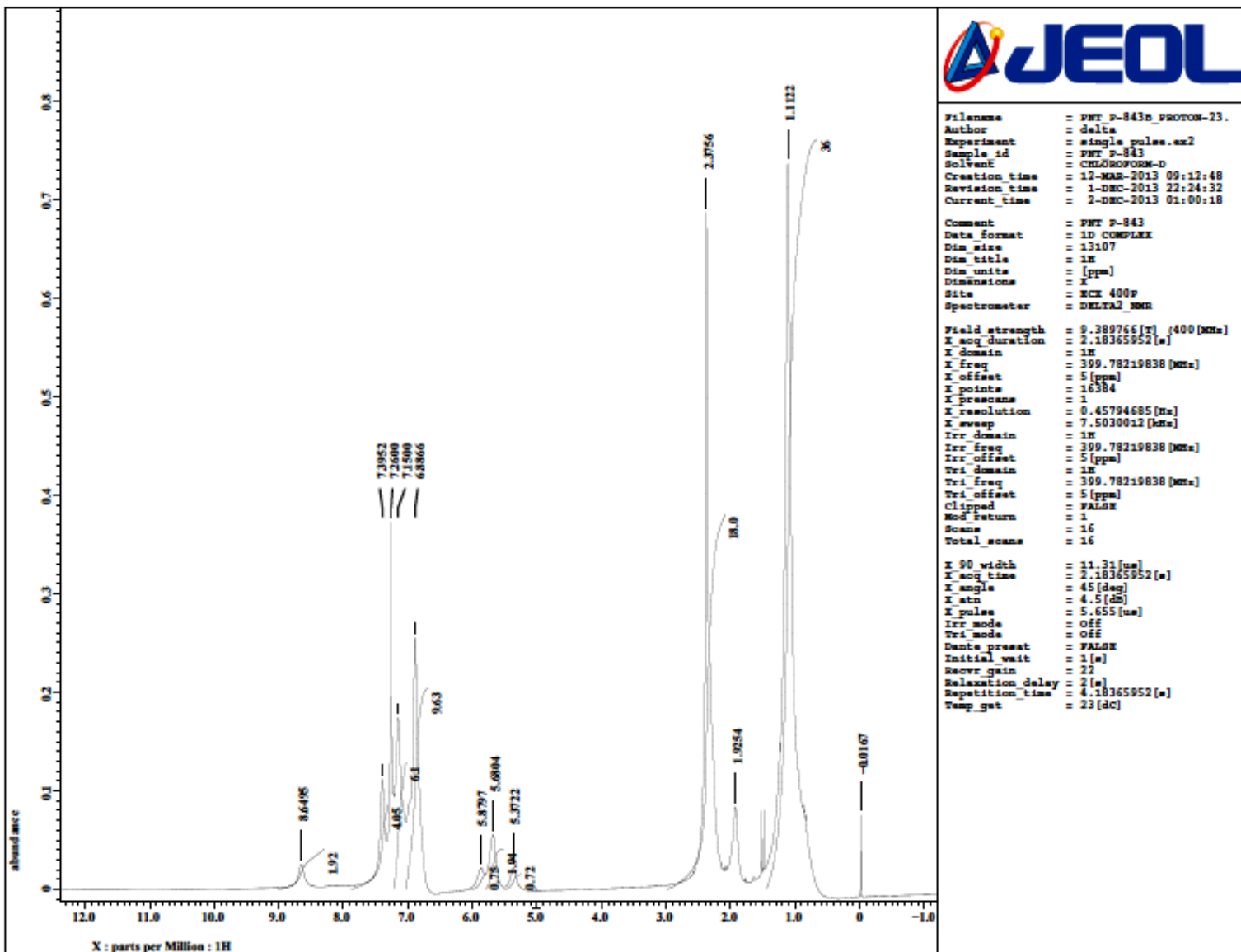


Fig. S133 ^1H NMR spectrum of **18** (CDCl_3 , 400.0 MHz).

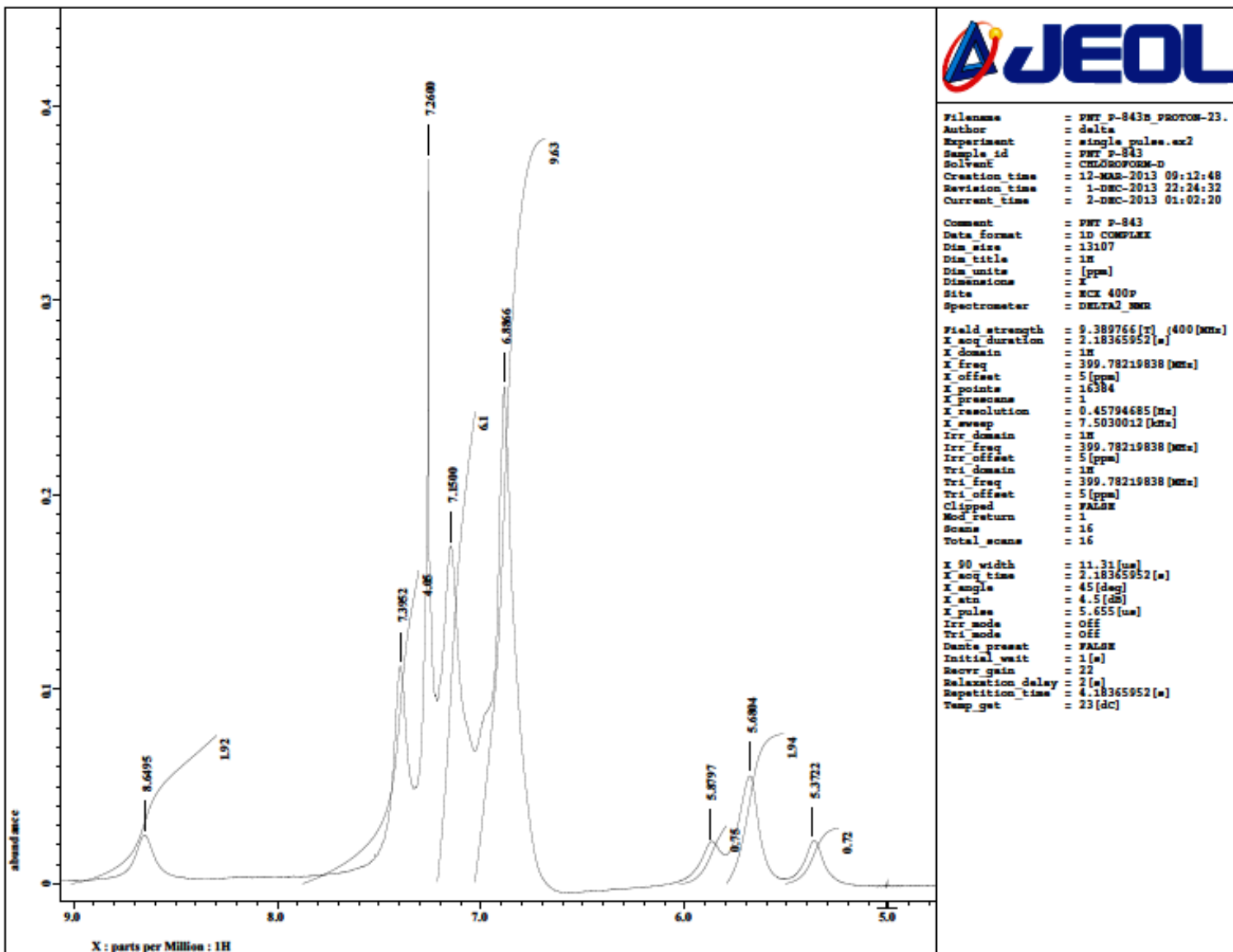


Fig. S134 Expansion of ^1H NMR spectrum of **18** (CDCl_3 , 400.0 MHz).

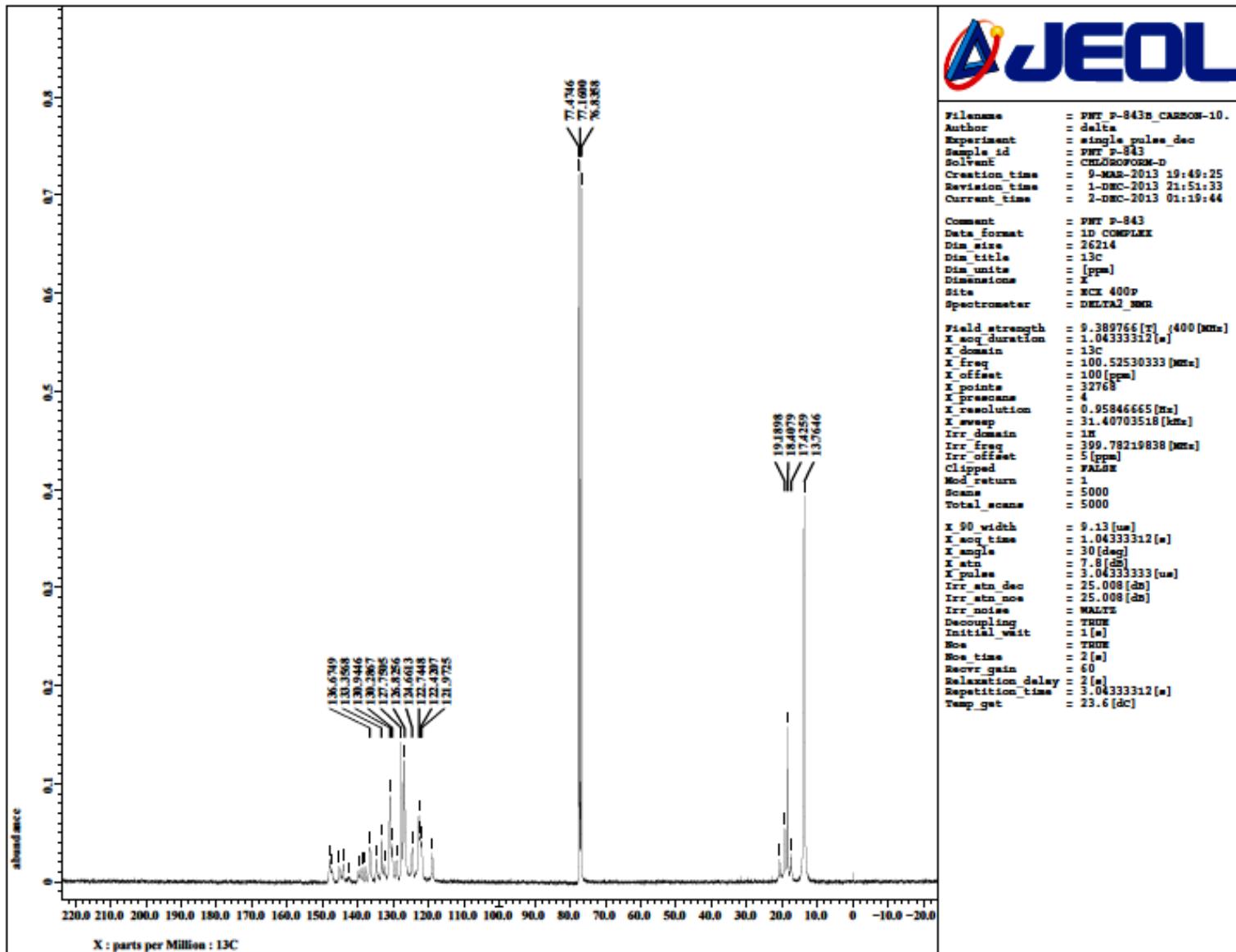


Fig. S135 ^{13}C NMR spectrum of **18** (CDCl_3 , 400.0 MHz).

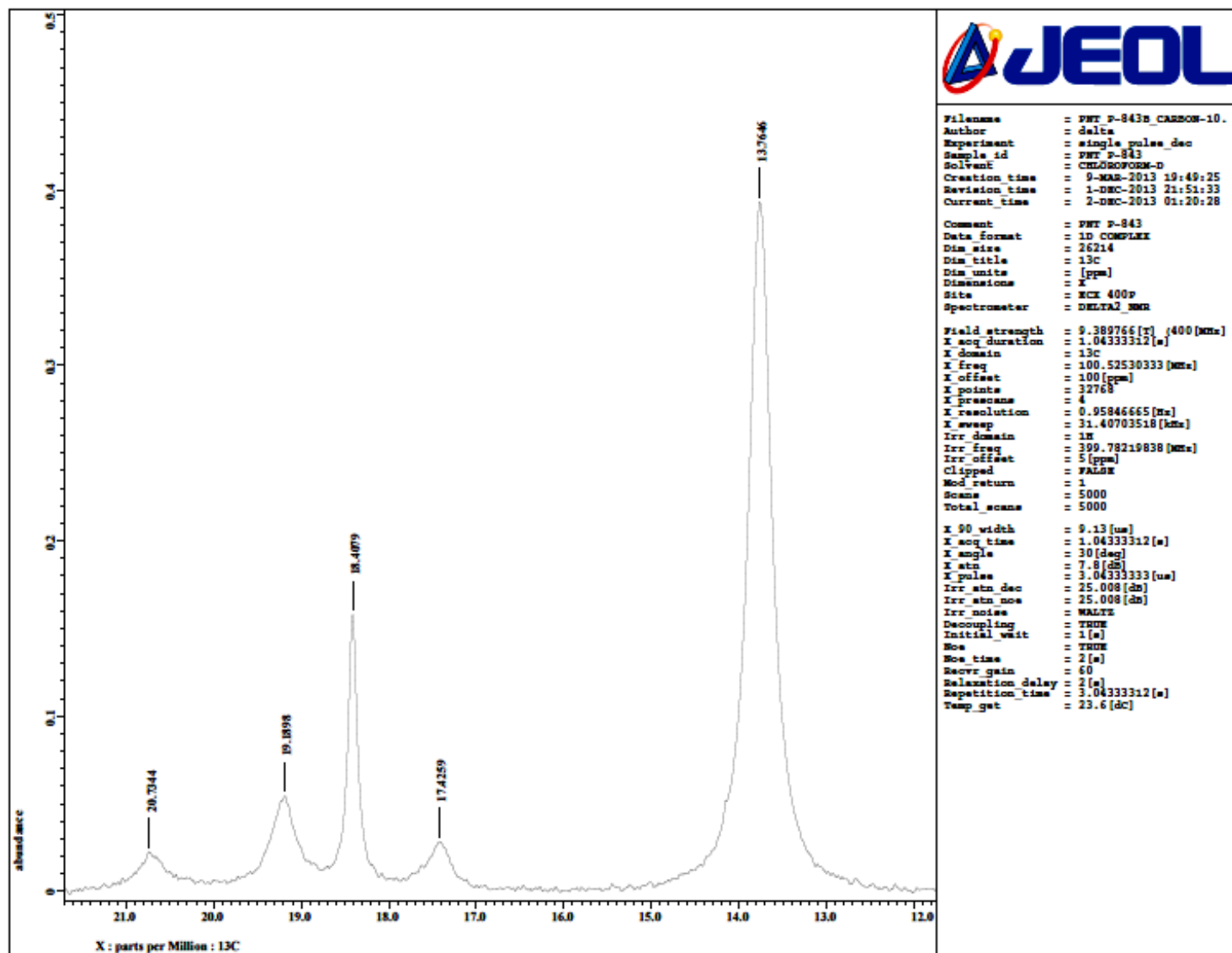


Fig. S136 Expansion of ^{13}C NMR spectrum of **18** (CDCl_3 , 400.0 MHz).

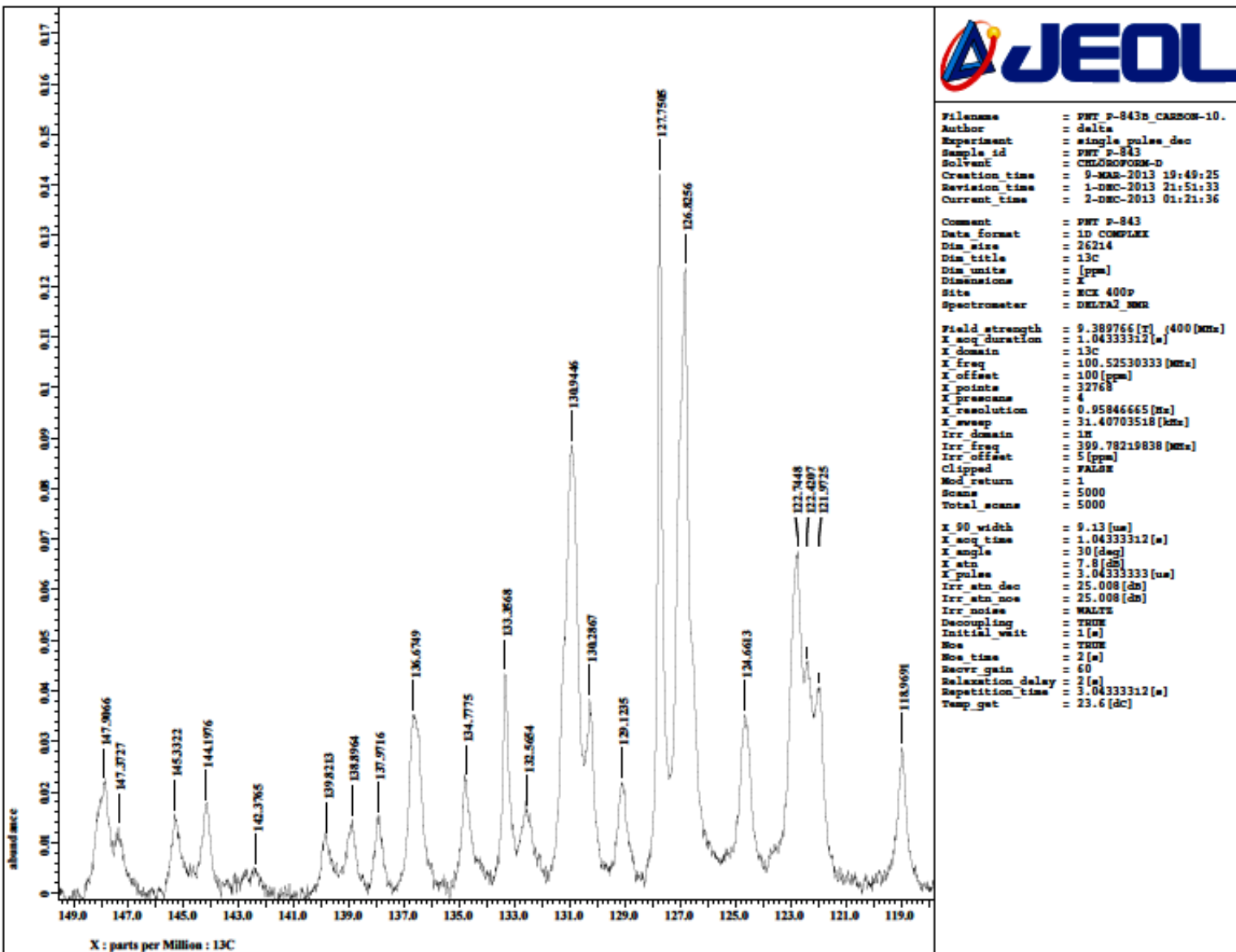


Fig. S137 Expansion of ^{13}C NMR spectrum of **18** (CDCl_3 , 400.0 MHz).

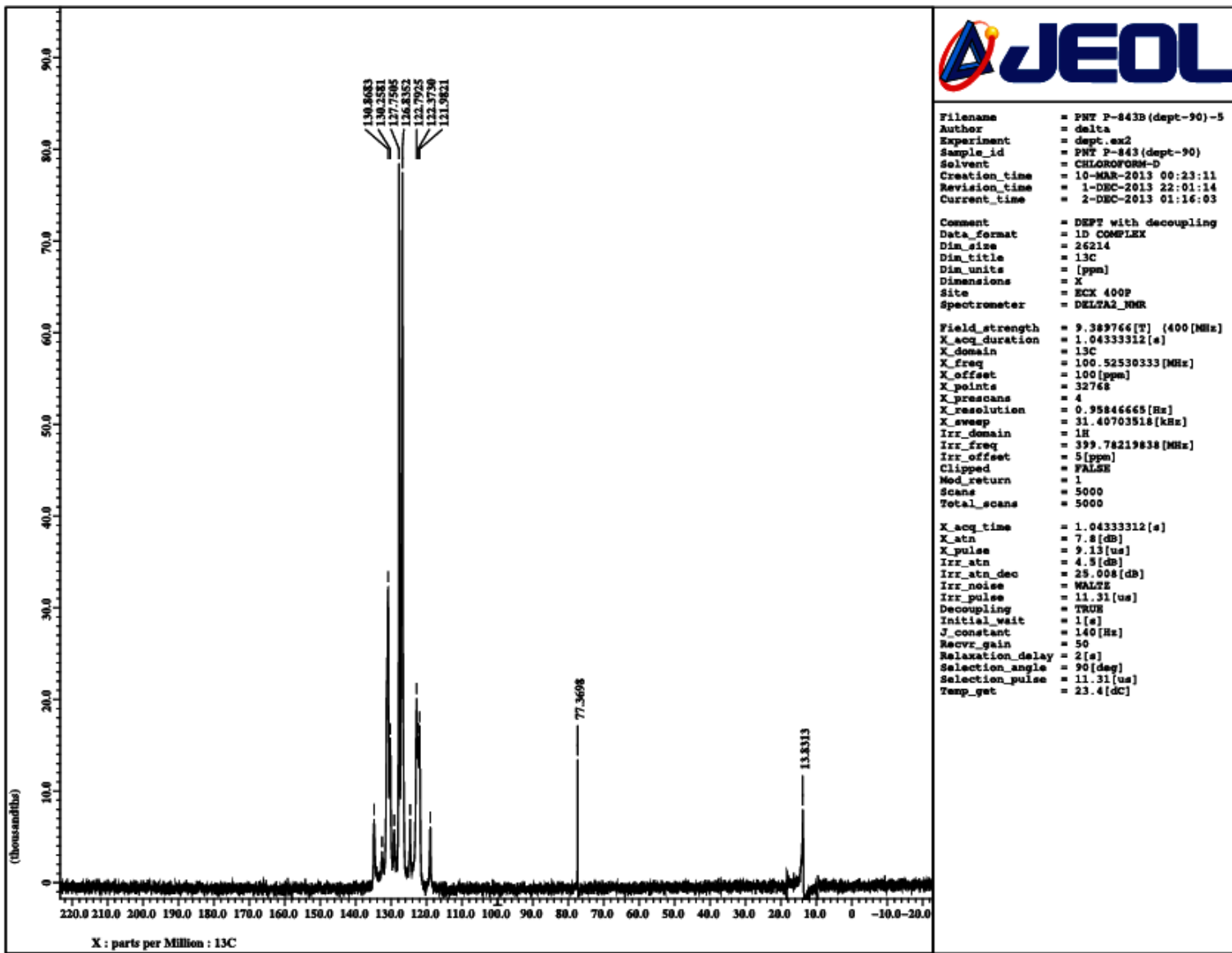


Fig. S138 DEPT 90 NMR spectrum of **18** (CDCl_3 , 100.5 MHz). Peak around δ 13 corresponds to residual peaks of CH_3 carbons.

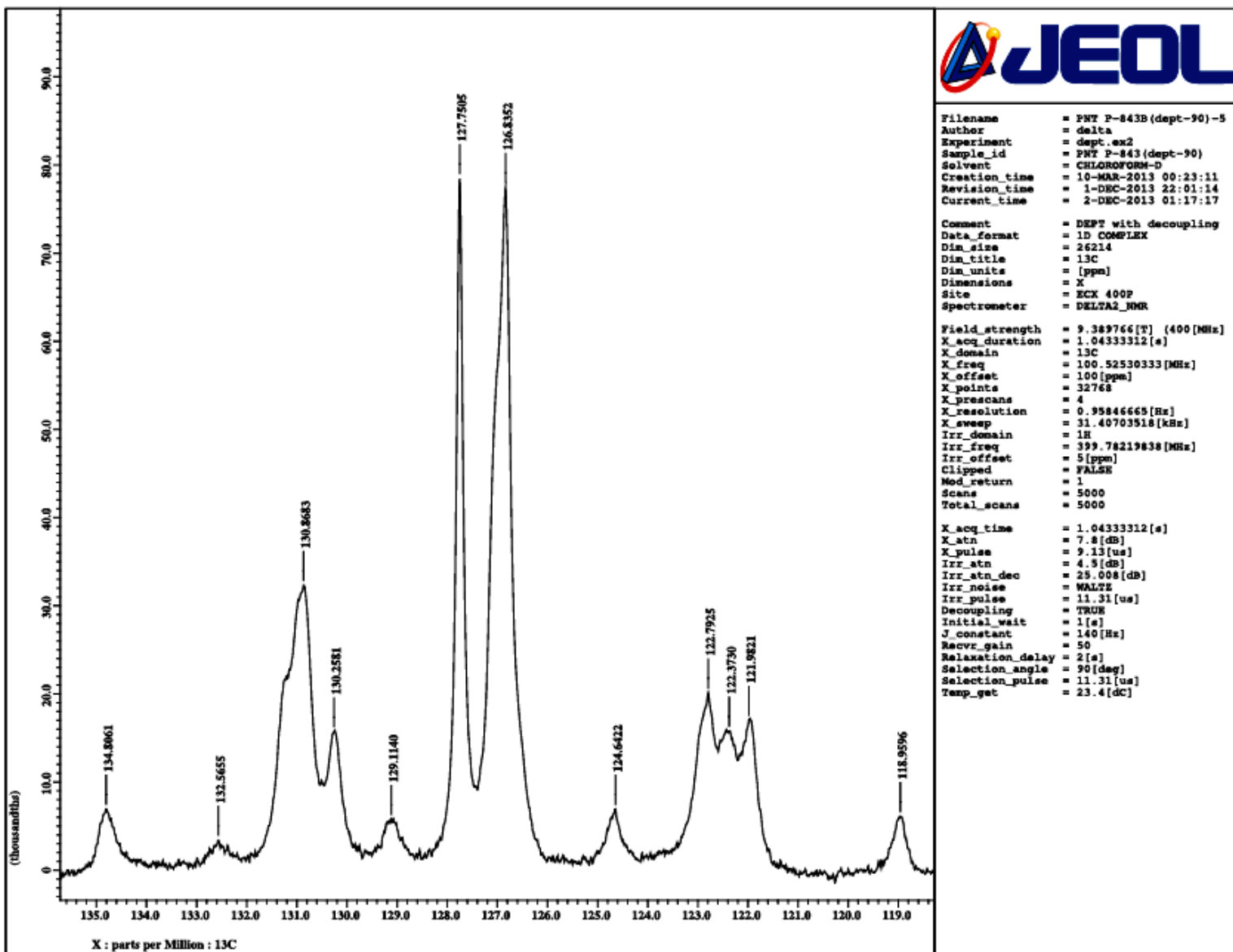


Fig. S139 Expansion of DEPT 90 NMR spectrum of **18**.

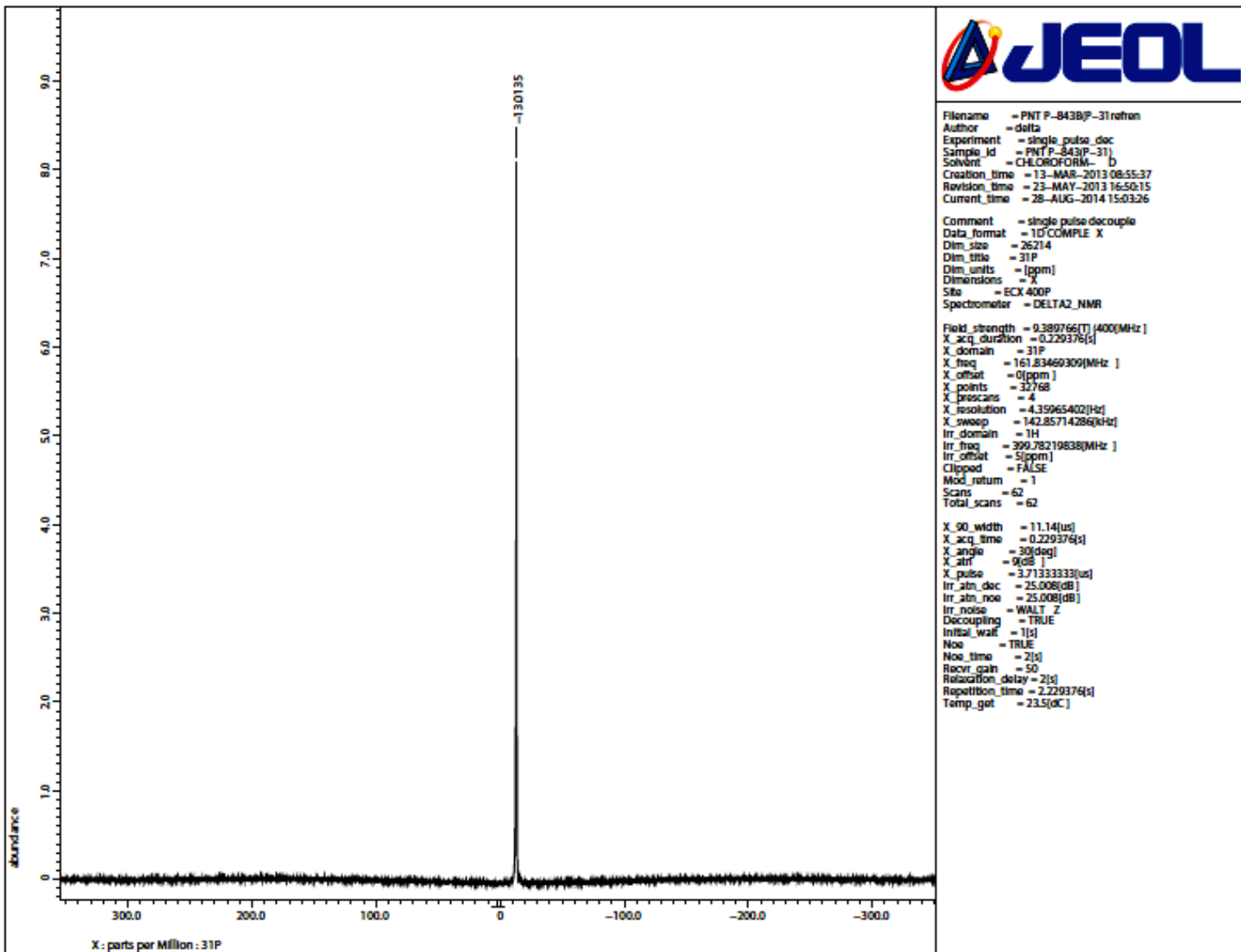


Fig. S140 $^{31}\text{P}\{\text{H}\}$ NMR spectrum of **18** (CDCl_3 , 161.8 MHz).